EXPLORING TRITHORAX GROUP COMPLEX ACTIVITY IN PANCREAS AND ENDOCRINE PROGENITOR CELL DEVELOPMENT

by

Stephanie Ann Campbell

B.Sc.H., Simon Fraser University, 2011

A THESIS SUBMITTED IN PARTIAL FULFILLMENT OF

THE REQUIREMENTS FOR THE DEGREE OF

DOCTOR OF PHILOSOPHY

in

THE FACULTY OF GRADUATE AND POSTDOCTORAL STUDIES

(Cell and Developmental Biology)

THE UNIVERSITY OF BRITISH COLUMBIA

(Vancouver)

March 2019

The following individuals certify that they have read, and recommend to the Faculty of Graduate and Postdoctoral Studies for acceptance, the dissertation entitled:

Exploring Trithorax Group complex activity in pancreas and endocrine progenitor cell development

submitted by Stephanie Ann Campbell in partial fulfillment of the requirements for

the degree of Doctor of Philosophy

in Cell and Developmental Biology

Examining Committee:

Dr. Bradford Hoffman, Cell and Developmental Biology
Supervisor

Dr. Pamela Hoodless, Cell and Developmental Biology
Supervisory Committee Member

Supervisory Committee Member

Dr. Angela Devlin, Experimental Medicine
University Examiner

Dr. Stefan Taubert, Cell and Developmental Biology
University Examiner

Additional Supervisory Committee Members:

Dr. Francis Lynn, Cell and Developmental Biology
Supervisory Committee Member

Dr. Timothy Kieffer, Cellular and Physiological Sciences
Supervisory Committee Member

Abstract

The pancreas derives from PDX1$^+$ multipotent progenitors that differentiate and mature into acinar, duct and endocrine cells. Pancreas cell differentiation and maturation is controlled by activation of lineage-specific genes, such as *Neurog3,* which drives endocrine cell specification. However, how these genes are activated and/or maintained during pancreas development is not clear. The Trithorax Group (TrxG) complexes are chromatin regulators that catalyze histone 3 lysine 4 (H3K4) methylation associated with active chromatin. The objective of this thesis was to investigate the role of TrxG-catalyzed H3K4 methylation in mediating the activation and maintenance of genes critical to pancreas and endocrine progenitor cell specification.

Using an *in vitro* spheroid model of pancreas development, TrxG complex formation and thus, catalytic and non-catalytic functions, were disrupted by *Wdr5* suppression in pancreas progenitors. *Wdr5* suppression significantly decreased the number of spheres generated per pancreas and sphere diameter. Activation of *Neurog3* and downstream endocrine genes was significantly reduced, and RNA-sequencing revealed that activation of acinar cell genes was also reduced. The catalytic role of TrxG complexes in pancreas development was examined *in vivo* by genetically deleting *Dpy30* in PDX1$^+$ and NEUROG3$^+$ cells. Loss of *Dpy30* from PDX1$^+$ cells resulted in loss of H3K4 methylation and decreased pancreas size due to a reduction in progenitor proliferation and an increase in apoptosis. *Neurog3* expression was decreased and the proportion of NEUROG3$^+$ endocrine progenitors and differentiated endocrine cells was significantly reduced. Additionally, while acinar cell genes were activated, the proportion of differentiated acinar cells was decreased, acinar cell maturation was impaired and disorganized cystic structures developed. Loss of *Dpy30* from NEUROG3$^+$ cells resulted in loss of H3K4

methylation, without altering the proportion of differentiated endocrine cells, but led to impaired postnatal glucose tolerance. RNA-sequencing of pancreatic islets from these mice demonstrated that while the majority of genes were unaffected, the expression of a subset of islet-specific genes was significantly reduced. Collectively, these results suggest that the non-catalytic functions of the TrxG complexes are required for activation of a subset of lineage-specific genes while H3K4 methylation is necessary for their active maintenance during pancreas development.

Lay Summary

Central to diabetes are the specialized pancreatic β-cells that sense glucose levels in the blood and secrete the hormone insulin, which acts on various tissues to reduce blood glucose levels. In diabetes, β-cell dysfunction leads to reduced insulin levels and/or action which results in high blood glucose over time. It is important to understand how the pancreas and β-cells normally develop in order to identify the causes of β-cell dysfunction in diabetes. This thesis focuses on investigating the role of the Trithorax Group (TrxG) protein complexes during pancreas and β-cell development. Using mouse models, I found that the loss of activity of the TrxG complexes in the pancreas resulted in high blood glucose levels due to fewer and dysfunctional insulin-producing β-cells. The results in this study may improve the process of generating functional insulin-producing β-cells from stem cells to replace dysfunctional β-cells as a potential diabetes therapy.

Preface

Animal experiments conducted herein were ethically approved by the University of British Columbia's Animal Care Committee under Protocols A14-0032, A14-0033 and A17-0045.

Research data described herein were designed and conceived by S.A. Campbell and B.G. Hoffman. Experiments were performed and analyzed by S.A. Campbell, with technical assistance as follows:

Chapter 3: C.J. Whiting assisted with lentivirus generation and C.L. McDonald assisted with embryo collection, *in vitro* pancreas spheroid assays, sphere measurements and qPCR. B.G. Hoffman analyzed RNA-sequencing data.

Chapter 4: N.A.J. Krentz performed cumulative EdU labeling experiments, including embryo collection, tissue processing and sectioning, immunostaining, imaging and quantification. C.L. McDonald performed pHH3 and TUNEL experiments, including embryo collection, tissue processing and sectioning, immunostaining, imaging and quantification. E.E. Xu assisted with custom CellProfiler pipelines.

Chapter 5: C.L. McDonald and T.L. Stephan assisted with mouse monitoring, embryo and pancreas collection, tissue processing, sectioning, immunostaining, imaging and quantification. B. Vanderkruk assisted with islet isolations.

Part of Chapter 1 has been published in Campbell, S.A. and Hoffman, B.G. (2016) Chromatin Regulators in Pancreas Development and Diabetes. ***Trends in Endocrinology and Metabolism***. 27(3): 142-152. S.A. Campbell wrote the manuscript with revisions from B.G. Hoffman.

A version of Chapters 3 and 4 are peer-reviewed and under revision as Campbell, S.A., McDonald, C.L., Krentz, N.A.J., Lynn, F.C. and Hoffman, B.G. (2019) Loss of TrxG activity in pancreas progenitors impairs cell cycle progression shifting specification towards the acinar lineage. ***Cell Reports***. S.A. Campbell, C.L. McDonald and N.A.J. Krentz performed experiments and analyzed data. B.G. Hoffman analyzed sequencing data. S.A. Campbell wrote the manuscript with revisions from B.G. Hoffman.

This dissertation was written by S.A. Campbell with revisions from B.G. Hoffman.

Table of Contents

List of Tables

List of Figures

List of Abbreviations

Ac	Acetylation
ANOVA	Analysis of variance
ATP	Adenosine triphosphate
BMP	Bone morphogenetic protein
BPC	Bipotent progenitor cell
BPE	Bovine pituitary extract
CBP	CREB-binding protein
cDNA	Complementary DNA
CHD1	Chromodomain-helicase-DNA-binding-protein 1
DBA	*Dolichos* bifluros agglutinin
DNA	Deoxyribonucleic acid
DNMT	DNA methyltransferase
Dpy30ΔN	*Neurog3*-Cre; *Dpy30*$^{flox/flox}$
Dpy30ΔP	*Pdx1*-Cre; *Dpy30*$^{flox/flox}$
E	Embryonic day
EdU	5-ethynyl-2'-deoxyuridine
EMT	Epithelial-to-mesenchymal transition
FBS	Fetal bovine serum
FDR	False discovery rate
FGF	Fibroblast growth factor
G	Gap
H	Histone
HAT	Histone acetyltransferase
HBSS	Hank's Balanced Salt Solution
HDAC	Histone deacetylase
HEK	Human embryonic kidney
hESC	Human embryonic stem cell
IGF	Insulin-like growth factor
ING	Inhibitor of growth
IF	Immunofluorescence
IP	Intraperitoneal
IPGTT	Intraperitoneal glucose tolerance test
iPSC	Induced pluripotent stem cell
K	Lysine
KDM	Lysine demethylase
M	Mitosis
me1, me2, me3	Mono-, di- and tri-methylation
mESC	Mouse embryonic stem cell
MIP-GFP	Mouse insulin promoter green fluorescent protein
MOI	Multiplicity of infection
MPC	Multipotent progenitor cell

ncRNA	Non-coding RNA
NuRD	Nucleosome remodeling and deacetylase
NuRF	Nucleosome remodeling factor
P	Postnatal day
PAF	Polymerase associated factor
PanIN	Pancreatic intraepithelial neoplasia
PcG	Polycomb Group
PDAC	Pancreatic ductal adenocarcinoma
PFA	Paraformaldehyde
pHH3	Phospho-histone H3
Pol II	RNA polymerase II
PRC	Polycomb repressive complex
PrEBM	Prostate epithelial cell growth basal medium
qPCR	Quantitative PCR
RA	Retinoic acid
RNA	Ribonucleic acid
RPMI	Roswell Park Memorial Institute medium
S	Synthesis
SD	Standard deviation
SEM	Standard error of the mean
SET	Su(var)3-9, Enhancer-of-zeste and Trithorax
SHH	Sonic hedgehog
shRNA	Short hairpin RNA
SWI/SNF	Switch/sucrose non-fermentable
T1D	Type 1 diabetes
T2D	Type 2 diabetes
TF	Transferrin
TFIID	Transcription factor II D
TGFβ	Transforming growth factor β
Trr	Trithorax-related
Trx	Trithorax
TrxG	Trithorax Group
TU	Transducing units
TUNEL	Terminal deoxynucleotidyl transferase dUTP nick end labeling
VEGF	Vascular endothelial growth factor

Acknowledgements

My PhD training has been a rewarding and fulfilling experience thanks to many individuals who have been instrumental to the completion of my degree. This work would not be possible without your mentorship, support and guidance.

First, I am grateful to my PhD supervisor, Dr. Brad Hoffman, for encouraging me to undertake doctoral research, for many valuable scientific discussions over the years and for the critical reading of this thesis. Thank you for sharing your interest in pancreas development with me, for providing me with experimental and academic guidance, for pushing me to succeed and for your patience.

Thank you to the members of my committee, Dr. Pamela Hoodless, Dr. Timothy Kieffer and Dr. Francis Lynn, for your continued mentorship, support and advice that has extended beyond committee meetings. I would also like to thank my undergraduate Honours thesis supervisor, Dr. Rosemary Cornell, for providing me with exceptional training and for inspiring my love of science and research.

To the members of the Hoffman lab, thank you for providing technical expertise and training, as well as intellectual discussions and friendship. Bryan Tennant, Cheryl Whiting, Peter Hurley, Ben Vanderkruk, Cassie McDonald, Tabea Stephan, Yuka Obayashi and Nina Maeshima, thank you for making the lab a fun, learning and mentoring environment. Your assistance with islet isolations, weekend experiments and support during both scientific successes and failures is greatly appreciated. You have taught me the value of work-life balance and the importance of Friday Starbucks.

I would also like to thank the members of the Verchere, Lynn, Luciani, Gibson, Kieffer and Johnson labs for providing reagents, equipment and expertise throughout my degree. A special thank you to my strong, female scientists and role models, Nicole Krentz, Sigrid Alvarez, Alexis Shih, Helen Chen, Sumin Jo, Michal Aharoni-Simon, Dominika Nackiewicz, Heather Denroche and Søs Skovsø. It has been a pleasure learning from each of you.

Finally, I am forever grateful to my family and friends for their support and encouragement throughout my graduate education, and especially during the writing of this dissertation. Mom and Dad, thank you for providing me with financial support and the confidence to pursue a PhD. Last, thank you Darren Kimura for your patience while I completed my second degree, and for being the most supportive in every way possible. You're nothing but the best.

To my parents & Darren Kimura
for your endless love and support

Chapter 1: Introduction

1.1 Exocrine and endocrine pancreatic functions and diseases

The pancreas is composed of exocrine and endocrine cells specialized for enzymatic digestion and glucose regulation, respectively [1]. The majority of the pancreas consists of exocrine tissue, including the acinar and duct cells, with a small proportion of endocrine cells that cluster into the islets of Langerhans [2,3]. Acinar cells secrete digestive enzymes (i.e. amylase, lipases, nucleases and proteases) and duct cells secrete bicarbonate into the pancreatic ductal network, duodenum and small intestine where proteins, carbohydrates and fat are digested [3]. There are five types of endocrine cells, including insulin-secreting β-cells, glucagon-secreting α-cells, somatostatin-secreting δ-cells, ghrelin-secreting ε-cells and pancreatic polypeptide-secreting γ-cells [2,4]. In response to various stimuli (e.g. hyperglycemia or hypoglycemia), pancreatic endocrine cells secrete hormones into the islet vasculature and systemic circulation where they regulate blood glucose levels. Genetic or environmental factors that cause dysregulation of either endocrine or exocrine pancreas function can lead to diseases such as pancreatitis, pancreatic cancer, and most commonly, diabetes mellitus. Diabetes mellitus is a chronic metabolic disease of the endocrine pancreas characterized by hyperglycemia resulting from insulin insufficiency or resistance, and currently affects 3.5 million Canadians and 425 million people worldwide [5,6].

1.2 Diabetes mellitus

The first documented reports of diabetes symptoms, including polydipsia, polyuria and body wasting, were found in ancient Egyptian civilizations [7], but the term “diabetes” – meaning “to pass through” – was established in the 2nd century by the Greco-Roman physician Aretaeus

of Cappadocia [8]. Much later, English physician Thomas Willis noted that the urine and blood of diabetic patients were "sweet" tasting and added the term "mellitus" in the 17th century. In 1776, English physician Matthew Dobson confirmed that the cause of the sweet taste was sugar, and in 1815 French chemist Michael Chevreal identified the sugar as glucose [7]. In the mid-19th century, French physiologist Claude Bernard examined the liver of dogs fed either carbohydrate- or protein-rich diets and discovered that the liver stored glucose in the form of glycogen. Based on these observations, Bernard hypothesized that secretions from the liver caused diabetes [8].

In 1869, German pathologist Paul Langerhans described the microscopic anatomy of the pancreas, including clusters of pancreatic "islands" of unknown function that were later named the islets of Langerhans [7]. At the University of Strasbourg in 1889, Oskar Minkowski and Joseph von Mering performed pancreatectomies on dogs and noted that this caused symptoms of diabetes. These experiments demonstrated for the first time that the pancreas regulated glucose homeostasis [8]. In 1921, further groundbreaking experiments were performed by Frederick Banting and Charles Best in John McLeod's laboratory at the University of Toronto. Pancreatic duct ligation caused atrophy of the exocrine pancreas in dogs and allowed isolation of a "concentrated internal secretion" – later termed "insulin" – from the remaining islets of Langerhans [9]. This crude insulin extract was purified with assistance by James Collip and injected into pancreatectomized dogs and diabetic patients to reverse hyperglycemia [9,10]. In 1923, the Nobel Prize was awarded to Banting and McLeod for the discovery of insulin. This Canadian discovery provided the first evidence that secreted insulin from pancreatic islets of Langerhans regulates glucose homeostasis and was instrumental for diabetes management and patient survival.

1.2.1 The major types of diabetes and health complications

Diabetes mellitus is characterized by hyperglycemia that develops as a result of insufficient insulin secretion and/or utilization [11]. There are two main types of diabetes: autoimmune type 1 diabetes (T1D) and type 2 diabetes (T2D). T1D is defined as a disease of insulin deficiency and accounts for ~5-10% of all diabetes cases [12]. T2D is the most common form of diabetes and is estimated to account for ~90% of all cases [13]. This type of diabetes is characterized by β-cell dysfunction and insulin resistance at target tissues, with reduced insulin secretion and β-cell death as the disease progresses [11]. While both types of diabetes are associated with genetic and environmental risk factors [11], the precise cause of diabetes is currently unknown.

The long-term health risks of diabetes are a primary result of uncontrolled hyperglycemia and include atherosclerosis, nephropathies, neuropathies and retinopathies. Diabetes is a leading cause of heart disease, stroke, blindness, renal failure and foot amputations, and is estimated to reduce life expectancy by 5-10 years [5,14]. The World Health Organization recognizes that diabetes and associated complications are a significant cause of death and disability [15] and treatment of complications related to diabetes is a huge economic burden for many countries [5,16]. Strict management of blood pressure and glucose levels can prevent or delay many of the complications, and this is becoming more attainable with the development of more sophisticated technology such as closed-loop continuous glucose monitoring and insulin infusion systems (i.e. an artificial pancreas). Despite our education, awareness, and technological and scientific advances, diabetes remains a global health problem that is increasing in prevalence each year, and the International Diabetes Federation predicts the number of people living with diabetes will be 629 million by 2045 [5].

1.2.2 Diabetes management by insulin and drug therapy

Hyperglycemia in T1D is managed with regular injections of exogenous insulin and continuous blood glucose measurements to adjust insulin dosage [12]. As a result of the pioneering work by Banting and Best [9,10], recombinant human insulin preparations are available for lifelong blood glucose management. The most effective treatment for T2D is prevention of obesity through diet and exercise [17]. In addition to lifestyle changes, treatment for T2D includes drugs that inhibit gluconeogenesis, promote the incretin effect, reduce insulin resistance, inhibit glucose excursions or reabsorption and others that promote insulin secretion. The gold standard for T2D treatment is metformin, either as a monotherapy or in combination with other oral glucose- or lipid-lowering agents [5]. However, some patients require exogenous insulin in addition to metformin to maintain glucose homeostasis as T2D progresses.

1.2.3 Human islet transplants for diabetes treatment

Treatment of diabetes with exogenous insulin (T1D) or pharmaceuticals (T2D) certainly aid in lowering blood glucose levels, but these therapies rely on patient input, glucose monitoring and do not prevent the progressive complications that result from hyperglycemia. A therapy that achieves an improved level of glucose control is the transplantation of human islets via the Edmonton protocol [18,19]. Purified islets from cadaveric donors are transplanted into the portal vein and travel to the liver where they secrete insulin in response to glucose fluctuations in a regulated manner. This treatment is currently reserved for the most brittle type 1 diabetics as islet cells are limited, and patients still require immunosuppressive therapy to prevent autoimmunity and alloimmune graft rejection [20]. Although islet transplantation is an initially effective treatment, current success rates and insulin independence are reduced to ~50% at 5 years post-transplant [21]. As a result, research to improve islet transplantation is underway, including

development of islet encapsulation devices that prevent immune cell infiltration and the bioengineering of pseudoislets from donor tissue [22].

1.2.4 Proliferation, transdifferentiation and stem cell-based β-cell therapies

To address the shortfall in donor-derived tissue for islet transplantation, research efforts are focused on generating β-cell replacements by i) stimulation of endogenous β-cell proliferation, ii) the transdifferentiation of pancreas and other cell types to β-cells, or iii) through directed stem cell differentiation towards β-cells. Overall, the primary objective is to increase the supply of glucose-responsive insulin secreting β-cells using either *in vitro* or *in vivo* approaches.

One potential method for diabetes therapy is the stimulation of *in vivo* pancreatic β-cell proliferation. The majority of β-cell proliferation occurs during early post-natal development and declines into adulthood [23]; however, there is evidence that β-cell proliferation also occurs during pregnancy, tissue injury and weight gain [24]. Understanding how β-cells replicate in these situations and why proliferation is reduced in adult β-cells has provided insight into how β-cell regeneration could occur. To date, a myriad of pancreatic β-cell mitogenic factors have been identified in rodents [24,25]. These include aminopyrazines [26], protease inhibitors [27], WNT signaling molecules [28], glucose alone [29] or in combination with fatty acids [30], insulin signaling proteins [31-33] and many others [25]. Mechanistically, these approaches promote β-cell proliferation by activation of downstream cell cycle proteins such as Cyclin D1, Cyclin D2 and CENP-A [31-33]. Unfortunately, these promising targets are less effective in stimulating human β-cell proliferation [24,25], arguing against their utility as a human β-cell therapy.

Another potential method to increase the supply of β-cells is the *in vitro* or *in vivo* transdifferentiation of other cells in the pancreas to β-cells. Evidence of cell transdifferentiation

has mostly been observed under extreme conditions, such as in tissue injury models or forced expression of transcription factors [34]. Additionally, transdifferentiation is more likely to occur if the cells are developmentally related and possess similar epigenetic landscapes [35]. Therefore, in order to transdifferentiate cells to β-cells, it is important to examine cellular plasticity in the pancreas and understand how β-cells are generated and maintained. In mouse models of pancreas injury, there is support for transdifferentiation from α-cells to β-cells, and duct cells to β-cells [36-38], suggesting transdifferentiation to some extent can occur in this artificial environment. Recent evidence demonstrates that α-cell to β-cell transdifferentiation also normally occurs at the islet periphery of healthy mouse islets [39]. Additionally, overexpression of the transcription factor MAFA is sufficient to induce insulin expression in non-β-cell lines, but insulin induction is improved when combined with PDX1 and NEUROD1 [40]. Similarly, the forced expression of a combination of three transcription factors, NEUROG3, PDX1 and MAFA, converts acinar cells to β-like cells *in vitro* and *in vivo* [41,42]. Overall, these examples are evidence that transdifferentiation is possible; however, the forced expression methods do not completely convert non-β-cells to β-cells and significant safety barriers limit the application of tissue injury models to generate new human β-cells.

Another approach to generate cells for islet cell therapy is the *in vitro* directed differentiation of human embryonic stem cells (hESCs) or induced pluripotent stem cells (iPSCs) towards a pancreatic β-cell fate. Protocols for differentiation of stem cells towards pancreatic β-cells use soluble signaling molecules at specific concentrations and are designed to mimic the stages of β-cell development. Although establishment of definitive endoderm, pancreas endoderm [43,44], endocrine progenitors [45] and glucagon-secreting α-cells [46] are relatively efficient,

current *in vitro* differentiation protocols towards pancreatic β-cells have not efficiently generated cells that match the insulin secretory dynamics of primary β-cells [47-50]. The resulting β-like cells are often more phenotypically similar to neonatal β-cells which directly reflects our lack of understanding of β-cell maturation [50]. However, functional maturation of stem cell-derived pancreas progenitors can occur when transplanted into mice and reverse pre-existing diabetes [45,51]. This indicates that *in vitro*-derived pancreas cells have the potential to differentiate towards mature, glucose-responsive insulin-secreting β-cells, and several groups are actively researching stem cell-based β-cell therapies [47,48,50,52-54]. Regardless, the current advances in stem cell differentiation protocols and immunoprotective cell encapsulation devices are promising solutions for β-cell therapies and several clinical trials are underway to assess their safety and efficacy.

1.3 Pancreas development

The pancreas is derived from multipotent progenitor cells (MPCs) within the endoderm that give rise to the three lineages of the pancreas – acinar, ductal and endocrine cells [55]. Development of pancreas MPCs involves external signaling pathways that mediate cell autonomous gene expression changes that guide cell specification, lineage commitment, differentiation and maturation [3,4]. A subset of lineage-specific transcription factors that control gene expression programs largely define the pancreas cell types throughout development [3,56]. Overall, a balance of cell proliferation, differentiation and apoptosis drives patterning and morphogenesis into the fully functional organ [2,4]. Pancreas development is discussed below in four sections: 1) patterning from the endoderm and initial pancreas budding; 2) commitment to

the pancreas lineage, branching morphogenesis and MPC expansion; 3) MPC specification and differentiation; and 4) pancreas cell maturation.

1.3.1 Early pancreas specification and budding from the endoderm

Specification of the mouse pancreas begins with dorsoventral patterning in the posterior foregut endoderm [2]. Patterning is guided by external signaling from the surrounding mesenchyme (e.g. fibroblast growth factor 4 (FGF4) and retinoic acid (RA)) [2,57,58], the aortic endothelium (e.g. VEGFs) [2] and the notochord (e.g. activin-βB and FGF2) [1,59-61]. These factors converge to inhibit BMP, SHH and WNT signaling in a region designated for pancreas budding and drive the expression of critical transcription factors, including FOXA1, FOXA2, GATA4, GATA6 and ONECUT1, that induce expression of *Pdx1* at E8.5 [1,3,4,61-68]. PDX1 is central to pancreas development and pancreas agenesis occurs in its absence [69,70]. The pancreas is first evident as two $PDX1^+$ epithelial buds evaginating from the gut tube and surrounded by mesenchymal cells at E9 (dorsal bud) and E9.5 (ventral bud) [1,3,4,62].

1.3.2 The primary transition and growth of pancreas progenitors

Early studies by Pictet and Rutter describe a biphasic model of pancreas development where a primary transition and "proto-differentiated" state are followed by a secondary transition and a "differentiated" state [71]. During the primary transition from E9-E12.5 [2], the unpolarized $PDX1^+$ pancreatic buds undergo dramatic proliferation, stratification and branching morphogenesis, and the "first wave" of endocrine cells appear. The pancreatic buds contain MPCs that are defined by their ability to generate all pancreas lineages and by the expression of *Cpa1, Nkx2-2, Nkx6-1, Pdx1* and *Sox9* (Figure 1) [2,4,55]. The number of MPCs that form during the primary transition determines the eventual size of the mature pancreas [72].

Maintenance of pancreas MPCs in the proto-differentiated state is controlled by many transcription factors and extrinsic signals that promote growth and prevent differentiation. In particular, HNF1β, PDX1, PTF1A and SOX9 are necessary for progenitor proliferation [3]. Together, these transcription factors sustain growth of the pancreas, and deletion of any of these factors reduces progenitor proliferation and causes pancreas hypoplasia [69,73-75]. Although the primary transition is described as the period of pancreas growth, there is a "first wave" of mostly glucagon$^+$ endocrine cells that are present starting at E9. These "first wave" endocrine cells arise from induction of the pro-endocrine factor *Neurog3*, but do not contribute to the final endocrine compartment [2,76].

Expansion of MPCs is mostly driven by FGF and WNT signaling from the mesenchyme. For example, expression of FGF10 promotes SOX9, PDX1 and PTF1A expression and maintenance of progenitors in the undifferentiated state [77,78]. Secreted FGF10 promotes Notch signaling in the pancreas epithelium through expression of RBPJ and HES1, and this drives progenitor proliferation and represses differentiation of acinar and endocrine cells [2,78-81]. Pancreas progenitor proliferation is also driven by WNT/β-catenin signaling [82,83]. When the mesenchymal gene *Pygo2* is disrupted in mice or the mesenchyme is removed altogether, pancreas progenitor cells fail to proliferate due to disrupted WNT signaling [84]. Additionally, although disruption of β-catenin in PDX1$^+$ cells does not impair pancreas bud formation, progenitor proliferation was significantly reduced in E11.5 embryos and led to a smaller pancreas at birth [85].

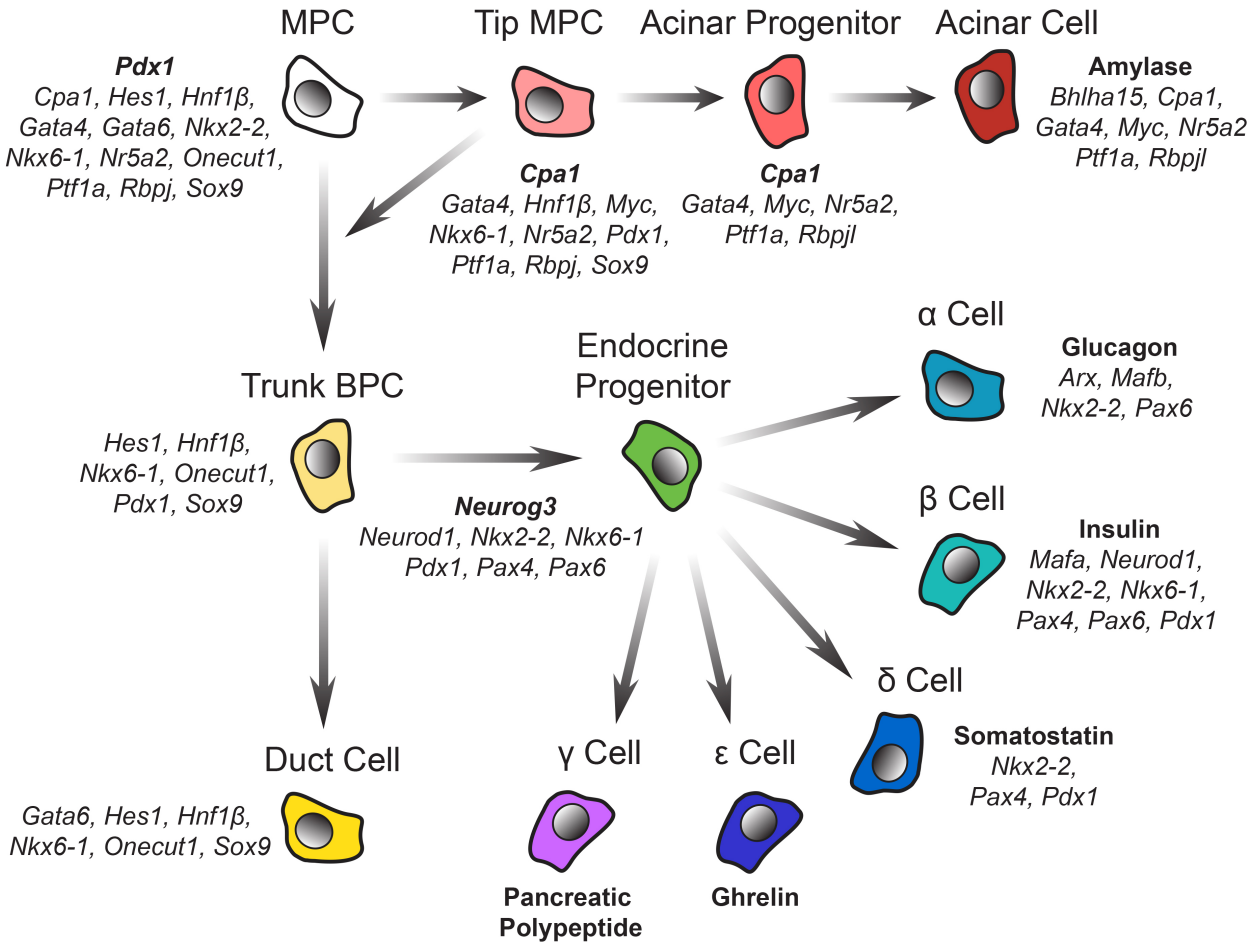

Figure 1: Overview of pancreas progenitor development into acinar, duct and endocrine cells.
Pancreas multipotent progenitor cells (MPCs) are patterned into tip MPCs and trunk bipotent progenitor cells (BPCs) before acinar, duct and endocrine cell specification. NEUROG3^{+} endocrine progenitors differentiate into either α-, β-, δ-, ε- or γ-cells. Genes expressed in each cell type are italicized. Critical transcription factors, digestive enzymes or hormones are bolded.

At E11.5, the multilayered pancreas epithelium acquires apical-basal cell polarity and apical constriction initiates microlumen and rosette formation [3]. Remodeling and fusion of microlumina results in the appearance of a branched tubular network or "plexus" [1,86]. The basal cell surfaces are in contact with the surrounding mesenchyme via a basal lamina, whereas the apical cell surfaces form a ductal lumen. This polarity is maintained throughout cell division and branching morphogenesis [2,71]. At the end of the primary transition, the resulting "proto-differentiated" pancreas epithelium is polarized, resembles an organized tree structure supported

by surrounding mesenchymal cells and contains low levels of exocrine and endocrine proteins [2,71].

1.3.3 The secondary transition and pancreas progenitor differentiation

Between E12.5 and E15.5, the "proto-differentiated" pancreas undergoes tip-trunk progenitor segregation and differentiation throughout the secondary transition [3,56,61]. During this phase, digestive enzymes and endocrine hormones start to accumulate as MPCs specify into acinar, duct and endocrine cells [1,3,55,56]. Pancreas cell differentiation is controlled by organization of the epithelial "plexus" into specific niche environments that respond to local feedback signals [87]. During this stage, the multi-layered pancreas epithelium is remodeled into monolayer branches with a single lumen [88]. Beginning at E11.5, Notch signaling progressively divides the pancreas epithelium into MPCs at branch "tips" and bipotent progenitor cells (BPCs) within branch "trunks" (Figure 1) [2,3,55,89]. The tip cells are found at the ends of the $PDX1^{+}SOX9^{+}$ epithelial branches and are demarcated by their expression of CPA1 [55,90]. The remaining $PDX1^{+}SOX9^{+}$ cells in the pancreas epithelium directly adjacent to the tip cells constitute the trunk BPCs which express HES1 and NKX6-1, and only give rise to duct or endocrine cells [3]. Growth of the pancreas at this stage is mostly driven by proliferation of MPCs at the tips [88], which divide and contribute to the BPC pool or undergo acinar cell specification [3,55,56]. Tip MPC specification into acinar progenitors also restricts SOX9 expression to trunk cells by E14 [3,56,91,92]. The tip vs. trunk domains are patterned by Notch signaling and the antagonistic transcription factors NKX6-1 and PTF1A which promote endocrine or acinar cell differentiation, respectively [93,94]. As MPCs and BPCs specify to the duct, endocrine or acinar cell lineages, proliferation slows until the progenitor pool is depleted.

1.3.3.1 Duct and endocrine cell specification

Notch signaling maintains SOX9^{+} trunk BPCs [81,95] and regulates maintenance of *Sox9* expression in the ducts [89]. Many of the genes expressed in early pancreas progenitors persist in BPCs and duct cells, including *Hnf1β, Onecut1* and *Sox9*, and are required for duct cell development [96-98]. To date, a pro-duct cell specifier remains unidentified, leading to the hypothesis that duct cells are the default differentiation state [2]. Although SOX9 is required for the specification of acinar, duct and endocrine cells [73,97], failed downregulation of SOX9 expression in NEUROG3^{+} endocrine progenitors maintains a BPC or duct cell fate [89].

Endocrine cell specification commences with the transient, high level expression of NEUROG3 in a subset of trunk BPCs (Figure 1) and subsequent exit from the cell cycle driven by CDKN1A upregulation [4,99,100]. The importance of *Neurog3* to endocrine cell development is highlighted in studies that show a complete absence of endocrine cells after loss of *Neurog3* [100,101]. *Neurog3* expression is controlled by several transcription factors including NKX6-1, PDX1 and SOX9 [97,102-105]. *Neurog3* expression begins at E9 during the primary transition, but these early endocrine progenitors only contribute to the "first wave" of endocrine cells [100]. During the secondary transition, the number of NEUROG3^{+} cells peaks at E15.5 and drives differentiation of the "second wave" of endocrine cells [100].

Specification of BPCs into endocrine cells depends on several feedback mechanisms, including Notch signaling, lateral inhibition and cell cycle control. Lower levels of Notch signaling decreases *Hes1* expression in SOX9^{+} cells and promotes *Neurog3* induction by SOX9 [89,97,104]. Low level *Neurog3* gene expression is associated with a subset of mitotic BPCs (termed NEUROG3^{LO}) that are not committed to endocrine cell fate [106-109]. NEUROG3^{+} cells activate Notch signaling and *Hes1* expression in adjacent cells which prevents further *Neurog3* induction

through lateral inhibition [56,110]. High level *Neurog3* gene expression and robust protein levels (NEUROG3^{HI} cells) in turn decreases *Sox9* and duct lineage commitment, and reinforces NEUROG3 stability and endocrine lineage commitment [106,107,110,111].

Once high level activation of *Neurog3* is achieved in select trunk cells, NEUROG3 is rapidly degraded as endocrine progenitors commit to a single islet cell type, delaminate from the trunk epithelium and organize with other committed endocrine cells into epithelial cords [2,56,112]. A cascade of pro-endocrine transcription factors are induced downstream of *Neurog3* activation and drive endocrine cell differentiation (Figure 1) [3,56]. *Neurod1* and *Pax6* are some of the first factors activated and are involved in the general development of all endocrine cell types [56,113,114]. Additional factors control the relative proportions of differentiated islet cells, including *Nkx2-2, Nkx6-1,* and *Pdx1* [3,115-117]. Differentiation of insulin$^+$ β-cells requires NEUROD1, NKX2-2, PAX4 and high level PDX1 expression [3,118,119]. Endocrine cells coalesce to form non-polar proto-islet structures [3,71] which expand in size by further recruitment of *de novo* endocrine cells from the trunk [2,120].

1.3.3.2 Acinar cell specification

Signals from the mesenchyme during the secondary transition promote acinar cell fate rather than endocrine commitment. For example, secreted FGF7 favours acinar cell specification and inhibits specification of NEUROG3$^+$ endocrine cells [80,121]. Acinar cell differentiation is also driven by suppression of Notch signaling [95,122], inhibition of TGFβ and activation of WNT/β-catenin signaling [3,123,124]. In the absence of WNT/β-catenin signaling, the pancreas is hypoplastic [85,124] due to reduced proliferation of PTF1A$^+$ tip MPC/acinar cells [3,95,124]. Furthermore, loss of β-catenin in developing PDX1$^+$ cells specifically impairs acinar cell specification [85,124].

Between E12.5 and E14, PTF1A^{+}CPA1^{+} tip MPCs undergo specification to acinar progenitors, a process that is marked by an increase in CPA1 levels and a decrease in SOX9 expression [1,56]. During acinar cell specification, the PTF1A-RBPJ complex represses *Nkx6.1* and is followed by the exchange of RBPJ for RBPJL which facilitates acinar cell differentiation [3,56,125,126]. The PFT1A-RBPJL complex drives further acinar cell differentiation by promoting expression of *Bhlha15*, *Ptf1a*, *Nr5a2* and *Rbpjl*, which activate expression of acinar cell digestive enzymes [90,94,125,127,128]. Differentiated acinar cells are defined by their restricted expression of transcription factors, such as BHLHA15, PTF1A, NR5A2 and RBPJL [3,90,128,129], and expression of ~25 different digestive enzymes, including amylase, carboxypeptidases, chymotrypsin, elastases, lipases and trypsin [2].

1.3.4 Maturation of the pancreas lineages

At the end of the secondary transition, differentiated acinar, duct and endocrine cells continue to terminally differentiate and mature from E15.5 onward into postnatal development [2]. The differentiated endocrine cords and trunk cells separate as acinar tissue expands and the cords undergo fission and mature into spherical islet structures composed of a β-cell core surrounded by a mantle of α-, δ-, ε- and γ-cells [2,56]. During this period, proliferation expands the acinar and endocrine cell compartments and terminal differentiation creates a mature and functional pancreas organ capable of regulating secretion of digestive enzymes and endocrine hormones in response to glucose.

Following differentiation, exocrine and endocrine pancreas cells mature at different rates in the period from E15.5 until weeks after birth. Although maturation of each pancreas lineage is progressive, endocrine cells do not fully mature into functional islets until after weaning [61,130]. Maturation of endocrine islet cells is completed postnatally when functional glucose sensing

machinery enables cells to respond to glucose by secreting hormones in a regulated fashion. At birth, immature β-cells have high basal insulin secretion and proper glucose-stimulated insulin secretion is not acquired until several weeks later [50,130]. The transition from immature to mature β-cells involves expression of functional glucose-sensing transporters (e.g. SLC2A2), glucose-processing enzymes (e.g. expression of low-affinity GCK and silencing of high-affinity HK), proteins involved in insulin secretion (e.g. K_{ATP} and Ca^{2+} channels) and several metabolic changes to promote oxidative phosphorylation, including downregulation of LDHA, MCT1, PDGFRα and REST [50,130].

The terminal differentiation and maturation of islet cells is controlled by many transcription factors. In particular, MAFA and MAFB have important roles in the regulation of mouse β-cell and α-cell maturation, respectively [56]. In mature β-cells, high expression of PDX1 activates *Gck, Glut2*, *Ins1* and *Iapp* and is required for glucose-stimulated insulin secretion [115,131,132]. NKX6-1 is also highly expressed in mature β-cells and is required for maintenance of mature β-cell identity and glucose-stimulated insulin secretion [133].

By E16.5, mature pyramidal acinar cells contain zymogen granules and are organized into clusters of acini [134]. As acinar cells proliferate and mature during embryonic and postnatal development, expression of digestive enzymes is significantly enhanced and the cytoplasm of acinar cells expand to accommodate the increased production [2,56,71]. The mature acinar cell phenotype is established and maintained by expression of *Bhlha15, Gata4, Ptf1a, Rbpjl* and *Nr5a2*, which regulate transcription of digestive enzymes and control acinar cell proliferation and differentiation [3,56,135].

1.3.5 Mouse vs. human pancreas development

Most of the mouse pancreas developmental pathways and lineage determinants are evolutionarily conserved in humans, with some species-specific differences in overall pancreas morphology and transcription factor expression [25]. During human pancreas specification, expression of the transcription factor *PDX1* and budding occur at a slightly later stage compared to mouse development [25,136]. Interestingly, the human embryonic pancreas develops from the endoderm as one dorsal and two ventral buds [25]. During the primary transition, human MPCs co-express PDX1 and CK19 [25,137], a marker normally observed in mature mouse duct cells, and lack expression of NKX2-2 until endocrine specification is induced [138]. In contrast to mouse endocrine cell development, NEUROG3 is not expressed during the primary transition (i.e. there are no "first wave" endocrine cells), but is transiently expressed during the secondary transition [2,3,25]. Additionally, insulin$^+$ β-cells appear before glucagon$^+$ α-cells in humans [2,3,25]. The proportion of bihormonal insulin$^+$glucagon$^+$ endocrine cells is also higher in the human embryonic pancreas, a phenomenon also observed in hESC-derived endocrine cell protocols [46,51,139]. Finally, the transcription factor MAFB has restricted expression in mature mouse α-cells, but is expressed in both α- and β-cells in humans [140].

Islet architecture is perhaps the most striking difference between species. Rodent islets have a large proportion of β-cells that occupy the mature islet core and are surrounded by α-cells and other endocrine cells in the mantle. It is estimated that murine islets contain 60-80% insulin$^+$ β-cells, 15-20% glucagon$^+$ α-cells, 5-10% somatostatin$^+$ δ-cells, and <2% are pancreatic polypeptide$^+$ γ-cells or ghrelin$^+$ ε-cells [4,141]. In humans, early fetal islets resemble rodent islet architecture, but eventually α-cells become higher in proportion and both α- and β-cells are

interspersed throughout the late fetal and mature human islets [3]. In humans, islets contain 50-70% β-cells and 20-40% α-cells, with δ-cells and γ-cells comprising <10% of the islet [141].

1.4 The regulation of transcription by chromatin

A unifying concept in both mouse and human pancreas development is the underlying chromatin which mediates progenitor cell lineage decisions and transcription factor expression. Genetic and epigenetic information is organized into chromatin – a macromolecular complex of DNA, protein and RNA in which regions of DNA are wound around histone proteins to form nucleosomes and then packaged into higher-order structures. Non-coding RNAs (ncRNAs) can function as scaffolds to create looped chromatin domains [142] and are involved in gene-specific recruitment of chromatin-modifying complexes [143,144]. Chromatin is classified as euchromatin or heterochromatin, based on post-translational DNA or histone modifications and transcriptional activity or lack thereof [145-147]. Transcription is regulated by *cis*-regulatory DNA elements within non-coding regions of the genome, such as promoters and enhancers [148]. The structure of chromatin, including nucleosome placement, histone variants, post-translational modifications and higher-order chromatin domains, controls DNA accessibility and gene expression by creating a permissive or obstructive environment for recruitment of proteins to *cis*-regulatory loci [149]. These include general and lineage-specific transcription factors, enzyme complexes that modify DNA or histones and remodel nucleosomes, RNA polymerase II (Pol II) and its co-factor proteins (e.g. the Mediator complex), as well as ncRNAs [150,151].

Nucleosome remodeling complexes displace, reposition or remodel nucleosomes which can promote or inhibit transcription factor binding to *cis*-regulatory loci [152]. DNA methylation catalyzed by DNA methyltransferases (DNMTs) promotes tightly wrapped DNA around

nucleosomes which makes *cis*-regulatory regions less accessible [153]. Histones are chemically modified by chromatin-modifying complexes that establish a "histone code" which includes acetylation, methylation and others [154]. Histone acetylation is catalyzed by histone acetyltransferases (HATs) which are recruited to transcriptional start sites in concert with Pol II where transcription factors are bound [146,155]. The reversal of histone acetylation is accomplished by histone deacetylases (HDACs) and promotes chromatin compaction and transcriptional repression [146]. Different histone methylation marks are associated with active versus repressed chromatin and are controlled by opposing protein complexes [156]. For example, the Trithorax Group (TrxG) complexes are involved in deposition of histone 3 (H3) lysine 4 (K4) methylation that is associated with active chromatin [157]. In contrast, the Polycomb Group (PcG) complexes are involved in deposition of H3K27 methylation that is associated with repressed chromatin [158]. Erasure of histone lysine methylation is accomplished by a family of lysine demethylases (KDMs) that remove mono- (me1), di- (me2) and trimethylation (me3) of H3K4, K9, K27 and K36 [146,159,160].

Transcription factors bind to DNA-recognition sequences within *cis*-regulatory elements and elicit either an activating or repressive response through further co-factor recruitment [151,161]. Through chromatin looping by the Mediator complex and Cohesin, distant enhancers bound by transcription factors are brought in contact with the transcriptional machinery at target gene promoters and transcription is initiated [162,163]. Transcription factor density at *cis*-regulatory elements regulates transcriptional output, whereby higher levels of transcription factors recruit additional co-activators and Pol II to increase mRNA levels [164]. This results in gene expression that varies from ubiquitous to cell-type specific, constitutive or regulated, across a broad range of expression levels [161].

1.4.1 DNA methylation and histone modifications define chromatin state

Chromatin immunoprecipitation (ChIP) experiments have determined that *cis*-regulatory loci exist in several different chromatin "states" demarcated by specific distributions of DNA or histone modifications, including active, poised, inactive, bivalent and facultatively or constitutively repressed (Figure 2). Several post-translational histone modifications are associated with specific *cis*-regulatory sites in active chromatin (Figure 2A). These include acetylation of H3 at K4, K9, K14 and K27, acetylation of H4 at K5 and methylation of H3 at K4, K36 and K79 [145,146,165]. In particular, the promoters and enhancers of actively transcribed genes contain high levels of H3K4 methylation and H3K27 acetylation and are devoid of H3K27me3 [151,156,162,166-168]. H3K4 can be mono-, di- or tri-methylated and the distribution of H3K4 methylation is distinct at different *cis*-regulatory elements [156,169,170]. For example, active enhancer regions are enriched for H3K4me1 [162,171,172], whereas active promoter regions are enriched for H3K4me3 [166,173].

Relative to active *cis*-regulatory elements, poised promoters are identified by low level H3K4me3 [166,172] and poised enhancers are identified by low level H3K4me1, but both in the absence of H3K27 acetylation (Figure 2B) [162,170,174,175]. Thus, poised promoters and enhancers have not yet been activated by H3K27 acetylation, Pol II is absent and are transcriptionally inactive [170]. Inactive chromatin is defined by a relative absence of DNA or histone modifications (Figure 2C). Bivalent *cis*-regulatory regions contain high level H3K27me3 in addition to low level H3K4 methylation (Figure 2D), and are highly associated with developmentally regulated transcription factors [148,156,176]. Transcriptional repression can be facultative or constitutive, with facultative heterochromatin characterized by H3K27me3 (Figure 2E) and constitutive heterochromatin by H3K9me3 and DNA methylation (Figure 2F) [146,151,177,178].

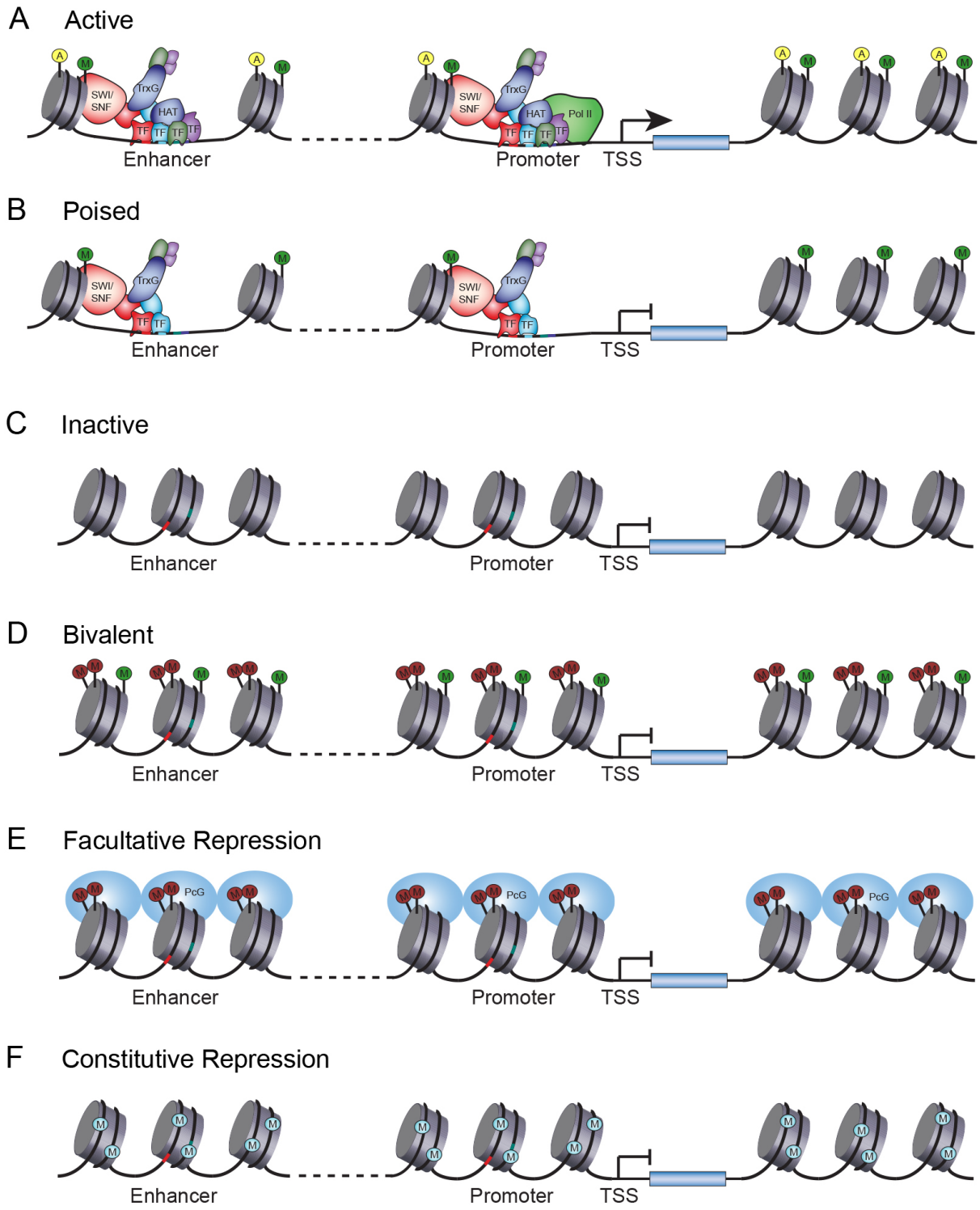

Figure 2: Chromatin state is determined by DNA and histone modifications.
DNA and histone modifications associated with chromatin in an **(A)** active; **(B)** poised; **(C)** inactive; **(D)** bivalent; **(E)** facultatively repressed; or **(F)** constitutively repressed state. Chromatin modifiers include histone acetyltransferases (HATs), nucleosome remodelers (e.g. SWI/SNF) and histone methyltransferases (PcG and TrxG). Pol II, RNA polymerase II; TSS, transcription start site; TF, transcription factor; yellow A, histone acetylation; green M, H3K4 methylation; red M, H3K27me3; blue M, DNA methylation.

The conversion of poised, inactive, bivalent or repressed chromatin to an active state requires nucleosome remodeling, transcription factor binding and recruitment of chromatin regulators and Pol II [162]. Transcriptional maintenance requires the coordinated activity of the same proteins that are involved in the establishment of active chromatin [179]. Conversion of poised to active chromatin is facilitated by recruitment of transcriptional co-activators including transcription factors, HATs and other chromatin regulators which mediate recruitment of Pol II and its co-factor proteins to initiate transcription [149,151]. At inactive chromatin, pioneer transcription factors bind and destabilize DNA-histone interactions through recruitment of nucleosome remodelers, HATs and additional co-activators such as general and lineage-specific transcription factors which bind to exposed DNA binding sites [180,181]. In response to developmental signals, bivalent chromatin is activated by increased and/or broader H3K4 methylation by TrxG complexes [148,159]. Additionally, KDMs remove H3K27me3 at bivalent and facultatively repressed chromatin [159]. Removal of DNA methylation associated with constitutive heterochromatin is facilitated by the TET family of demethylases [153].

1.5 The Trithorax Group complexes and H3K4 methylation

In mammals, the majority of H3K4 methylation is catalyzed by the six TrxG complexes [182]. The TrxG complex proteins were discovered in *Drosophila* as important developmental regulators of *Hox* gene clusters together with the antagonistic PcG complexes [159]. The SET domain responsible for histone lysine methyltransferase activity is well-conserved from yeast to metazoans [159,163,167,172]. In yeast, there is a single Set1 H3K4 methyltransferase, while the *Drosophila* TrxG proteins include Set1, Trithorax-related (Trr) or Trithorax (Trx) [159]. Additional TrxG histone methyltransferase proteins have emerged in metazoans through divergent evolution

– SET1A/B, MLL1/2 and MLL3/4 – and are homologs of the *Drosophila* TrxG proteins Set1, Trx and Trr proteins, respectively [159,183]. In all species, TrxG complexes catalyze H3K4 mono-, di- or trimethylation [172,183-187].

All TrxG complexes contain at minimum the core proteins ASH2L, DPY30, RBBP5 and WDR5 which exist as an independent sub-complex that associates with the SET domain of any of the six H3K4 methyltransferase proteins (Figure 3) [167,182]. Although there are six mammalian TrxG complexes, they do not have completely redundant methyltransferase activity. The majority of bulk H3K4 mono-, di- and trimethylation at active promoters is established by SET1A/B methyltransferases [159,163]. In contrast, the majority of H3K4me1 at enhancers is established by MLL3/4 methyltransferases [159,163,188]. Additionally, MLL2 establishes H3K4me3 specifically at bivalent promoters, whereas MLL1 only catalyzes H3K4me3 at a subset of genes [159,189]. While the core TrxG proteins regulate complex stability and activity, additional co-factor proteins are TrxG complex-specific, alter complex function and contribute to site-specific recruitment through unique transcription factor interactions [172,182]. For example, H3K4 trimethylation is established by the MLL1/2 and SET1A/B complexes when in association with the subunits menin and WDR82, respectively [172]. In addition, MLL3/4 complexes can associate with the KDM6 demethylases to remove repressive H3K27me3 at bivalent domains [183,190].

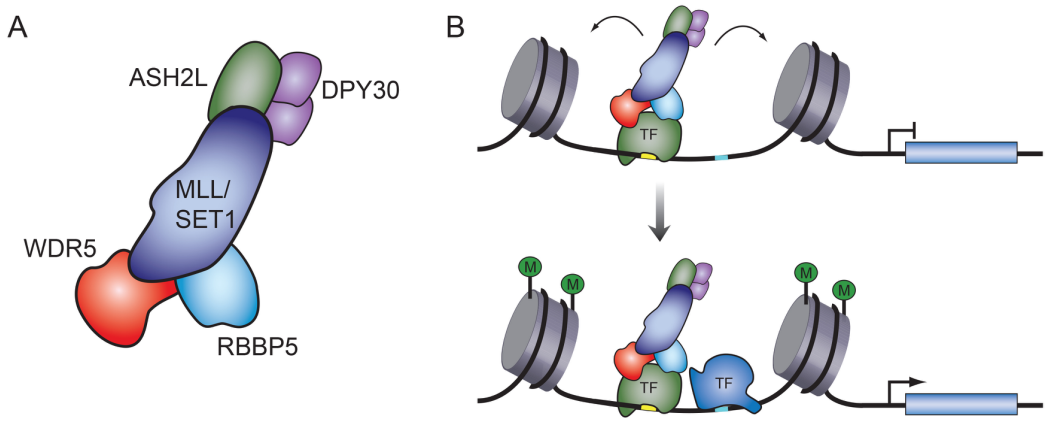

Figure 3: The structure and function of Trithorax Group (TrxG) complexes.
(A) TrxG complexes contain 1 of 6 histone methyltransferases (MLL1-4, SET1A/B) and a minimum of 4 core proteins (ASH2L, DPY30, RBBP5 and WDR5). **(B)** TrxG complexes catalyze H3K4 methylation that is associated with active chromatin. TF, transcription factor.

In addition to histone methyltransferase catalytic activity, TrxG complexes also have enzyme-independent or non-catalytic functions [172,191,192]. Several studies suggest that the non-enzymatic functions of TrxG complex proteins have a larger biological effect than their histone methyltransferase activity. For example, while deletion of the entire *SET1A* gene reduces mESC proliferation and causes apoptosis [191,193], deletion of only the catalytic SET domain from *SET1A* in mESCs does not affect cell proliferation and instead only impairs mESC differentiation due to reduced H3K4 methylation at bivalent genes [191]. In agreement, loss of MLL3 and MLL4 proteins significantly reduces Pol II occupancy and transcription, while disruption of the MLL3 and MLL4 catalytic SET domain in mESCs does not affect self-renewal and has minor effects on transcription [192,194]. TrxG complexes interact either directly or indirectly with other chromatin regulators or transcription machinery and function as non-enzymatic co-activators. For example, the SET1A/B complex component WDR82 interacts with Pol II and the MLL1/2 complexes interact with the Pol II-associated factor PAF1 [182]. MLL3/4 complexes are involved in the recruitment of P300 and enhancer activation [188,195]. Additionally, WDR5 interacts with the

nucleosome remodeling and deacetylase (NuRD) complex and DPY30 interacts with the NuRF complex [196,197]. Overall, these studies demonstrate that TrxG complexes have context-specific co-activator roles in biological processes and enzyme-independent functions that include the recruitment of other proteins.

Although H3K4 methylation is associated with active chromatin, its precise function is unknown [162,198] and several studies have called into question whether it has any role in gene activation or transcriptional maintenance [192,194,199,200]. For example, Dorighi *et. al.* [192] generated catalytically deficient MLL3/4 mutant mESC lines and demonstrated that loss of H3K4me1 has minor effects on transcription. In agreement, gene expression was largely unaffected following disruption of H3K4 methyltransferase activity either by mutation of the *Mll3* and *Mll4* *Drosophila* homolog *Trr* or by deletion of the MLL3/4 catalytic SET domain in mESCs [194]. By creating non-methylatable H3K4 *Drosophila* mutants, Hödl *et. al.* [199] found that gene activation and transcriptional maintenance is unaffected in the absence of H3K4 methylation. Further, Pérez-Lluch *et. al.* [200] examined *Drosophila* and *C. elegans* RNA-seq and ChIP-seq profiles and discovered a relative absence of H3K4 methylation at developmentally activated genes. These reports suggest that H3K4 methylation is not necessary for transcription, and that potentially the TrxG complexes that deposit these histone modifications mediate gene activation. Regardless, H3K4 histone methylation has been proposed to be involved in a) the establishment and/or maintenance of active chromatin; b) high level and/or stable gene expression; c) recruitment of chromatin regulators; and d) prevention of chromatin repression [156,159,162,163,167,182,201,202].

Evidence for H3K4 methylation in the establishment and/or maintenance of active chromatin comes from *in vitro* studies and by disrupting H3K4 methyltransferase activity. For example, gene activation by MLL2 in an *in vitro* system was dependent on catalytic H3K4

methyltransferase activity [203]. In mESCs, catalytically-deficient MLL2 reduced activation of genes required for primordial germ cell specification [204]. Rather than initial gene activation, H3K4 methylation has been linked to the maintenance of expression of a subset of lineage-specific genes in several cell types [205,206]. Further, H3K4me3 may contribute to stable gene expression by recruiting the general transcription factor TFIID and permitting efficient Pol II loading during transcription initiation [172,182,198]. Also, there is a strong correlation between H3 acetylation and H3K4 methylation level with transcriptional activity, suggesting that histone modifications may recruit and/or stabilize Pol II to increase output [145,151,167,207].

H3K4 methylation may also function to recruit chromatin regulators through interactions with proteins that contain H3K4me-recognition domains [162,167]. Support for this hypothesis comes from experiments showing several proteins associated with chromatin regulators can recognize H3K4 methylation marks [162,172]. For example, nucleosome remodelers (e.g. SWI/SNF, NuRF, CHD1), histone acetyltransferases (e.g. ING family proteins), histone deacetylases (e.g. JMJD2A) and histone methyltransferases (e.g. SET1A/B) are recruited directly or indirectly to H3K4 methylation marks [167,172,201]. However, as there are many different proteins that recognize H3K4 methylation, rather than serving as the primary recruitment mechanism, histone methylation most likely provides secondary stabilization of complexes/proteins that were initially recruited by transcription factors or ncRNAs [167]. Finally, an alternate function of H3K4 methylation may be to directly prevent chromatin repression rather than to indirectly assist in chromatin activation. For example, H3K4 methylation protects *cis*-regulatory elements from *de novo* DNA methylation [163] and also disrupts the binding of the NuRD repressive complex [156]. Further, the H3K4me3 modification allosterically inhibits the H3K27me3 repressive activity of PRC2 by association with the histone acetyltransferase CBP [159,202].

1.6 Chromatin regulators in pancreas development

During pancreas development, nucleosome positioning, DNA methylation and histone modifications regulate transcription in order to balance proliferation and differentiation [148,156,176,208-210]. Most of the evidence indicating nucleosome remodelers have an important role during pancreas development comes from mouse studies on the SWI/SNF complex catalytic subunit BRG1. For example, disruption of *Brg1* in PTF1A$^+$ pancreas progenitors causes a significant reduction in exocrine pancreas mass and enlargement of ducts [211]. In addition, PDX1 interacts with BRG1 and other components of the SWI/SNF complex in E12.5 multipotent progenitors and later in development in insulin$^+$ β-cells [212]. These results suggest a role for BRG1 and the SWI/SNF complexes in controlling acinar vs. duct cell fate during pancreas development.

The DNA methyltransferases DNMT1 and DNMT3 also have a role in the development of pancreas cell types. Initial studies of DNMTs in zebrafish demonstrated that acinar cells in *Dnmt1* mutants undergo apoptosis, without affecting endocrine or duct cells [213]. In contrast, disruption of *Dnmt1* in mouse PDX1$^+$ pancreatic progenitors disrupts the correct architecture and differentiation of all three pancreas lineages [214]. Further, the maturation and function of β-cells is regulated by DNMT3A, which is highly expressed in neonatal insulin$^+$ cells and is required for glucose-stimulated insulin secretion [215]. Recent single-cell RNA sequencing of E16.5 NEUROG3$^+$ endocrine progenitors also confirmed that *Dnmt3a* is enriched in this β-cell-biased population [109].

Although histone acetylation is upregulated during differentiation of pancreas progenitors [216], studies of histone acetyltransferases in pancreas development are limited. A recent report demonstrates that disruption of P300 and/or CBP in NEUROG3$^+$ endocrine progenitors

specifically impairs proliferation of α- and β-cells and this leads to glucose intolerance [217]. Further experiments are necessary to understand the role of P300 and/or CBP in the development of pancreas acinar and duct cells.

During pancreas development, the expression of histone deacetylases (HDACs) and histone deacetylation are decreased [216,218], suggesting that inhibition of HDACs may improve differentiation. Interestingly, treatment of developing E13.5 pancreas explants with HDAC inhibitors reduces acinar lineage specification, but increases the number of duct cells and NEUROG3$^+$ endocrine progenitors [218]. Further, HDAC inhibitors increase specification of NEUROG3$^+$ endocrine progenitors towards the α- and PP-cell lineages *in vitro*; however, depending on which inhibitor is used, β- and δ-cell differentiation is either increased or decreased [216,218]. Additionally, treatment of E13.5 rat pancreas explants with an HDAC inhibitor enhances *Pax4, Ins1/2* and *Sst* transcripts [219]. Embryonic disruption of *Hdac5* or *Hdac9* increases insulin$^+$ β-cells, while *Hdac4* and *Hdac5* disruption increases somatostatin$^+$ δ-cells [219]. These experiments suggest a pivotal role for HDACs in mediating endocrine pancreas development.

Several studies provide evidence that PcG proteins have an integral role in pancreas development. In the endoderm, *cis*-regulatory regions of pancreas-specific genes such as *Pdx1* are enriched for the PRC2 component EZH2 and H3K27me3 [35,220]. Several PcG proteins are upregulated as hESCs are directed to the pancreatic lineage *in vitro*, suggesting a regulatory role for repressive histone methylation in defining cell fate decisions [221]. Loss of *Ezh2* from pancreas progenitors increases the number of NEUROG3$^+$ endocrine progenitor cells, as well as insulin$^+$ β-cells [222]. Interestingly, more than half of the H3K27me3 histone modifications in adult β-cells are formed *de novo* during β-cell specification, suggesting the importance of PcG complexes in this process [35]. Consistently, *Ezh2* is enriched in E14.5 endocrine progenitor cells [109]. Complete

endocrine specification from hESCs requires reductions in H3K27me3 at bivalent regulatory genes, implicating KDMs as critical regulators of endocrine cell specification [223]. In support of this hypothesis, the transition from NEUROG3^{LO} to NEUROG3^{HI} endocrine-committed cells involves removal of H3K27me3 by KDM6B [224]. A recent study also suggests that the PRC2-associated subunit JARID2 is also critical for endocrine cell differentiation downstream of NEUROG3^{+} progenitor cell specification [225].

To date, there is very limited research on the role of TrxG complexes or other histone methyltransferases in pancreatic development [176]. However, several studies have suggested that TrxG-driven H3K4 methylation and activation of pancreas-enriched *cis*-regulatory loci is necessary for pancreas and islet development, although this has not been directly tested [180,223,226].

1.7 Thesis Investigation

Given the above, the objective of my thesis was to clarify the catalytic and non-catalytic functions of the TrxG complexes with respect to gene activation and maintenance during pancreas development. While DNA methyltransferases [214], nucleosome remodelers [211], HATs [217], HDACs [216,218,219] and PcG complexes [222,227] have been implicated in pancreas progenitor development, there is a relative absence of research on the TrxG complexes in this context [176]. To address this, I examined the catalytic and non-catalytic roles of the TrxG complexes in gene activation during mouse pancreas and endocrine progenitor differentiation by targeting WDR5 and DPY30 to disrupt either complex assembly or catalytic activity, respectively. Since TrxG complex activity is associated with lineage-specific gene activation and/or maintenance [179,191,205,206], I **hypothesized** that disruption of TrxG complex activity in pancreas and endocrine

progenitor cells would reduce activation and/or maintenance of lineage-specific genes during pancreas cell differentiation.

In Chapter 3, I describe the expression of DPY30 and WDR5 in mouse embryonic pancreas and explore the effect of *Wdr5* suppression and loss of TrxG complex assembly on *in vitro* growth and differentiation of pancreas progenitor spheroids. In Chapter 4, I determine the *in vivo* role of H3K4 methylation in the survival and differentiation of mouse $PDX1^{+}$ pancreas progenitors by embryonic deletion of *Dpy30*. Finally, in Chapter 5, I discuss the *in vivo* function of H3K4 methylation in the differentiation and maturation of mouse $NEUROG3^{+}$ endocrine progenitors into glucose-responsive pancreatic islets.

Chapter 2: Materials & Methods

2.1 Animal husbandry, mouse strains and embryo collection

All mice were housed at the British Columbia Children's Hospital Research (BCCHR) Animal Care Facility (ACF) and ethical procedures were followed according to protocols approved by the University of British Columbia (UBC) Animal Care Committee (ACC). All mice were maintained on a regular chow diet *ad libitum* and housed up to 5 mice per cage on a 12-hour light/dark cycle. Experiments with pancreas progenitor spheres were performed with ICR (CD-1) mice (obtained from Charles River) or Ins1-EGFP (MIP-GFP) mice (obtained from The Jackson Laboratory, Stock No. 006864). Timed matings were used to determine embryonic stages and the morning of vaginal plug discovery was considered embryonic day 0.5 (E0.5).

Two heterozygous *Dpy30*$^{tm1a(KOMP)Wtsi}$ male mice (on a C57BL/6NJ background) were obtained from the International Knockout Mouse Consortium (EMMA ID EM:09575) and bred to *Rosa26*^{FLPe} (FLP deleter) female mice (obtained from The Jackson Laboratory, Stock No. 009086). This removed the *Dpy30* knockout-first cassette (containing a splice acceptor between FRT sites) and generated heterozygous floxed *Dpy30* mice. Progeny were bred to produce floxed *Dpy30* mice that when crossed to Cre driver mice, conditional deletion of *Dpy30* exon 4 in the pancreas or endocrine lineage was attained. Exon 4 is the largest coding exon and its deletion causes a frameshift mutation in every protein-coding transcript and generates a non-functional protein. The Cre driver strains Tg(Pdx1-cre)89.1Dam/Mmucd (*Pdx1*-Cre, on an ICR (CD-1) background) and Tg(Neurog3-cre)C1Able/J (*Neurog3*-Cre) were gifted from Dr. Francis Lynn (University of British Columbia) and originally obtained from the Mutant Mouse Resource and Research Centers (MMRRC, Stock No. 000353-UCD) [120] and The Jackson Laboratory (Stock No. 005667) [228], respectively. *Pdx1*-Cre; *Dpy30*$^{flox/flox}$ knockout mice (*Dpy30ΔP*) were generated

by breeding male *Pdx1*-Cre; *Dpy30*$^{fl/wt}$ transgenic mice to female *Dpy30*$^{fl/fl}$ animals. *Neurog3*-Cre; *Dpy30*$^{flox/flox}$ knockout mice (*Dpy30ΔN*) were generated by breeding either male or female *Neurog3*-Cre; *Dpy30*$^{fl/wt}$ transgenic mice to *Dpy30*$^{fl/fl}$ animals. All knockout mice were compared to littermate controls (*Dpy30*$^{flox/flox}$ and *Dpy30*$^{flox/wt}$). Genotyping primers are listed in Table 1.

At noon on the day of the experimentally determined timepoint (e.g. E14.5), embryos were harvested by hysterectomy, dissected under an Olympus dissecting microscope in ice-cold phosphate buffered saline (PBS) and tail clippings were taken for genotyping. All knockout embryos were stained for DPY30 and/or H3K4 methylation to determine recombination efficiency prior to further analysis. Embryos with insufficient loss of DPY30 or H3K4 methylation (<80%) were not studied.

Table 1: Genotyping primer sequences

Genotyping PCR	Left Primer Sequence	Right Primer Sequence
Mutant *Dpy30*^{tm1a}	AATTCAGCACCAGCACTTGG	TCGTGGTATCGTTATGCGCC
Flp Deleted *Dpy30*^{tm1a}	GGGGGTGTGTTCGTATTCTG	AGCCTGGGCTACACAGAGAA
Floxed *Dpy30*	GTGAGTGCCAGGAACCAAAT	GTTGTGAGCTGCCATGAAGA
Pdx1-Cre	CGTAGAGAGTCCGCGAGCCA	CCCCAGAAATGCCAGATTACG
Neurog3-Cre	GGAAACTCCAAAGGGTGGAT	AGGCAAATTTTGGTGTACGG
Cre	TCCCGCAGAACCTGAAGATG	CCCCAGAAATGCCAGATTACG

2.2 Embryonic pancreas dissection and *in vitro* spheroid formation

Dorsal pancreatic buds were dissected from E13.5 embryos using fine-tipped forceps under a dissecting microscope, pooled into a single tube and digested in 250 μL TrypLE Express media (Gibco) for 5 minutes at 37°C. The reaction was neutralized by dilution with RPMI 1640 Complete media and the pancreas was further mechanically dispersed by pipetting. Single cells

were then spun at 750xg for 4 minutes, the pellet was resuspended in Pancreas Growth Media (see composition below) ± lentivirus, and an 8 μL suspension was plated at one pancreas per well into a 96-well plate. Spin-infection of lentivirus was performed at 1,020xg at 34°C for 90 minutes, during which the plate was covered with an adhesive seal to prevent evaporation. To the cell suspension at the bottom rim of the well, 12 μL of Matrigel (Corning) was overlayed and solidified at 37°C for 60 minutes on a 45° angle. 100 μL of Pancreas Growth Media was added per well and infected cells were selected with 1 μg/mL puromycin ~5 hours post-infection. Media was changed every other day and 0.33 μM retinoic acid (RA, Sigma-Aldrich) was added every day for 3 days to induce sphere proliferation. Pancreas Differentiation Media (see composition below) was added on Days 4 and 6 to induce differentiation of the spheres.

2.3 Culture and *in vitro* differentiation of spheres

The pancreas sphere assay was modified from a previously published protocol [229]. To improve the size of the biological replicates (where one replicate corresponds to one litter of embryonic pancreas), CD-1 (ICR) mice were used for timed matings as their litter sizes are substantially larger than mice on a C57BL6 background. Briefly, dispersed E13.5 pancreas cells (both progenitors and mesenchyme) were initially cultured for 3 days in Pancreas Growth media containing: basal PrEBM (Lonza) supplemented with 0.1% (wt/vol) recombinant human insulin (Sigma-Aldrich); 0.4% (vol/vol) bovine pituitary extract (BPE, Lonza); 150 ng/mL recombinant human FGF-10 (R&D Systems); 20 ng/mL recombinant mouse IGF-1 (R&D Systems); 0.1% (vol/vol) human transferrin (TF, Lonza); 2% (vol/vol) B-27 supplement (Thermo Fisher Scientific) and 0.33 μM RA. Growth media was changed every other day and retinoic acid was

supplemented every day. On Day 4, the proliferating spheres were switched to Pancreas Differentiation media containing: basal PrEBM media supplemented with 0.1% (wt/vol) recombinant human insulin; 0.4% (vol/vol) BPE; 50 ng/mL recombinant human FGF-10; 20 ng/mL recombinant mouse IGF-1; 0.1% (vol/vol) human TF and 10 mM nicotinamide (Sigma-Aldrich). Since spheres were grown in the absence of antibiotics, media was filter-sterilized and prepared fresh every week. Sphere cultures were maintained at ambient oxygen (21% O_2) and the day of pancreas dissection was considered Day 0.

2.4 Lentivirus generation

Short hairpin RNA (shRNA) lentiviral constructs targeting the TrxG complex component *Wdr5* were ordered from Sigma-Aldrich (sh*Wdr5* #1, clone TRCN000034415; sh*Wdr5* #2, clone TRCN000034416) as bacterial glycerol stocks and a control shScramble sequence was cloned into the pLKO.1 backbone. Lentiviral DNA and packaging components were transfected into HEK 293T cells and lentiviral particles were collected 46 hours later. Supernatants were filtered with a 0.45 μM filter, ultra-centrifuged at 25,000xg for 100 minutes at 4°C and viral pellets were resuspended in 40 μL of PBS with a lentiviral titer of ~1 x 10^{10} TU/mL. Pancreas progenitors were transduced with a multiplicity of infection (MOI) of ~30 (assuming ~30,000 E13.5 pancreas cells treated with 1:100 dilution of lentivirus in PBS at 2.7 μL per well). Transduced cells were cultured with puromycin for selection.

2.5 Sphere measurements

The number of spheres generated per pancreas was counted manually on Days 1, 4 and 7, and the average of 5 wells was determined per treatment each day. Images of the spheres were

captured on a Canon DSLR camera attached to an Olympus CKX41 inverted microscope and sphere diameters were measured using ImageJ software.

2.6 RNA extraction and qPCR analysis

RNA was extracted from lysed cells by pipetting in TRIzol reagent (Thermo Fisher Scientific) and combined with $^1/_5$ the total volume of chloroform. Samples were inverted 10x before centrifugation at 12,000xg for 15 minutes at 4°C. The aqueous layer was mixed with an equal volume of ice-cold 70% ethanol and further processed with the PureLink RNA Mini Kit (Ambion). Complementary DNA (cDNA) was generated using SuperScript III Reverse Transcriptase (Thermo Fisher Scientific) and qPCR experiments were carried out using 0.25-2 µL of cDNA per reaction. Both Fast SYBR Green and TaqMan chemistry (Thermo Fisher Scientific) was used with purchased or custom designed primers (Primer3) to detect exon-intron boundaries (Table 2). Samples were loaded onto 384-well plates in triplicate and run on a ViiA 7 Real-Time PCR system (Thermo Fisher Scientific) where gene expression was normalized to β-actin (*Actb*) and determined using the $\Delta\Delta C_t$ formula.

Table 2: List of qPCR primer sequences

Gene Name	Chemistry	Probe Dyes & Sequence	Left qPCR Primer Sequence	Right qPCR Primer Sequence
Actb	TaqMan	FAM/ZEN/IABkFQ CCCATTCCCACC ATCACACCCT	GCCTCGTCACC CACATAG	CTGTATTCCCCTC CATCGTG
Dpy30	SYBR		TTGCAGAAAAT CCTCACTCTGA	ATCCAGGTAGGCA CGAGTTG
Gcg	SYBR		TGCAGTGGTTG ATGAACACC	TGGTAAAGGTCCC TTCAGCATG
Hes1	SYBR		GAAAGATAGCT CCCGGCATT	GTCACCTCGTTCA TGCACTC
Ins1	SYBR		TCAGAGACCAT CAGCAAGCA	CTCCCAGAGGGCA AGCAG

Ins2	SYBR		GCTTCTTCTACA CACCCATGT	ACGACTGATCTAC AATGCCAC
Neurog3	TaqMan	FAM/ZEN/IABkFQ CGCCATCCTAGT TCTCCCGACTCA	GAAAAGGTTGT TGTGTCTCTGG	ACTGACCTGCTGC TCTCTA
Notch1	SYBR		CCCTTGCTCTGC CTAACG	ACAGGCTTCAGTG CCGTTG
Pdx1	TaqMan	FAM/ZEN/IABkFQ TTCCGCTGTGTA AGCACCTCCTG	GTACGGGTCCT CTTGTTTTCC	GATGAAATCCACC AAAGCTCAC
Rbpj	SYBR		TGGGGATGTAG AAGCCGAAA	GCTGGTGGAGTAA ATGACCC
Rbpjl	SYBR		AACAGACCCCT CGTTGCC	AGGATCCACACAG TCTGCTC
Sox9	TaqMan	FAM/ZEN/IABkFQ AGGGTCTCTTCT CGCTCTCGTTCA	CAAGACTCTGG GCAAGCTC	GGGCTGGTACTTG TAATCGG
Wdr5	SYBR		TGACAATCCTC CAGTGTCCTT	CCCTTGCTGTAGT CCCAGAG

2.7 RNA-sequencing

Samples from Day 7 shScramble and sh*Wdr5* #1 spheres were pooled from ≥ 5 replicates into TRIzol to obtain 2 μg RNA. cDNA libraries were prepared from an Illumina TruSeq RNA Sample Preparation Low Throughput (LT) kit using Ampure XP beads for size selection and validated on an Agilent Bioanalyzer High Sensitivity DNA chip before sequencing on an Illumina HiSeq sequencing platform. The Tuxedo 2.0 suite of tools [230] was used to map reads to known Refseq transcripts, and to identify differentially expressed genes. Sequence reads were aligned to the NCBI37/mm9 mouse genome using TopHat software, with Cufflinks software to identify peaks and analyze enrichment [230], essentially as has been done previously [231]. In order to determine differential gene expression, a histogram of the frequency distribution of the $\log_2$ fold change (sh*Wdr5* #1/shScramble) values was plotted and thresholds were established using the graph inflection points. 340 genes with a $\log_2$ fold change above 2.0 were considered increased

and 1,586 genes below -1.0 were considered impaired. The top 30 underrepresented and overrepresented genes are listed in Appendices A & B, with lineage-specific gene expression listed in Appendix C.

Islets from 3 control and 3 *Dpy30ΔN* male mice were isolated at 4 weeks of age (P28-P32) and handpicked into 1 mL of TRIzol. Extracted RNA was treated with TURBO DNase I (Thermo Fisher Scientific) to remove genomic DNA before 100 ng was ribodepleted with the RiboGone kit (Takara Bio). In total, 6 cDNA libraries were prepared from <10 ng RNA using the SMARTer Stranded RNA-seq kit (Clontech Laboratories, Inc.) and SPRIselect beads (Beckman Coulter). As quality control prior to sequencing, the libraries were validated on an Agilent Bioanalyzer High Sensitivity DNA chip and quantified using the qPCR-based KAPA library quantification kit, where final cDNA concentrations ranged from ~7-40 nM. Libraries were denatured, diluted to 1.6 pM and sequenced on an illumina NextSeq500 system with a 150 cycle high output cartridge. According to the SMARTer Stranded RNA-seq protocol, the first 3 bases that correspond to the SMARTer Stranded Oligo were trimmed from Read 1 (as well as Read 2) using the FASTQ Toolkit Base Trimmer (BaseSpace Labs). The trimmed FastQ files were aligned to the NCBI37/mm9 mouse genome using the RNA-seq Alignment tool (Illumina, Inc.) and STAR aligner. Aligned reads were then normalized and differential expression analysis was performed using DESeq2 (BaseSpace Labs). 415 genes with a $\log_2$ fold change above 1.0 were considered elevated and 521 genes below -1.0 were considered decreased.

2.8 Flow cytometry

Spheres generated from E13.5 MIP-GFP pancreas cells treated with shScramble or sh*Wdr5* #1 were released from Matrigel on Day 7 of differentiation and dispersed into single cells (as above). The number of GFP^+ cells was counted on a BD LSRII flow cytometer.

2.9 Tissue processing and histology

Pancreas progenitor spheres were released from Matrigel (Corning) using 100 μL per well of Dispase II (Sigma-Aldrich) dissolved at 1 mg/mL in PrEBM media (Lonza) for 2 hours at 37°C. An additional 100 μL per well of RPMI 1640 Complete with fetal bovine serum (FBS, Thermo Fisher Scientific) was overlayed to stop the reaction by dilution, and spheres were subsequently mechanically released from Matrigel by pipetting and collected into a single Eppendorf tube. Spheres were pelleted at 750xg for 4 minutes, supernatant was removed, and either 200 μL of TRIzol reagent (Thermo Fisher Scientific) was added for RNA extraction, or 200 μL of 4% paraformaldehyde (PFA, Sigma-Aldrich) was added for a 10 minute fixation followed by liquefied 2% agarose for further immunohistochemical processing.

Embryonic and pancreatic tissue was fixed at 4°C in 4% PFA overnight (whole embryos) or for 5 hours (dissected stomach, pancreas, spleen and intestine ≥ E15.5). All tissue was processed through a series of graded ethanol and xylene de-hydration steps before embedding in paraffin wax. Briefly, fixed embryos and tissues were washed 3x 10 minutes in PBS and processed in cassettes through 50% ethanol (embryos only), 70% ethanol, 2x 30 minutes of 95% and 100% ethanol, 2x 30 minutes of xylene, followed by 2x 1 hour in melted paraffin.

Embryonic or pancreatic tissue was cut into 5 μM sagittal sections using a microtome and mounted onto Superfrost Plus slides.

2.10 Immunostaining, imaging and analysis

Paraffin slides were processed through graded xylene and ethanol re-hydration steps, followed by a 10 minute heat-induced antigen retrieval (10 mM sodium citrate, pH 6.0) at 95°C and 1 hour blocking (5% FBS in PBS) at room temperature. Briefly, slides were processed through 3x 5 minutes xylene, 2x 5 minutes 100% ethanol, 5 minutes 95% ethanol, 5 minutes 70% ethanol and 10 minutes in PBS on a shaker prior to antigen retrieval. Slides were cooled for 5 minutes under cold running tap water and washed for 5 minutes each in de-ionized water and PBS on a shaker before circumscribing with a Super PAP pen (Thermo Fisher Scientific) and blocking. For EdU detection, slides were permeabilized prior to blocking with 0.5% Triton X-100 (Sigma-Aldrich) and incubated for 1 hour with: 100 mM Tris pH 8.5, 1 mM $CuSO_4$ (Sigma-Aldrich), 30 uM Alexa Fluor 594 azide triethylammonium (Thermo Fisher Scientific) and 100 mM ascorbate (Sigma-Aldrich) in H_20. For TUNEL detection, the *In Situ* Cell Death Detection kit, Fluorescein (Roche) was prepared as specified. Briefly, TUNEL reaction mixture was applied to permeabilized slides prior to blocking and incubated in a pre-warmed humid chamber at 37 ˚C for 1 hour in the dark. Embryonic spleen sections were used as positive controls. Primary antibodies were incubated at 4°C overnight with dilutions in blocking solution (see Table 3 for antibody information). The following day, slides were washed 3x 10 minutes in PBS and incubated with secondary antibodies in PBS for 1 hour at room temperature in a humidified dark chamber. Finally, slides were washed 3x 10 minutes in PBS before mounting with Prolong Gold mounting solution. Slides were imaged on a Leica TCS SP8 Confocal microscope or tiled

on an Olympus Bx61 microscope and analyzed using CellProfiler software with custom pipelines.

Table 3: List of primary and secondary antibodies

Antibody	Host Species	Manufacturer	Catalog #	Dilution
Amylase	Goat	Santa Cruz	sc-12821	1:100
Chromogranin A	Mouse	Santa Cruz	sc-393941	1:100
CPA1	Goat	R&D Systems	AF-2765	1:500
DPY30	Rabbit	Abcam	ab214010	1:500
DPY30	Rabbit	Bethyl	A304-296A	1:10,000
DPY30	Rabbit	Atlas Antibodies	HPA043761	1:1000
E-cadherin	Rabbit	Cell Signaling	3195S	1:400
Glucagon	Rabbit	Santa Cruz	sc-13091	1:500
Glucagon	Mouse	Sigma-Aldrich	G6254	1:2000
H3K4me1	Rabbit	Abcam	ab8895	1:1000
H3K4me3	Rabbit	Abcam	ab8580	1:1000
H3K4me3	Rabbit	Cell Signaling	C42D8	1:1000
Insulin	Guinea Pig	Abcam	ab7842	1:1000
Insulin	Guinea Pig	DAKO	IR-002	1:4
MAFA	Rabbit	Bethyl	IHC-00352	1:100
MUC1	Armenian Hamster	Neomarkers	HM-1630-PO	1:2000
NEUROG3	Mouse	DSHB	F25A1B3-c	1:100
NKX2-2	Mouse	DSHB	745A5-c	1:100
NKX6-1	Mouse	DSHB	F55A10-c	1:100
PAX6	Mouse	DSHB	PAX6-s	1:100
PDX1	Mouse	DSHB	F109-D12	1:100
Phospho-Histone H3	Rabbit	Cell Signaling	9701S	1:500
Somatostatin	Goat	Santa Cruz	sc-7819	1:1000
SOX9	Rabbit	Millipore	AB5535	1:2000
WDR5	Rabbit	Bethyl	A302-430A	1:1000
DAPI		Thermo Fisher Scientific	D9542	1:5000
DBA Lectin		Vector Laboratories	B-1035	1:200
TOPRO-3		Thermo Fisher Scientific	T3605	1:5000
Alexa Fluor 488 anti-Rabbit	Donkey	Thermo Fisher Scientific	A-21206	1:500
Alexa Fluor 555 anti-Guinea Pig	Goat	Thermo Fisher Scientific	A-21435	1:500
Alexa Fluor 546 anti-Mouse	Goat	Thermo Fisher Scientific	A-11003	1:500
Alexa Fluor 488 anti-Goat	Donkey	Thermo Fisher Scientific	A-11055	1:500

Antibody	Host Species	Manufacturer	Catalog #	Dilution
Alexa Fluor 488 anti-Armenian Hamster	Goat	Thermo Fisher Scientific	A-21110	1:500
Alexa Fluor 647 anti-Mouse	Donkey	Thermo Fisher Scientific	A-31571	1:500
Alexa Fluor 594 anti-Rabbit	Donkey	Thermo Fisher Scientific	A-21207	1:500

2.11 EdU cumulative labeling and quantification

Pregnant *Dpy30*$^{flox/flox}$ females bred to *Pdx1*-Cre; *Dpy30*$^{flox/wt}$ males were injected intraperitoneally (IP) with 1 mg 5-ethylnyl-2'-deoxyuridine (EdU, Sigma-Aldrich) beginning at 9 AM for cumulative labeling of E12.5 embryonic pancreas cells in S-phase as previously described [111,232]. Subsequent doses of 0.25 mg EdU were injected every 1.5 hours for up to 3 hours. Embryos were harvested 0.5 hour after the last injection and dissected, processed and paraffin embedded as above. The proportion of total PDX1^{+}EdU^{+} cells was measured from at least 8 sections across the pancreas of 4 control and *Dpy30ΔP* embryos.

2.12 Morphometric analysis

Quantifications were determined by taking serial sections at set intervals throughout the entire embryonic pancreas (every 30-60 μM) and postnatal pancreas (every 150-300 μM). At least 10 images per pancreas were captured on a Leica TCS SP8 Confocal microscope or tiled on an Olympus Bx61 microscope. Images were analyzed using CellProfiler software to quantify absolute cell numbers or relative cell fractions, or using ImageJ to quantify islet diameter from more than 250 islets. The number of NEUROG3^{+} nuclei was determined manually.

2.13 NanoString expression analysis

The pancreata from E15.5 and E18.5 control and *Dpy30ΔP* embryos were dissected directly into TRIzol and total RNA was extracted as above. Gene expression was analyzed according to the nCounter XT CodeSet Gene Expression Assay Protocol (NanoString Technologies). Briefly, 5 μL of RNA per sample was hybridized with a custom CodeSet (Table 4) and Capture ProbeSet at 65°C for 16 hours. Sample temperatures were ramped down to 4°C on ice and diluted with 20 μL of water before loading 32 μL onto the cartridge. A panel of 26 developmental pancreas genes were assessed on the nCounter *SPRINT* profiler and further normalization (to 4 housekeeping genes) and analysis was performed in nSolver Analysis Software 3.0.

Table 4: NanoString CodeSet sequences

Gene Name	Forward Sequence	Reverse Sequence
Actb	CGCGAGCACAGCTTCTTT	GACCCATTCCCACCATCA
B2m	AGAATGGGAAGCCGAACA	GGCCATACTGGCATGCTT
Bhlha15	TCCATCCTCCTGCCTCAG	AACAGACACACAGGCCCC
Cpa1	CCAGTGGGGTCTGGTTTG	CATCCCAAAGGCAGCATC
Dpy30	GGGCTCACAGACAGCGTT	CGATCTTCAAACTGCGCC
Foxa2	TCACTGGGGACAAGGGAA	CCAAAGGCTCCTTTAAAACAA
Gapdh	TGACTCCACTCACGGCAA	CCTTTTGGCTCCACCCTT
Gata4	TTCCCAGGACTCTAGCTTGC	GCCCTGGGGACATCTTCT
Gata6	GGCCTGAGCTGGTGCTAC	TTCCTGCAAAAGCCCATC
Gcg	CACAGGGCACATTCACCA	TCACCAGCCAAGCAATGA
Hes1	TGCCTTTCTCATCCCCAA	GGGTAGCAGTGGCCTGAG
Hnf1b	AGCTCCAACCAGACGCAC	AAACCGACTGGCTGGTCA
Hnf4a	AGCCCCTGCAAAGTGTCA	TGGCCCCATTACTCCTCA
Ins1	CCTCTGGCCATCTGCCTA	GGAAGTGCACCAACAGGG
Ins2	CGTGAAGTGGAGGACCCA	TTGCAGAGGGGTAGGCTG
Mafa	ACTGAAACAGAAGCGGCG	TCCTTGTACAGGTCCCGC
Mnx1	TAACAATACCGGCCCCAA	GCGAGGGAAGTGACCAAG
Myc	CAGACAGCCACGACGATG	GTGGGAAGCAGCTCGAAT
Neurod1	AGAGACACTGCGCTTGGC	ATGTCCGGGTTCTGCTCA
Neurog3	CGCTCCAAGCATTTGAGAA	TGCATGTAGCGGGCAGTA
Nkx2-2	GGGAGAGCCACGAATTGA	CCCTTCGCTCTCCTCCTC
Nkx6-1	AGTGATGCAGAGTCCGCC	TCCGTCATCCCCAGAGAA

Gene Name	Forward Sequence	Reverse Sequence
Nr5a2	CTCCCACCACCACCACC	CGAACACACGACAAAACAAA
Onecut1	GCAAGAACACGGGAAGGA	TCCTCCTCCTGGCATTCA
Pdx1	AAGCTCACGCGTGGAAAG	CCACTTCATGCGACGGTT
Ptf1a	CCCAGAGGACCCCAGAAA	TTGCCATTAGAAAAATGTGGTC
Rbpj	TCCCTTAAAACAGGAGCCA	ACAAGCCAAGGAGGAGCC
Rbpjl	GCGGTTACATGGGACTGG	TGATGAGGCGACTGTGGA
Rplp0	CTGCCAAAGCTGAAGCAA	GCGGTTTTGCTTTTTCATC
Sox9	CGTCCTCGTGGGGTTTTT	AGGCATGTGTTGTCCCGT

2.14 Blood glucose measurements

Male *Dpy30ΔN* knockout mice (and littermate controls) were monitored after weaning for body mass and random blood glucose until hyperglycemia was detected (two measurements above 20 mM). Around 2 PM, the mice were weighed, the tail vein was pricked with a 30G needle and blood glucose measurements were obtained using a OneTouch® Ultra® 2 glucometer. For intraperitoneal glucose tolerance tests (IPGTTs), male *Dpy30ΔN* knockout mice (and littermate controls) were fasted for 6 hours prior to IP injection of 2 g/kg 20% D-glucose (Sigma-Aldrich) in water with a 26G needle. Blood glucose measurements were obtained prior to injection (T_0) and 15, 30, 45, 60 and 120 minutes after injection.

2.15 Pancreas and islet isolations

Mice were anesthetized with isoflurane inhalation and checked for toe pinch reflexes prior to euthanasia by cervical dislocation. To open the chest cavity, two lateral incisions were made in the abdomen away from the midline, followed by medial incisions up and down the midline and through the ribcage and diaphragm. The pancreas was dissected by cutting all connections to the spleen, stomach, intestine and liver before placing the tissue directly into 4% PFA in PBS on ice, followed by fixation overnight at 4°C.

For islet isolations from control and *Dpy30ΔN* mice, anesthesia and opening of the chest cavity were performed as above, but mice were euthanized by decapitation and blood was drained. The common bile duct was clamped at the duodenum and a 30G needle was used for perfusion of 3 mL Collagenase XI (1000 U/mL, Sigma-Aldrich) in Hank's Balanced Salt Solution (HBSS) with 1 mM $CaCl_2$ into the common bile duct. The pancreas was dissected as above and further enzymatically digested in 2 mL Collagenase XI for 15 minutes in a 37°C water bath before 4 minutes of mechanical shaking. Pancreas tissue was washed twice with 25 mL HBSS with 1 mM $CaCl_2$ before and filtering through a 70 μM filter. Islets collected on the strainer were inverted and rinsed into a petri dish with RPMI 1640 Complete media (11 mM D-glucose) supplemented with 10% FBS, 50 U/mL penicillin/streptomycin and 2 mM L-glutamine, and either recovered overnight at 37°C in a 5% CO_2 humidified incubator or immediately handpicked for experiments under a dissecting microscope.

2.16 Statistics

Data are expressed as mean ± standard error of the mean (SEM) unless otherwise specified and all experiments were carried out at minimum in triplicate. Statistical analyses were performed using GraphPad Prism 7 Software. Statistical significance was determined using unpaired, two-tailed Student's t-tests for comparisons between two groups, and one-way ANOVA with Dunnett's multiple comparisons post-hoc tests were used for comparisons between more than two groups (unless otherwise specified), with * indicating $P < 0.05$, ** indicating $P < 0.01$, *** indicating $P < 0.001$ and **** indicating $P < 0.0001$.

Chapter 3: TrxG complexes are essential for gene activation during pancreas progenitor spheroid cell specification to the endocrine and acinar lineages

3.1 Background

Spheroids and organoids from multiple human and mouse cell types are 3D *ex vivo* models of organ development and disease [233-235]. Spheroids are defined as a spherical monolayer of self-renewing progenitors with a central lumen, whereas organoids are characterized by branched, non-spherical clusters that resemble the original organ in terms of function and structure [229,234,235]. Although both have self-renewing and self-organizing potential when co-cultured with an extracellular matrix substitute, organoids are derived from more differentiated cells than spheroids [233,236]. The *in vitro* 3D culture system of spheroids and organoids is attractive for many reasons, including the ability to visualize and reconstruct cell development, to study the effects of exogenous morphogens, to perform viral-mediated gene manipulations in single cells, to expand progenitor cells in culture, and for disease modeling. Compared to 2D cell culture and tissue explants, spheroid and organoid models more closely resemble *in vivo* tissues in terms of cell architecture, composition and differentiation potential [235].

Several groups have developed pancreas spheroid and organoid models from mouse embryonic or adult cells, human stem and progenitor cells or from tumor cells [229,237-253]. Two models in particular have been developed for the study of mouse pancreas progenitor development. For example, over seven days of *in vitro* culture, E11.5 $SOX9^{+}$ pancreas progenitors develop into spheroids that express endocrine genes when cultured with RA, or organoids that express acinar genes when cultured in the absence of RA [229]. Using two different 7-day culture protocols, Greggio *et al.* [237] generated organoids from E10.5 mouse pancreas

progenitors that recapitulate tip and trunk progenitor segregation with partial endocrine and exocrine cell differentiation and spheroids that differentiate into acinar and endocrine cells.

Chromatin modifiers have diverse roles in pancreas progenitor differentiation and have the potential to enhance protocols to produce β-like-cells from hESCs [176,254-257]. Several reports describe enrichment of H3K4 methylation or removal of H3K27me3 during activation of pancreas- or islet-specific *cis*-regulatory loci in human and mouse pancreas and endocrine cells [180,210,226], suggesting that H3K4 methyltransferases and H3K27me3 demethylases are necessary for conversion of these loci during pancreas development. In support of this hypothesis, suppression of the H3K4 methyltransferase *Prdm16* in mouse pancreas spheroids and the study of *Prdm16*$^{-/-}$ mice demonstrated that *Prdm16* is required for *in vitro* and *in vivo* islet development [229]. However, the TrxG complexes are the major H3K4 methyltransferases and also associate with H3K27 demethylase proteins, suggesting that the TrxG complexes may have a prominent role in gene activation during pancreas development.

Within the TrxG complexes, the core TrxG subunit WDR5 is essential for the catalytic function and assembly of all six mammalian TrxG complexes [183,187,258-260]. WDR5 is described as the key adapter protein that links the core TrxG proteins to the H3K4 methyltransferase, and without the WDR5 subunit, the TrxG complex does not assemble and H3K4 methyltransferase activity is undetectable [185,258,259,261-263]. WDR5 has a prominent role in cell cycle progression, differentiation and self-renewal of an array of progenitor cells and is upregulated in several cancers [182,264-273].

In this Chapter, I determined the localization of TrxG complex proteins in the mouse embryonic pancreas. The catalytic and non-catalytic roles of the TrxG complexes in gene activation during differentiation of mouse pancreas progenitors were investigated by suppression

of *Wdr5* in an *in vitro* pancreas progenitor spheroid model [229]. Given that the TrxG complexes recruit nucleosome remodelers, Pol II and are associated with activation of developmental genes [167,179,182,191,196,197], I **hypothesized** that the TrxG complexes were required for activation and/or maintenance of lineage-specific genes during pancreas progenitor spheroid cell specification.

3.2 Results

3.2.1 Localization of TrxG complex proteins in the embryonic mouse pancreas

Although the TrxG complexes are considered ubiquitously expressed, several TrxG proteins shuttle between the nucleus and the cytoplasm to control complex activity [274,275]. To address whether core TrxG subunits are nuclear or cytoplasmic at key pancreas developmental stages, I analyzed the core TrxG proteins DPY30 and WDR5 [183-185,187,258-260]. To determine the localization of DPY30 and WDR5 in the embryonic pancreas, I utilized immunofluorescence (IF) staining of E12.5 and E14.5 mouse paraffin sections. DPY30 and WDR5 immunoreactivity was detected in the mesenchymal and epithelial cells of the pancreas, including in $PDX1^{+}$ pancreas progenitors at E12.5 (Figure 4A), and in $NEUROG3^{+}$ endocrine progenitors (Figure 4B) and $insulin^{+}$ or $glucagon^{+}$ endocrine cells at E14.5 (Figure 5). In the pancreas epithelium at both stages, DPY30 and WDR5 immunoreactivity was highly nuclear and weakly cytoplasmic. Upon closer examination of the E14.5 pancreas, the cells with the strongest DPY30 and WDR5 immunoreactivity localized with $PDX1^{HI}$ cells and $insulin^{+}$ and $glucagon^{+}$ endocrine cells (Figure 5, white and yellow arrowheads). These results confirm the ubiquitous expression of DPY30 and WDR5 in the mouse embryonic pancreas and demonstrate their nuclear and cytoplasmic localization in pancreas and endocrine progenitors, as well as endocrine cells.

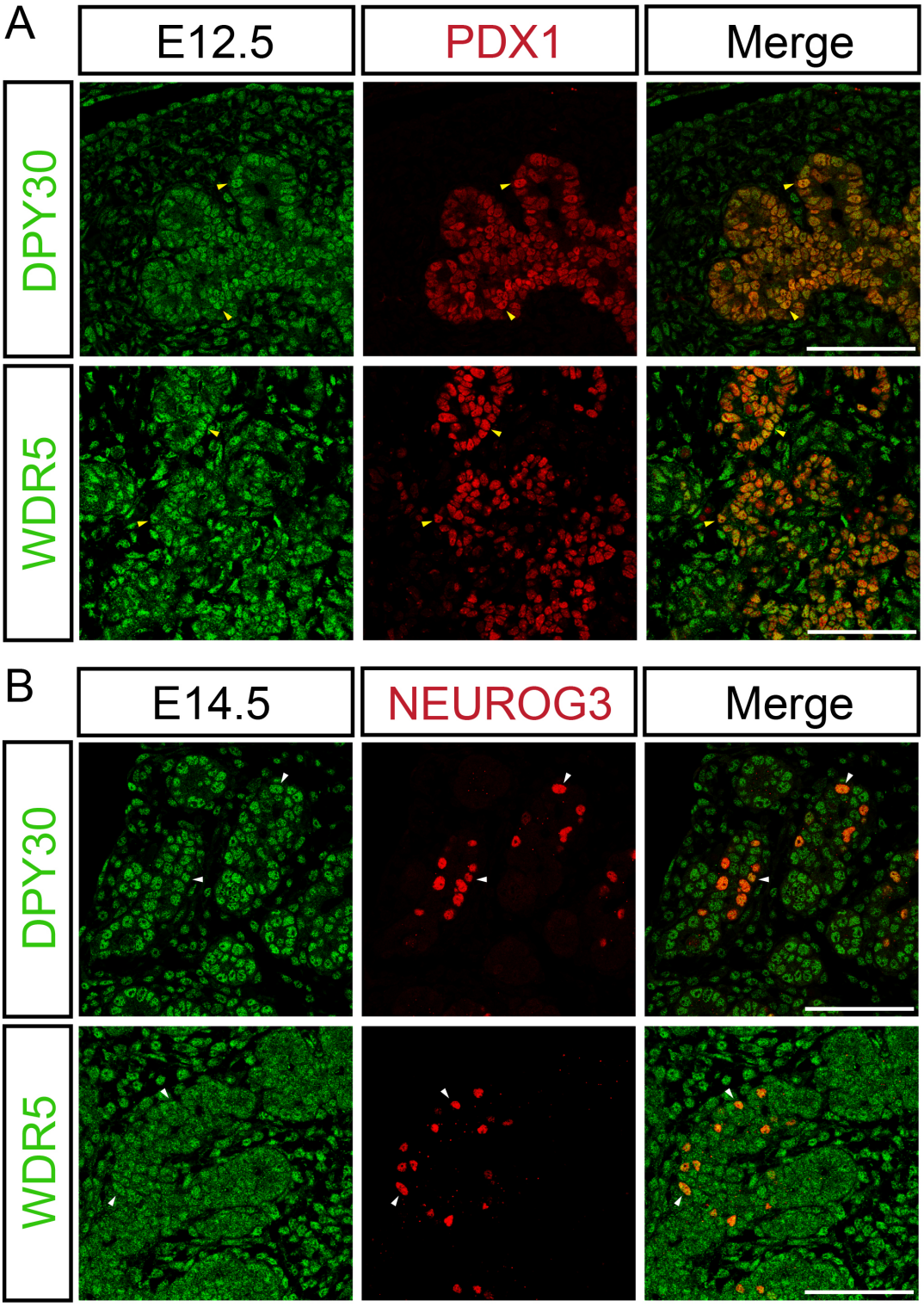

Figure 4: TrxG proteins DPY30 and WDR5 are detected in mouse pancreas and endocrine progenitors. Immunoreactivity of DPY30 and WDR5 (green) in mouse pancreas at **(A)** E12.5 with PDX1^{+} cells (red, yellow arrowheads) and **(B)** E14.5 with NEUROG3^{+} cells (red, white arrowheads). Scale bar, 100 μM.

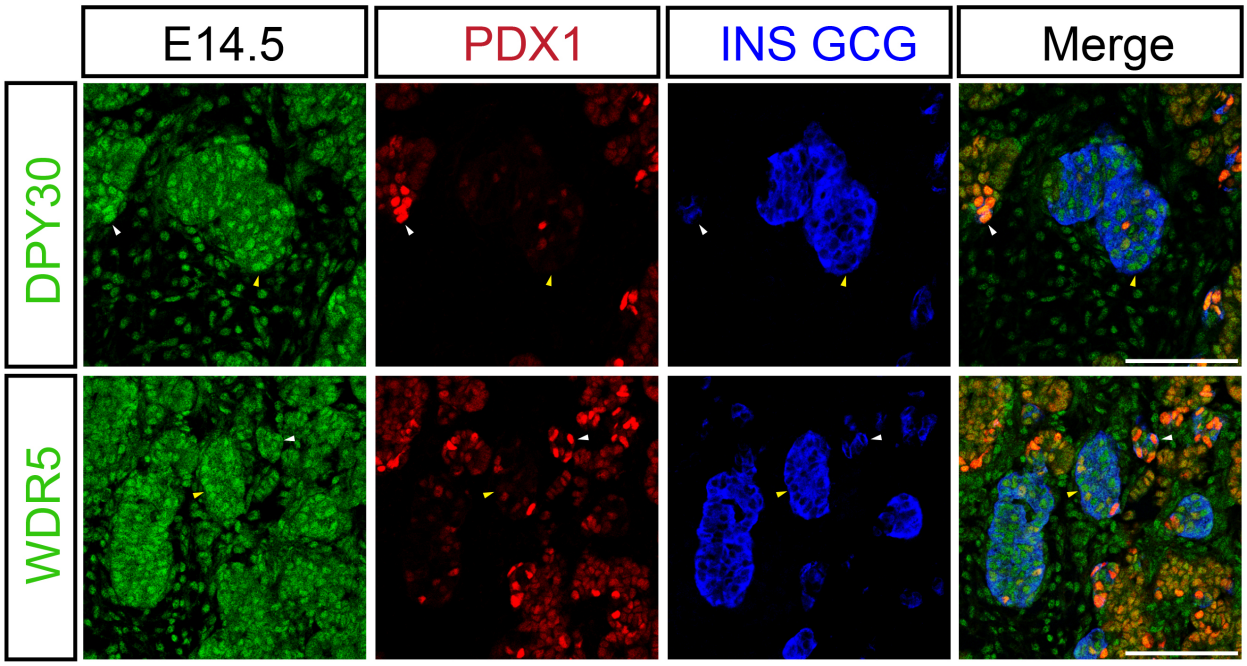

Figure 5: TrxG proteins DPY30 and WDR5 are detected in endocrine cells.
Immunoreactivity of DPY30 and WDR5 (green) in mouse pancreas at E14.5 with PDX1^{+} cells (red), insulin^{+} and glucagon^{+} cells (blue). White arrowheads, DPY30^{HI} or WDR5^{HI} cells co-localized with PDX1^{HI} cells; yellow arrowheads, DPY30^{HI} or WDR5^{HI} cells co-localized with endocrine cells. Scale bar, 100 μM

3.2.2 Pancreas spheroids as an *in vitro* model of development

To examine whether the TrxG complexes have a functional role in the differentiation of pancreas progenitors into the three pancreas lineages, I adapted an *in vitro* pancreas progenitor spheroid model [229]. Briefly, the pancreas was dissected from E13.5 mouse embryos, dispersed into single cells and grown as spheroids in 3D Matrigel culture for up to seven days. Once established, I confirmed cell differentiation in the spheroid model by measuring qPCR expression of pancreas lineage markers. Over seven days in culture, spheres expressed the pancreas progenitor markers *Pdx1* and *Sox9,* the endocrine progenitor marker *Neurog3*, the endocrine cell transcripts *Gcg*, *Ins1* and *Ins2*, and expressed the TrxG component *Wdr5* (Figure 6). From Day 1 to Day 7, *Pdx1* and *Sox9* were consistently expressed, whereas expression of *Neurog3* peaked on Days 2-5. *Gcg* expression decreased from Day 1 to Day 4, and then steadily

increased again to Day 7. Expression of *Ins1* and *Ins2* steadily increased from Day 1 to Day 7. Finally, *Wdr5* expression decreased slightly over seven days of sphere culture.

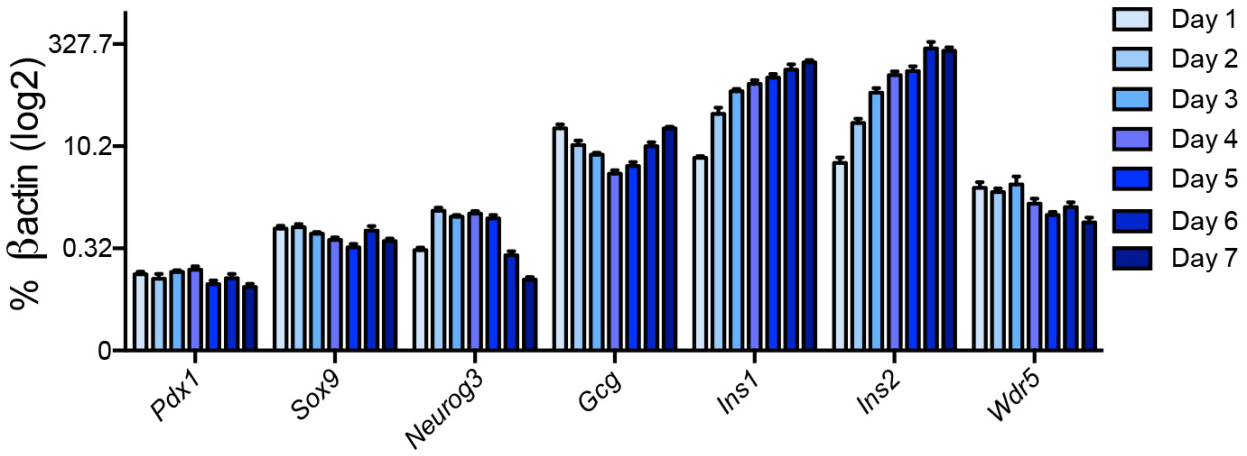

Figure 6: Pancreas spheroids upregulate endocrine genes during *in vitro* differentiation.
qPCR expression of select pancreas progenitor (*Pdx1, Sox9*), endocrine (*Neurog3, Gcg, Ins1* and *Ins2*) and TrxG (*Wdr5*) genes over seven days of spheroid differentiation. Data are represented as $\log_2$ % βactin; n = 3-5.

To examine protein expression in the pancreas spheroids, Day 7 differentiated spheres were embedded in paraffin and immunostained for several pancreas lineage proteins. A high proportion of the sphere cells were immunoreactive for PDX1 and SOX9 (Figure 7A-B). Staining for the duct cell markers mucin (MUC1) and *Dolichos* biflorous agglutinin (DBA) lectin showed that MUC1 marked the sphere lumen and the majority of the sphere cells expressed cytosolic DBA lectin (Figure 7C-D). A small fraction of the pancreas sphere cells showed evidence of endocrine lineage proteins, with NEUROG3$^+$ endocrine progenitors, glucagon$^+$ α-cells and insulin$^+$ β-cells detected (Figure 7E-G). In addition, pancreas spheroids ubiquitously expressed the TrxG complex protein WDR5 (Figure 7H). Together, these results suggest that Day 7 pancreas spheroids are mostly composed of progenitor or duct cells, and that a fraction of sphere cells are capable of endocrine cell differentiation.

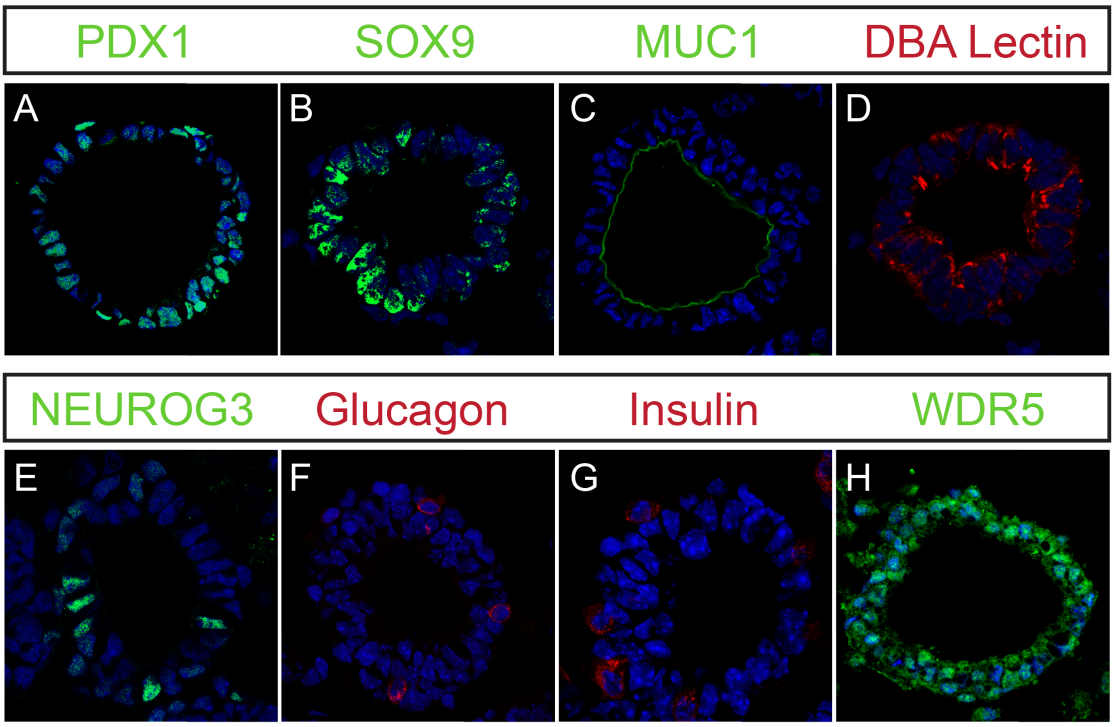

Figure 7: Progenitor, duct, endocrine and TrxG complex proteins are detected in pancreas spheroids. IF staining of pancreas spheroids on Day 7 of differentiation shows immunoreactivity of **(A, B)** progenitor (PDX1 and SOX9); **(C, D)** duct (MUC1 and DBA lectin); **(E-G)** endocrine (NEUROG3, glucagon and insulin) and **(H)** TrxG complex (WDR5) proteins. Nuclei are stained with TOPRO-3 (blue).

3.2.3 Suppression of *Wdr5* reduces sphere number and diameter

To assess the role of the TrxG complexes in gene activation during pancreas progenitor differentiation, I suppressed the TrxG core subunit *Wdr5* in the pancreas spheroid assay. For these experiments, I generated two different lentiviral shRNAs targeting *Wdr5* (sh*Wdr5* #1 and sh*Wdr5* #2). Relative to an shScramble control lentivirus, sh*Wdr5* #1 and sh*Wdr5* #2 effectively suppressed *Wdr5* transcripts by ~80 and ~90% respectively, in Day 7 pancreas spheres (Figure 8). Over the course of the seven-day pancreas spheroid culture, I observed a decrease in sphere number after sh*Wdr5* treatment compared to the shScramble control (Figure 9). Scoring the number of spheres generated per pancreas revealed that although there were equivalent numbers of spheres on Day 1, there were significantly fewer (~50% less) sh*Wdr5*-treated spheres on Days

4 and 7 (Figure 10). Additionally, measuring sphere diameter over seven days of culture demonstrated that the spheres ranged in size, with most spheres between 0-30 μm on Day 1 and growing to 31-60 μm in diameter on Days 4 and 7 (Figure 11). On Days 1 and 4, sh*Wdr5* treatment had no significant effect on sphere size compared to shScramble controls. However, on Day 7 there were more sh*Wdr5*-treated spheres in the 31-60 μm range and fewer sh*Wdr5* spheres that were larger than 60 μm (Figure 11). Together, these data suggest that suppression of *Wdr5* in pancreas spheroids may either reduce sphere cell proliferation or survival.

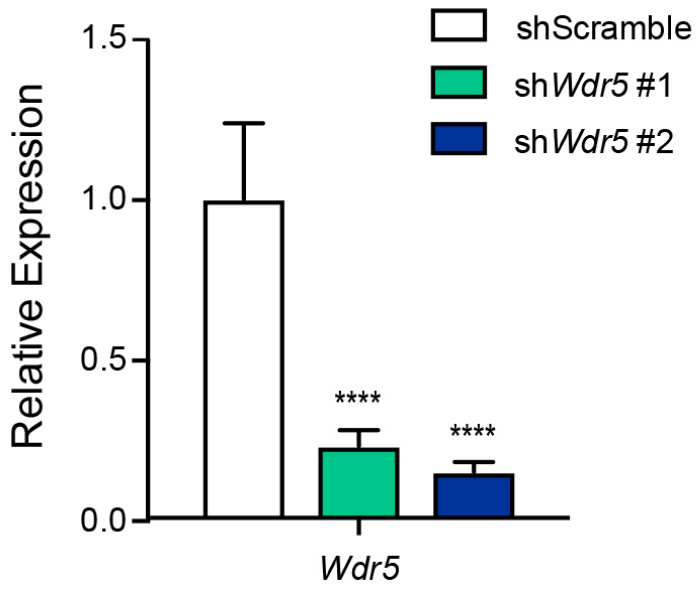

Figure 8: Efficient suppression of *Wdr5* in pancreas spheroids by sh*Wdr5* lentivirus.
Relative expression of *Wdr5* transcripts in pancreas spheres treated with shScramble, sh*Wdr5* #1 and sh*Wdr5* #2. Data are relative to β-actin; n = 6-12; **** denotes $P < 0.0001$ sh*Wdr5* vs. shScramble; one-way ANOVA with Dunnett's multiple comparisons post-hoc test.

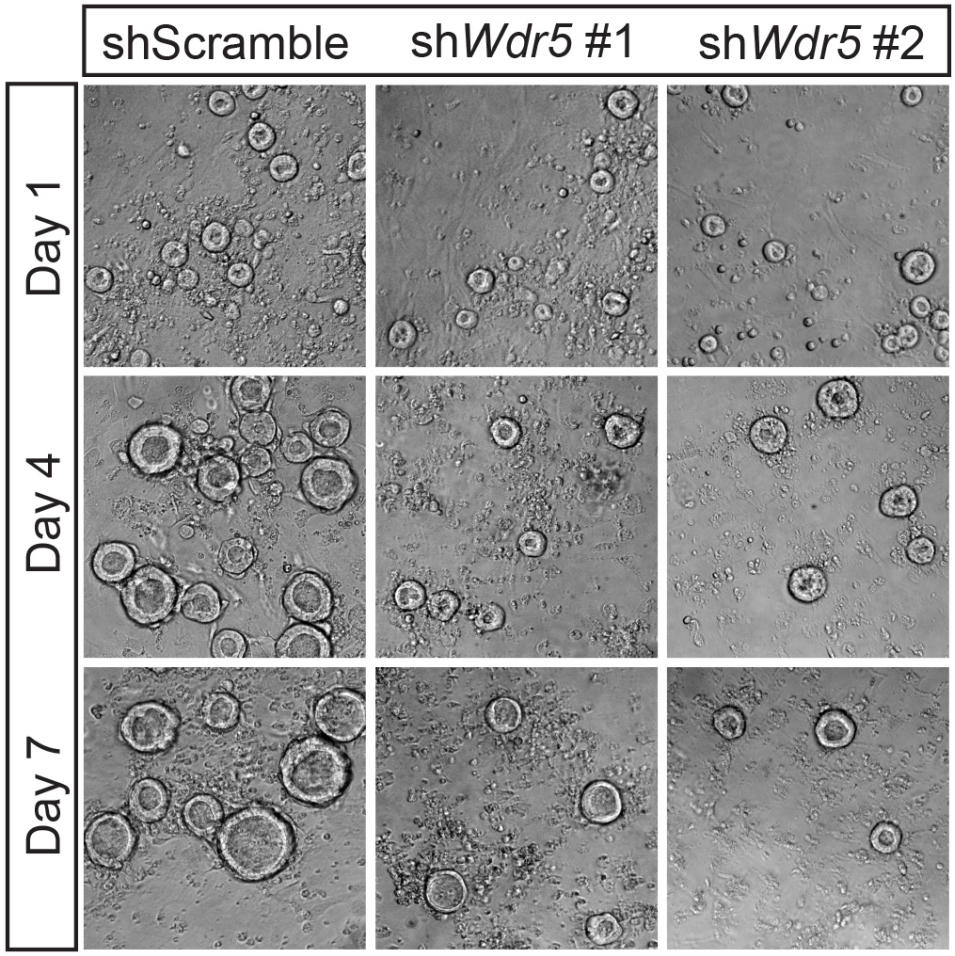

Figure 9: Suppression of *Wdr5* reduces sphere number and size.
Bright field images of shScramble, sh*Wd5* #1 and sh*Wdr5* #2 spheres on Days 1, 4 and 7 of differentiation.

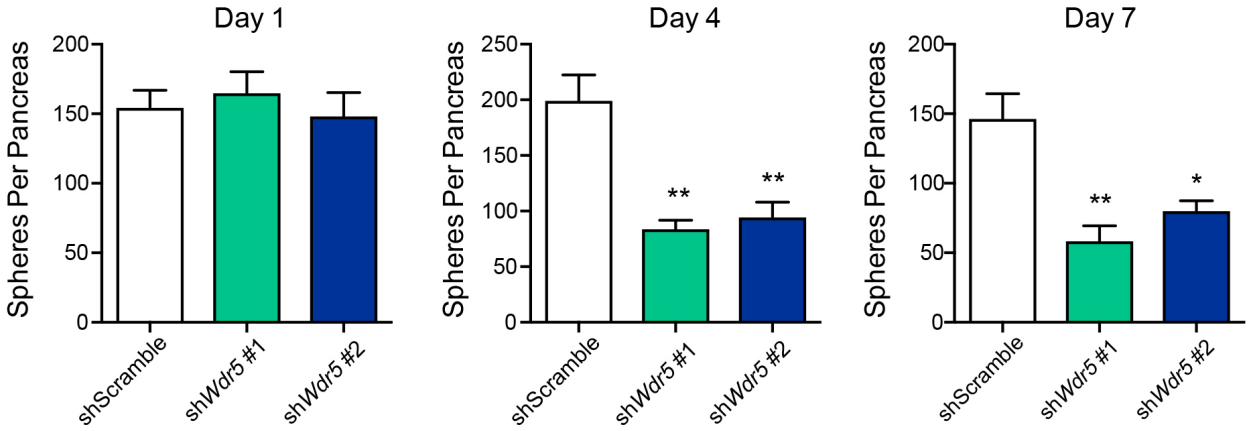

Figure 10: Suppression of *Wdr5* reduces the number of spheroids per pancreas after seven-day culture.
Quantification of the number of shScramble, sh*Wdr5* #1 and sh*Wdr5* #2 spheres generated per pancreas on Days 1, 4 and 7 of differentiation. Data are represented as mean ± SEM; n = 4-14; * denotes $P < 0.05$ and ** denotes $P < 0.01$ sh*Wdr5* vs. shScramble; one-way ANOVA with Dunnett's multiple comparisons post-hoc test.

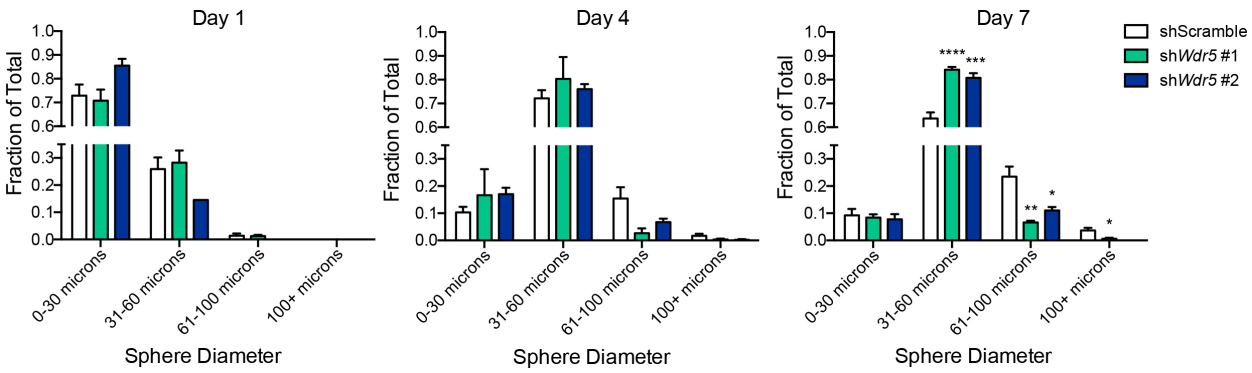

Figure 11: The diameter of sh*Wdr5* spheroids is reduced compared to shScramble.
Sphere diameter measurements as a fraction of the total number of spheres for shScramble, sh*Wd5* #1 and sh*Wdr5* #2 treatments on Days 1, 4 and 7 of differentiation. Data are represented as mean ± SEM; n = 3-9; * denotes $P < 0.05$, ** denotes $P < 0.01$, *** denotes $P < 0.001$ and **** denotes $P < 0.0001$ sh*Wdr5* vs. shScramble; one-way ANOVA with Dunnett's multiple comparisons post-hoc test. Note that no statistically significant differences were detected on Days 1 and 4.

3.2.4 Suppression of *Wdr5* impairs endocrine and acinar gene activation in pancreas progenitors

To determine whether suppression of *Wdr5* has an effect on gene activation during specification of pancreas spheroids to the endocrine lineage, I measured endocrine transcript expression by qPCR in Day 7 spheres treated with sh*Wdr5* #1, sh*Wdr5* #2 or an shScramble control. Although sh*Wdr5* treatment did not significantly affect the expression of progenitor markers *Pdx1* or *Sox9*, there were significant reductions in the endocrine progenitor cell transcript *Neurog3* (> 53-fold) and endocrine cell transcripts *Ins1* (> 16-fold), *Ins2* (> 17-fold) and *Gcg* (> 14-fold) compared to shScramble controls (Figure 12).

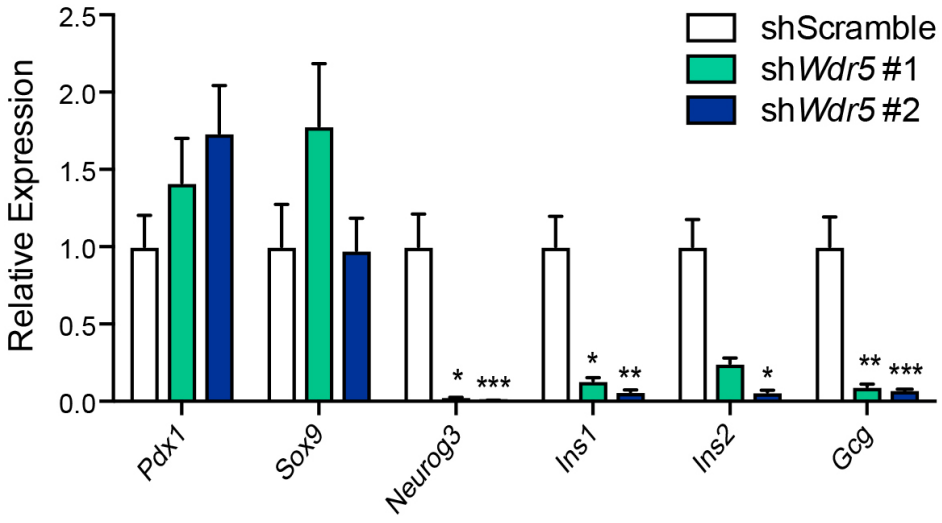

Figure 12: Suppression of *Wdr5* in pancreas spheroids impairs islet gene activation.
Relative expression of progenitor (*Pdx1* and *Sox9*), endocrine progenitor (*Neurog3*) and endocrine (*Ins1*, *Ins2* and *Gcg*) cell transcripts in Day 7 spheroids from shScramble control, sh*Wdr5* #1 and sh*Wdr5* #2 treatment. Data are relative to β-actin; n = 3-11; * denotes $P < 0.05$, ** denotes $P < 0.01$ and *** denotes $P < 0.001$ sh*Wdr5* vs. shScramble; one-way ANOVA with Dunnett's multiple comparisons post-hoc test.

To further validate that *Wdr5* suppression decreased endocrine cell differentiation, I performed the sphere assay with mice expressing GFP under control of the mouse insulin promoter (MIP-GFP). This mouse model allowed me to use the GFP transgene as a readout for insulin promoter activity and visualize GFP^+ cells directly in the sphere culture. In agreement, suppression of *Wdr5* by sh*Wdr5* #1 in MIP-GFP pancreas spheroids significantly reduced the proportion of GFP^+ sphere cells by > 4-fold compared to shScramble spheres on Day 7 (Figure 13A-B). This result further suggests that treatment of pancreas spheres with sh*Wdr5* reduces their differentiation to $insulin^+$ β-cells.

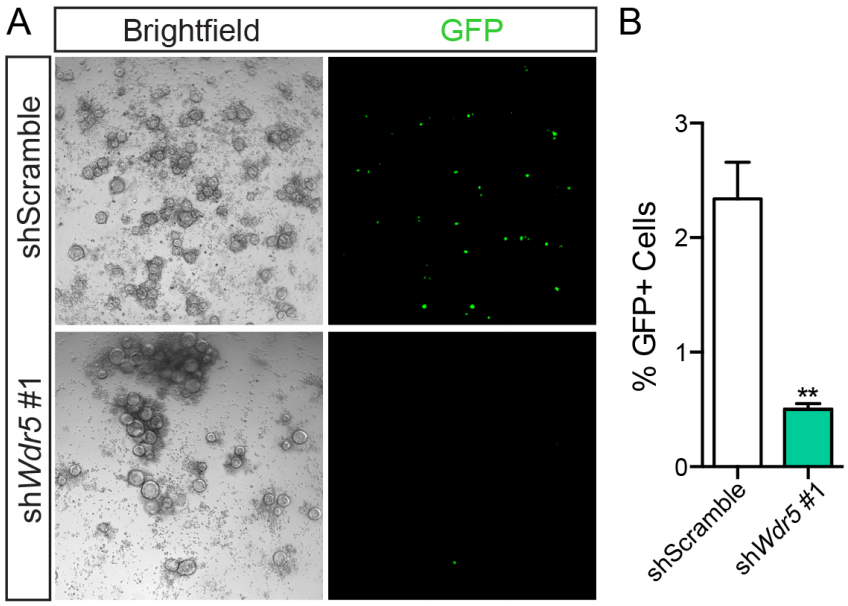

Figure 13: GFP⁺ cells are reduced in MIP-GFP sh*Wdr5* spheroids.
(A) Bright field and GFP images from Day 7 mouse insulin promoter-driven GFP (MIP-GFP) spheres treated with shScramble and sh*Wdr5* #1. **(B)** The % of GFP⁺ cells in shScramble and sh*Wdr5* #1 spheres measured by flow cytometry. Data are represented as mean ± SEM; n = 4; ** denotes $P < 0.01$ sh*Wdr5* vs. shScramble; unpaired, two-tailed Student's t test.

To determine the genome-wide effect of *Wdr5* suppression on acinar, duct and endocrine gene activation during spheroid differentiation, I generated RNA-sequencing (RNA-seq) data from Day 7 sh*Wdr5* #1 and shScramble spheres (see Materials & Methods and Appendices A & B). Gene Ontology (GO) term analysis indicated that underrepresented genes were associated with pancreas development, glucose homeostasis, insulin secretion and cell proliferation (Figure 14A). Overrepresented genes were associated with cell adhesion, apoptosis, cell proliferation, regulation of cell differentiation and assembly of cell junctions (Figure 14B).

Activation of endocrine lineage-specific genes was essentially abolished in spheres treated with sh*Wd5* #1 compared to shScramble controls (Figure 14C, Appendix C). These reductions included genes expressed in endocrine progenitors (i.e. *Neurog3*, > 165-fold; *Neurod1*, > 60-fold; *Pax6*, > 250-fold) and endocrine hormones (i.e. *Gcg*, >80-fold; *Iapp,* > 70-fold; *Ins1*, >

100-fold; *Ins2,* > 70-fold; *Ppy*, >80-fold; *Sst*, >190-fold). Even though gene expression levels were low compared to the endocrine lineage (see Appendix C for FPKM values), activation of acinar lineage-specific genes, including *Amy2b*, *Bhlha15, Cel, Clps, Cpa1*, *Cpa2*, *Pnliprp1* and *Prss2,* was also decreased between 2- to 18-fold (Figure 14C, Appendix C). The acinar cell regenerating factors *Reg1, Reg3b* and *Reg3g* were increased between 4- to 20-fold by *Wdr5* suppression. Genes expressed in early pancreas progenitor cells, including *Hes1, Pdx1, Rbpj* and *Sox9*, were either unaltered or slightly elevated by *Wdr5* suppression compared to controls (Figure 14C, Appendix C). Finally, genes expressed in the duct cell lineage, including *Car2, Krt7*, *Krt19*, *Muc1, Muc4* and *Muc20*, were elevated between 4- to 22-fold in sh*Wdr5* #1 spheres compared to controls (Figure 14C, Appendix C). Overall, these data suggest that the TrxG complexes are required for activation of acinar and endocrine lineage-specific genes, but are not necessary for gene expression maintenance of progenitor and duct cell genes.

A

Underrepresented Genes	
GO Term Category	**Gene Symbol**
Pancreas development	*Isl1, Insm1, Igf1, Neurog3, Gck, Iapp, Nkx2-2, Rfx6, Pax6, Acvr2b, Il6, Myt1, Bmp6, Prox1, Neurod1, Foxa3, Ildr2, Ift88, Ins1, Nkx6-1*
Cellular glucose homeostasis	*Ptprn2, Cartpt, Igf1, Kcnb1, Ogt, Gck, Rab11fip2, Abcc8, Mixipl, Pik3r1, Myt1, Neurod1, Foxa3, Vcam1*
Positive regulation of insulin secretion	*Gcg, Pfkm, Isl1, Park2, Tmem27, Cacna1d, Nnat, Slc30a8, Gpr27, Gck, Baiap3, Rbp4, Rfx6, Ghrl, Glp1r, Nkx6-1*
Positive regulation of epithelial cell proliferation	*Scg2, Akt3, Gas1, Ptn, Hmgb2, Has2, Fgf1, Htra1, Egr3, Igf1, Ang, Figf, Cav1, Fgf2, Ccl5, Il6, Arg1, Sfrp1 Dysf, Osr1, Ghrl, Bmp6, Prox1, Osr2, Cyp7b1, Twist2, Egfl7*

B

Overrepresented Genes	
GO Term Category	**Gene Symbol**
Cell-cell adhesion	*Cldn3, Wnt7b, Tnf, Lama3, Lmo7, Cldn2, Cdh13, Adam8, Slc7a11, Mpzl2, Perp, Dscaml1, Ceacam1, Cdh17*
Intrinsic apoptotic signaling pathway	*Sfn, Phlda3, Nupr1, Crip1, Cdkn1a, Tnf, Clu, Ddit4, Perp*
Cell proliferation	*Rnf43, Wnt7b, Bmper, Ereg, Nurp1, Tnf, Sdcbp2, Nrarp, Clu, Cdh13, Tspan1, Areg, Dmbt1, Ccnd1, Txnrd1, Tgfa, Ddit4, Wnt7a, Ceacam1*
Regulation of epithelial cell differentiation	*Sfn, Tnf, Serpine1, Jag1, Lif, Dmbt1, Foxj1, Reg3g, Ceacam1*
Cell junction assembly	*Cldn3, Itga2, Lama3, Zfp703, Cdh13, Micall2, Itgb4, Cdh17*

C

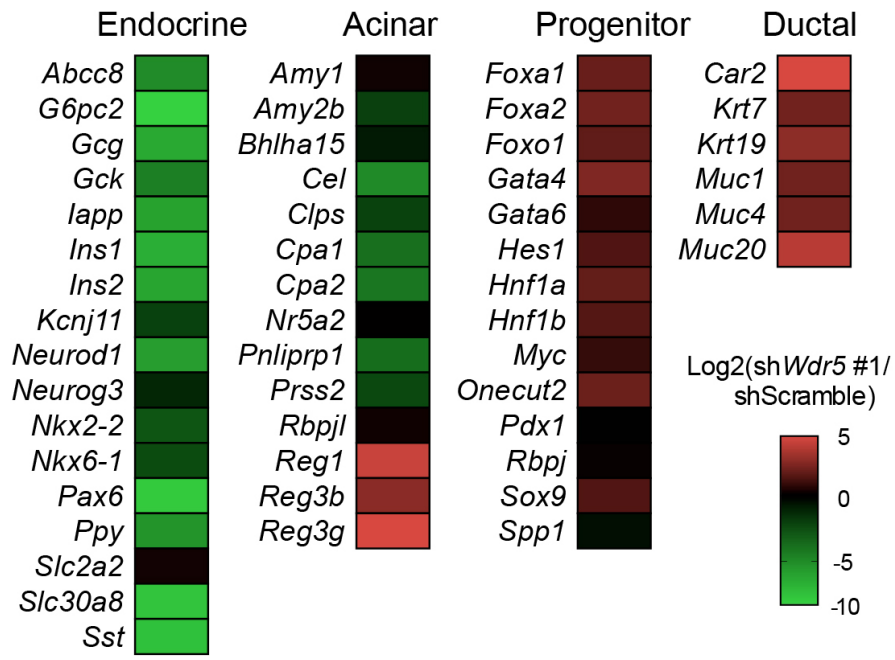

Figure 14: RNA-sequencing reveals impaired endocrine and acinar gene activation in sh*Wdr5* spheroids. Gene Ontology (GO) term analysis of **(A)** underrepresented genes and **(B)** overrepresented genes in Day 7 sh*Wdr5* #1 spheres compared to shScramble spheres. **(C)** Heat map showing relative expression of Day 7 sh*Wdr5* #1 spheres compared to shScramble spheres. RNA-sequencing data was generated from combining ≥ 5 sphere differentiations (n = 1 pooled replicate) to achieve 2 µg of RNA and is represented as $\log_2$ fold change of sh*Wdr5* #1/shScramble.

3.3 Discussion

In this Chapter, I determined the expression of TrxG complex proteins in the mouse embryonic pancreas and established a role for the TrxG complexes in activation of genes necessary for the specification of pancreas progenitors. The TrxG core proteins DPY30 and WDR5 were localized in the nucleus and the cytoplasm of PDX1^{+} and NEUROG3^{+} progenitors and in endocrine cells. In an *in vitro* pancreas spheroid model, suppression of *Wdr5* reduced spheroid diameter and the number of spheres after seven-day culture. While genes expressed in pancreas progenitors or duct cells were unaffected or elevated in sh*Wdr5* spheres compared to controls, activation of genes in the acinar and endocrine cell lineages was markedly decreased. This suggests that the TrxG complexes are not required for the maintenance of progenitor or duct cell gene expression but are essential for acinar and endocrine lineage-specific gene activation.

The pancreas spheroid model used herein was adapted from a previously established protocol that permits gene manipulation by lentiviral transduction of shRNA [229]. In addition, this protocol models pancreas development *in vitro* – isolated mouse E11.5 dorsal pancreas SOX9^{+} MPCs grow as polarized spheres, differentiate to the endocrine and duct lineages and secrete insulin in response to glucose. From mouse E13.5 dorsal pancreas, I generated spheroids with a similar architecture and differentiation potential. For example, a high proportion of the sphere cells were immunoreactive for PDX1 and SOX9. These proteins are found in early pancreas MPCs, but later in development PDX1 is restricted to insulin^{+} β-cells and SOX9 is maintained in BPCs and duct cells. Similar to the organization of mouse pancreas epithelial cells, the spheroids exhibited apical-basal cell polarity where mucin^{+} duct cells lined the sphere lumens. Further, a high proportion of sphere cells were immunoreactive for DBA lectin, indicating mature duct cell differentiation.

Since the established protocol used mouse E11.5 pancreas [229] whereas I used E13.5 pancreas to generate spheroids, one might expect the difference in pancreas progenitor cell sources to have an effect on sphere cell development. However, both sphere protocols showed evidence of duct and endocrine lineage markers and were not very conducive to acinar cell differentiation. Although I detected low expression of acinar cell transcripts by RNA-seq, digestive enzymes such as amylase and CPA1 were not detected by IF staining (data not shown) and this was also reported in the original protocol [229].

Spheroid culture exhibited endocrine cell differentiation reminiscent of *in vivo* pancreas development. For example, gene expression profiling demonstrated that *Neurog3* transcripts peaked between Days 2-5 of the sphere assay, and after *Neurog3* activation, expression of *Ins1* and *Ins2* steadily increased from Day 1 to Day 7. This aligns well with the transient induction of *Neurog3* in mouse endocrine progenitors and downstream β-cell differentiation. Interestingly, *Gcg* expression decreased from Day 1 to Day 4, and then steadily increased again to Day 7. These changes in sphere *Gcg* expression correspond to the switch from Pancreas Growth media to Pancreas Differentiation media on Day 4. This suggests that either Pancreas Growth media is not conducive to *Gcg* gene induction, or that Days 1-4 represent a gradual reduction in first wave glucagon$^+$ cells and Days 4-7 represent induction of glucagon$^+$ cells of the secondary transition. At the protein level, few individual sphere cells expressed markers of the endocrine lineage. However, this is consistent with *in vivo* development where relatively few cells activate NEUROG3 from BPCs and specify to the endocrine lineage in proportion to the entire pancreas epithelium. Furthermore, a subset of luminal sphere cells induced NEUROG3 whereas insulin$^+$ and glucagon$^+$ cells were observed in peripheral sphere cells. This may be suggestive of an EMT event where NEUROG3$^+$ cells migrate away from the sphere lumen during endocrine

differentiation. Overall, these data demonstrate that endocrine cell differentiation occurs during *in vitro* pancreas progenitor spheroid culture.

Using this spheroid model, I tested the hypothesis that the TrxG complexes are required for gene activation during pancreas progenitor differentiation. First, I confirmed expression of WDR5 in the mouse embryonic pancreas as well as in pancreas-derived spheroids. After lentiviral *Wdr5* suppression in the spheroid assay, I observed significantly reduced sphere number and size compared to shScramble controls. This implies that either cell proliferation is reduced or cell death is increased in sh*Wdr5* spheres. The TrxG complex and the core protein WDR5 have a well-documented role in cell proliferation [267,269,271,276-280], and in cancer growth [264-266,268,281-283]. In particular, suppression of *Wdr5* in a pancreatic cancer spheroid model reduces sphere counts and the proliferation marker Ki67 [265]. There are conflicting reports on whether WDR5 has a role in apoptosis depending on the cell type [231,266,267,271].

Although proliferation and cell death were not directly tested in the spheroid assay, GO term analysis of the sphere RNA-seq data suggests that both pathways are affected by *Wdr5* suppression. For example, genes associated with cell proliferation, including several growth factors (e.g. *Bmp6, Figf, Fgf1, Fgf2, Egfl7, Egr3* and *Prox1*), were underrepresented in the sh*Wdr5* spheres. In contrast, genes associated with apoptosis, such as *Ddit4, Cdkn1a, Perp* and *Tnf*, were overrepresented in sh*Wdr5* spheres. Interestingly, expression of acinar cell regenerating transcripts *Reg1, Reg3b* and *Reg3g* was increased in sh*Wdr5* spheres compared to shScramble controls. These regenerating factors promote duct cell proliferation through *Ccnd1* induction and are consistently upregulated in models of pancreas cell injury such as pancreatitis [284-286]. These results may suggest that suppression of *Wdr5* in pancreas progenitors reduces proliferation, increases apoptosis and stimulates a compensatory regenerative pathway.

Unexpectedly, sh*Wdr5* spheres were enriched for cell adhesion molecules such as cadherins, integrins and laminins, which are upregulated in pancreatic cancer [287]. For example, *Cecam1* is expressed in pancreatic intraepithelial neoplasia (PanIN) lesions and is used as an early biomarker for pancreatic adenocarcinoma [288].

The most striking observation from suppression of *Wdr5* during pancreas spheroid differentiation was the significant reduction in endocrine cell transcripts. Expression of *Neurog3*, *Ins1*, *Ins2* and *Gcg* were reduced more than 70-fold compared to shScramble controls, and GFP^+ cells were also reduced more than 4-fold after *Wdr5* suppression in the MIP-GFP sphere model. GO term analysis of RNA-seq data confirmed that many additional endocrine genes were underrepresented in the sh*Wdr5* spheres, including those involved in islet development, glucose homeostasis and insulin secretion. The reduction in endocrine cell fate in sh*Wdr5* spheres suggests that the cells may remain as progenitors, get shunted to the duct or acinar cell lineages, or undergo apoptosis. Although message levels were low in the RNA-seq data as discussed above, acinar cell transcripts were also reduced after *Wdr5* suppression. In contrast, duct cell transcripts were elevated compared to shScramble spheres, including the duct-specific gene *Car2* and several cytokeratins and mucins. These results suggest that the TrxG complexes are required for activation of a subset of genes during endocrine and acinar cell specification.

This raises the question as to why the endocrine and acinar cell lineages were particularly affected by *Wdr5* suppression but not the duct cell lineage. One explanation is that acinar and endocrine lineage-specific genes require activation by the TrxG complexes, whereas duct genes have already been activated in pancreas progenitors and do not require further maintenance by the TrxG complexes. In support of this hypothesis, the expression of genes already activated in pancreas progenitors, such as *Foxa1, Foxa2, Gata4, Gata6* and *Pdx1*, were unaffected by *Wdr5*

suppression and are already in an active chromatin state in MPCs [35]. This suggests that genes in an active chromatin state in pancreas progenitors do not require the TrxG complexes for gene expression maintenance. However, the endocrine lineage master regulator *Neurog3* and downstream genes *Neurod1, Nkx2-2, Nkx6-1* and *Pax6* are marked by H3K27me3 in pancreas progenitors [35]. This suggests that *Neurog3* activation and endocrine specification requires removal of the repressive H3K27me3 modification by TrxG-associated KDMs such as KDM6A and KDM6B. Disruption of TrxG complex assembly by *Wdr5* suppression in pancreas progenitors could therefore impair recruitment of KDMs to *Neurog3* during endocrine specification. There is also evidence that the TrxG complexes interact with nucleosome remodeling complexes and proteins associated with Pol II [182,196,197], suggesting that disruptions of these interactions could prevent activation of endocrine and acinar lineage-specific genes. In addition, DNA methylation prevents gene activation and is removed at developmentally regulated genes during differentiation [153]. Thus, failed demethylation at endocrine and acinar lineage-specific genes is another potential mechanism that may prevent differentiation of the endocrine and acinar lineages in sh*Wdr5* progenitors.

Collectively, these results demonstrate that the TrxG complex proteins DPY30 and WDR5 are expressed in the mouse embryonic pancreas and that the TrxG complexes have a role in pancreas spheroid development. My data suggests that pancreas progenitors require the TrxG complexes for cell proliferation and/or survival. Further, these findings support a hypothesis whereby the catalytic and/or non-catalytic activities of the TrxG complexes are required for activation of a subset of lineage-specific genes during endocrine and acinar cell specification but not for maintenance of progenitor or duct cell gene expression.

Chapter 4: TrxG catalytic activity regulates pancreas progenitor survival, endocrine cell specification and acinar cell differentiation

4.1 Background

Pancreas development is mediated by external signals, transcription factors and chromatin regulators that direct gene expression and regulate cell proliferation and differentiation [1,176]. In both mouse and human development, pancreas- and islet-specific *cis*-regulatory elements become poised for activation with enrichment for H3K4 methylation [180,226], suggesting a role for H3K4 methylation in driving gene expression in the pancreas. In Chapter 3, I discovered that suppression of *Wdr5* in pancreas progenitor spheroids decreased endocrine and acinar cell differentiation. However, in addition to loss of H3K4 methyltransferase activity, the TrxG complexes do not assemble in the absence of the WDR5 subunit [185,258,259,261-263]. Since the TrxG complexes have non-enzymatic co-activator roles that include the recruitment of nucleosome remodeling complexes and KDMs [183,190,196,197], it was unclear in this model whether the catalytic or non-catalytic co-activator functions of the TrxG complexes were essential for the activation of endocrine and acinar critical genes.

Thus, to clarify whether the catalytic or non-catalytic activities of the TrxG complexes are required for the activation of acinar and endocrine lineage-specific genes, I next focused on DPY30, a TrxG core protein that is not required for formation of the TrxG complexes [206] but is essential for full methyltransferase activity and methyl group specificity at H3 [197,263,280,289,290]. In the absence of DPY30, TrxG complex H3K4 methyltransferase activity is marginally reduced *in vitro* but completely lost *in vivo* [291], suggesting that DPY30 acts as a catalytic enhancer. The role of DPY30 in pancreas development has not been examined, but DPY30 has reported roles in cell

proliferation and differentiation in other tissues [206,279,280,289,292]. For example, suppression of *Dpy30* in a human neuron-committed cell line impairs proliferation and drives cellular senescence [279]. Suppression of *DPY30* in hESCs decreases endoderm specification and differentiation into pancreas and liver cells [206]. Importantly, impaired cell specification was the result of decreased H3K4 methylation and impaired expression of lineage-specific genes [206,280]. Thus, I **hypothesized** that the catalytic activity of TrxG complexes, and thus H3K4 methylation, is required for the activation of acinar and endocrine lineage-specific genes during pancreas progenitor differentiation.

In this Chapter, I investigate this using *Pdx1*-Cre driver mice to obtain embryonic deletion of *Dpy30* in PDX1^{+} progenitors. In these mice, I show that H3K4 methylation is rapidly depleted in the absence of DPY30, and I assessed the formation of pancreas progenitors, patterning into multipotent tip and bipotent trunk progenitors, and differentiation into the acinar and endocrine cell lineages.

4.2 Results

4.2.1 H3K4 methylation is reduced in *Dpy30ΔP* PDX1^{+} progenitors

To determine whether TrxG catalytic activity is required for activation of lineage-specific genes during *in vivo* pancreas progenitor differentiation, *Dpy30* was genetically deleted from PDX1^{+} progenitor cells using Cre-*lox* recombination (Figure 15A) [120]. Mice harbouring *loxP* sites flanking the 4th *Dpy30* exon (*Dpy30*$^{flox/flox}$) were bred to *Pdx1*-Cre driver mice to achieve recombination in the pancreas (*Pdx1*-Cre; *Dpy30*$^{flox/flox}$, or *Dpy30ΔP*). In all experiments, littermate *Dpy30*$^{flox/flox}$ or *Dpy30*$^{flox/WT}$ (*Pdx1*-Cre-negative) embryos were used as controls. Since PDX1 is highly expressed in pancreas progenitors from E8.5 and is required for pancreas growth [2,4,69], *Pdx1*-Cre mice are commonly used for "pancreas-specific" recombination. However, PDX1 is also expressed in the duodenum, stomach, common bile duct and the brain [1,293,294] and recombination also occurs in these cells.

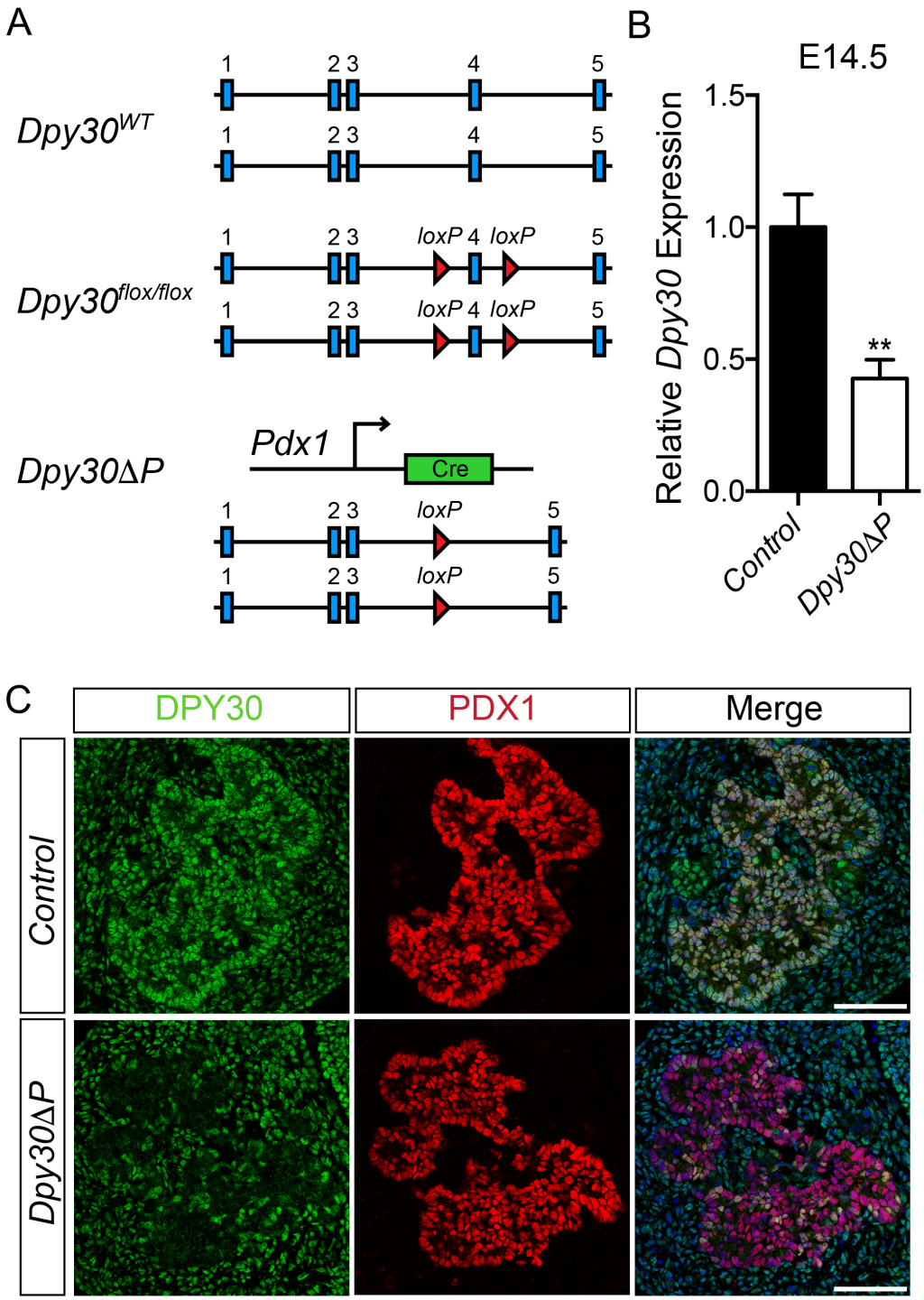

Figure 15: Efficient *Dpy30* recombination in PDX1^{+} pancreas cells of *Dpy30ΔP* embryos.
(A) Schematic of a wildtype *Dpy30* locus (*Dpy30*^{WT}) with 5 coding exons, an exon 4 targeted *Dpy30* locus (*Dpy30*$^{flox/flox}$) and a *Pdx1*-Cre recombined *Dpy30* locus (*Dpy30ΔP*). **(B)** Relative expression of *Dpy30* at E14.5 from control (*Dpy30*$^{flox/flox}$ or *Dpy30*$^{flox/WT}$) and *Dpy30ΔP* pancreas. Data are relative to β-actin; n = 7; ** denotes $P < 0.01$ *Dpy30ΔP* vs. control; unpaired, two-tailed Student's t test. **(C)** IF staining of DPY30 (green) and PDX1 (red) in E12.5 control and *Dpy30ΔP* pancreas. Merged images include nuclei stained with TOPRO-3 (blue). Scale bar, 75 μM.

To examine *Pdx1*-Cre-driven *Dpy30* recombination in the embryonic pancreas, I measured *Dpy30* transcript levels by qPCR and protein expression by immunofluorescence (IF). In the E14.5 *Dpy30*Δ*P* pancreas, *Dpy30* transcripts were decreased by ~57% compared to controls (Figure 15B). Given that the mesenchyme constitutes ~45% of total pancreas cells at E14.5 [109], a ~57% reduction in *Dpy30* suggested efficient recombination in PDX1$^+$ *Dpy30*Δ*P* epithelial cells. To confirm the disruption of *Dpy30* in PDX1$^+$ cells, I co-stained for DPY30 and PDX1 in E12.5 control and *Dpy30*Δ*P* whole embryonic sections. Confirming efficient disruption of *Dpy30*, DPY30 immunoreactivity was absent from ~85% of PDX1$^+$ cells in the *Dpy30*Δ*P* pancreas (Figure 15C). H3K4me1 and H3K4me3 immunoreactivity was also absent from ~85% of PDX1$^+$ cells in the *Dpy30*Δ*P* pancreas (Figure 16A-B). Together, these results demonstrate that *Pdx1*-Cre-mediated deletion of *Dpy30* results in loss of DPY30 protein and global loss of H3K4 methylation in PDX1$^+$ pancreas progenitors.

Next, I examined whether the global loss of H3K4 methylation from PDX1$^+$ cells perturbed expression of markers of MPCs, including NKX2-2, NKX6-1, PDX1 and SOX9, in the E12.5 pancreas. Despite the absence of H3K4me3 in the *Dpy30*Δ*P* pancreatic epithelium, NKX2-2 and NKX6-1 immunoreactivity was similar to controls (Figure 17A-B). In addition, immunoreactivity of PDX1 and SOX9 was unchanged in the E12.5 *Dpy30*Δ*P* pancreas (Figure 18A) and the total number of PDX1$^+$ and SOX9$^+$ cells was not significantly different from controls (Figure 18B-C). Overall, these results suggest that formation of multipotent pancreas progenitor cells is unaffected by loss of *Dpy30* or H3K4 methylation.

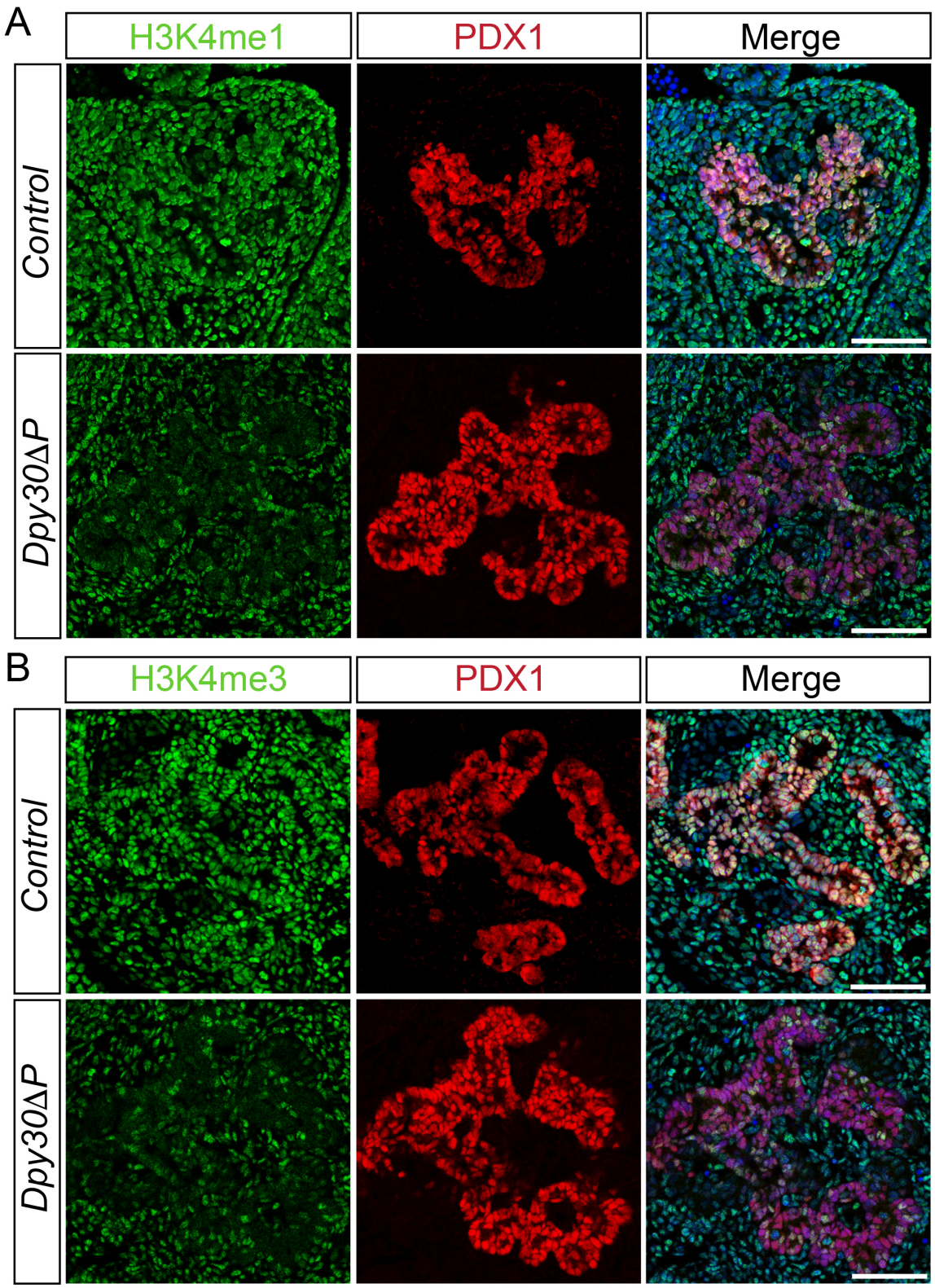

Figure 16: Global loss of H3K4 methylation in *Dpy30ΔP* PDX1^{+} pancreas cells.
Immunofluorescence staining of **(A)** H3K4me1 and **(B)** H3K4me3 in green with PDX1 (red) at E12.5 in control and *Dpy30ΔP* pancreas. Merged images include nuclei stained with TOPRO-3 (blue). Scale bar, 75 μM.

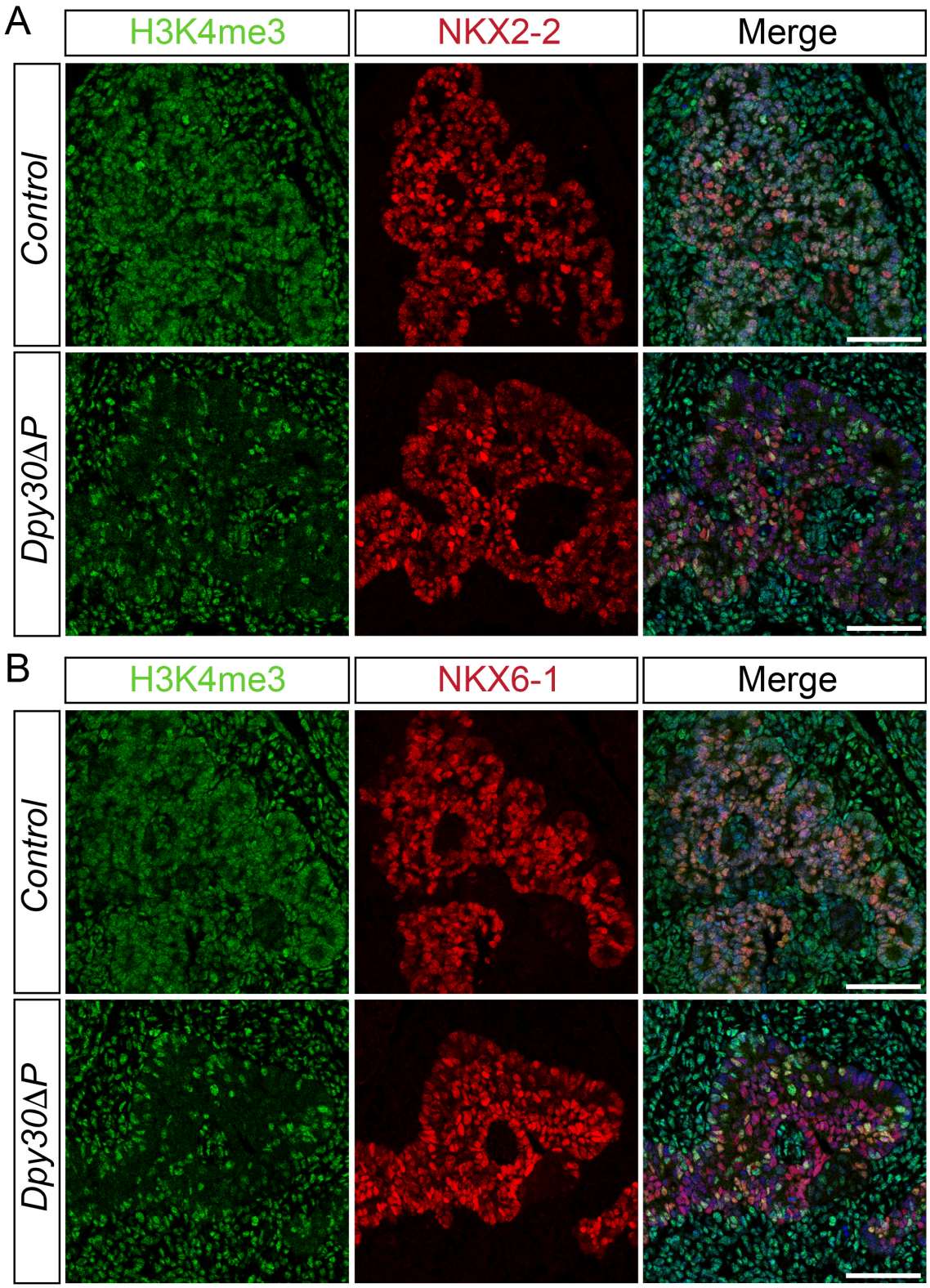

Figure 17: Maintenance of pancreas progenitors in *Dpy30ΔP* pancreas.
Immunofluorescence staining of H3K4me3 (green) with **(A)** NKX2-2 and **(B)** NKX6-1 (red)**.** Nuclei are stained with TOPRO-3 (blue). Scale bar, 75 μM.

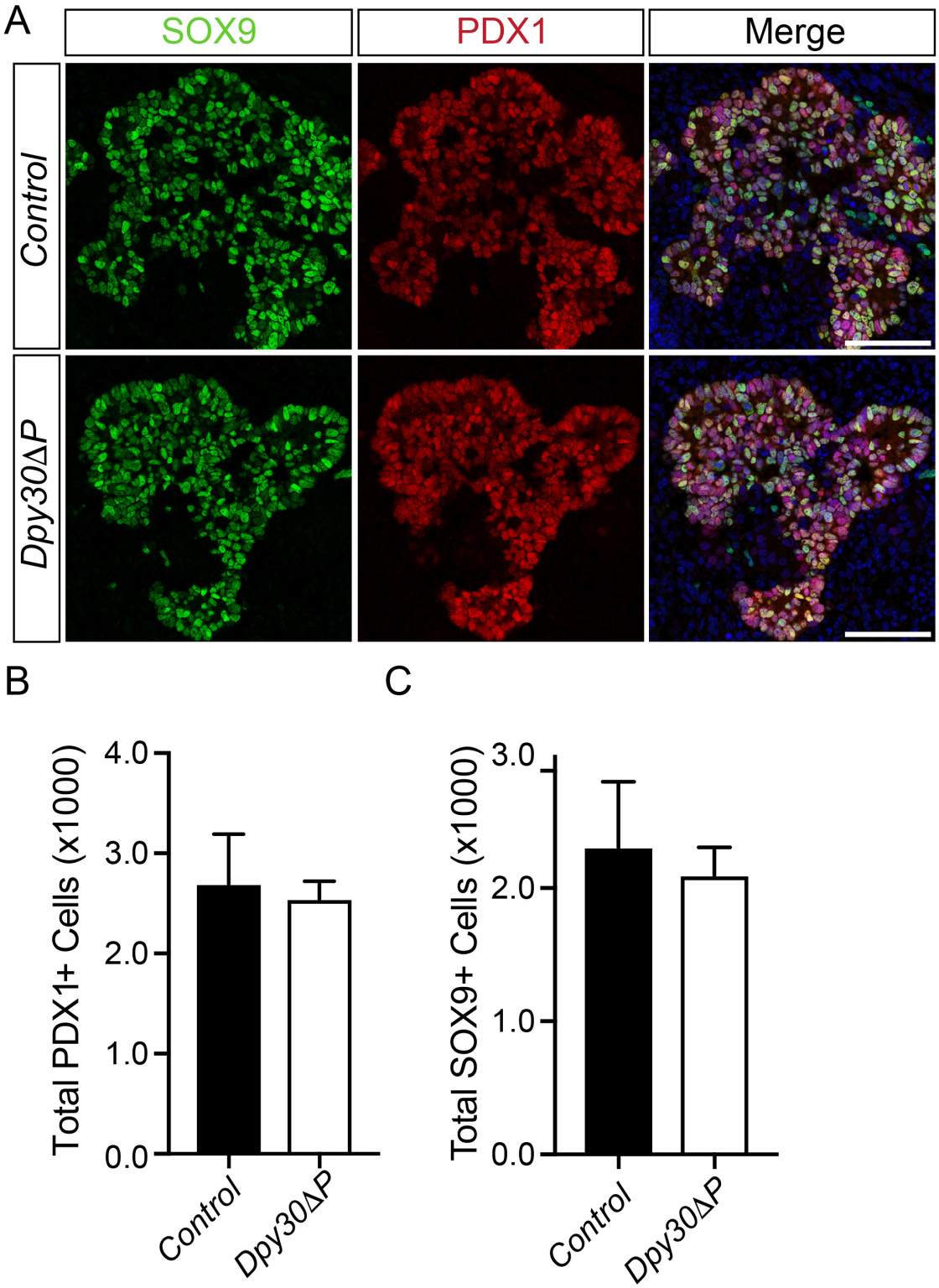

Figure 18: The total number of PDX1^{+} and SOX9^{+} cells is unchanged in E12.5 *Dpy30ΔP* pancreas.
(A) Immunofluorescence staining of SOX9 (green) and PDX1 (red) at E12.5 in control and *Dpy30ΔP* pancreas. Nuclei are stained with TOPRO-3 (blue). Scale bar, 75 μM. The total number of **(B)** PDX1^{+} and **(C)** SOX9^{+} cells at E12.5 in control and *Dpy30ΔP* pancreas. Data are represented as mean ± SEM; n = 3.

4.2.2 The *Dpy30ΔP* pancreas is hypoplastic

Although PDX1$^+$ and SOX9$^+$ cells were unaltered at E12.5, the total number of *Dpy30*Δ*P* pancreas cells was significantly decreased by ~50% at both E15.5 and E18.5 (Figure 19A). Accordingly, I also observed a decrease in the overall size of the E18.5 *Dpy30*Δ*P* pancreas compared to controls during pancreas dissections (Figure 19B). The equivalent reductions in total *Dpy30*Δ*P* pancreas cells at these stages suggested that an earlier progenitor defect in either proliferation or survival may have occurred. To investigate this, cumulative 5-ethylnyl-2'-deoxyuridine (EdU) incorporation was used to measure the proportion of proliferating PDX1$^+$ progenitors in E12.5 embryos [111]. A small (~15%) but significant reduction in the fraction of PDX1$^+$EdU$^+$ cells in the *Dpy30*Δ*P* pancreas was detected compared to controls (Figure 19C-D), suggesting that the ~50% reduction in pancreas cells may be partly due to a reduction in progenitor proliferation. To examine whether progenitor survival was also affected, I assessed apoptosis in E12.5 SOX9$^+$ progenitors by terminal deoxynucleotidyl transferase dUTP nick end labeling (TUNEL) staining. Compared to controls, the fraction of TUNEL$^+$SOX9$^+$ cells relative to total SOX9$^+$ cells was increased 1.7-fold ($P = 0.06$) in the E12.5 *Dpy30*Δ*P* pancreas (Figure 19E-F). Together, these findings suggest that the combined decrease in progenitor cell proliferation and an increase in progenitor cell apoptosis results in *Dpy30*Δ*P* pancreas hypoplasia over time.

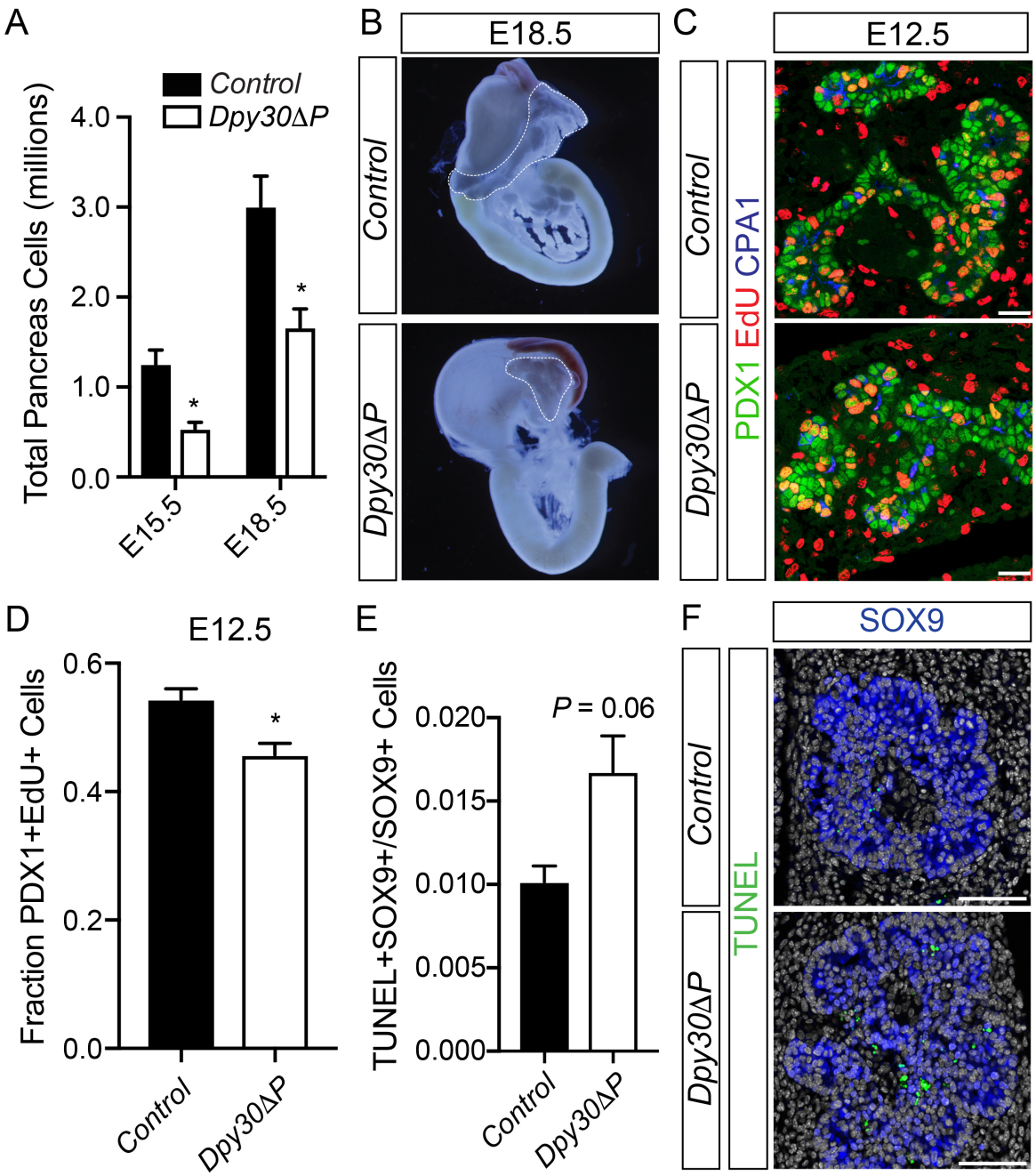

Figure 19: The *Dpy30ΔP* pancreas is hypoplastic.
(A) Total pancreas cells at E15.5 and E18.5 in control and *Dpy30ΔP* pancreas. Data represents mean ± SEM; n = 3; * denotes $P < 0.05$ *Dpy30ΔP* vs. control; unpaired, two-tailed Student's t test. **(B)** E18.5 control and *Dpy30ΔP* gut organs. Dorsal pancreas is outlined in white. **(C)** IF staining for PDX1 (green), EdU (red) and CPA1 (blue) in control and *Dpy30ΔP* pancreas at E12.5. Scale bar, 25 μM. **(D)** The fraction of proliferating $PDX1^{+}EdU^{+}$ pancreas progenitor cells relative to total $PDX1^{+}$ cells in E12.5 control and *Dpy30ΔP* pancreas following 3.5 hours of EdU labeling. Data are represented as mean ± SEM; n = 4; * denotes $P < 0.05$ *Dpy30ΔP* vs. control; unpaired, two-tailed Student's t test. **(E)** The fraction of $TUNEL^{+}SOX9^{+}$ cells relative to $SOX9^{+}$ cells from E12.5 control and *Dpy30ΔP* pancreas. Data are represented as mean ± SEM; n = 3; unpaired, two-tailed Student's t test. **(F)** IF staining for TUNEL (green) and SOX9 (blue) in control and *Dpy30ΔP* pancreas at E12.5. Nuclei are stained with DAPI (grey). Scale bar, 75 μM.

4.2.3 CPA1 immunoreactivity is reduced in the *Dpy30ΔP* pancreas

The multipotent pancreas progenitors undergo further branching morphogenesis between E12.5 and E15.5 and begin differentiation into the endocrine and exocrine lineages [2,3]. To assess the developmental morphology of the *Dpy30ΔP* pancreas during this stage, I examined hematoxylin and eosin (H&E) staining of pancreas paraffin sections from E12.5 to E15.5. Compared to controls, branching morphogenesis and overall pancreas structure appeared unaffected at all stages in the *Dpy30ΔP* pancreas (Figure 20). These results suggest that loss of *Dpy30* from PDX1^{+} progenitors does not affect pancreas morphology during these stages of development.

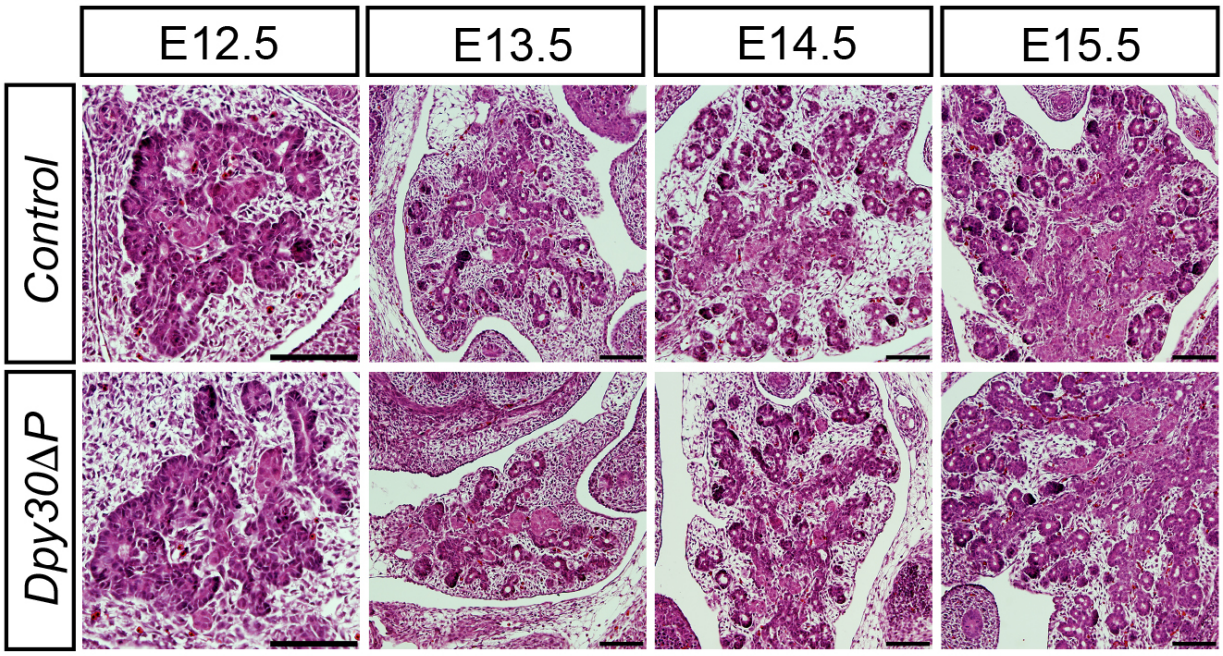

Figure 20: Developmental morphology of the embryonic *Dpy30ΔP* pancreas.
Hematoxylin and eosin (H&E) staining in control and *Dpy30ΔP* pancreas from E12.5 to E15.5. Scale bar, 100 μM.

Starting at E11.5, the pancreas epithelium becomes progressively more patterned with $CPA1^{+}SOX9^{+}$ multipotent progenitor cells (MPCs) and $CPA1^{+}$ acinar progenitors at "tips" and $SOX9^{+}$ bipotent progenitor cells (BPCs) in "trunks" [3,55]. Tip MPCs start to undergo acinar cell specification at ~E12.5 as SOX9 becomes restricted to trunk cells and enhanced cytosolic CPA1 expression is evident in differentiated acinar cells by E15.5 [2,55,90,91]. To assess tip and trunk patterning in the *Dpy30*Δ*P* pancreas, I co-stained for SOX9 and CPA1 between E12.5 and E15.5. At all stages, SOX9 immunoreactivity in the *Dpy30*Δ*P* pancreas was equivalent to controls (Figures 21 and 22). Although CPA1 staining was comparable between the control and *Dpy30*Δ*P* pancreas at E12.5, CPA1 immunoreactivity appeared decreased from *Dpy30*Δ*P* tip cells at E13.5 (Figure 21). While the control pancreas showed strong cytoplasmic CPA1 staining in E14.5 and E15.5 acinar cells at the epithelial tips, CPA1 immunoreactivity was comparatively decreased in the *Dpy30*Δ*P* pancreas at both stages (Figure 22). Collectively, these results suggest that tip and trunk patterning is maintained but CPA1 expression is reduced in the *Dpy30*Δ*P* pancreas starting at E13.5.

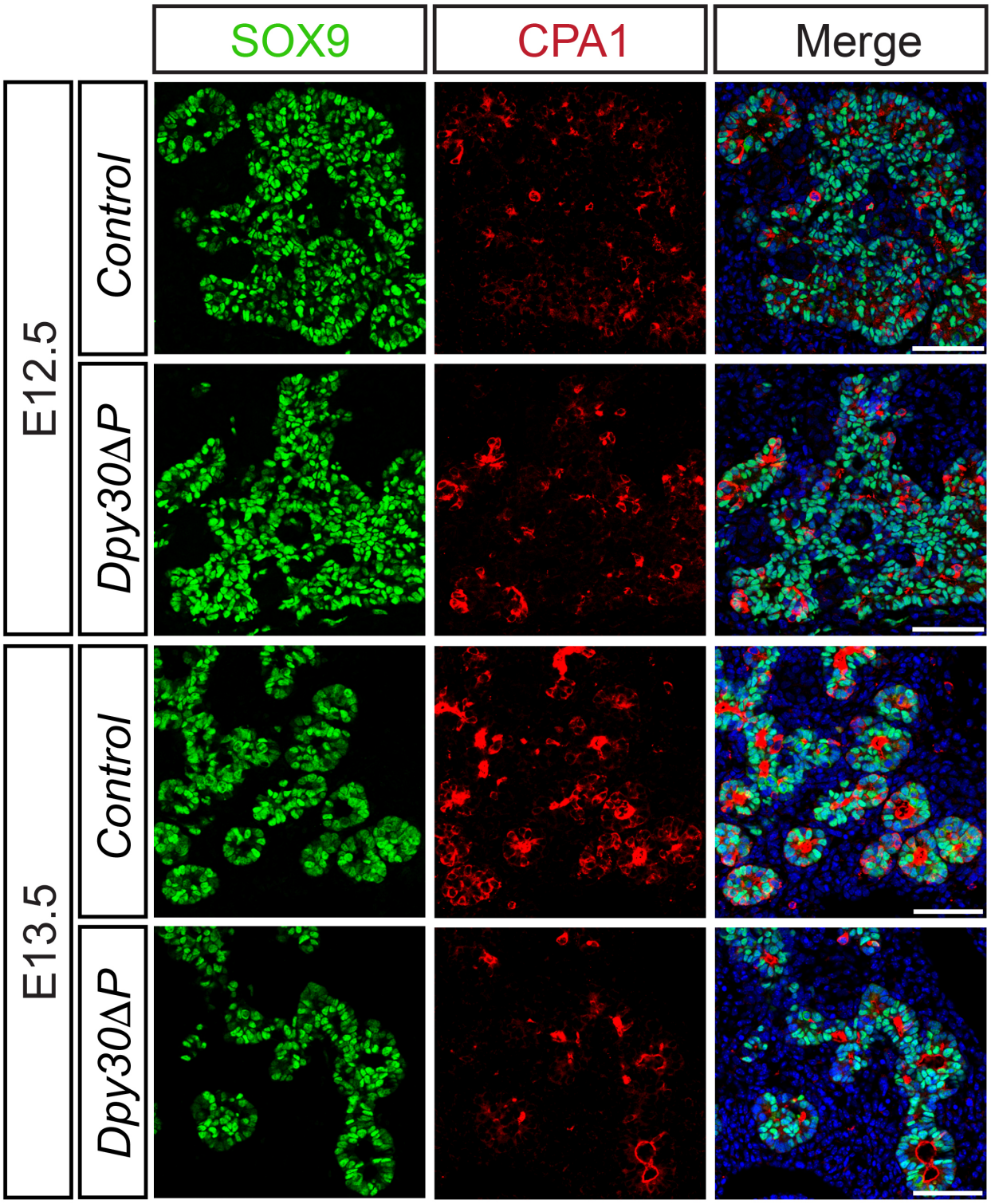

Figure 21: CPA1 immunoreactivity is reduced in E13.5 *Dpy30ΔP* tip cells.
Immunofluorescence staining of SOX9 (green) and CPA1 (red) at E12.5 and E13.5 in control and *Dpy30ΔP* pancreas. Nuclei are stained with TOPRO-3 (blue). Scale bar, 75 μM.

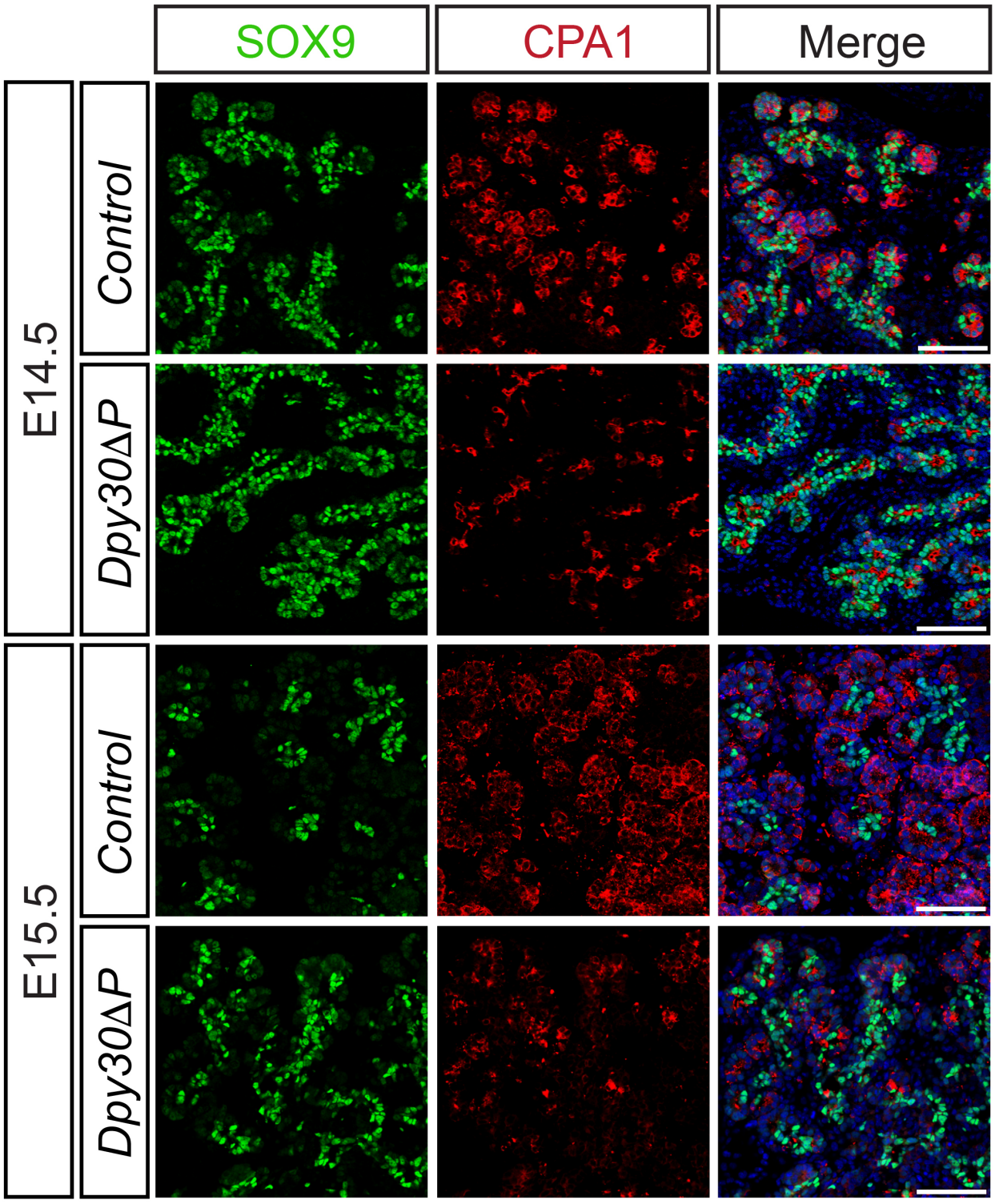

Figure 22: CPA1 immunoreactivity is decreased in *Dpy30ΔP* acinar cells.
Immunofluorescence staining of SOX9 (green) and CPA1 (red) at E14.5 and E15.5 in control and *Dpy30ΔP* pancreas. Nuclei are stained with TOPRO-3 (blue). Scale bar, 75 μM.

4.2.4 *Dpy30ΔP* acinar cell differentiation and maturation is impaired

Decreased CPA1 immunoreactivity in the E15.5 *Dpy30*Δ*P* pancreas suggested that the proportion of pancreatic acinar cells is reduced. Compared to controls, the fraction of amylase$^+$ cells relative to total pancreas cells was reduced by ~60% in the E15.5 *Dpy30*Δ*P* pancreas (Figure 23A-B). At E18.5, the proportion of *Dpy30*Δ*P* amylase$^+$ pancreatic area was decreased by ~40% (Figure 23C-D). Given that the major source of acinar tissue expansion from E15.5 onward is from proliferation of differentiated acinar cells [2], I examined whether acinar cell proliferation was reduced in the *Dpy30*Δ*P* pancreas. Co-staining of amylase with the G2M mitotic marker phospho-histone H3 (pHH3) at E15.5 revealed that the fraction of pHH3$^+$amylase$^+$ acinar cells was not changed in the *Dpy30*Δ*P* pancreas compared to controls (Figure 24A-B). These results suggest that the reduction in *Dpy30*Δ*P* acinar cells was not due to impaired acinar cell proliferation.

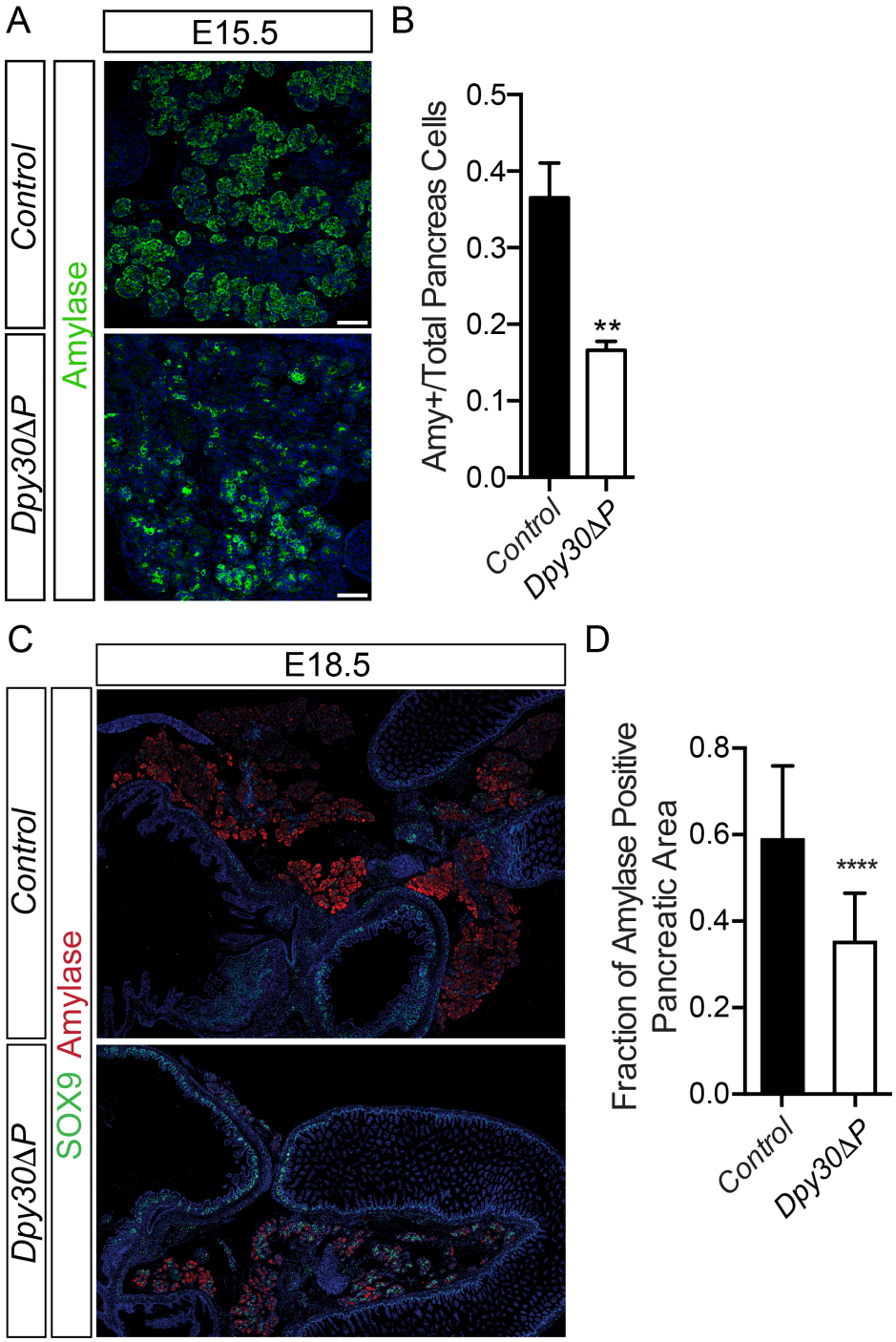

Figure 23: Amylase$^+$ acinar cells are reduced in the *Dpy30ΔP* pancreas.
(A) IF staining for amylase (green) in E15.5 control and *Dpy30ΔP* pancreas. Nuclei are stained with TOPRO-3 (blue). Scale bar, 75 μm. **(B)** The fraction of amylase$^+$ cells relative to total pancreas cells from E15.5 control and *Dpy30ΔP* pancreas. Data are represented as mean ± SEM; n = 3; ** denotes $P < 0.01$ *Dpy30ΔP* vs. control; unpaired, two-tailed Student's t test. **(C)** IF staining for Sox9 (green) and amylase (red) in E18.5 control and *Dpy30ΔP* pancreas. Nuclei are stained with TOPRO-3 (blue). **(D)** The fraction of amylase$^+$ area relative to total pancreas area from E18.5 control and *Dpy30ΔP* pancreas. Data are represented as mean ± SD; n = 3; **** denotes $P < 0.0001$ *Dpy30ΔP* vs. control; unpaired, two-tailed Student's t test.

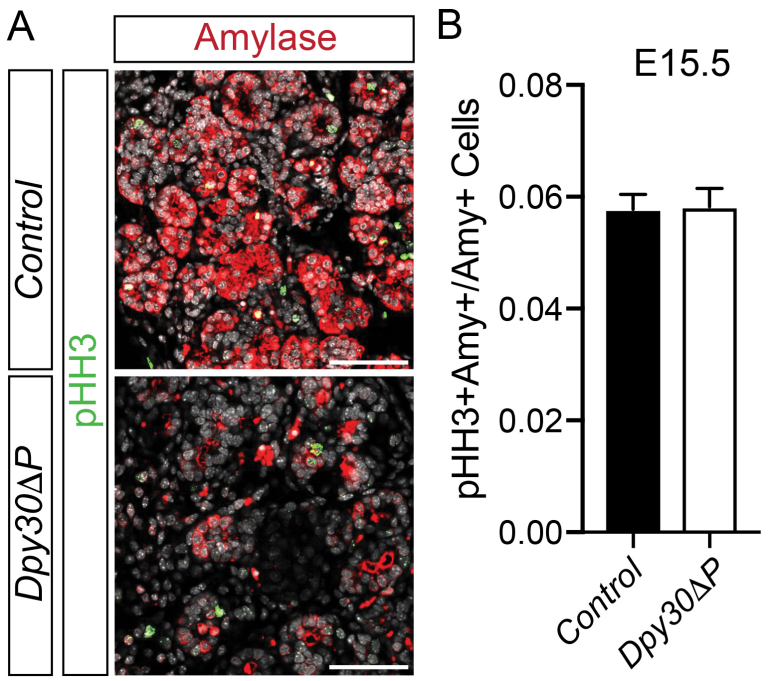

Figure 24: Acinar cell proliferation is not altered in the *Dpy30ΔP* pancreas.
(A) IF staining for pHH3 (green) and amylase (red) in control and *Dpy30ΔP* pancreas at E15.5. Nuclei are stained with DAPI (grey). Scale bar, 75 M. **(B)** The fraction of pHH3^{+}amylase^{+} cells relative to amylase^{+} cells from E15.5 control and *Dpy30ΔP* pancreas. Data are represented as mean ± SEM; n = 3.

To determine whether acinar cells in the *Dpy30ΔP* pancreas were differentiated, I first assessed acinar cell gene expression. Given that specification of acinar cells occurs when RBPJ is replaced with RBPJL in the PTF1A complex (Masui et al. 2007; Arda et al., 2013), I evaluated *Rbpj* and *Rbpjl* transcript levels by qPCR at E14.5. While *Rbpj* expression was unaffected, *Rbpjl* transcripts were significantly decreased by ~50% in the *Dpy30ΔP* pancreas compared to controls (Figure 25A). Further acinar cell gene expression was performed using NanoString *SPRINT* profiling at E15.5. While significant reductions were detected in *Dpy30* (>3-fold) and *Cpa1* (>3-fold) (Figure 25B), as well as *Bhlha15* (2-fold), *Gata4* (1.6-fold) and *Rbpjl* (1.8-fold) (Figure 25C), expression of *Myc, Nr5a2, Ptf1a* and *Rbpj* were not significantly altered (Figure 25C). These results demonstrate decreased expression of a subset of genes involved in acinar cell differentiation after disruption of *Dpy30* in the pancreas.

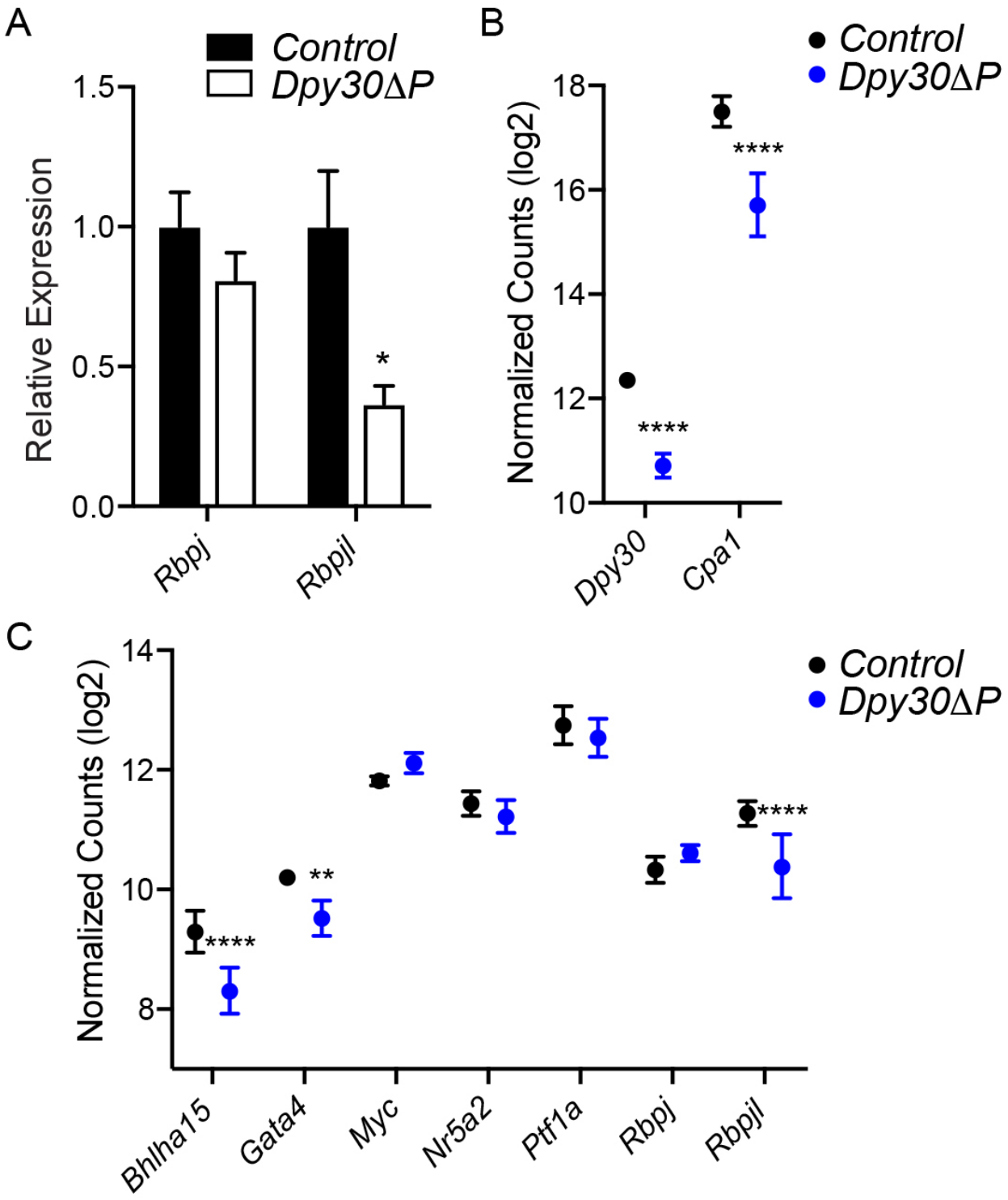

Figure 25: Acinar cell differentiation is impaired.
(A) Relative expression of *Rbpj* and *Rpbjl* transcripts from E14.5 control and *Dpy30ΔP* pancreas. Data are relative to β-actin; n = 4-7; * denotes $P < 0.05$ *Dpy30ΔP* vs. control; unpaired, two-tailed Student's t test. **(B-C)** Acinar gene expression analysis from E15.5 control and *Dpy30ΔP* pancreas. Data are represented as the geometric mean ± geometric SD; n = 5; ** denotes $P < 0.01$ and **** denotes $P < 0.0001$ *Dpy30ΔP* vs. control; unpaired, two-tailed Student's t test with a Benjamini, Krieger and Yekutieli 1% FDR correction for multiple comparisons.

To investigate whether reduced acinar cell gene expression in the *Dpy30*Δ*P* pancreas impacted acinar cell histology, I examined acinar cell morphology by H&E staining at E15.5 and E18.5. Although H&E staining was similar in the E15.5 control and *Dpy30*Δ*P* pancreas, a visible impairment in *Dpy30*Δ*P* acinar cell morphology was observed at E18.5 (Figure 26). The control illustrated an organized pancreas with compact acinar cells displaying enlarged cytoplasmic area staining strongly for eosin (in pink), surrounding the duct and endocrine cells stained for hematoxylin (in blue/violet). In contrast, the E18.5 *Dpy30*Δ*P* pancreas was disorganized and loosely associated, with many abnormal clusters of cystic cells that did not have the characteristic morphology of either acinar or duct cells (Figure 26A, black arrowheads). Compared to the acinar cells in the E18.5 control pancreas, these *Dpy30*Δ*P* cystic cells displayed increased luminal space and decreased cytoplasmic area identified by decreased eosin staining.

To determine whether the abnormal cells in the E18.5 *Dpy30*Δ*P* pancreas were acinar or duct cells, I immunostained E18.5 control and *Dpy30*Δ*P* pancreas for acinar and duct cell markers. Co-staining with H3K4me3 revealed that the cystic structures in the *Dpy30*Δ*P* pancreas were absent for H3K4me3 immunoreactivity, in addition to the mature acinar enzymes Cpa1 and amylase, or the mature duct cell marker DBA lectin (Figure 27A, white arrowheads). While mature duct cells formed and stained for DBA lectin and SOX9 in the *Dpy30*Δ*P* pancreas (Figure 27A-B), the cystic cells were neither DBA lectin^{+} or SOX9^{+}, but did stain for E-cadherin and MUC1 (Figure 27B). Further, duct cell gene expression analysis at E15.5 by NanoString *SPRINT* profiling demonstrated that none of the duct cell transcripts examined, including *Hes1, Hnf1b, Gata6*, *Onecut1* and *Sox9,* were affected in the *Dpy30*Δ*P* pancreas [1,81]. Together, these results suggest that disruption of *Dpy30* in the pancreas impairs acinar cell differentiation and maturation, leading to the abnormal development of cysts.

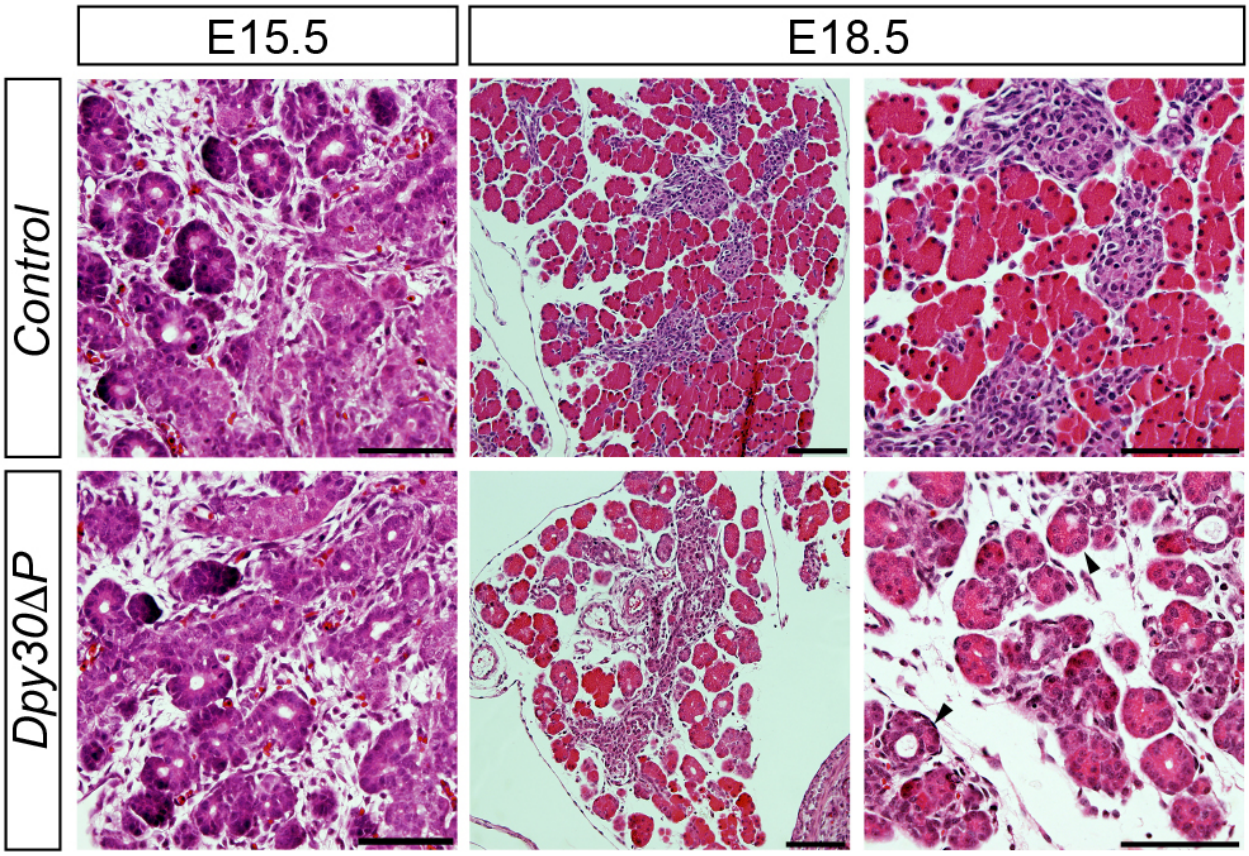

Figure 26: Abnormal cell morphology in the *Dpy30ΔP* pancreas.
H&E staining at E15.5 and E18.5 in control and *Dpy30ΔP* pancreas. Black arrowheads = disorganized, cystic cells. Scale bar, 100 μM.

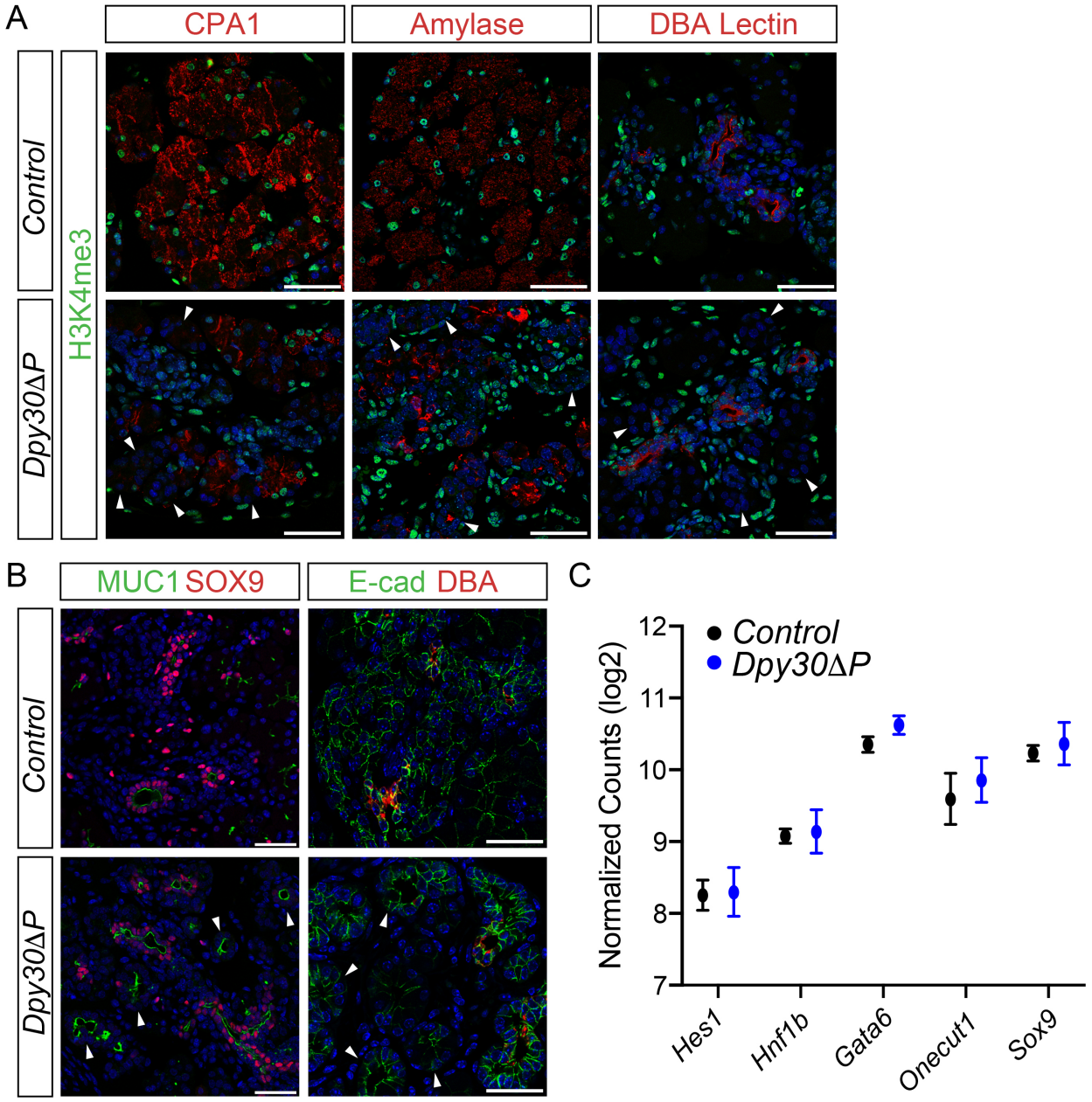

Figure 27: Abnormal *Dpy30ΔP* cells do not stain for mature acinar or duct cell markers.
(A) IF staining of H3K4me3 (green) with CPA1, amylase or DBA lectin (red) in control and *Dpy30ΔP* pancreas at E18.5. White arrowheads = low level or CPA1-, amylase- or DBA lectin-negative *Dpy30ΔP* cells. Nuclei are stained with TOPRO-3 (blue). Scale bar, 50 μM. **(B)** IF staining of MUC1 (green) with SOX9 (red) and E-cadherin (green) with DBA lectin (red) in control and *Dpy30ΔP* pancreas at E18.5. White arrowheads = *Dpy30ΔP* cells that do not stain for SOX9 or DBA lectin, but are positive for MUC1 and E-cadherin. Nuclei are stained with TOPRO-3 (blue). Scale bar, 50 μM. **(C)** Duct gene expression analysis from E15.5 control and *Dpy30ΔP* pancreas. Data are represented as the geometric mean ± geometric SD; n = 5.

4.2.5 Loss of *Dpy30* impairs NEUROG3$^+$ endocrine progenitor cell specification

To determine whether the endocrine cell lineage was impacted by loss of *Dpy30*, I first assessed the specification of SOX9$^+$ BPCs into NEUROG3$^+$ endocrine progenitors at E14.5. Although NEUROG3$^+$ cells were detected in the absence of H3K4me3 (Figure 28A), the NEUROG3$^+$/SOX9$^+$ cell ratio was significantly reduced in the *Dpy30*Δ*P* pancreas compared to controls, equating to ~50% fewer NEUROG3$^+$ endocrine progenitors (Figure 28B-C). Further, the reduced NEUROG3$^+$/SOX9$^+$ ratio was due to a ~50% reduction in NEUROG3$^+$ cells (Figure 28D) and not changes in the number of SOX9$^+$ cells (Figure 28E). During endocrine progenitor specification, reduced Notch signaling in BPCs decreases expression of the pro-endocrine repressor *Hes1,* allowing SOX9 to activate *Neurog3* (Shih et al., 2012). To assess whether decreased NEUROG3$^+$ cells in the *Dpy30*Δ*P* pancreas resulted from continued Notch and HES1-mediated repression of *Neurog3*, I measured *Notch1* and *Hes1* mRNA by qPCR in E14.5 control and *Dpy30*Δ*P* pancreas. Although *Neurog3* transcripts were reduced by ~50% (consistent with the ~50% reduction in NEUROG3$^+$ cells), expression of *Hes1, Notch1* and *Sox9* were not significantly altered (Figure 29), suggesting that Notch signaling did not contribute to the reductions in NEUROG3$^+$ cells. Overall, these data demonstrate that in the absence of H3K4 methylation in trunk progenitors, the total number of specified NEUROG3$^+$ endocrine progenitor cells is reduced by 50%.

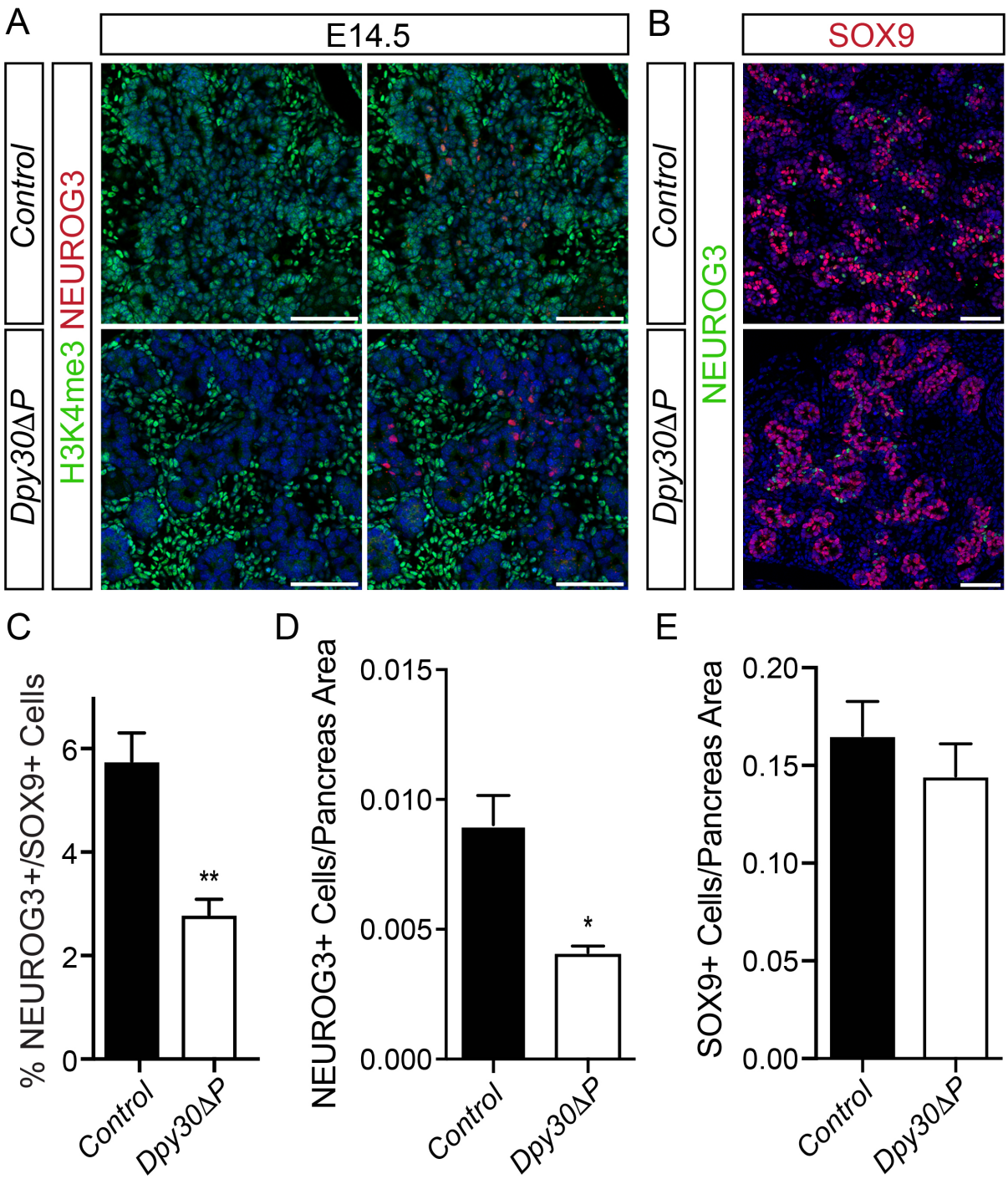

Figure 28: NEUROG3$^+$ endocrine progenitors are decreased by 50% in the *Dpy30ΔP* pancreas.
(A-B) IF staining of E14.5 control and *Dpy30ΔP* pancreas with **(A)** H3K4me3 (green) and NEUROG3 (red) or **(B)** SOX9 (red) and NEUROG3 (green). Nuclei are stained with TOPRO-3 (blue). Scale bar, 75 μM. **(C)** Quantification of % NEUROG3$^+$ cells relative to SOX9$^+$ cells in E14.5 control and *Dpy30ΔP* pancreas. Data are represented as mean ± SEM; n = 3; ** denotes $P < 0.01$ *Dpy30ΔP* vs. control; unpaired, two-tailed Student's t test. **(D-E)** The fraction of **(D)** NEUROG3$^+$ or **(E)** SOX9$^+$ cells relative to pancreas area in E14.5 control and *Dpy30ΔP* pancreas. Data are represented as mean ± SEM; n = 3; * denotes $P < 0.05$ *Dpy30ΔP* vs. control; unpaired, two-tailed Student's t test.

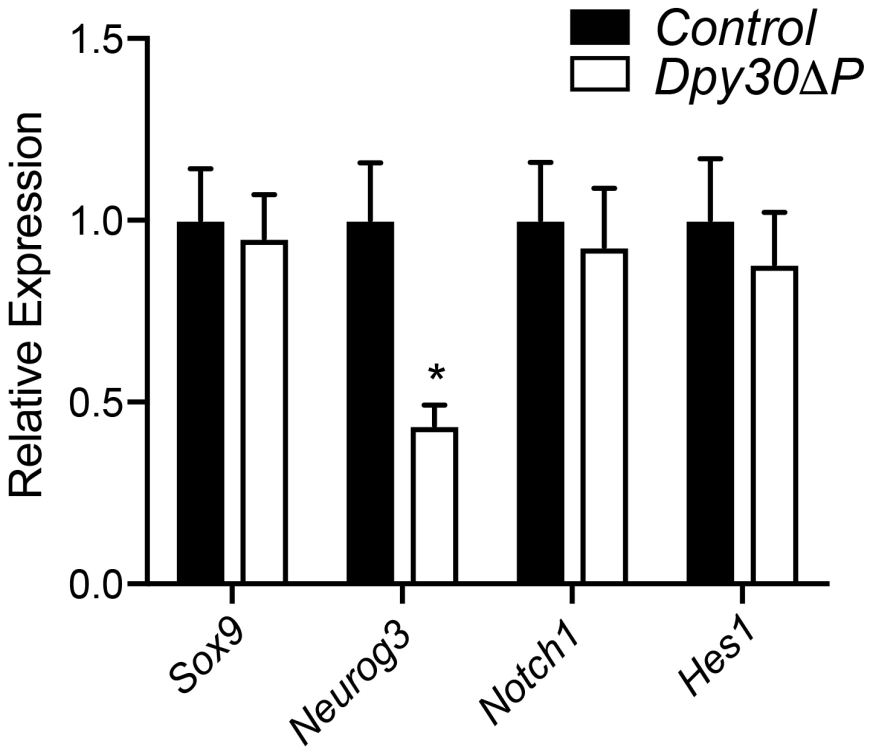

Figure 29: Notch signaling is unaffected in the *Dpy30ΔP* pancreas.
Relative expression of *Sox9, Neurog3, Notch1* and *Hes1* transcripts in E14.5 control and *Dpy30ΔP* pancreas. Data are relative to β-actin; n = 4-7; * denotes $P < 0.05$ *Dpy30ΔP* vs. control; unpaired, two-tailed Student's t test.

4.2.6 Endocrine cell differentiation is unaffected in the *Dpy30ΔP* pancreas

To investigate whether the reduced number of NEUROG3$^+$ endocrine progenitors in the *Dpy30ΔP* pancreas completed differentiation into hormone-expressing endocrine cells, I first examined the proportion of insulin$^+$ β-cells and glucagon$^+$ α-cells at E15.5 and E18.5. At both stages, insulin$^+$ and glucagon$^+$ cells were detected by IF staining but were visibly reduced in number in the *Dpy30ΔP* pancreas compared to controls (Figure 30A). Quantitatively, the fractions of insulin$^+$ β-cells and glucagon$^+$ α-cells relative to total pancreas cells were respectively decreased by ~40% and ~50% at E15.5, and by ~60% and ~50% at E18.5 (Figure 30B). These results demonstrate that the reduced proportion of NEUROG3$^+$ endocrine progenitors differentiate to a similar proportion of α- and β-cells in the E15.5 and E18.5

*Dpy30*Δ*P* pancreas. In confirmation, endocrine cell proliferation was measured by co-staining pHH3 with the pan-endocrine marker chromogranin A (CHGA), and the fraction of $pHH3^{+}CHGA^{+}$ cells was not changed between control and *Dpy30*Δ*P* pancreas at E15.5 (Figure 31A-B) or at E18.5 (Figure 31C). Together, these results suggest that loss of H3K4 methylation does not impair endocrine cell proliferation, but rather, the reduced proportions of differentiated α- and β-cells in the *Dpy30*Δ*P* pancreas are due to decreased $NEUROG3^{+}$ endocrine progenitors.

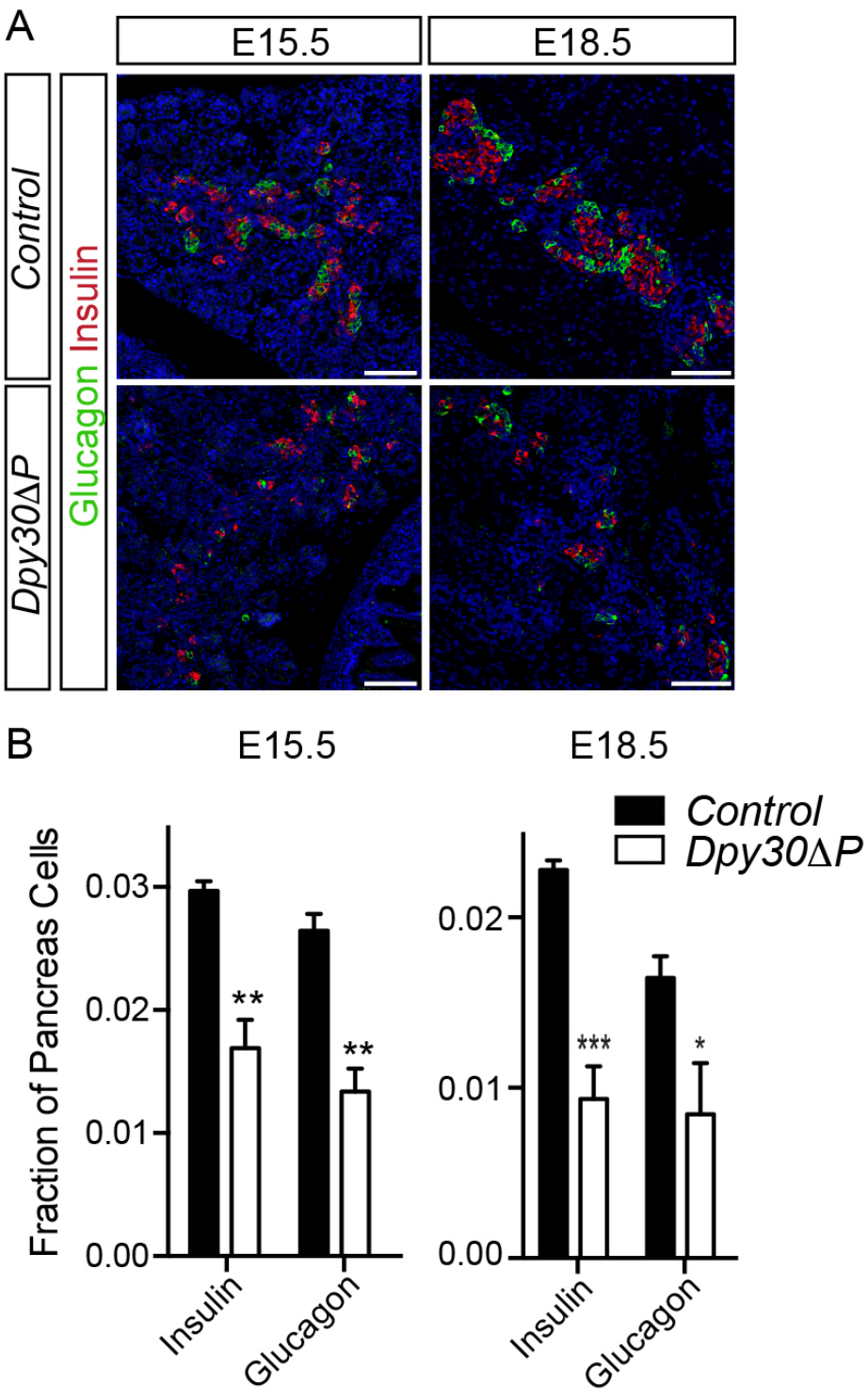

Figure 30: The number of α- and β-cells is reduced in the *Dpy30ΔP* pancreas.
(A) IF staining for insulin (red) and glucagon (green) in control and *Dpy30ΔP* pancreas at E15.5 and E18.5. Nuclei are stained with TOPRO-3 (blue). Scale bar, 100 μm. **(B)** The fraction of insulin$^+$ and glucagon$^+$ cells relative to total pancreas cells at E15.5 and E18.8 in control and *Dpy30ΔP* pancreas. Data are represented as mean ± SEM; n = 3; * denotes $P < 0.05$, ** denotes $P < 0.01$ and *** denotes $P < 0.001$ *Dpy30ΔP* vs. control; unpaired, two-tailed Student's t test**.**

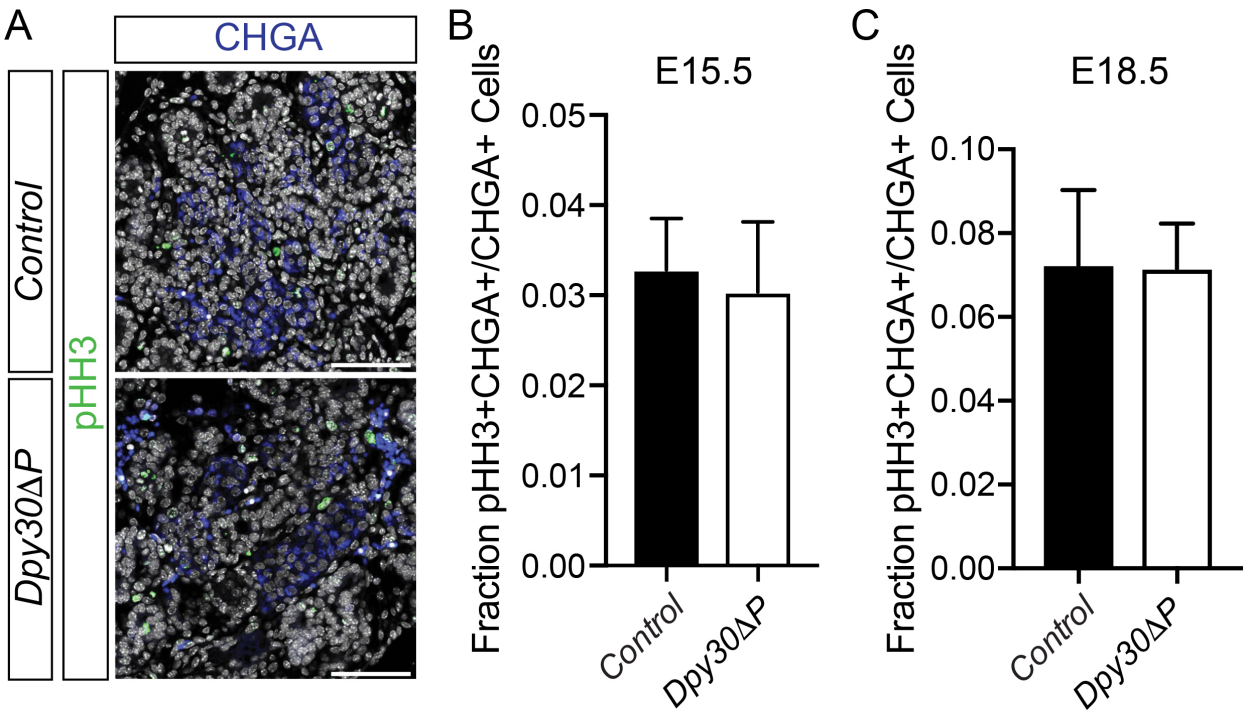

Figure 31: Endocrine cell proliferation is unchanged.
(A) IF staining for pHH3 (green) and chromogranin A (CHGA, blue) in control and *Dpy30ΔP* pancreas at E15.5. Scale bar, 75 M. **(B-C)** The fraction of pHH3^{+}CHGA^{+} cells relative to CHGA^{+} cells from **(B)** E15.5 and **(C)** E18.5 control and *Dpy30ΔP* pancreas. Data are represented as mean ± SEM; n = 3.

To examine whether the insulin^{+} β-cells that form in the *Dpy30*Δ*P* pancreas express transcription factors involved in β-cell differentiation or maturation, I co-stained for insulin and MAFA, NKX2-2, NKX6-1 or PAX6 in the E18.5 pancreas. Compared to controls, the fraction of insulin^{+} cells that stained for MAFA, NKX2-2, NKX6-1 and PAX6 was not significantly different in the *Dpy30*Δ*P* pancreas (Figure 32A-B). Importantly, insulin^{+} β-cells in the *Dpy30*Δ*P* pancreas were mosaic for H3K4me3 immunoreactivity (Figure 32C), demonstrating that the β-cells detected did not solely arise from unrecombined cells in the *Dpy30*Δ*P* pancreas. These results suggest that terminal β-cell markers are not affected by loss of H3K4 methylation and suggest that endocrine cell differentiation is unaffected in the *Dpy30*Δ*P* pancreas.

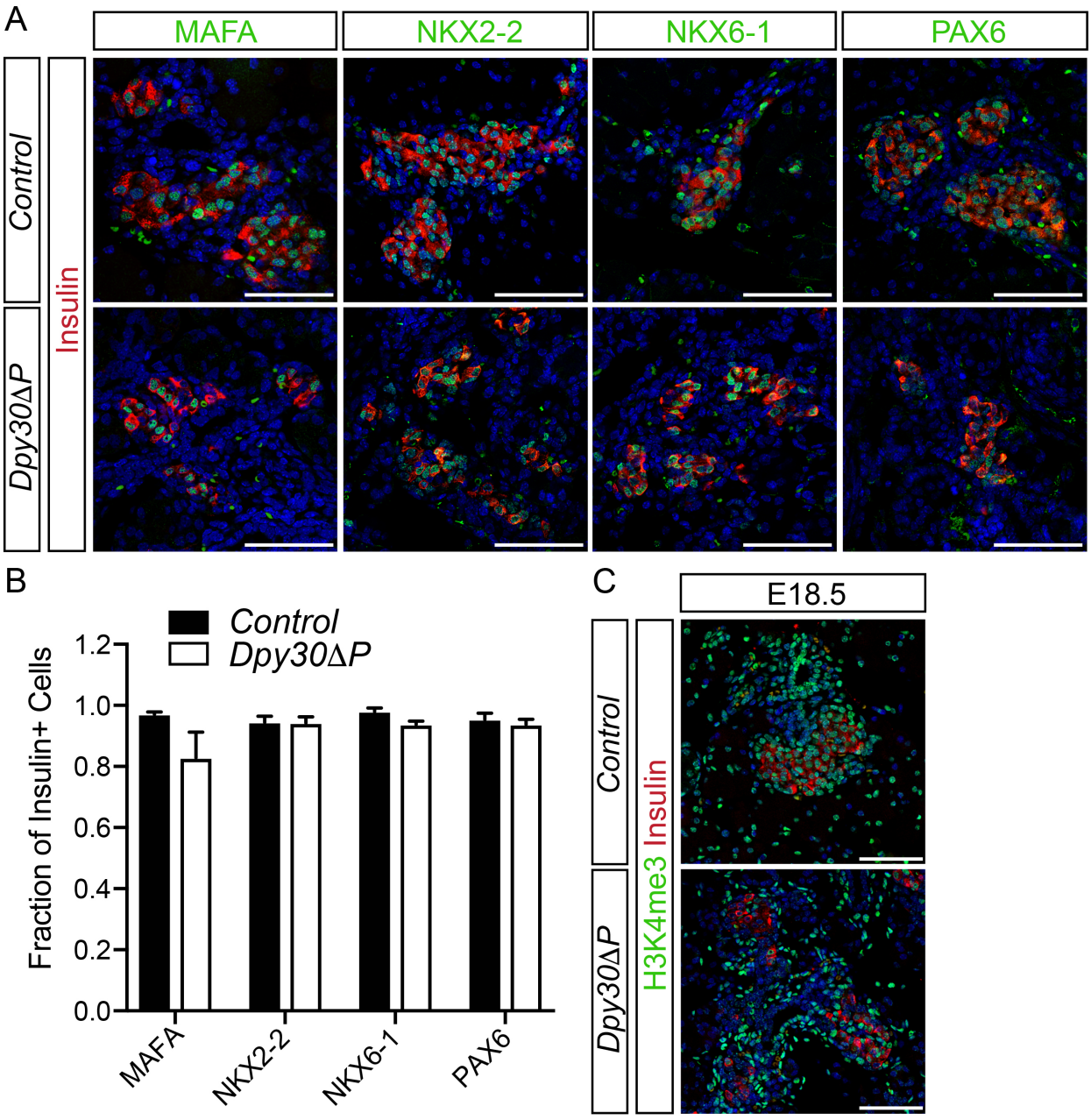

Figure 32: *Dpy30ΔP* endocrine cells express terminal islet transcription factors.
(A) IF staining for insulin (red) and MAFA, NKX2-2, NKX6-1 and PAX6 (green) in control and *Dpy30ΔP* pancreas at E18.5. Nuclei are stained with TOPRO-3 (blue). Scale bar 75 μM. **(B)** The fraction of insulin^{+} cells that stained for MAFA, NKX2-2, NKX6-1 and PAX6 in control and *Dpy30ΔP* pancreas at E18.5. Data are represented as mean ± SEM; n = 3-7. (**C**) IF staining in E18.5 control and *Dpy30ΔP* pancreas for insulin (red) with H3K4me3 (green). Nuclei are stained with TOPRO-3 (blue). Scale bar, 75 μm.

4.3 Discussion

In this Chapter, I determined the role of TrxG catalytic activity in mediating gene expression during mouse pancreas progenitor differentiation. Disruption of *Dpy30* in PDX1$^+$ cells resulted in a global loss of H3K4 methylation in E12.5 embryos, but did not impair the formation of pancreas progenitor cells. However, reduced progenitor proliferation and increased apoptosis in the early *Dpy30ΔP* pancreas decreased the overall pancreas size later in development. While loss of H3K4 methylation impaired NEUROG3$^+$ endocrine progenitor specification, further differentiation into α- and β-cells was not affected. In contrast, TrxG catalytic activity appears to be particularly required for acinar cell differentiation and maturation as disorganized cystic structures develop in the exocrine pancreas in its absence.

In the E12.5 *Dpy30*Δ*P* pancreas, global loss of H3K4 methylation did not disturb MPC formation or the patterning of tip and trunk cells. The total number of PDX1$^+$ and SOX9$^+$ cells was not altered and IF staining for CPA1, NKX2-2, NKX6-1, PDX1 and SOX9 was also unchanged. In addition, H&E staining indicated that the overall *Dpy30*Δ*P* pancreas morphology was not affected at E12.5, suggesting normal branching morphogenesis. Despite this, the first impairment in *Dpy30*Δ*P* pancreas development was detected at E12.5. Cumulative EdU labeling demonstrated that proliferation of PDX1$^+$ cells was marginally (~15%) but significantly reduced. Further, TUNEL staining at E12.5 indicated that the proportion of SOX9$^+$ cells undergoing apoptosis was increased by ~60% in the *Dpy30*Δ*P* pancreas. This is consistent with many other reports that indicate a role for DPY30 and other TrxG complex proteins in cell proliferation and/or survival [265,266,268,269,271,277-280,283]. Since progenitor cell number was maintained at E12.5 but cell proliferation and death were altered, this is likely the start of the developmental defect in the *Dpy30*Δ*P* pancreas. Given that the final size of the pancreas depends on the pool of

progenitors at E12.5 [2], it is not surprising that the E12.5 *Dpy30*Δ*P* progenitor cell defect progressed to a ~50% decrease in overall pancreas size by E15.5. Additionally, the ~50% decrease in total pancreas cells remained constant at E18.5, suggesting no further reductions in cell number occurred between these stages. Together, these data suggest that H3K4 methylation is required to maintain pancreas progenitor cell proliferation and survival.

Although acinar cells did develop in the *Dpy30*Δ*P* pancreas, the proportion of amylase^{+} acinar cells was decreased by ~50% at E15.5 and E18.5. This reduction was not the result of impaired acinar cell proliferation, since co-staining of amylase with pHH3 demonstrated that acinar cell proliferation was not altered in the E15.5 *Dpy30*Δ*P* pancreas. However, acinar cells failed to completely differentiate and mature. Differentiation of acinar cells begins during the secondary transition with the replacement of RBPJ with RBPJL in the PTF1A complex [125]. The RBPJL-PTF1A complex drives acinar cell maturation with robust induction of digestive enzymes, such as CPA1 and amylase, and is mostly completed by E17.5 [90,126]. In the *Dpy30*Δ*P* pancreas, the expression level of several acinar cell markers was reduced compared to controls. Beginning at E14.5, expression of *Rbpjl* was reduced by ~60% while expression of the immature form, *Rbpj*, was maintained in the *Dpy30*Δ*P* pancreas. This reduction in *Rbpjl* suggested that the initial step in acinar cell differentiation was impaired in the *Dpy30*Δ*P* pancreas. Significant reductions in expression of the acinar cell genes *Bhlha15*, *Cpa1* and *Gata4* (~50-70%) were also detected at E15.5, indicating impaired acinar cell differentiation downstream of *Rbpjl*. In addition, immunostaining for CPA1 and amylase was reduced in the *Dpy30*Δ*P* pancreas compared to controls, suggesting expression of these digestive enzymes was not as robust as it should be. Consistent with these observations, others have reported that embryonic disruption of *Bhlha15, Gata4* or *Rbpjl* results in reduced pancreas size, fewer acinar cells, decreased

expression of digestive enzymes and incomplete acinar cell differentiation [126,128,295-297]. Overall, these data suggest that loss of H3K4 methylation from PDX1^{+} cells impairs the maintenance of a subset of genes required for acinar cell differentiation.

Late in gestation, differentiated acinar cells acquire a characteristic pyramidal shape with expanded cytoplasmic area and the apical duct lumen that borders each acinus begins to close [71]. In *Dpy30ΔP* embryos, H&E staining revealed that pancreas morphology remained intact at E15.5 but a striking disorganization of the exocrine pancreas and development of cystic structures were evident at E18.5. These structures did not develop the characteristic morphology of mature acinar cells and instead retained characteristics of immature acinar cells, including increased centroacinar space of acini and decreased cytoplasmic area, identified by eosin staining. In support of this immature phenotype, the cystic cells were not immunoreactive for the mature acinar enzymes amylase or CPA1. Furthermore, several other studies have reported that impaired acinar cell differentiation leads to the loss of acinar tissue and/or the development of disorganized cysts [85,90,128,214,298,299].

The development of pseudocysts is also characteristic of mouse models of pancreatitis or pre-cancerous lesions [128,295,296,300], suggesting that the cystic cells in the *Dpy30ΔP* pancreas may alternatively represent development of either of these exocrine pancreatic diseases. However, these diseases develop in the postnatal pancreas, rather than in the embryo, and result from the dedifferentiation of mature acinar cells or acinar-to-ductal metaplasia [301]. In addition, the cysts present in these models typically express duct cell markers [128,301]. While mature ductal cells were detected in the *Dpy30ΔP* pancreas by DBA lectin and SOX9 staining, the cystic structures did not express these markers. In agreement, duct cell gene expression was not altered in the E15.5 *Dpy30ΔP* pancreas, suggesting that the cystic structures were not evidence of acinar-to-ductal

metaplasia. Thus, these results suggest that loss of H3K4 methylation in pancreas progenitors impairs acinar cell maturation.

Developmental defects in the endocrine lineage were also observed in the *Dpy30*Δ*P* pancreas at E14.5 with a ~50% reduction in specified NEUROG3^{+} endocrine progenitors, and a proportional reduction in *Neurog3* transcripts. Initially, I hypothesized that reduced expression of NEUROG3 in *Dpy30*Δ*P* embryos was due to a concomitant increase in (or maintenance of) Notch signaling, a negative regulator of *Neurog3* expression [102,110,302]. However, expression of the Notch signaling genes, *Notch1*, *Hes1* and *Rbpj* was not significantly different. This suggested that failure to completely activate *Neurog3* in *Dpy30*Δ*P* embryos was independent of Notch signaling.

An alternative explanation is that H3K4 methylation is required for high level or stable transcription of *Neurog3*. Initially, *Neurog3* is expressed at low levels in cycling BPCs (NEUROG3^{LO}) and transitions to high level *Neurog3* expression upon cell cycle exit (NEUROG3^{HI}) [106]. Potentially, loss of H3K4 methylation impairs high level *Neurog3* expression in BPCs, where only NEUROG3^{HI} cells are immuno-detectable and therefore observed at lower levels in the *Dpy30*Δ*P* pancreas [106]. Others have suggested that H3K4 methylation has a role in establishing transcriptional stability and high level expression rather than initial gene activation [194,200,303-305]. Together, these reports suggest that loss of H3K4 methylation may prevent high level transcription or maintenance of *Neurog3* expression, leading to a reduction in endocrine cell specification in the *Dpy30*Δ*P* pancreas.

Another possibility is that the establishment of pre-committed BPCs that normally activate *Neurog3* may be affected [106], rather than *Neurog3* activation itself. Progenitor cell fate decisions are tightly linked to the cell cycle, whereby proliferation requires cell cycle progression, and

differentiation is associated with cell cycle exit (Soufi and Dalton, 2016). It was also recently established that BPC cell cycle length increases during development, and this is linked to the activation of *Neurog3* [111]. However, cumulative EdU labeling in the E12.5 *Dpy30ΔP* pancreas demonstrated a ~15% reduction in PDX1$^+$ progenitor proliferation. This decreased progenitor proliferation in the *Dpy30ΔP* pancreas may predominantly occur in MPCs and not in BPCs, which could lead to premature MPC specification, thereby affecting BPC formation and thus endocrine cell specification. In addition, failure to achieve high level *Neurog3* expression and endocrine cell specification from BPCs has been reported to drive duct or acinar cell commitment [89,107,108]. These studies suggest that a closer examination of BPC, duct and acinar cell specification in the *Dpy30ΔP* pancreas is warranted.

Consistent with the reduction in NEUROG3$^+$ cells, differentiated endocrine cells were also proportionally diminished at E15.5 and E18.5 in the *Dpy30ΔP* pancreas, without affecting endocrine cell proliferation at either stage. The fractions of insulin$^+$ β-cells and glucagon$^+$ α-cells were respectively decreased by ~40% and ~50% at E15.5, and by ~60% and ~50% at E18.5. Given that the fraction of NEUROG3$^+$ endocrine progenitors was decreased by ~50%, these results suggest that loss of H3K4 methylation does not significantly alter differentiation into the correct proportion of α- and β-cells. Further, an equal fraction of insulin$^+$ β-cells were immunoreactive for MAFA, NKX2-2, NKX6-1 and PAX6 in the E18.5 control and *Dpy30ΔP* pancreas, suggesting terminal transcription factor expression was not affected either. These data suggest that H3K4 methylation is not required for endocrine cell differentiation in the pancreas.

Taken together, these data demonstrate that disruption of *Dpy30* in PDX1$^+$ cells reduces pancreas progenitor cell proliferation and survival, contributing to decreased total pancreas cells later in development. Additionally, loss of H3K4 methylation impaired acinar cell differentiation

and endocrine cell specification, leading to fewer differentiated acinar and endocrine cells. In conclusion, my examination of the *Dpy30ΔP* pancreas supports the hypothesis that TrxG complex catalytic activity has a minimal role in gene activation or maintenance throughout pancreas development. However, H3K4 methylation may be particularly important for transcriptional maintenance of genes involved in cell division and survival, and a subset of acinar lineage-specific genes.

Chapter 5: TrxG catalytic activity is essential for pancreas endocrine cell maturation

5.1 Background

Endocrine cell specification is initiated by high level induction of the pro-endocrine factor *Neurog3* and subsequent exit from the cell cycle [56,306,307]. NEUROG3 drives expression of downstream transcription factors, such as *Neurod1, Nkx2-2, Nkx6-1, Pax6* and *Pdx1*, that determine further differentiation of endocrine progenitors into hormone-expressing endocrine cells that form proto-islet structures [3,56]. After birth, an increase in endocrine cell proliferation drives islet remodeling into the mature spherical architecture [3,56]. At P14, islets undergo a process of functional maturation which involves acquisition of glucose-sensing and hormone-secretion machinery [3,56,130,308]. For β-cell maturation in particular, the transition from immature to mature β-cells involves a switch from *Mafb* to *Mafa* expression, metabolic gene expression changes (e.g. switch from high-affinity hexokinase (*Hk*) to low-affinity glucokinase (*Gck*)) and increased glucose exposure improves glucose-stimulated insulin secretion [130,309].

In Chapter 4, the fraction of NEUROG3^{+} progenitors and differentiated endocrine cells was significantly decreased in the *Dpy30ΔP* pancreas, suggesting TrxG catalytic activity has an important role in endocrine cell specification. While loss of TrxG catalytic activity had a minimal effect on bulk gene activation, my data suggested a role for H3K4 methylation in transcriptional maintenance of a subset of genes in the acinar lineage. However, this model left unresolved whether TrxG catalytic activity has a role in the activation or maintenance of genes required for the differentiation or functional maturation of endocrine cells. TrxG complex proteins are enriched in mature islets [231] and interact with the maturation factors MAFA and

MAFB in mature β-cells [310], suggesting a role for these complexes in maintenance of islet identity. Notably, deletion of the TrxG gene *Ncoa6* in embryonic β-cells does not affect MAFA expression but results in reduced downstream activation of MAFA target genes and impaired glucose-stimulated insulin secretion [310]. Importantly, decreased gene expression was correlated with reductions in H3K4 methylation and Pol II at the TSS of affected genes. In addition, H3K4 methylation deposited by the SET7/9 histone methyltransferase was linked to transcriptional maintenance of genes involved in glucose-stimulated insulin secretion in primary islets [311]. Thus, in this Chapter, I tested the **hypothesis** that H3K4 methylation is required for maintenance of genes involved in endocrine cell maturation and glucose homeostasis.

5.2 Results

5.2.1 Loss of DPY30 and H3K4 methylation from *Dpy30ΔN* endocrine cells

To investigate the role of H3K4 methylation in endocrine cell maturation, I disrupted *Dpy30* in NEUROG3^{+} endocrine progenitor cells using *Neurog3*-Cre driver mice [228]. This generated experimental *Neurog3*-Cre; *Dpy30*$^{flox/flox}$ mice (hereafter known as *Dpy30ΔN*) and littermate *Dpy30*$^{flox/flox}$ (Cre-negative) control mice. DPY30 immunoreactivity was absent from >95% of insulin^{+} and glucagon^{+} endocrine cells at E14.5 (Figure 33, white arrowheads), P0 and P7 (Figure 34), but was maintained in the surrounding *Dpy30ΔN* exocrine pancreas, validating deletion of *Dpy30* in the endocrine lineage. Co-staining of endocrine cells with the pan-endocrine marker chromogranin A (CHGA) and H3K4me3 revealed a delay between loss of DPY30 protein and H3K4 methylation. At P0, H3K4me3 immunoreactivity was maintained in CHGA^{+} *Dpy30ΔN* islets similar to controls (Figure 35). However, from P0 onward, H3K4me3 immuno-staining was progressively decreased and was consistently absent from P14 endocrine cells and thereafter (Figure 35). These data suggest that disruption of *Dpy30* in NEUROG3^{+} cells results in loss of DPY30 protein from embryonic endocrine cells and delayed loss of H3K4 methylation in postnatal islets.

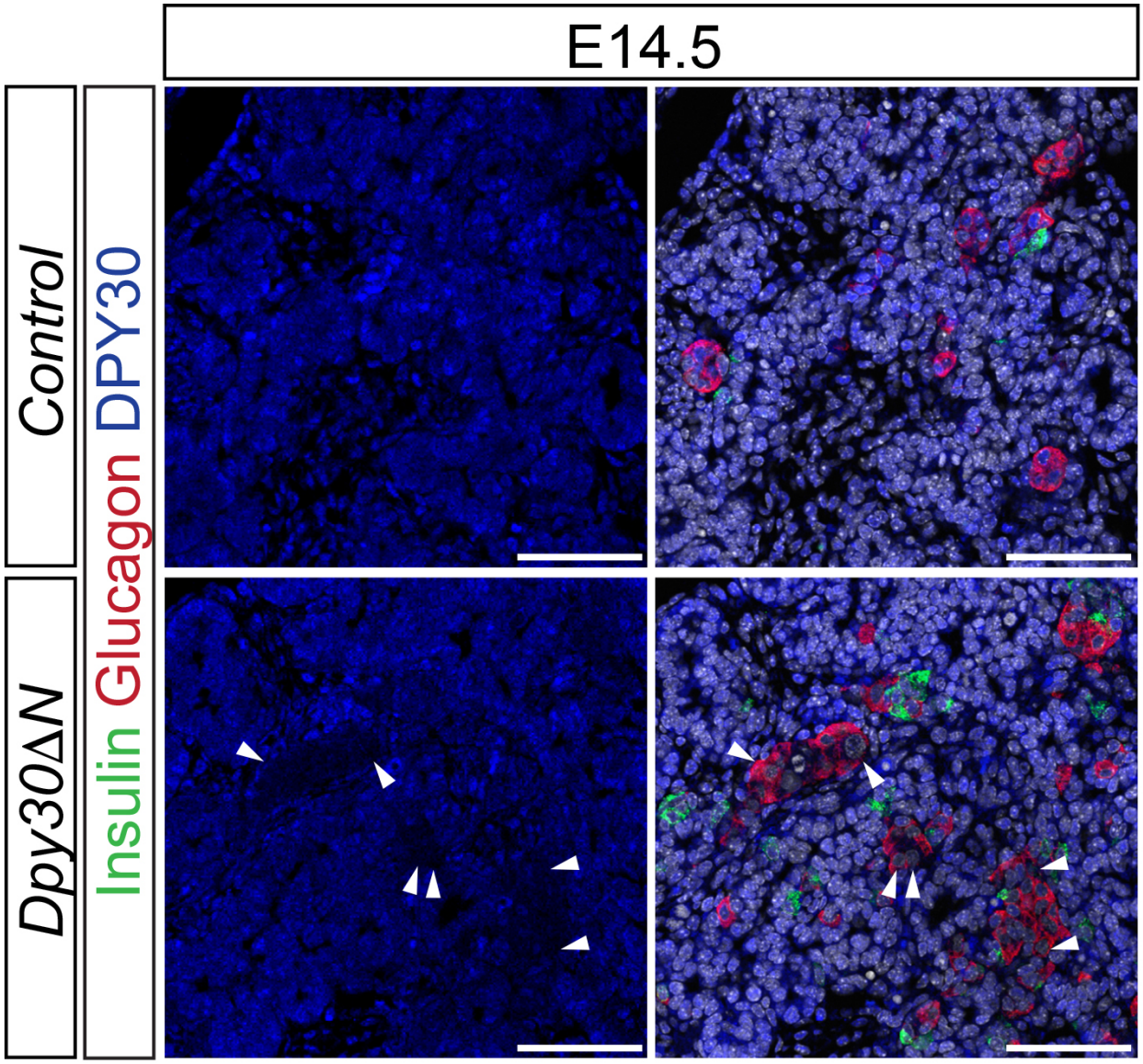

Figure 33: DPY30 is absent from E14.5 endocrine cells.
IF staining of insulin (green), glucagon (red) and DPY30 (blue) in E14.5 control and *Dpy30ΔN* pancreas. Nuclei are stained with DAPI (grey). White arrowheads = loss of DPY30 from *Dpy30ΔN* endocrine cells. Scale bar, 75 μM.

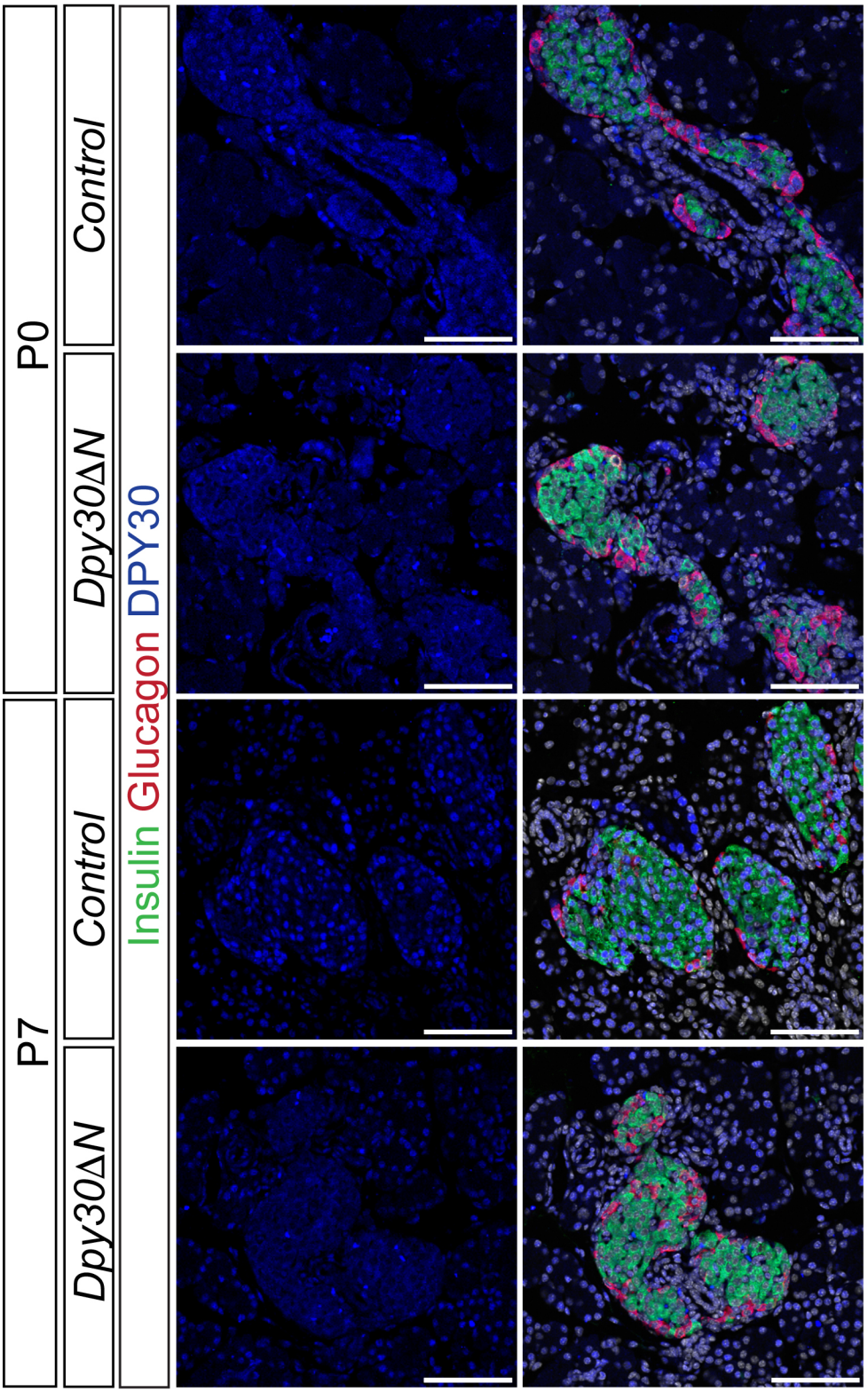

Figure 34: Loss of DPY30 in *Dpy30ΔN* endocrine cells.
IF staining of insulin (green), glucagon (red) and DPY30 (blue) in control and *Dpy30ΔN* pancreas at P0 and P7. Nuclei are stained with DAPI (grey). Scale bar, 75 μM.

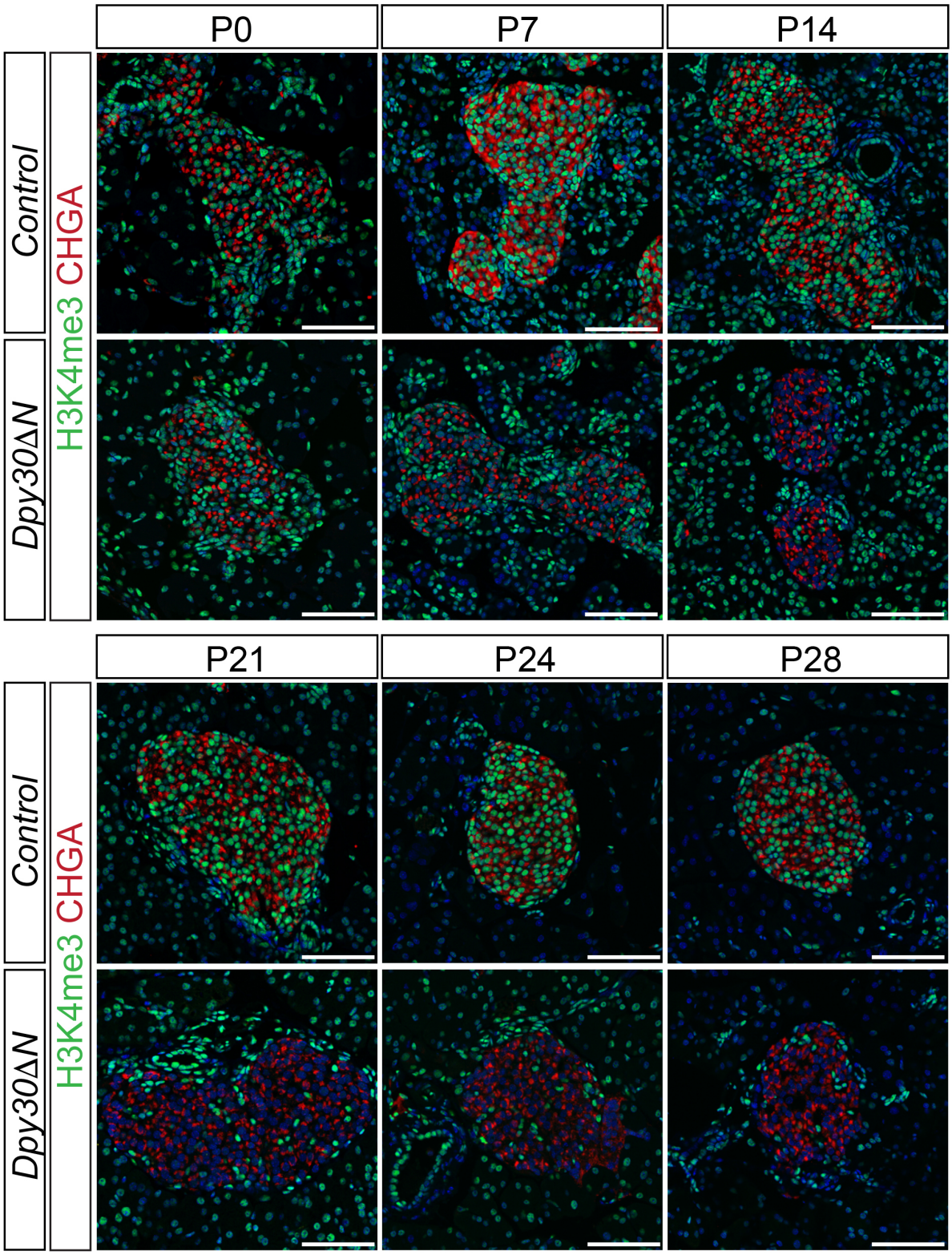

Figure 35: H3K4 methylation is progressively lost from *Dpy30ΔN* islets.
IF staining of H3K4me3 (green) and CHGA (red) in control and *Dpy30ΔN* pancreas from P0 to P28. Nuclei are stained with DAPI (blue). Scale bar, 75 μM.

To determine whether deletion of *Dpy30* in NEUROG3^{+} endocrine progenitors altered the proportion of endocrine cells, I first confirmed that the NEUROG3^{+}/SOX9^{+} cell ratio was not significantly different in E14.5 control and *Dpy30ΔN* pancreas (Figure 36A-B). Next, co-staining for insulin^{+} β-cells, glucagon^{+} α-cells and somatostatin^{+} δ-cells demonstrated that the sum of these endocrine cells relative to total pancreas cells was not altered in the E18.5 *Dpy30ΔN* pancreas compared to controls (Figure 36C-D). The relative proportion of insulin^{+} β-cells, glucagon^{+} α-cells and somatostatin^{+} δ-cells was also normal in the E18.5 *Dpy30ΔN* pancreas (Figure 37). These data suggest that disruption of *Dpy30* in NEUROG3^{+} cells does not affect the proportion of pancreatic endocrine cells in the embryo.

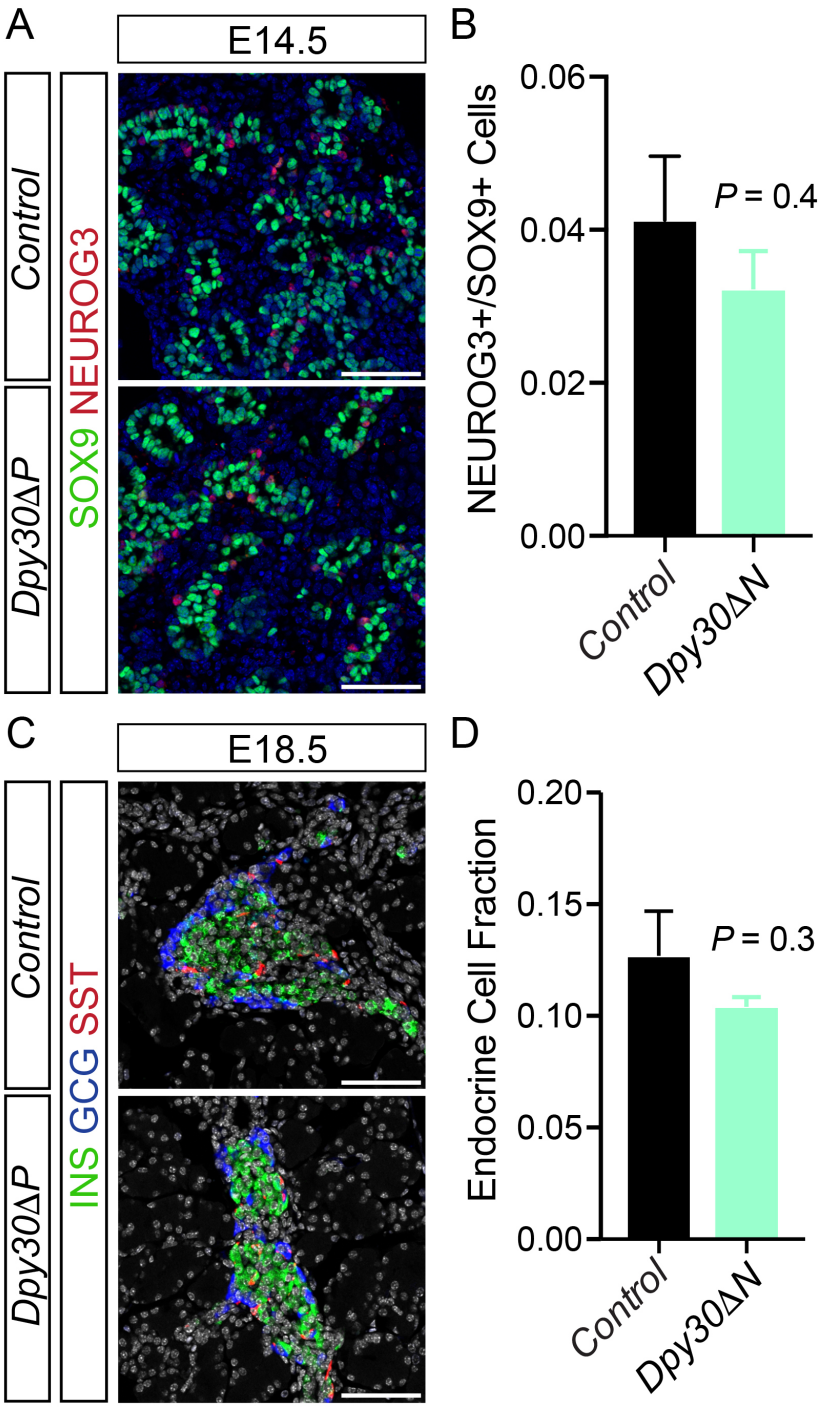

Figure 36: The fraction of NEUROG3$^+$ endocrine progenitors and endocrine cells in *Dpy30ΔN* embryonic pancreas is equivalent to controls.
(A) IF staining for SOX9 (green) and NEUROG3 (red) in E14.5 control and *Dpy30ΔN* pancreas. Nuclei are stained with DAPI (blue). Scale bar, 75 µM. **(B)** The NEUROG3$^+$/SOX9$^+$ cell ratio in E14.5 control and *Dpy30ΔN* pancreas. **(C)** Co-staining for insulin (INS, green), glucagon (GCG, blue) and somatostatin (SST, red) in E18.5 control and *Dpy30ΔN* pancreas. Nuclei are stained with DAPI (grey). Scale bar, 75 µM. **(D)** The fraction of endocrine cells (sum of INS$^+$, GCG$^+$ and SST$^+$ cells) relative to pancreas cells in E18.5 control and *Dpy30ΔN* pancreas. Data are represented as mean ± SEM; n = 3; *Dpy30ΔN* vs. control; unpaired, two-tailed Student's t test.

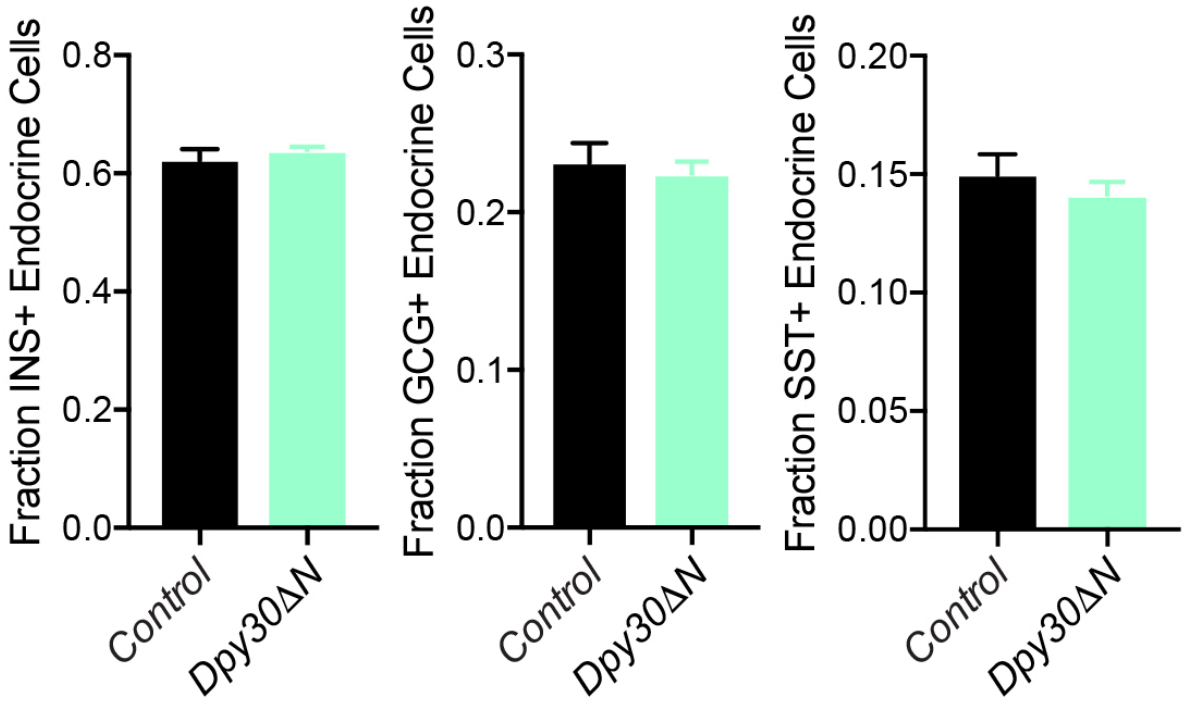

Figure 37: The fraction of insulin$^+$ β-cells, glucagon$^+$ α-cells and somatostatin$^+$ δ-cells is normal in embryonic *Dpy30ΔN* pancreas.
The proportions of insulin$^+$ β-cells (INS$^+$), glucagon$^+$ α-cells (GCG$^+$) and somatostatin$^+$ δ-cells (SST$^+$) relative to total endocrine cells in E18.5 control and *Dpy30ΔN* pancreas. Data are represented as mean ± SEM; n = 3.

5.2.2 *Dpy30ΔN* mice develop hyperglycemia and impaired glucose tolerance

To investigate whether the postnatal islet reduction in H3K4 methylation had a biological effect in *Dpy30ΔN* mice, I first monitored body mass and random fed blood glucose. Daily tracking between P24 and P38 indicated that while body mass was not significantly altered in male *Dpy30ΔN* mice compared to controls (Figure 38A), mean *ad libitum* glycemia was over 18 mM by P28 and worsened over time (Figure 38B). A similar trend was observed in female *Dpy30ΔN* mice (data not shown). Further, 6 hour fasting blood glucose levels were equivalent in control and *Dpy30ΔN* mice at P23 (Figure 39A), but significantly increased to ~12 mM in *Dpy30ΔN* males by P25 (Figure 39B). These data demonstrate that male *Dpy30ΔN* mice develop random and fasting hyperglycemia.

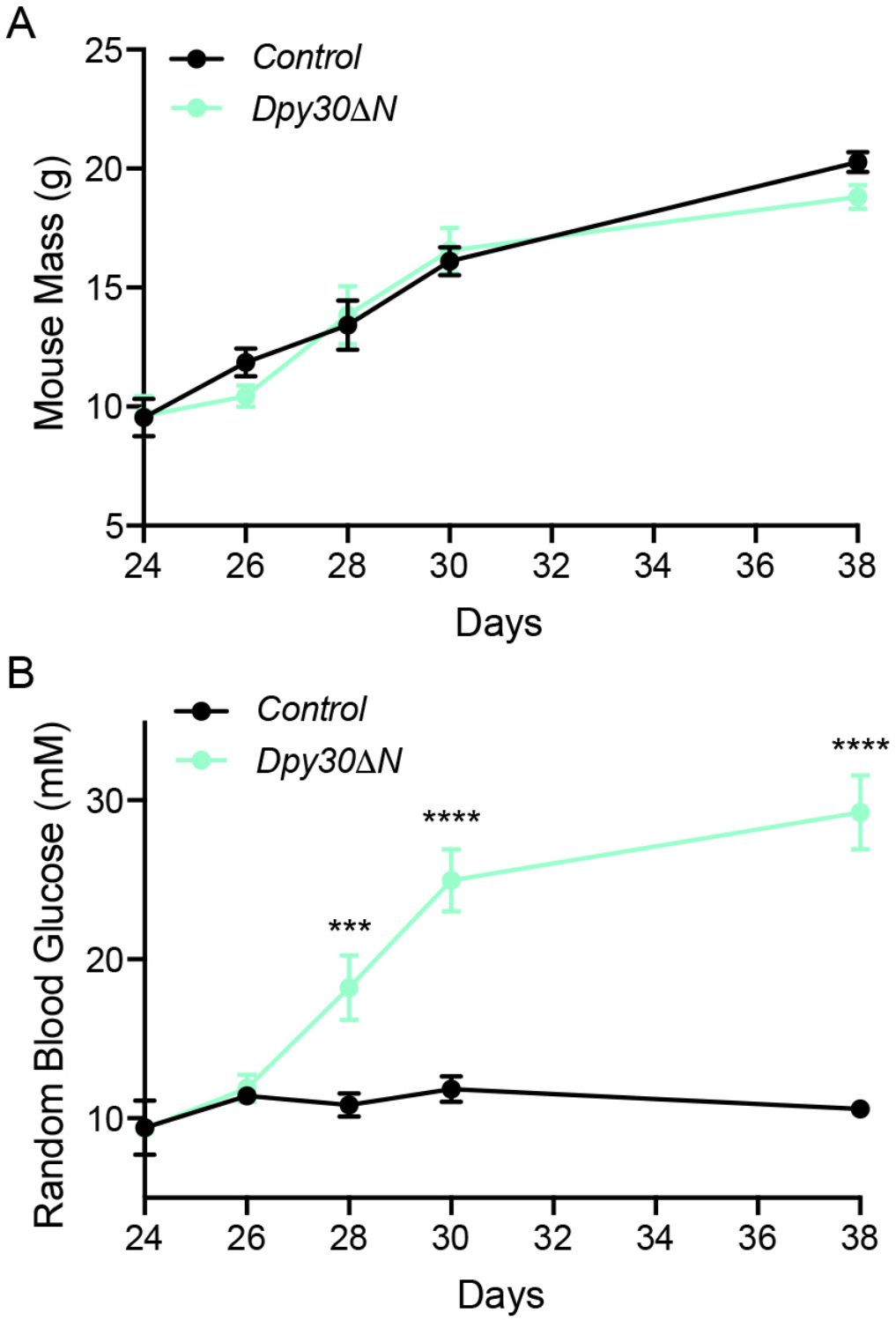

Figure 38: Random blood glucose levels are elevated in male *Dpy30ΔN* mice.
(A) Mouse body mass measurements between P24 and P38 in male control and *Dpy30ΔN* animals. Data are represented as mean ± SEM; n = 4-8. **(B)** Random blood glucose measurements from male *Dpy30ΔN* and control mice between P24 and P38. Data are represented as mean ± SEM; n = 3-10; *** denotes $P < 0.001$ and **** denotes $P < 0.0001$ *Dpy30ΔN* vs. control; multiple t tests with Holm-Sidak correction for multiple comparisons.

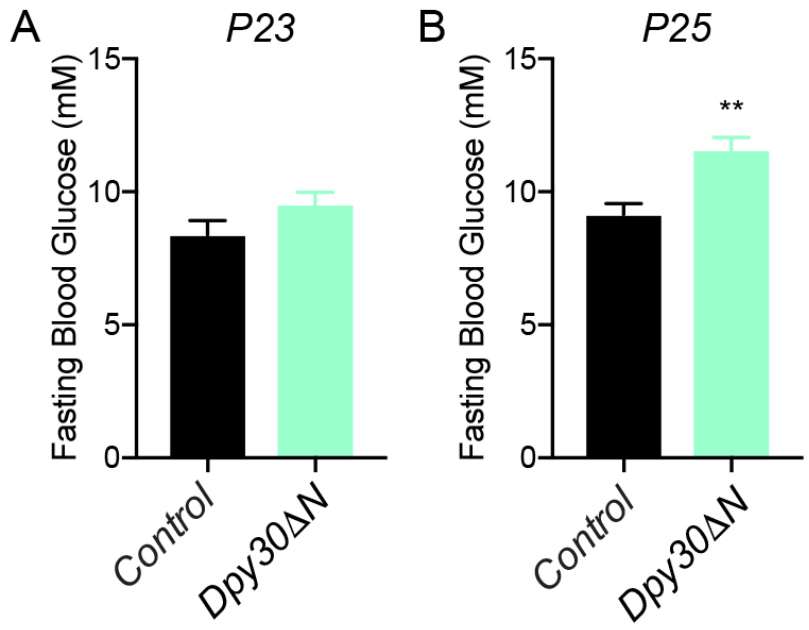

Figure 39: Male *Dpy30ΔN* mice develop fasting hyperglycemia.
Blood glucose measurements after a 6 hour fast in male control and *Dpy30ΔN* mice at **(A)** P23 and **(B)** P25. Data are represented as mean ± SEM; n = 4-8; ** denotes $P < 0.01$ *Dpy30ΔN* vs. control; unpaired, two-tailed Student's t test.

Next, I examined glucose tolerance in male *Dpy30ΔN* mice by performing intraperitoneal glucose tolerance tests (IPGTTs) at P23 and P25. Following a 6 hour fast, glucose was injected IP at 2 g per kg body mass and blood glucose was measured at 15, 30, 60 and 120 minutes post-injection. At P23, a marginal but significant increase to ~19 mM was detected at 30 minutes in *Dpy30ΔN* male mice, but blood glucose measurements at other time points were otherwise comparable to controls (Figure 40A). In addition to elevated fasting glycemia at P25 (Figure 37B), blood glucose levels were above the limit of detection (33.3 mM) at 15 and 30 minutes post-injection in *Dpy30ΔN* mice at P25 (Figure 40B). A significant increase to ~23 mM was detected at 60 minutes post-injection but glycemia returned to control levels by 120 minutes, suggesting that *Dpy30ΔN* mice were not completely glucose intolerant (Figure 40B). These results suggest that male *Dpy30ΔN* mice develop impaired glucose tolerance.

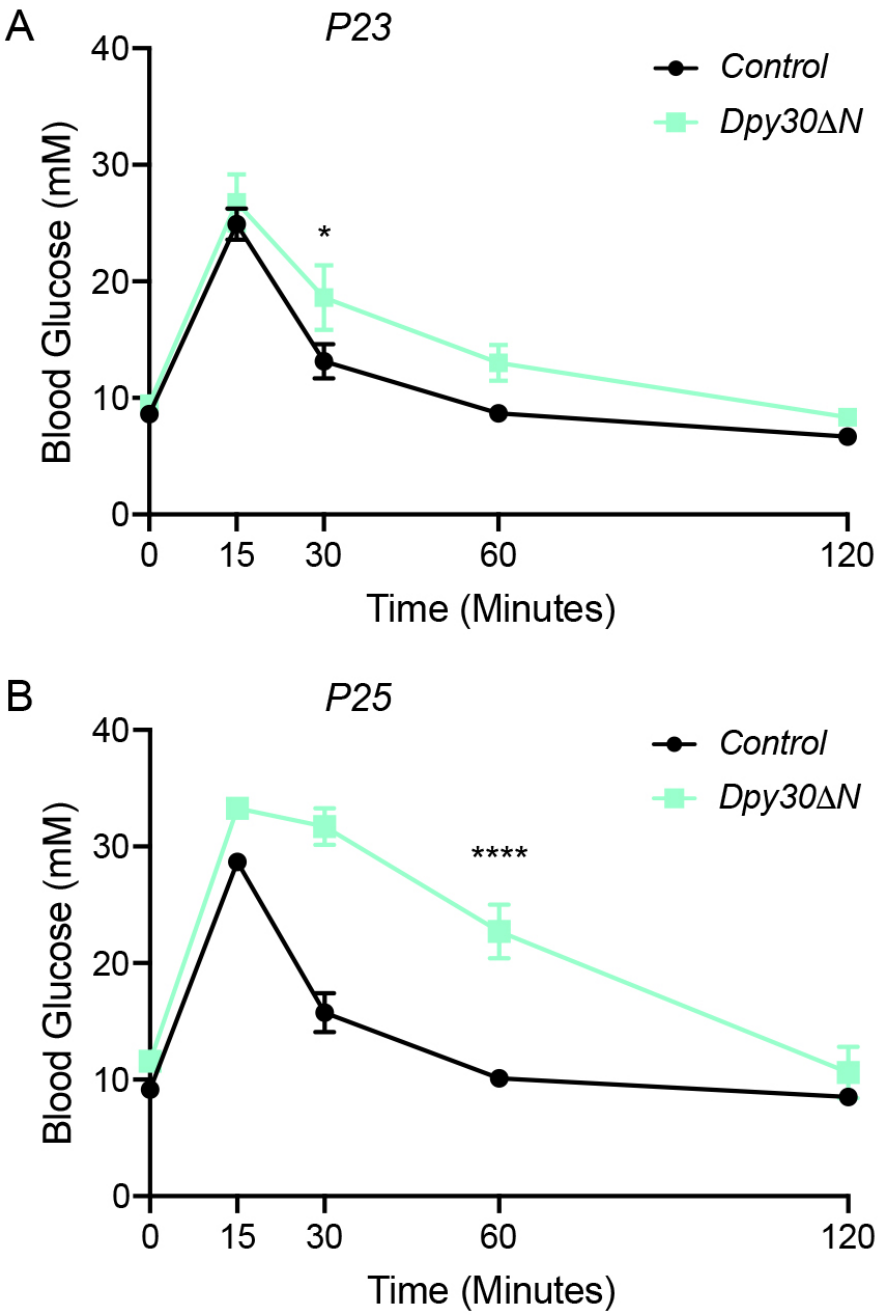

Figure 40: Male *Dpy30ΔN* mice develop impaired glucose tolerance.
IPGTT of 2 g per kg body mass IP glucose in male control and *Dpy30ΔN* mice following a 6 hour fast at **(A)** P23 and **(B)** P25. Data are represented as mean ± SEM; n = 4-9; * denotes $P < 0.05$ and **** denotes $P < 0.0001$ *Dpy30ΔN* vs. control; repeated measures two-way ANOVA with Sidak's multiple comparison post-hoc test. Note that statistical testing was not performed at 15 and 30 minutes as measurements were above the detection limit (33.3 mM).

5.2.3 Islet maturity is compromised in *Dpy30ΔN* mice

To understand the underlying mechanism for hyperglycemia and impaired glucose tolerance in *Dpy30ΔN* mice, I assessed whether postnatal islet size, number or proportion of endocrine cells was impaired. *Dpy30ΔN* and control pancreas sections from 5-week-old mice were immunostained for endocrine hormones and islet diameter measurements were segregated based on small (0-75 μM), medium (76-150 μM) or large (≥ 151 μM) diameters, but no significant differences were detected at any size range (Figure 41A). Similarly, neither the number of islets quantified per image (Figure 41B) nor the proportion of α-, β- or δ-cells per islet (Figure 42A-B) were significantly altered in the *Dpy30ΔN* pancreas. These results suggest that hyperglycemia in *Dpy30ΔN* mice is not due to a change in islet size, number or endocrine cell proportion.

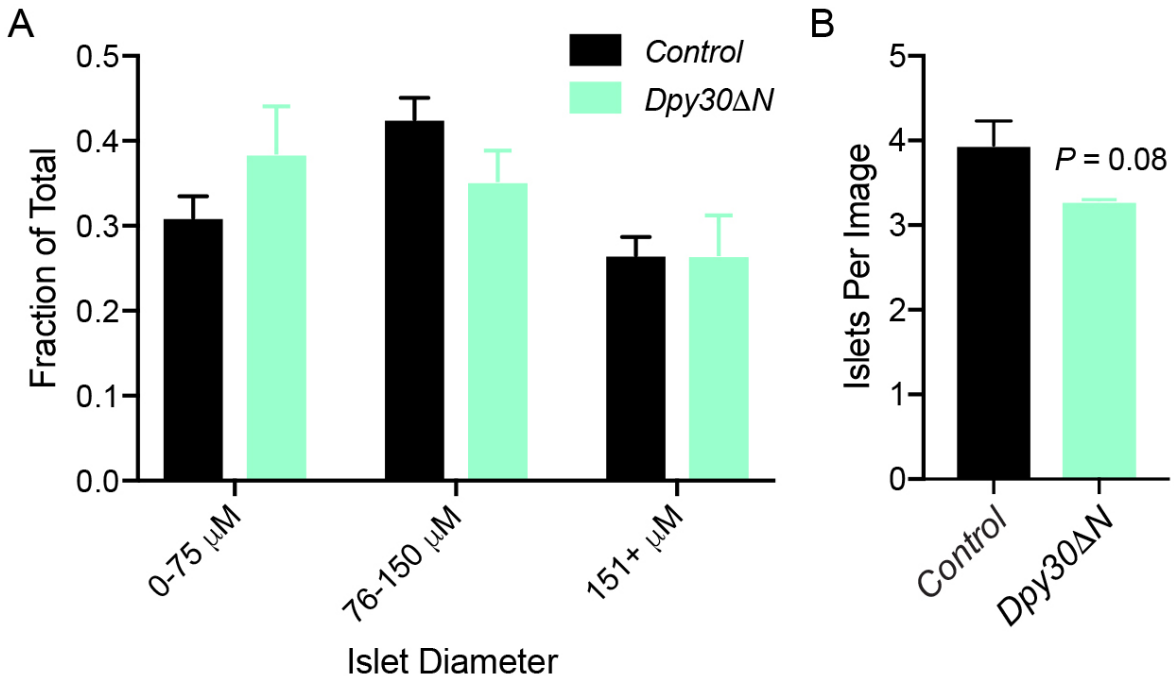

Figure 41: Islet diameter and islet number is not significantly altered in *Dpy30ΔN* mice.
Quantification of **(A)** islet diameter or **(B)** islet number from *Dpy30ΔN* and control pancreas at 5 weeks. Paraffin sections were immunostained for endocrine hormones to identify islets. Islet diameter measurements were divided into bins and represented as a fraction of the total. Data are represented as mean ± SEM; n ≥ 4; *Dpy30ΔN* vs. control; unpaired, two-tailed Student's t test.

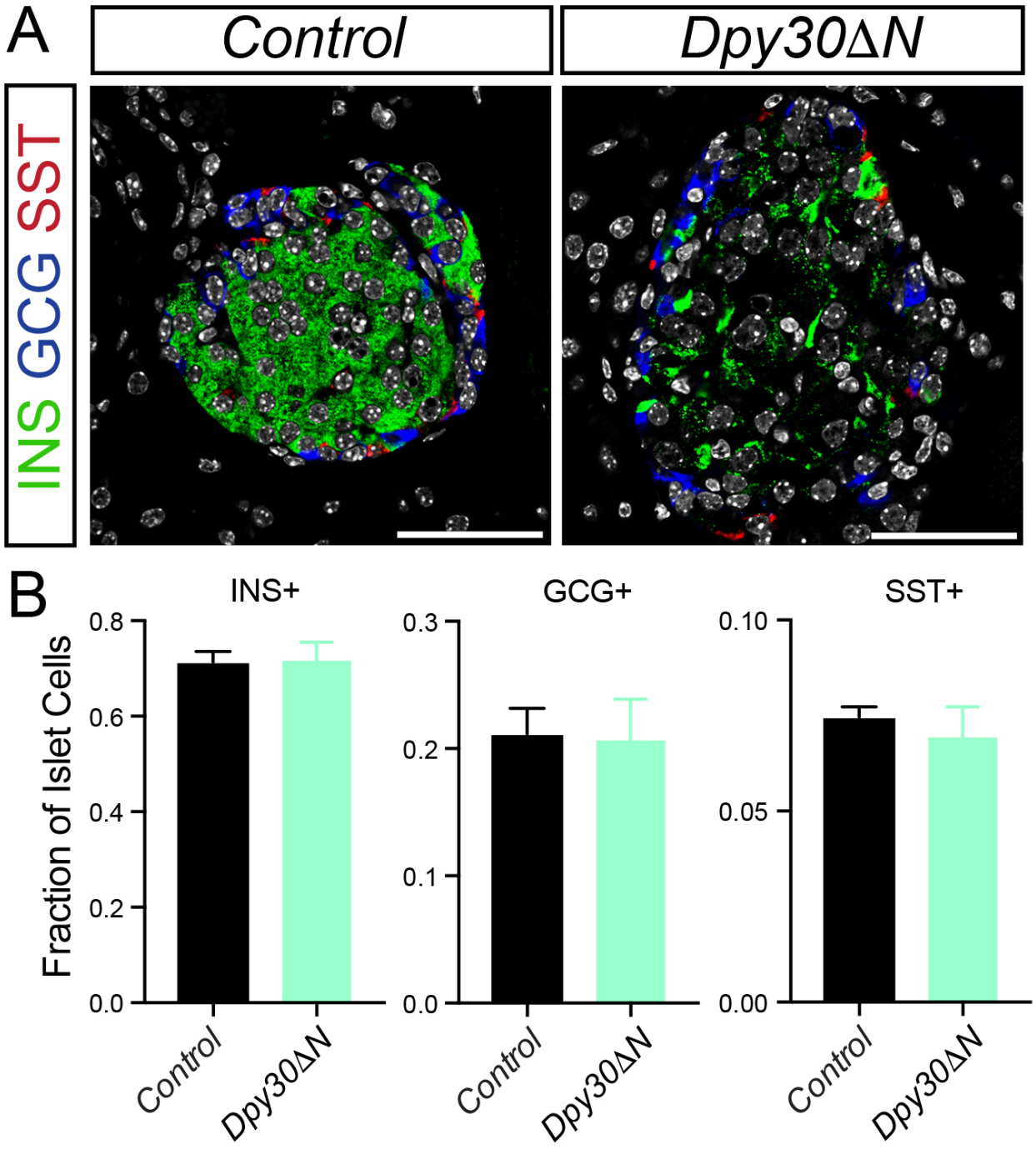

Figure 42: Endocrine cell fractions are unchanged in *Dpy30ΔN* islets.
(A) IF staining for insulin (INS, green), glucagon (GCG, blue) and somatostatin (SST, red) in 5 week control and *Dpy30ΔN* pancreas. Nuclei are stained with DAPI (grey). Scale bar, 50 μM. **(B)** The fraction of insulin$^+$ (INS$^+$), glucagon$^+$ (GCG$^+$) and somatostatin$^+$ (SST$^+$) islet cells in 5 week control and *Dpy30ΔN* pancreas. Data are represented as mean ± SEM; n = 3.

As the insulin staining in *Dpy30ΔN* islets appeared reduced compared to controls (Figure 42A), I next examined whether impaired glucose tolerance and hyperglycemia in *Dpy30ΔN* animals was instead the result of reduced endocrine cell maturity. To assess islet maturation, islets from male *Dpy30ΔN* and control mice were collected when two consecutive random blood glucose measurements > 20 mM were obtained in *Dpy30ΔN* animals (~4 weeks of age) and RNA-sequencing (RNA-seq) was performed. A key determinant of β-cell maturity is the ability to effectively respond to glucose, which includes efficient glucose transport and metabolism as well as regulated insulin secretion. Thus, I focused the RNA-seq analysis on expression of genes associated with islet maturity or immaturity, critical islet transcription factors and islet hormones. In general, genes associated with mature β-cells were lowered in *Dpy30ΔN* islets (Figure 43A), whereas genes associated with immature β-cells were elevated in *Dpy30ΔN* islets (Figure 43B). For example, significant decreases were detected in the β-cell glucose transporter (i.e. *Slc2a2*, > 18-fold), mature β-cell hormone (i.e. *Ucn3,* 6-fold) [308], mature hexokinase (i.e. *Gck*, 1.4-fold) and K_{ATP} channel (i.e. *Abcc8,* 1.8-fold; *Kcnj11*, > 7-fold) genes (Figure 43A). This coincided with significantly elevated levels of the immature hexokinase (i.e. *Hk2*, 2.2-fold), the aldehyde dehydrogenase gene (i.e. *Aldh1a3*, 2.4-fold) [312] and the fetal endocrine hormone gastrin (i.e. *Gast*, > 7-fold) [313] (Figure 43B). Differential expression of mature islet transcription factors indicated that while *Mafa* and *Nkx6-1* were not affected, significant decreases in *Mafb* (1.7-fold), *Neurod1* (1.5-fold), *Nkx2-2* (1.5-fold), *Pax6* (1.7-fold) and *Pdx1* (1.4-fold) were detected in *Dpy30ΔN* islets (Figure 43C). Consistently, significant decreases in islet hormones *Gcg* (2.4-fold), *Iapp* (2.8-fold), *Ins1* (1.8-fold), *Ins2* (7.2-fold), *Ppy* (7.5-fold) and *Sst* (2.9-fold) were detected in *Dpy30ΔN* islets (Figure 43D). Combined, these results suggest that hyperglycemia

and impaired glucose tolerance in *Dpy30ΔN* mice may manifest from reduced insulin secretion and/or compromised islet β-cell maturity.

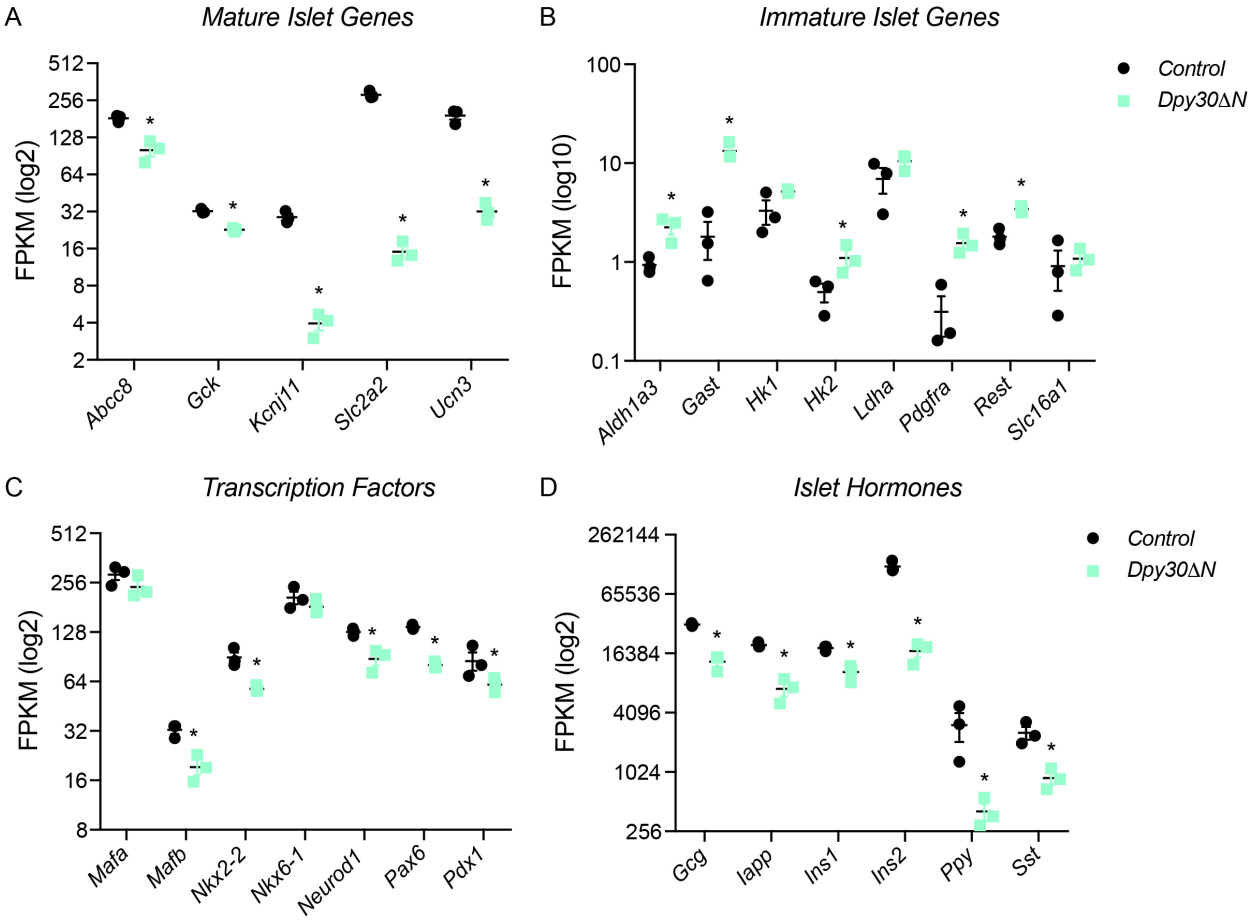

Figure 43: Islet β-cell failure in *Dpy30ΔN* mice.
RNA-sequencing of 4 week (P28-P32) islets from control and *Dpy30ΔN* male mice with genes categorized by **(A)** mature islet genes; **(B)** immature islet genes; **(C)** transcription factors; and **(D)** islet hormones. Gene expression is represented as Fragments Per Kilobase of transcript per Million (FPKM) mapped reads on a $\log_2$ or $\log_{10}$ scale as indicated. Data are represented as mean ± SEM; n = 3; * denotes $P < 0.05$ *Dpy30ΔN* vs. control; Wald test with corrections for multiple comparisons and false discoveries.

5.3 Discussion

In this Chapter, I demonstrated that genetic inactivation of *Dpy30* in NEUROG3^{+} cells did not alter the proportion of endocrine progenitors or endocrine cells but led to the global loss of H3K4 methylation in postnatal islets. *Dpy30ΔN* mice displayed elevated random and fasting glycemia, in addition to impaired glucose tolerance. These phenotypes could not be explained by changes in *Dpy30ΔN* islet size, islet number or the relative proportions of islet cells. However, expression of insulin and genes associated with insulin secretion and islet maturity were reduced in islet RNA-sequencing analysis, suggesting a role for TrxG catalytic activity in islet cell functional maturation.

An interesting observation from the *Dpy30ΔN* mice was the delayed loss of endocrine cell H3K4 methylation. Although DPY30 immunoreactivity was absent from hormone^{+} endocrine cells at E14.5, loss of H3K4me3 did not occur until P14. This difference may be the result of failed H3K4me3 re-establishment during cell division. At the time when *Dpy30* is genetically inactivated, NEUROG3^{+} cells exit the cell cycle and differentiate into endocrine cells [99]. These cells remain non-proliferative until the early postnatal period when endocrine cell replication increases [2], suggesting that loss of H3K4 methylation does not occur until after several rounds of endocrine cell division. In addition, no phenotype was observed in *Dpy30ΔN* mice until after loss of H3K4 methylation, suggesting that loss of DPY30 has a minimal effect and that the impaired endocrine cell maturation in *Dpy30ΔN* mice is due to the absence of H3K4 methylation.

Notably, the loss of H3K4 methylation from *Dpy30ΔN* islets at P14 overlaps with the period of endocrine cell maturation. During the first few weeks after birth, endocrine cells undergo functional maturation and develop glucose-stimulated hormone secretion by P14 [1,130,308].

In particular, immature β-cells secrete insulin at low glucose levels, whereas mature β-cells secrete more insulin in response to higher glucose levels [130]. This transition involves important gene expression changes, where immature genes (e.g. *Hk1, Ldha, Rest, Pdgfra* and *Mafb*) become repressed and mature genes (e.g. *Gck, Ucn3* and *Mafa*) are induced [130]. In *Dpy30ΔN* islets, the expression of several mature genes required for glucose transport (*Slc2a2*), glucose sensing (*Gck*) and insulin secretion (*Abcc8, Kcnj11*) were significantly reduced, and in addition the mature β-cell marker *Ucn3* was also reduced [308]. Meanwhile, several genes associated with endocrine cell immaturity such as *Aldh1a3, Gast, Hk2, Pdgfra* and *Rest* [130] were relatively elevated in *Dpy30ΔN* islets. Furthermore, transcript levels of *Ins1*, *Ins2, Gcg, Sst* and other islet hormones were also significantly reduced in *Dpy30ΔN* islets. This is consistent with the observed reduction in insulin immunostaining in *Dpy30ΔN* islets and suggests incomplete islet maturity in *Dpy30ΔN* mice.

The transcription factors MAFA, NEUROD1, NKX2-2, NKX6-1, PAX6 and PDX1 are particularly important for expression of the insulin genes and for regulated glucose-stimulated insulin secretion [116,133,314-318], and are consistently reduced in mouse models of diabetes and in T2D [319]. In *Dpy30ΔN* islets, small but significant reductions in expression of *Neurod1, Nkx2-2, Pax6* and *Pdx1* were detected compared to controls, without affecting *Mafa* or *Nkx6-1* transcript levels. Although complete disruption of either *Neurod1, Nkx2-2, Pax6* or *Pdx1* in pancreatic β-cells leads to impaired glucose-stimulated insulin secretion [115,315,317,320], it is unlikely that slight reductions in these factors contribute to large changes in *Ins2* and *Slc2a2* expression and impaired glucose homeostasis in *Dpy30ΔN* mice. This hypothesis is supported by evidence that mice harbouring heterozygous mutations in either *Nkx2-2* or *Pdx1* do not have a hyperglycemic

phenotype [69,118]. Consistent with these results, expression of MAFA was not significantly affected in the *Dpy30ΔP* pancreas (Chapter 4) or after disruption of *Ncoa6* in embryonic β-cells [310]. However, expression levels of downstream β-cell critical genes such as *G6pc2, Gck, Pdx1, Slc2a2* and *Slc30a8* [321] were affected in *Dpy30ΔN* mice. This suggests that H3K4 methylation may be important for expression of a subset of β-cell critical genes rather than initial gene activation.

Given that RNA-sequencing was performed on P28-P32 *Dpy30ΔN* islets, a time point when blood glucose measurements were consistently above 20 mM for ~2-4 days, hyperglycemia could be a confounding variable in this analysis. Prolonged elevated glucose exposure leads to reduced islet gene expression, glucose-stimulated insulin secretion and islet survival [322]. However, although high glucose exposure can impair insulin gene expression, this occurs after several weeks of exposure rather than several days [322]. In addition, it is clear that disruption of *Dpy30* and loss of H3K4 methylation is the initial driver of elevated glucose levels since this does not occur in the controls. Thus, it is unlikely that the gene expression changes observed in *Dpy30ΔN* mice are due to hyperglycemia.

Following weaning at P21, *Dpy30ΔN* mice developed hyperglycemia and impaired glucose tolerance. During normal pancreatic development, glucose-stimulated insulin secretion improves gradually in the postnatal period, and β-cells are considered functionally mature by P14 [308]. In addition, β-cell maturation is triggered by exposure to a carbohydrate-rich diet [309]. The transition to glucose metabolism as the primary energy source exposes maturing islets to increased glucose levels, and this stimulates β-cell proliferation, enhances insulin secretion and promotes oxidative phosphorylation [309]. In *Dpy30ΔN* mice, no differences in islet size or number were detected,

suggesting that impaired β-cell proliferation was unlikely to result in hyperglycemia. IPGTTs demonstrated that fasting blood glucose and glucose tolerance was significantly impaired by P25, suggesting that either glucose-stimulated insulin secretion, insulin levels or insulin action may be affected at this stage. Although glucose-stimulated insulin secretion was not directly tested on *ex vivo Dpy30ΔN* islets, RNA-sequencing analysis indicated that the expression of genes involved in insulin secretion and insulin transcript levels were significantly decreased in 4 week *Dpy30ΔN* islets compared to controls. This suggests that during a glucose challenge, *Dpy30ΔN* mice have insufficient insulin secretion to reduce blood glucose levels, likely due to reduced levels of insulin and/or insulin secretion machinery.

In summary, results in this Chapter suggest that TrxG catalytic activity is important for transcriptional maintenance of a subset of islet genes required for endocrine cell functional maturation. However, this conclusion would be strengthened by future experiments directed at better addressing whether islet maturation is impaired at earlier stages (i.e. prior to P28) and if glucose-stimulated insulin secretion is impaired in *Dpy30ΔN* mice. Overall, these data suggest that endocrine cells do not completely mature in the absence of H3K4 methylation.

Chapter 6: Conclusion

6.1 Overall Conclusions

The overarching goal of this thesis was to examine the role of the TrxG complexes in gene activation during mouse pancreas and endocrine progenitor differentiation. Using lentiviral suppression and genetic Cre-lox approaches that disrupted core TrxG complex subunits, I tested the hypothesis that the TrxG complexes and/or H3K4 methylation are required for activation of lineage-specific genes during pancreas and endocrine progenitor cell differentiation. Since WDR5 is critical for assembly of the TrxG complexes [259] whereas DPY30 is required for H3K4 methyltransferase activity [291], disruption of *Wdr5* or *Dpy30* was used to study the non-catalytic or catalytic roles of the TrxG complexes, respectively. Although disruption of TrxG complex assembly by *Wdr5* suppression prevented lineage-specific gene activation, disruption of TrxG catalytic H3K4 methyltransferase activity by genetic deletion of *Dpy30* did not affect bulk gene activation, but specifically reduced the expression of a subset of lineage-specific genes. This is in agreement with other studies that demonstrate H3K4 methylation is not essential for the expression of most genes [192,194,199,200].

Gene activation involves nucleosome remodeling (e.g. by SWI/SNF), transcription factor binding, recruitment of additional chromatin modifying complexes and co-activators (e.g. HATs, KDMs and TrxG) and Pol II to initiate transcription [162]. These same proteins and complexes are involved in transcriptional maintenance of gene expression [179]. Combined with previous reports which suggest the TrxG complexes have an enzyme-independent role in gene activation [167,179,191,205,206], results in this thesis support a model whereby the non-catalytic activity of TrxG complexes is required for pancreas lineage-specific gene activation (Figure 44), whereas TrxG catalytic H3K4 methyltransferase activity is required for the maintenance and transcriptional

consistency of a subset of pancreas lineage-critical genes (Figure 45). In this model, DNA methylation or repressive H3K27me3 may increase in the absence of H3K4 methylation, or H3K4 methylation may stabilize Pol II and chromatin regulators at active chromatin in order to maintain consistent gene expression [167].

Progenitor cells respond to developmental signals that either promote proliferation and the maintenance of the progenitor state, or induce expression of lineage-restricted genes that drive cell differentiation. The major findings presented in this thesis are that TrxG complexes and/or H3K4 methylation contribute to transcriptional activation or maintenance of genes involved in both of these fundamental processes, in pancreas progenitors and in the maturation of acinar and endocrine cells. These results are consistent with other evidence in the literature that suggests DPY30, WDR5 and/or H3K4 methylation have a role in the proliferation and differentiation of other cell types through transcriptional activation or maintenance [205,206,271,272,289,323].

In Chapter 3, suppression of *Wdr5* in pancreas progenitor spheroids impaired the activation of genes required for endocrine (i.e. *Neurog3*) and acinar cell differentiation, without affecting the maintenance of genes expressed in progenitor and duct cells (i.e. *Pdx1, Sox9*). These results support a model whereby the TrxG complexes are required for the initial activation of lineage-specific genes (Figure 44). Activation of gene expression is dependent on chromatin state, but requires nucleosome remodeling (e.g. by SWI/SNF) to expose *cis*-regulatory loci, transcription factor binding, histone acetylation by HATs and recruitment of Pol II at minimum. Using a bivalent chromatin state as an example (i.e. *Neurog3*), additional removal of H3K27me3 by KDMs such as KDM6A and KDM6B is necessary to initiate transcription (Figure 44A) [222-224]. The drastic reduction in *Neurog3* expression in sh*Wdr5* spheroids supports the hypothesis that disruption of TrxG complex assembly prevents the initial establishment of active chromatin at

lineage-specific factors such as *Neurog3* (Figure 44B). Given that the TrxG complexes interact with nucleosome remodelers [196,197], other chromatin regulators and Pol II [172,182,198], these proteins are likely not recruited in the absence of TrxG complexes and gene activation does not occur.

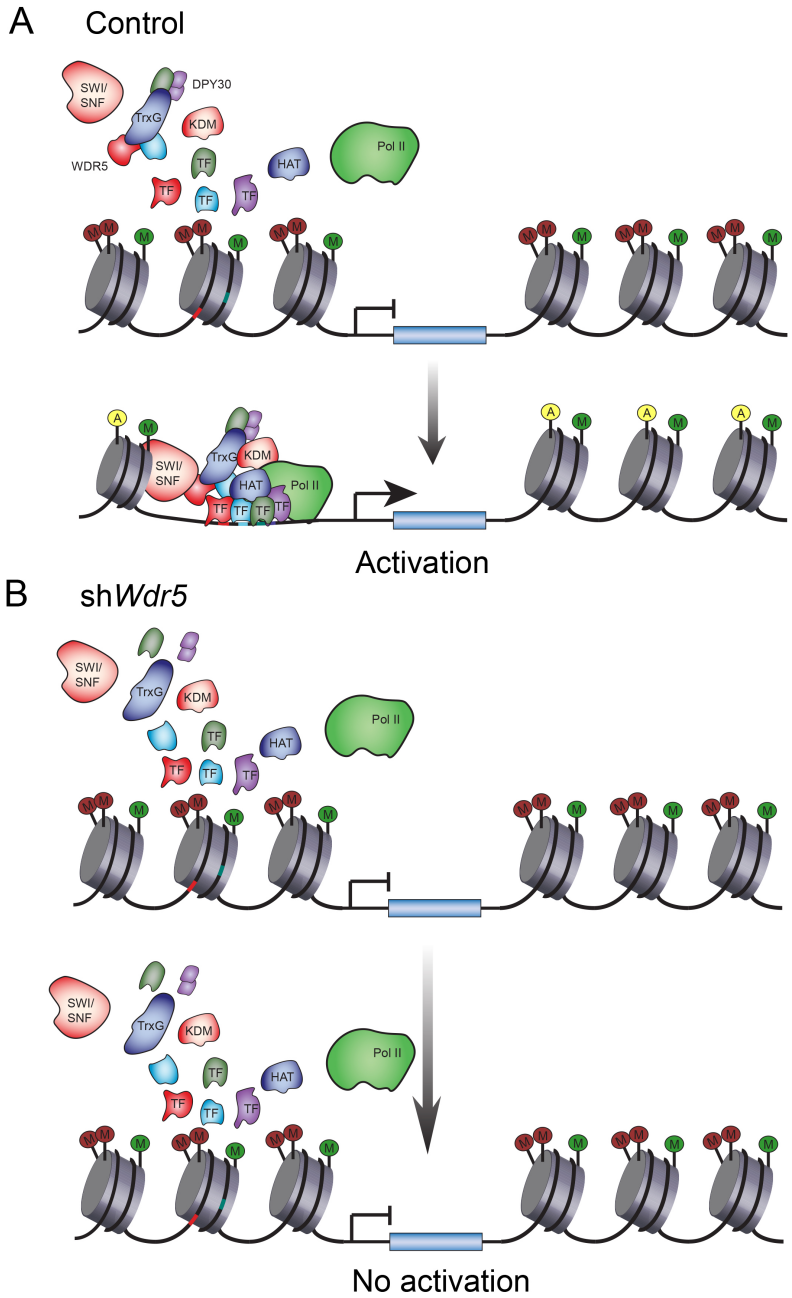

Figure 44: Model of TrxG complex-mediated gene activation.
(A) Cooperative gene activation via transcription factor (TF) binding, nucleosome remodeling (e.g. SWI/SNF) and recruitment of histone acetyltransferases (HATs), lysine demethylases (KDMs), histone methyltransferases (e.g. TrxG complexes) and RNA polymerase II (Pol II). **(B)** In the absence of TrxG complex assembly, gene activation does not occur. Yellow A, histone acetylation; green M, H3K4 methylation; red M, H3K27me3.

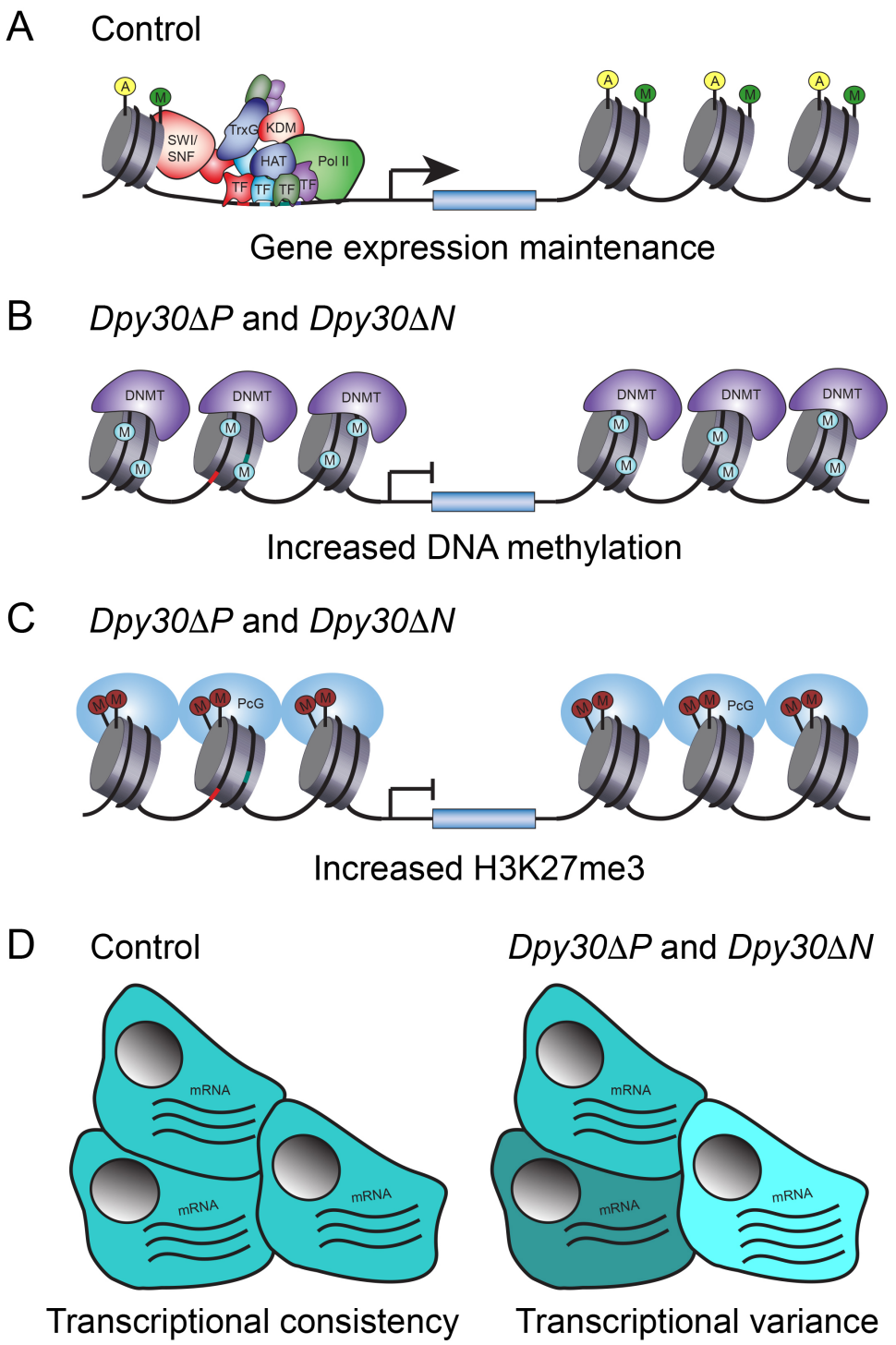

Figure 45: H3K4 methylation promotes gene expression maintenance.
(A) Gene expression is maintained in the presence of H3K4 methylation. **(B-D)** Gene expression maintenance may be reduced at lineage-specific genes in the absence of H3K4 methylation due to **(B)** increased DNA methylation, **(C)** increased H3K27me3, or **(D)** increased transcriptional variance. DNMT, DNA methyltransferase; HAT, histone acetyltransferase; KDM, lysine demethylase; PcG, Polycomb Group complexes; Pol II, RNA polymerase II; SWI/SNF, nucleosome remodeler; TF, transcription factor; yellow A, histone acetylation; green M, H3K4 methylation; red M, H3K27me3; blue M, DNA methylation.

In Chapter 4, disruption of *Dpy30* in PDX1^{+} cells decreased endocrine cell specification and acinar cell differentiation, resulting in diminished numbers of differentiated endocrine and acinar cells. Maturation of acinar cells was also impaired in this model, with reduced amylase and CPA1 immunoreactivity, and correlated with disorganized cystic structures in the exocrine pancreas. While disruption of TrxG complex assembly by *Wdr5* suppression prevented gene activation, loss of H3K4 methyltransferase activity by *Dpy30* disruption had no noticeable effect on gene activation or the expression of most genes. However, the expression of a subset of acinar and endocrine lineage-specific genes was significantly impaired in the absence of H3K4 methylation. Together, these results support a model whereby the TrxG H3K4 methyltransferase activity is required for maintaining the transcriptional output at a subset of genes (Figure 45).

In Chapter 5, disruption of *Dpy30* in NEUROG3^{+} cells significantly impaired expression of a subset of genes involved in endocrine cell functional maturation, including those required for glucose metabolism (i.e. *G6pc2, Gck, Slc2a2*) and insulin secretion (i.e. *Abcc8, Ins1, Ins2, Kcnj11*). Similar to the results presented in Chapter 4, loss of H3K4 methylation from endocrine progenitors did not prevent downstream lineage-specific gene activation but affected gene expression maintenance at a subset of genes (Figure 45).

Using *Cpa1* and *Ins2* as examples, repressed chromatin is activated and maintained via nucleosome remodeling, transcription factor binding, recruitment of TrxG complexes, KDMs, HATs and Pol II (Figure 45A). In *Dpy30ΔP* mice, recruitment of these complexes and co-activators likely still occurs since disruption of *Dpy30* does not impair TrxG complex assembly [206]. However, *Cpa1* and *Ins2* expression is not appropriately maintained after loss of H3K4 methylation. This suggests that in the absence of H3K4 methylation, either DNA methylation is increased, H3K27me3 is re-established, or loss of H3K4 methylation may reduce the stability

and/or residence time of the TrxG complexes, co-activators and Pol II, and thus increase transcriptional variance (Figure 45B-D).

At loci that are constitutively repressed outside the pancreas, e.g. *Cpa1*, active chromatin may not be maintained in the absence of H3K4 methylation and DNA methyltransferases may re-establish the repressive state (Figure 45B). This hypothesis is supported by evidence that DNMT3 can re-establish DNA methylation in the absence of H3K4 methylation [324]. The hypothesis that H3K27me3 is re-established after loss of H3K4 methylation (Figure 45C) is supported by other reports that demonstrate reductions in H3K27ac and increased H3K27me3 in the absence of H3K4 methylation [159,192,194]. There are several lines of evidence that lend support to the hypothesis that H3K4 methylation may stabilize Pol II recruitment and promote transcriptional consistency (Figure 45D). H3K4 methylation has been linked to the Pol II-associated factor (PAF) that is required for transcriptional elongation and also stabilizes transcription through a direct interaction with the general transcription factor TFIID [151,198]. Thus, H3K4 methylation may act as a secondary stabilizer to maintain active chromatin [167]. Other reports have shown that H3K4 methylation correlates with transcription levels and transcriptional stability – the sustained expression of activated genes [200] – and specifically the maintenance of lineage-specific genes [205,206]. For example, loss of H3K4 methylation in mouse cardiomyocytes resulted in transcriptional instability of differentiated cardiac cells, with particular reductions at lineage-specific genes [205]. Additionally, decreased H3K4 methylation by knockdown of *DPY30* in hESCs reduced endoderm gene expression due to impaired Pol II recruitment [206]. Given that broad domains of H3K4 methylation are associated with lineage-specific genes and increased transcriptional output and/or consistency [303,304], the shortening of broad H3K4 methylation domains may result in reduced and/or variable lineage-specific gene

expression. In support of this hypothesis, suppression of *Wdr5* in mouse neural progenitor cells resulted in narrowing of broad H3K4 methylation domains and increased transcriptional variance [303]. However, given that *Wdr5* suppression disrupts TrxG complex assembly in addition to catalytic activity, it is unclear whether reductions in H3K4 methylation or impaired TrxG recruitment results in increased transcriptional variance in this model. The *Dpy30* deletion models developed herein suggest that transcriptional variance is increased after loss of H3K4 methylation, suggesting that loss of H3K4 methylation may result in increased gene expression variance at a subset of lineage-specific genes.

Together, these models support the conclusion that the non-enzymatic function of TrxG complexes has a larger biological impact than H3K4 methylation itself. For example, disruption of TrxG complex formation via suppression of *Wdr5* had a larger effect on pancreas progenitor cell differentiation compared to the genetic deletion of *Dpy30*, which does not disturb TrxG assembly but affects H3K4 methylation. *Neurog3* and downstream endocrine lineage-specific genes were not activated in sh*Wdr5* spheres; however, maintenance of a subset of lineage-specific genes was reduced in *Dpy30ΔP* and *Dpy30ΔN* mice. Supporting this model, several studies have demonstrated that loss of TrxG complex proteins has a larger effect compared to inactivation of histone methyltransferase activity [191,192,325]. This is likely because TrxG complexes mediate gene expression by interactions with transcription factors and recruitment of co-activators and Pol II [162,183], functions that are abolished when the complexes do not assemble.

In addition to impaired expression of genes involved in pancreas progenitor cell differentiation, genes involved in progenitor cell proliferation and survival were also affected. In sh*Wdr5* spheres, genes associated with cell proliferation were decreased and genes associated with apoptosis were increased, resulting in fewer and smaller spheres. Consistently, disruption of

Dpy30 in PDX1^{+} cells reduced progenitor proliferation and increased apoptosis, reducing the overall pancreas size. This suggests that the gene expression changes resulting in reduced proliferation and increased apoptosis are mediated by H3K4 methylation rather than an enzyme-independent role of the TrxG complexes. Although RNA-sequencing revealed that mitotic genes were underrepresented in *Dpy30ΔN* islets, no evidence of altered islet size or number was detected. This is likely because at the stage when H3K4 methylation was lost in this model (P14), endocrine cell proliferation is relatively low.

In conclusion, this thesis reveals that during pancreas progenitor differentiation, the TrxG complexes are important regulators of transcriptional activation at lineage-specific genes. Further, TrxG catalytic activity is not broadly required for gene expression, but has a critical role in promoting the transcriptional maintenance or stability of a subset of lineage-specific genes during pancreas and endocrine progenitor differentiation. Overall, this thesis contributes to our understanding of how the TrxG complexes and H3K4 methylation regulate gene activation and transcriptional maintenance during pancreas and endocrine progenitor differentiation.

6.2 Future Directions

A major application for the continued study of pancreas developmental biology is to improve development of functionally mature human stem cell-derived pancreatic β-cells for diabetes therapy. This will require identification of novel external signals and transcription factors, a greater understanding of how transcription factors regulate pancreas development and maintain β-cell identity, and importantly, exactly how β-cells acquire a functionally mature insulin secretion response [4,50]. The models examined in this thesis suggest that specific targeting of TrxG complexes to lineage-specific loci during hESC-derived pancreas cell differentiation

may stabilize gene expression and improve the efficiency of β-cell functional maturation. Further investigations that address the role of the TrxG complexes and/or H3K4 methylation in β-cell maturation or in the maintenance of β-cell identity, using *Ins1*-Cre or *Ins1*-CreER drivers, would improve our understanding of these processes and help identify target loci.

The minimal effect on progenitor cell maintenance but altered downstream expression of a subset of genes is a common theme observed in all three models described in this thesis and adds strength to these findings. Additionally, *in vitro* pancreas spheroid suppression experiments were complemented by *in vivo* gene targeting, where endocrine cell specification was impaired in both models and further strengthening this result. The suppression of *Wdr5* versus genetic deletion of *Dpy30* in pancreas progenitors allowed for a comparison between the non-catalytic versus catalytic roles of the TrxG complexes, respectively, in pancreas development. Notably, *Wdr5* suppression had a larger biological effect compared to *Dpy30* deletion and loss of H3K4 methylation in $PDX1^+$ cells. However, these conclusions would be strengthened with complementary experiments where *Dpy30* is suppressed in pancreas spheroids and *Wdr5* is genetically deleted from $PDX1^+$ cells. Although *Wdr5* targeted mice are not currently available, preliminary results not presented in this thesis suggest that *Dpy30* suppression in spheroids has a minimal effect on gene expression, including *Neurog3* or downstream endocrine genes. This is consistent with the notion that H3K4 methylation has a minimal role in transcriptional activation.

Although the biological effects of the models examined in this thesis were presumed to be due to loss of TrxG complex activity, both WDR5 and DPY30 associate with other non-TrxG complexes and the additional loss of these functions cannot be completely ruled out. For example, DPY30 also associates with the nucleosome remodeling NuRF complex [197]. In *Dpy30ΔN* mice, however, a phenotype was only observed after loss of H3K4 methylation, rather

than loss of DPY30, suggesting that gene expression changes are dependent on H3K4 methylation and not DPY30 in this model. Additionally, many chromatin regulators have other non-histone substrates, which makes it challenging to delineate whether the histone modification deposited by the chromatin regulator causes the biological effect [156]. Thus, it is entirely possible that methylation of non-histone proteins is also disrupted in the models described herein and the effect of this is currently unknown. As the roles of WDR5, DPY30 and H3K4 methylation were examined in mouse pancreas development in this thesis, it would be interesting to explore the relevance to human pancreas development. Possible strategies to examine this would be to use hESC-derived pancreas progenitor cells in the spheroid assay or during hESC differentiation protocols. Since *DPY30* is required for hESC pluripotentcy [206], an inducible suppression or deletion approach would be required. In light of a current study that developed a method for both the inducible suppression and deletion of *DPY30* during hESC differentiation [326], the controlled deletion of *DPY30* in $PDX1^+$ and $NEUROG3^+$ cells could be examined during hESC-derived pancreas cell differentiation.

A limitation of work in this thesis is that reductions in gene expression were not directly correlated with alterations in histone modifications or Pol II recruitment at *cis*-regulatory loci. Further investigations could address the chromatin state of genes with decreased expression by H3K4me1/3, H3K27ac, H3K27me3 and Pol II ChIP-seq experiments. In the absence of H3K4 methylation at these sites, H3K27ac and Pol II enrichment would also likely be reduced, whereas H3K27me3 enrichment may be increased [159,192,194]. In addition, the absence of H3K4 methylation may permit nucleosome reformation and the re-establishment of DNA methylation by DNMT3 [324]. Further, although TrxG proteins are known to interact with lineage-specific factors (e.g.

FOXA1, MAFA, MAFB and PAX6 [310,327,328]), studies herein have not directly demonstrated an interaction during pancreas development.

Given the exocrine pancreas phenotype in the *Dpy30ΔP* model, an interesting extension of this work would be to examine the role of DPY30 and/or H3K4 methylation in the maintenance of acinar cell identity. Preliminary results not presented in this thesis demonstrate the progressive worsening of the cystic *Dpy30ΔP* pancreas postnatally, with reduced mouse mass and severe hyperglycemia. These phenotypes in combination with the *Dpy30ΔP* pancreas histology may be early indicators of exocrine pancreas diseases such as chronic pancreatitis or pancreatic cancer [300,329-331]. In support of this hypothesis, mutations in the MLL TrxG proteins are linked to pancreatic cancer [331] and the acinar cell identity factor *Bhlha15,* which was decreased in *Dpy30ΔP* embryos, has been linked to mouse models of pancreatitis [128]. Consistently, suppression of *Wdr5* in pancreas spheroids upregulated expression of genes that are described as biomarkers for pancreatitis and pancreatic cancer.

Overall, data presented in this thesis demonstrate that TrxG-mediated H3K4 methylation has a relatively minor role in gene transcription during pancreas and endocrine progenitor development. However, the expression of several lineage-specific genes was affected by disruption of *Wdr5* and *Dpy30*, supporting a role for the TrxG complexes and/or H3K4 methylation in the activation or maintenance of a subset of lineage critical genes. Collectively, these findings provide an improved understanding of how TrxG complexes and H3K4 methylation contribute to pancreas development and endocrine cell maturation.

References

1. Pan, F. C. & Wright, C. Pancreas organogenesis: from bud to plexus to gland. *Dev. Dyn.* **240,** 530–565 (2011).
2. Cleaver, O. & MacDonald, R. J. *Developmental Molecular Biology of the Pancreas*. *Pancreatic Cancer* 71–117 (2010).
3. Bastidas-Ponce, A., Scheibner, K., Lickert, H. & Bakhti, M. Cellular and molecular mechanisms coordinating pancreas development. *Development* **144,** 2873–2888 (2017).
4. Edlund, H. Pancreatic organogenesis--developmental mechanisms and implications for therapy. *Nat. Rev. Genet.* **3,** 524–532 (2002).
5. International Diabetes Federation. *IDF Diabetes Atlas, Eighth Edition*. 1–150 (International Diabetes Federation, 2017).
6. Canadian Diabetes Association. Diabetes in Canada. *www.diabetes.ca* 1–4 (2018).
7. Ahmed, A. M. History of diabetes mellitus. *Saudi Med J* **23,** 373–378 (2002).
8. Karamanou, M., Protogerou, A., Tsoucalas, G., Androutsos, G. & Poulakou-Rebelakou, E. Milestones in the history of diabetes mellitus: The main contributors. *World J Diabetes* **7,** 1–7 (2016).
9. Banting, F. G., Best, C. H., Collip, J. B., Campbell, W. R. & Fletcher, A. A. Pancreatic Extracts in the Treatment of Diabetes Mellitus. *Can Med Assoc J* **12,** 141–146 (1922).
10. Best, C. H. & Scott, D. A. The preparation of insulin. *J. Biol. Chem.* **57,** 709–723 (1923).
11. Powers, A. C. Diabetes Mellitus: Diagnosis Classification, and Pathophysiology in *Harrisons Principles of Internal Medicine* 1–25 (2018).
12. BMJ Publishing Group. *Type 1 diabetes mellitus*. 1–46 (BMJ Publishing Group, 2018).
13. Stumvoll, M., Goldstein, B. J. & van Haeften, T. W. Type 2 diabetes: principles of pathogenesis and therapy. *Lancet* **365,** 1333–1346 (2005).
14. Little, J. W., Miller, C. S. & Rhodus, N. L. *Diabetes Mellitus*. *Little and Falace's Dental Management of the Medically Compromised Patient* 230–254 (Elsevier, 2013).
15. World Health Organization. *Global report on diabetes.* 1–88 (World Health Organization, 2016).
16. Canadian Diabetes Association. *An economic tsunami: the cost of diabetes in Canada*. 1–13 (Canadian Diabetes Association, 2010).
17. BMJ Publishing Group. *Type 2 diabetes mellitus in adults*. 1–72 (BMJ Publishing Group, 2018).
18. Shapiro, A. M. J., Ricordi, C., Hering, B. J., Auchincloss, H., Lindblad, R., Robertson, R. P., Secchi, A., Brendel, M. D., Berney, T., Brennan, D. C., Cagliero, E., Alejandro, R., Ryan, E. A., DiMercurio, B., Morel, P., Polonsky, K. S., Reems, J.-A., Bretzel, R. G., Bertuzzi, F., Froud, T., Kandaswamy, R., Sutherland, D. E. R., Eisenbarth, G., Segal, M., Preiksaitis, J., Korbutt, G. S., Barton, F. B., Viviano, L., Seyfert-Margolis, V., Bluestone, J. & Lakey, J. R. T. International trial of the Edmonton protocol for islet transplantation. *N. Engl. J. Med.* **355,** 1318–1330 (2006).
19. Shapiro, A. M., Lakey, J. R., Ryan, E. A., Korbutt, G. S., Toth, E., Warnock, G. L., Kneteman, N. M. & Rajotte, R. V. Islet transplantation in seven patients with type 1

diabetes mellitus using a glucocorticoid-free immunosuppressive regimen. *N. Engl. J. Med.* **343,** 230–238 (2000).
20. Shapiro, A. M. J. Islet transplantation in type 1 diabetes: ongoing challenges, refined procedures, and long-term outcome. *Rev Diabet Stud* **9,** 385–406 (2012).
21. Pepper, A. R., Bruni, A. & Shapiro, A. M. J. Clinical islet transplantation: is the future finally now? *Curr Opin Organ Transplant* **23,** 428–439 (2018).
22. Yu, Y., Gamble, A., Pawlick, R., Pepper, A. R., Salama, B., Toms, D., Razian, G., Ellis, C., Bruni, A., Gala-Lopez, B., Lu, J. L., Vovko, H., Chiu, C., Abdo, S., Kin, T., Korbutt, G., Shapiro, A. M. J. & Ungrin, M. Bioengineered human pseudoislets form efficiently from donated tissue, compare favourably with native islets in vitro and restore normoglycaemia in mice. *Diabetologia* **61,** 2016–2029 (2018).
23. Meier, J. J., Butler, A. E., Saisho, Y., Monchamp, T., Galasso, R., Bhushan, A., Rizza, R. A. & Butler, P. C. Beta-cell replication is the primary mechanism subserving the postnatal expansion of beta-cell mass in humans. *Diabetes* **57,** 1584–1594 (2008).
24. Aguayo-Mazzucato, C. & Bonner-Weir, S. Pancreatic β Cell Regeneration as a Possible Therapy for Diabetes. *Cell Metab.* **27,** 57–67 (2018).
25. Baeyens, L., Lemper, M., Staels, W., De Groef, S., De Leu, N., Heremans, Y., German, M. S. & Heimberg, H. (Re)generating Human Beta Cells: Status, Pitfalls, and Perspectives. *Physiological Reviews* **98,** 1143–1167 (2018).
26. Shen, W., Taylor, B., Jin, Q., Nguyen-Tran, V., Meeusen, S., Zhang, Y.-Q., Kamireddy, A., Swafford, A., Powers, A. F., Walker, J., Lamb, J., Bursalaya, B., DiDonato, M., Harb, G., Qiu, M., Filippi, C. M., Deaton, L., Turk, C. N., Suarez-Pinzon, W. L., Liu, Y., Hao, X., Mo, T., Yan, S., Li, J., Herman, A. E., Hering, B. J., Wu, T., Martin Seidel, H., McNamara, P., Glynne, R. & Laffitte, B. Inhibition of DYRK1A and GSK3B induces human β-cell proliferation. *Nature Communications* **6,** 8372 (2015).
27. Ouaamari, El, A., Dirice, E., Gedeon, N., Hu, J., Zhou, J.-Y., Shirakawa, J., Hou, L., Goodman, J., Karampelias, C., Qiang, G., Boucher, J., Martinez, R., Gritsenko, M. A., De Jesus, D. F., Kahraman, S., Bhatt, S., Smith, R. D., Beer, H.-D., Jungtrakoon, P., Gong, Y., Goldfine, A. B., Liew, C. W., Doria, A., Andersson, O., Qian, W.-J., Remold-O'Donnell, E. & Kulkarni, R. N. SerpinB1 Promotes Pancreatic β Cell Proliferation. *Cell Metab.* **23,** 194–205 (2016).
28. Rulifson, I. C., Karnik, S. K., Heiser, P. W., Berge, ten, D., Chen, H., Gu, X., Taketo, M. M., Nusse, R., Hebrok, M. & Kim, S. K. Wnt signaling regulates pancreatic beta cell proliferation. *Proc Natl Acad Sci USA* **104,** 6247–6252 (2007).
29. Alonso, L. C., Yokoe, T., Zhang, P., Scott, D. K., Kim, S. K., O'Donnell, C. P. & Garcia-Ocaña, A. Glucose infusion in mice: a new model to induce beta-cell replication. *Diabetes* **56,** 1792–1801 (2007).
30. Moullé, V. S., Vivot, K., Tremblay, C., Zarrouki, B., Ghislain, J. & Poitout, V. Glucose and fatty acids synergistically and reversibly promote beta cell proliferation in rats. *Diabetologia* **60,** 879–888 (2017).
31. Stamateris, R. E., Sharma, R. B., Kong, Y., Ebrahimpour, P., Panday, D., Ranganath, P., Zou, B., Levitt, H., Parambil, N. A., O'Donnell, C. P., Garcia-Ocaña, A. & Alonso, L. C. Glucose Induces Mouse β-Cell Proliferation via IRS2, MTOR, and Cyclin D2 but Not the Insulin Receptor. *Diabetes* **65,** 981–995 (2016).

32. Shirakawa, J., Fernandez, M., Takatani, T., Ouaamari, El, A., Jungtrakoon, P., Okawa, E. R., Zhang, W., Yi, P., Doria, A. & Kulkarni, R. N. Insulin Signaling Regulates the FoxM1/PLK1/CENP-A Pathway to Promote Adaptive Pancreatic β Cell Proliferation. *Cell Metab.* **25,** 868–882.e5 (2017).
33. Szabat, M., Page, M. M., Panzhinskiy, E., Skovsø, S., Mojibian, M., Fernandez-Tajes, J., Bruin, J. E., Bround, M. J., Lee, J. T. C., Xu, E. E., Taghizadeh, F., O'Dwyer, S., van de Bunt, M., Moon, K.-M., Sinha, S., Han, J., Fan, Y., Lynn, F. C., Trucco, M., Borchers, C. H., Foster, L. J., Nislow, C., Kieffer, T. J. & Johnson, J. D. Reduced Insulin Production Relieves Endoplasmic Reticulum Stress and Induces β Cell Proliferation. *Cell Metab.* **23,** 179–193 (2016).
34. Merrell, A. J. & Stanger, B. Z. Adult cell plasticity in vivo: de-differentiation and transdifferentiation are back in style. *Nat. Rev. Mol. Cell Biol.* **17,** 413–425 (2016).
35. van Arensbergen, J., García-Hurtado, J., Morán, I., Maestro, M. A., Xu, X., Van De Casteele, M., Skoudy, A. L., Palassini, M., Heimberg, H. & Ferrer, J. Derepression of Polycomb targets during pancreatic organogenesis allows insulin-producing beta-cells to adopt a neural gene activity program. *Genome Res.* **20,** 722–732 (2010).
36. Thorel, F., Népote, V., Avril, I., Kohno, K., Desgraz, R., Chera, S. & Herrera, P. L. Conversion of adult pancreatic alpha-cells to beta-cells after extreme beta-cell loss. *Nature* **464,** 1149–1154 (2010).
37. Wang, R. N., Klöppel, G. & Bouwens, L. Duct- to islet-cell differentiation and islet growth in the pancreas of duct-ligated adult rats. *Diabetologia* **38,** 1405–1411 (1995).
38. Bonner-Weir, S., Toschi, E., Inada, A., Reitz, P., Fonseca, S. Y., Aye, T. & Sharma, A. The pancreatic ductal epithelium serves as a potential pool of progenitor cells. *Pediatr Diabetes* **5 Suppl 2,** 16–22 (2004).
39. van der Meulen, T., Mawla, A. M., DiGruccio, M. R., Adams, M. W., Nies, V., Dólleman, S., Liu, S., Ackermann, A. M., Cáceres, E., Hunter, A. E., Kaestner, K. H., Donaldson, C. J. & Huising, M. O. Virgin Beta Cells Persist throughout Life at a Neogenic Niche within Pancreatic Islets. *Cell Metab.* **25,** 911–926.e6 (2017).
40. Matsuoka, T.-A., Kaneto, H., Stein, R., Miyatsuka, T., Kawamori, D., Henderson, E., Kojima, I., Matsuhisa, M., Hori, M. & Yamasaki, Y. MafA regulates expression of genes important to islet beta-cell function. *Mol. Endocrinol.* **21,** 2764–2774 (2007).
41. Zhou, Q., Brown, J., Kanarek, A., Rajagopal, J. & Melton, D. A. In vivo reprogramming of adult pancreatic exocrine cells to beta-cells. *Nature* **455,** 627–632 (2008).
42. Akinci, E., Banga, A., Greder, L. V., Dutton, J. R. & Slack, J. M. W. Reprogramming of pancreatic exocrine cells towards a beta (β) cell character using Pdx1, Ngn3 and MafA. *Biochem. J.* **442,** 539–550 (2012).
43. D'Amour, K. A., Bang, A. G., Eliazer, S., Kelly, O. G., Agulnick, A. D., Smart, N. G., Moorman, M. A., Kroon, E., Carpenter, M. K. & Baetge, E. E. Production of pancreatic hormone-expressing endocrine cells from human embryonic stem cells. *Nat Biotechnol* **24,** 1392–1401 (2006).
44. Nostro, M. C., Sarangi, F., Yang, C., Holland, A., Elefanty, A. G., Stanley, E. G., Greiner, D. L. & Keller, G. Efficient generation of NKX6-1+ pancreatic progenitors from multiple human pluripotent stem cell lines. *Stem Cell Reports* **4,** 591–604 (2015).
45. Kroon, E., Martinson, L. A., Kadoya, K., Bang, A. G., Kelly, O. G., Eliazer, S., Young, H., Richardson, M., Smart, N. G., Cunningham, J., Agulnick, A. D., D'Amour, K. A.,

Carpenter, M. K. & Baetge, E. E. Pancreatic endoderm derived from human embryonic stem cells generates glucose-responsive insulin-secreting cells in vivo. *Nat Biotechnol* **26,** 443–452 (2008).
46. Rezania, A., Riedel, M. J., Wideman, R. D., Karanu, F., Ao, Z., Warnock, G. L. & Kieffer, T. J. Production of functional glucagon-secreting α-cells from human embryonic stem cells. *Diabetes* **60,** 239–247 (2011).
47. Rezania, A., Bruin, J. E., Arora, P., Rubin, A., Batushansky, I., Asadi, A., O'Dwyer, S., Quiskamp, N., Mojibian, M., Albrecht, T., Yang, Y. H. C., Johnson, J. D. & Kieffer, T. J. Reversal of diabetes with insulin-producing cells derived in vitro from human pluripotent stem cells. *Nat Biotechnol* **32,** 1121–1133 (2014).
48. Pagliuca, F. W., Millman, J. R., Gürtler, M., Segel, M., Van Dervort, A., Ryu, J. H., Peterson, Q. P., Greiner, D. & Melton, D. A. Generation of functional human pancreatic β cells in vitro. *Cell* **159,** 428–439 (2014).
49. Johnson, J. D. The quest to make fully functional human pancreatic beta cells from embryonic stem cells: climbing a mountain in the clouds. *Diabetologia* **59,** 2047–2057 (2016).
50. Kieffer, T. J. Closing in on Mass Production of Mature Human Beta Cells. *Cell Stem Cell* **18,** 699–702 (2016).
51. Rezania, A., Bruin, J. E., Riedel, M. J., Mojibian, M., Asadi, A., Xu, J., Gauvin, R., Narayan, K., Karanu, F., O'Neil, J. J., Ao, Z., Warnock, G. L. & Kieffer, T. J. Maturation of human embryonic stem cell-derived pancreatic progenitors into functional islets capable of treating pre-existing diabetes in mice. *Diabetes* **61,** 2016–2029 (2012).
52. Millman, J. R., Xie, C., Van Dervort, A., Gürtler, M., Pagliuca, F. W. & Melton, D. A. Generation of stem cell-derived β-cells from patients with type 1 diabetes. *Nature Communications* **7,** 11463 (2016).
53. Russ, H. A., Parent, A. V., Ringler, J. J., Hennings, T. G., Nair, G. G., Shveygert, M., Guo, T., Puri, S., Haataja, L., Cirulli, V., Blelloch, R., Szot, G. L., Arvan, P. & Hebrok, M. Controlled induction of human pancreatic progenitors produces functional beta-like cells in vitro. *The EMBO Journal* **34,** 1759–1772 (2015).
54. Cogger, K. F., Sinha, A., Sarangi, F., McGaugh, E. C., Saunders, D., Dorrell, C., Mejia-Guerrero, S., Aghazadeh, Y., Rourke, J. L., Screaton, R. A., Grompe, M., Streeter, P. R., Powers, A. C., Brissova, M., Kislinger, T. & Nostro, M. C. Glycoprotein 2 is a specific cell surface marker of human pancreatic progenitors. *Nature Communications* **8,** 331 (2017).
55. Zhou, Q., Law, A. C., Rajagopal, J., Anderson, W. J., Gray, P. A. & Melton, D. A. A multipotent progenitor domain guides pancreatic organogenesis. *Dev Cell* **13,** 103–114 (2007).
56. Larsen, H. L. & Grapin-Botton, A. The molecular and morphogenetic basis of pancreas organogenesis. *Semin. Cell Dev. Biol.* **66,** 51–68 (2017).
57. Golosow, N. & Grobstein, C. Epitheliomesenchymal interaction in pancreatic morphogenesis. *Dev. Biol.* **4,** 242–255 (1962).
58. Bayha, E., Jørgensen, M. C., Serup, P. & Grapin-Botton, A. Retinoic acid signaling organizes endodermal organ specification along the entire antero-posterior axis. *PLoS ONE* **4,** e5845 (2009).

59. Hebrok, M., Kim, S. K. & Melton, D. A. Notochord repression of endodermal Sonic hedgehog permits pancreas development. *Genes Dev* **12,** 1705–1713 (1998).
60. Hebrok, M. Hedgehog signaling in pancreas development. *Mechanisms of Development* **120,** 45–57 (2003).
61. Cleaver, O. & MacDonald, R. J. *Developmental Molecular Biology of the Pancreas*. *Pancreatic Cancer* 71–117 (2010).
62. Jensen, J. Gene regulatory factors in pancreatic development. *Dev. Dyn.* **229,** 176–200 (2004).
63. Hebrok, M., Kim, S. K., St Jacques, B., McMahon, A. P. & Melton, D. A. Regulation of pancreas development by hedgehog signaling. *Development* **127,** 4905–4913 (2000).
64. McLin, V. A., Rankin, S. A. & Zorn, A. M. Repression of Wnt/beta-catenin signaling in the anterior endoderm is essential for liver and pancreas development. *Development* **134,** 2207–2217 (2007).
65. Gerrish, K., Gannon, M., Shih, D., Henderson, E., Stoffel, M., Wright, C. V. & Stein, R. Pancreatic beta cell-specific transcription of the pdx-1 gene. The role of conserved upstream control regions and their hepatic nuclear factor 3beta sites. *J. Biol. Chem.* **275,** 3485–3492 (2000).
66. Gao, N., LeLay, J., Vatamaniuk, M. Z., Rieck, S., Friedman, J. R. & Kaestner, K. H. Dynamic regulation of Pdx1 enhancers by Foxa1 and Foxa2 is essential for pancreas development. *Genes Dev* **22,** 3435–3448 (2008).
67. Jacquemin, P., Lemaigre, F. P. & Rousseau, G. G. The Onecut transcription factor HNF-6 (OC-1) is required for timely specification of the pancreas and acts upstream of Pdx-1 in the specification cascade. *Dev. Biol.* **258,** 105–116 (2003).
68. Xuan, S. & Sussel, L. GATA4 and GATA6 regulate pancreatic endoderm identity through inhibition of hedgehog signaling. *Development* **143,** 780–786 (2016).
69. Jonsson, J., Carlsson, L., Edlund, T. & Edlund, H. Insulin-promoter-factor 1 is required for pancreas development in mice. *Nature* **371,** 606–609 (1994).
70. Stoffers, D. A., Zinkin, N. T., Stanojevic, V., Clarke, W. L. & Habener, J. F. Pancreatic agenesis attributable to a single nucleotide deletion in the human IPF1 gene coding sequence. *Nat. Genet.* **15,** 106–110 (1997).
71. Pictet, R. L., Clark, W. R., Williams, R. H. & Rutter, W. J. An ultrastructural analysis of the developing embryonic pancreas. *Dev. Biol.* **29,** 436–467 (1972).
72. Stanger, B. Z., Tanaka, A. J. & Melton, D. A. Organ size is limited by the number of embryonic progenitor cells in the pancreas but not the liver. *Nature* **445,** 886–891 (2007).
73. Seymour, P. A., Freude, K. K., Tran, M. N., Mayes, E. E., Jensen, J., Kist, R., Scherer, G. & Sander, M. SOX9 is required for maintenance of the pancreatic progenitor cell pool. *Proc Natl Acad Sci USA* **104,** 1865–1870 (2007).
74. De Vas, M. G., Kopp, J. L., Heliot, C., Sander, M., Cereghini, S. & Haumaitre, C. Hnf1b controls pancreas morphogenesis and the generation of Ngn3+ endocrine progenitors. *Development* **142,** 871–882 (2015).
75. Fukuda, A., Kawaguchi, Y., Furuyama, K., Kodama, S., Horiguchi, M., Kuhara, T., Kawaguchi, M., Terao, M., Doi, R., Wright, C. V. E., Hoshino, M., Chiba, T. & Uemoto, S. Reduction of Ptf1a gene dosage causes pancreatic hypoplasia and diabetes in mice. *Diabetes* **57,** 2421–2431 (2008).

76. Herrera, P. L. Adult insulin- and glucagon-producing cells differentiate from two independent cell lineages. *Development* **127,** 2317–2322 (2000).
77. Seymour, P. A., Shih, H. P., Patel, N. A., Freude, K. K., Xie, R., Lim, C. J. & Sander, M. A Sox9/Fgf feed-forward loop maintains pancreatic organ identity. *Development* **139,** 3363–3372 (2012).
78. Bhushan, A., Itoh, N., Kato, S., Thiery, J. P., Czernichow, P., Bellusci, S. & Scharfmann, R. Fgf10 is essential for maintaining the proliferative capacity of epithelial progenitor cells during early pancreatic organogenesis. *Development* **128,** 5109–5117 (2001).
79. Norgaard, G. A., Jensen, J. N. & Jensen, J. FGF10 signaling maintains the pancreatic progenitor cell state revealing a novel role of Notch in organ development. *Dev. Biol.* **264,** 323–338 (2003).
80. Duvillié, B., Attali, M., Bounacer, A., Ravassard, P., Basmaciogullari, A. & Scharfmann, R. The mesenchyme controls the timing of pancreatic beta-cell differentiation. *Diabetes* **55,** 582–589 (2006).
81. Kopinke, D., Brailsford, M., Shea, J. E., Leavitt, R., Scaife, C. L. & Murtaugh, L. C. Lineage tracing reveals the dynamic contribution of Hes1+ cells to the developing and adult pancreas. *Development* **138,** 431–441 (2011).
82. Murtaugh, L. C. The what, where, when and how of Wnt/β-catenin signaling in pancreas development. *Organogenesis* **4,** 81–86 (2008).
83. Papadopoulou, S. & Edlund, H. Attenuated Wnt signaling perturbs pancreatic growth but not pancreatic function. *Diabetes* **54,** 2844–2851 (2005).
84. Jonckheere, N., Mayes, E., Shih, H. P., Li, B., Lioubinski, O., Dai, X. & Sander, M. Analysis of mPygo2 mutant mice suggests a requirement for mesenchymal Wnt signaling in pancreatic growth and differentiation. *Dev. Biol.* **318,** 224–235 (2008).
85. Murtaugh, L. C., Law, A. C., Dor, Y. & Melton, D. A. Beta-catenin is essential for pancreatic acinar but not islet development. *Development* **132,** 4663–4674 (2005).
86. Kesavan, G., Sand, F. W., Greiner, T. U., Johansson, J. K., Kobberup, S., Wu, X., Brakebusch, C. & Semb, H. Cdc42-mediated tubulogenesis controls cell specification. *Cell* **139,** 791–801 (2009).
87. Bankaitis, E. D., Bechard, M. E. & Wright, C. V. E. Feedback control of growth, differentiation, and morphogenesis of pancreatic endocrine progenitors in an epithelial plexus niche. *Genes Dev* **29,** 2203–2216 (2015).
88. Villasenor, A., Chong, D. C., Henkemeyer, M. & Cleaver, O. Epithelial dynamics of pancreatic branching morphogenesis. *Development* **137,** 4295–4305 (2010).
89. Shih, H. P., Kopp, J. L., Sandhu, M., Dubois, C. L., Seymour, P. A., Grapin-Botton, A. & Sander, M. A Notch-dependent molecular circuitry initiates pancreatic endocrine and ductal cell differentiation. *Development* **139,** 2488–2499 (2012).
90. Hale, M. A., Swift, G. H., Hoang, C. Q., Deering, T. G., Masui, T., Lee, Y.-K., Xue, J. & MacDonald, R. J. The nuclear hormone receptor family member NR5A2 controls aspects of multipotent progenitor cell formation and acinar differentiation during pancreatic organogenesis. *Development* **141,** 3123–3133 (2014).
91. Pan, F. C., Bankaitis, E. D., Boyer, D., Xu, X., Van De Casteele, M., Magnuson, M. A., Heimberg, H. & Wright, C. V. E. Spatiotemporal patterns of multipotentiality in Ptf1a-

expressing cells during pancreas organogenesis and injury-induced facultative restoration. *Development* **140,** 751–764 (2013).
92. Kopp, J. L., Dubois, C. L., Schaffer, A. E., Hao, E., Shih, H. P., Seymour, P. A., Ma, J. & Sander, M. Sox9+ ductal cells are multipotent progenitors throughout development but do not produce new endocrine cells in the normal or injured adult pancreas. *Development* **138,** 653–665 (2011).
93. Afelik, S. & Jensen, J. Notch signaling in the pancreas: patterning and cell fate specification. *WIREs Dev Biol* **2,** 531–544 (2013).
94. Schaffer, A. E., Freude, K. K., Nelson, S. B. & Sander, M. Nkx6 transcription factors and Ptf1a function as antagonistic lineage determinants in multipotent pancreatic progenitors. *Dev Cell* **18,** 1022–1029 (2010).
95. Murtaugh, L. C., Stanger, B. Z., Kwan, K. M. & Melton, D. A. Notch signaling controls multiple steps of pancreatic differentiation. *Proc Natl Acad Sci USA* **100,** 14920–14925 (2003).
96. Solar, M., Cardalda, C., Houbracken, I., MartIn, M., Maestro, M. A., De Medts, N., Xu, X., Grau, V., Heimberg, H., Bouwens, L. & Ferrer, J. Pancreatic exocrine duct cells give rise to insulin-producing beta cells during embryogenesis but not after birth. *Dev Cell* **17,** 849–860 (2009).
97. Lynn, F. C., Smith, S. B., Wilson, M. E., Yang, K. Y., Nekrep, N. & German, M. S. Sox9 coordinates a transcriptional network in pancreatic progenitor cells. *Proc Natl Acad Sci USA* **104,** 10500–10505 (2007).
98. Pierreux, C. E., Poll, A. V., Kemp, C. R., Clotman, F., Maestro, M. A., Cordi, S., Ferrer, J., Leyns, L., Rousseau, G. G. & Lemaigre, F. P. The transcription factor hepatocyte nuclear factor-6 controls the development of pancreatic ducts in the mouse. *Gastroenterology* **130,** 532–541 (2006).
99. Miyatsuka, T., Kosaka, Y., Kim, H. & German, M. S. Neurogenin3 inhibits proliferation in endocrine progenitors by inducing Cdkn1a. *Proc. Natl. Acad. Sci. U.S.A.* **108,** 185–190 (2011).
100. Gradwohl, G., Dierich, A., LeMeur, M. & Guillemot, F. neurogenin3 is required for the development of the four endocrine cell lineages of the pancreas. *Proc Natl Acad Sci USA* **97,** 1607–1611 (2000).
101. McGrath, P. S., Watson, C. L., Ingram, C., Helmrath, M. A. & Wells, J. M. The Basic Helix-Loop-Helix Transcription Factor NEUROG3 Is Required for Development of the Human Endocrine Pancreas. *Diabetes* **64,** 2497–2505 (2015).
102. Lee, J. C., Smith, S. B., Watada, H., Lin, J., Scheel, D., Wang, J., Mirmira, R. G. & German, M. S. Regulation of the pancreatic pro-endocrine gene neurogenin3. *Diabetes* **50,** 928–936 (2001).
103. Dubois, C. L., Shih, H. P., Seymour, P. A., Patel, N. A., Behrmann, J. M., Ngo, V. & Sander, M. Sox9-haploinsufficiency causes glucose intolerance in mice. *PLoS ONE* **6,** e23131 (2011).
104. Seymour, P. A., Freude, K. K., Dubois, C. L., Shih, H. P., Patel, N. A. & Sander, M. A dosage-dependent requirement for Sox9 in pancreatic endocrine cell formation. *Dev. Biol.* **323,** 19–30 (2008).

105. Nelson, S. B., Schaffer, A. E. & Sander, M. The transcription factors Nkx6.1 and Nkx6.2 possess equivalent activities in promoting beta-cell fate specification in Pdx1+ pancreatic progenitor cells. *Development* **134,** 2491–2500 (2007).
106. Bechard, M. E., Bankaitis, E. D., Hipkens, S. B., Ustione, A., Piston, D. W., Yang, Y.-P., Magnuson, M. A. & Wright, C. V. E. Precommitment low-level Neurog3 expression defines a long-lived mitotic endocrine-biased progenitor pool that drives production of endocrine-committed cells. *Genes Dev* **30,** 1852–1865 (2016).
107. Wang, S., Yan, J., Anderson, D. A., Xu, Y., Kanal, M. C., Cao, Z., Wright, C. V. E. & Gu, G. Neurog3 gene dosage regulates allocation of endocrine and exocrine cell fates in the developing mouse pancreas. *Dev. Biol.* **339,** 26–37 (2010).
108. Beucher, A., MartIn, M., Spenle, C., Poulet, M., Collin, C. & Gradwohl, G. Competence of failed endocrine progenitors to give rise to acinar but not ductal cells is restricted to early pancreas development. *Dev. Biol.* **361,** 277–285 (2012).
109. Scavuzzo, M. A., Hill, M. C., Chmielowiec, J., Yang, D., Teaw, J., Sheng, K., Kong, Y., Bettini, M., Zong, C., Martin, J. F. & Borowiak, M. Endocrine lineage biases arise in temporally distinct endocrine progenitors during pancreatic morphogenesis. *Nature Communications* **9,** 3356 (2018).
110. Qu, X., Afelik, S., Jensen, J. N., Bukys, M. A., Kobberup, S., Schmerr, M., Xiao, F., Nyeng, P., Veronica Albertoni, M., Grapin-Botton, A. & Jensen, J. Notch-mediated post-translational control of Ngn3 protein stability regulates pancreatic patterning and cell fate commitment. *Dev. Biol.* **376,** 1–12 (2013).
111. Krentz, N. A. J., Van Hoof, D., Li, Z., Watanabe, A., Tang, M., Nian, C., German, M. S. & Lynn, F. C. Phosphorylation of NEUROG3 Links Endocrine Differentiation to the Cell Cycle in Pancreatic Progenitors. *Dev Cell* **41,** 129–142.e6 (2017).
112. Desgraz, R. & Herrera, P. L. Pancreatic neurogenin 3-expressing cells are unipotent islet precursors. *Development* **136,** 3567–3574 (2009).
113. Gasa, R., Mrejen, C., Leachman, N., Otten, M., Barnes, M., Wang, J., Chakrabarti, S., Mirmira, R. & German, M. Proendocrine genes coordinate the pancreatic islet differentiation program in vitro. *Proc Natl Acad Sci USA* **101,** 13245–13250 (2004).
114. Sander, M., Neubüser, A., Kalamaras, J., Ee, H. C., Martin, G. R. & German, M. S. Genetic analysis reveals that PAX6 is required for normal transcription of pancreatic hormone genes and islet development. *Genes Dev* **11,** 1662–1673 (1997).
115. Ahlgren, U., Jonsson, J., Jonsson, L., Simu, K. & Edlund, H. Beta-Cell-specific inactivation of the mouse Ipf1/Pdx1 gene results in loss of the beta-cell phenotype and maturity onset diabetes. *Genes Dev* **12,** 1763–1768 (1998).
116. Gao, T., McKenna, B., Li, C., Reichert, M., Nguyen, J., Singh, T., Yang, C., Pannikar, A., Doliba, N., Zhang, T., Stoffers, D. A., Edlund, H., Matschinsky, F., Stein, R. & Stanger, B. Z. Pdx1 maintains β cell identity and function by repressing an α cell program. *Cell Metab.* **19,** 259–271 (2014).
117. Schaffer, A. E., Taylor, B. L., Benthuysen, J. R., Liu, J., Thorel, F., Yuan, W., Jiao, Y., Kaestner, K. H., Herrera, P. L., Magnuson, M. A., May, C. L. & Sander, M. Nkx6.1 controls a gene regulatory network required for establishing and maintaining pancreatic Beta cell identity. *PLoS Genet* **9,** e1003274 (2013).
118. Sussel, L., Kalamaras, J., Hartigan-O'Connor, D. J., Meneses, J. J., Pedersen, R. A., Rubenstein, J. L. & German, M. S. Mice lacking the homeodomain transcription factor

Nkx2.2 have diabetes due to arrested differentiation of pancreatic beta cells. *Development* **125,** 2213–2221 (1998).
119. Sosa-Pineda, B., Chowdhury, K., Torres, M., Oliver, G. & Gruss, P. The Pax4 gene is essential for differentiation of insulin-producing beta cells in the mammalian pancreas. *Nature* **386,** 399–402 (1997).
120. Gu, G., Dubauskaite, J. & Melton, D. A. Direct evidence for the pancreatic lineage: NGN3+ cells are islet progenitors and are distinct from duct progenitors. *Development* **129,** 2447–2457 (2002).
121. Miralles, F., Czernichow, P., Ozaki, K., Itoh, N. & Scharfmann, R. Signaling through fibroblast growth factor receptor 2b plays a key role in the development of the exocrine pancreas. *Proc Natl Acad Sci USA* **96,** 6267–6272 (1999).
122. Afelik, S., Qu, X., Hasrouni, E., Bukys, M. A., Deering, T., Nieuwoudt, S., Rogers, W., MacDonald, R. J. & Jensen, J. Notch-mediated patterning and cell fate allocation of pancreatic progenitor cells. *Development* **139,** 1744–1753 (2012).
123. Murtaugh, L. C. Pancreas and beta-cell development: from the actual to the possible. *Development* **134,** 427–438 (2007).
124. Wells, J. M., Esni, F., Boivin, G. P., Aronow, B. J., Stuart, W., Combs, C., Sklenka, A., Leach, S. D. & Lowy, A. M. Wnt/beta-catenin signaling is required for development of the exocrine pancreas. *BMC Dev. Biol.* **7,** 4 (2007).
125. Masui, T., Long, Q., Beres, T. M., Magnuson, M. A. & MacDonald, R. J. Early pancreatic development requires the vertebrate Suppressor of Hairless (RBPJ) in the PTF1 bHLH complex. *Genes Dev* **21,** 2629–2643 (2007).
126. Masui, T., Swift, G. H., Deering, T., Shen, C., Coats, W. S., Long, Q., Elsässer, H. P., Magnuson, M. A. & MacDonald, R. J. Replacement of Rbpj with Rbpjl in the PTF1 complex controls the final maturation of pancreatic acinar cells. *Gastroenterology* **139,** 270–280 (2010).
127. Beres, T. M., Masui, T., Swift, G. H., Shi, L., Henke, R. M. & MacDonald, R. J. PTF1 is an organ-specific and Notch-independent basic helix-loop-helix complex containing the mammalian Suppressor of Hairless (RBP-J) or its paralogue, RBP-L. *Mol. Cell. Biol.* **26,** 117–130 (2006).
128. Pin, C. L., Rukstalis, J. M., Johnson, C. & Konieczny, S. F. The bHLH transcription factor Mist1 is required to maintain exocrine pancreas cell organization and acinar cell identity. *J. Cell Biol.* **155,** 519–530 (2001).
129. Krapp, A., Knöfler, M., Ledermann, B., Bürki, K., Berney, C., Zoerkler, N., Hagenbüchle, O. & Wellauer, P. K. The bHLH protein PTF1-p48 is essential for the formation of the exocrine and the correct spatial organization of the endocrine pancreas. *Genes Dev* **12,** 3752–3763 (1998).
130. Liu, J. S. E. & Hebrok, M. All mixed up: defining roles for β-cell subtypes in mature islets. *Genes Dev* **31,** 228–240 (2017).
131. MacFarlane, W. M., Read, M. L., Gilligan, M., Bujalska, I. & Docherty, K. Glucose modulates the binding activity of the beta-cell transcription factor IUF1 in a phosphorylation-dependent manner. *Biochem. J.* **303 (Pt 2),** 625–631 (1994).
132. Chakrabarti, S. K., James, J. C. & Mirmira, R. G. Quantitative assessment of gene targeting in vitro and in vivo by the pancreatic transcription factor, Pdx1. Importance of

chromatin structure in directing promoter binding. *J. Biol. Chem.* **277,** 13286–13293 (2002).
133. Taylor, B. L., Liu, F.-F. & Sander, M. Nkx6.1 is essential for maintaining the functional state of pancreatic beta cells. *Cell Rep.* **4,** 1262–1275 (2013).
134. Pin, C. & Fenech, M. Development of the Pancreas. *Pancreapedia: Exocrine Pancreas Knowledge Base* **1,** 1–10 (2017).
135. Jia, D., Sun, Y. & Konieczny, S. F. Mist1 regulates pancreatic acinar cell proliferation through p21 CIP1/WAF1. *Gastroenterology* **135,** 1687–1697 (2008).
136. Jennings, R. E., Berry, A. A., Strutt, J. P., Gerrard, D. T. & Hanley, N. A. Human pancreas development. *Development* **142,** 3126–3137 (2015).
137. Lyttle, B. M., Li, J., Krishnamurthy, M., Fellows, F., Wheeler, M. B., Goodyer, C. G. & Wang, R. Transcription factor expression in the developing human fetal endocrine pancreas. *Diabetologia* **51,** 1169–1180 (2008).
138. Jennings, R. E., Berry, A. A., Kirkwood-Wilson, R., Roberts, N. A., Hearn, T., Salisbury, R. J., Blaylock, J., Piper Hanley, K. & Hanley, N. A. Development of the human pancreas from foregut to endocrine commitment. *Diabetes* **62,** 3514–3522 (2013).
139. Riedel, M. J., Asadi, A., Wang, R., Ao, Z., Warnock, G. L. & Kieffer, T. J. Immunohistochemical characterisation of cells co-producing insulin and glucagon in the developing human pancreas. *Diabetologia* **55,** 372–381 (2012).
140. Artner, I., Le Lay, J., Hang, Y., Elghazi, L., Schisler, J. C., Henderson, E., Sosa-Pineda, B. & Stein, R. MafB: an activator of the glucagon gene expressed in developing islet alpha- and beta-cells. *Diabetes* **55,** 297–304 (2006).
141. Dolenšek, J., Rupnik, M. S. & Stožer, A. Structural similarities and differences between the human and the mouse pancreas. *Islets* **7,** e1024405 (2015).
142. Yamamoto, T. & Saitoh, N. Non-coding RNAs and chromatin domains. *Curr. Opin. Cell Biol.* **58,** 26–33 (2019).
143. Rinn, J. L. & Chang, H. Y. Genome regulation by long noncoding RNAs. *Annu. Rev. Biochem.* **81,** 145–166 (2012).
144. Flynn, R. A. & Chang, H. Y. Active chromatin and noncoding RNAs: an intimate relationship. *Current Opinion in Genetics & Development* **22,** 172–178 (2012).
145. Schübeler, D., MacAlpine, D. M., Scalzo, D., Wirbelauer, C., Kooperberg, C., van Leeuwen, F., Gottschling, D. E., O'Neill, L. P., Turner, B. M., Delrow, J., Bell, S. P. & Groudine, M. The histone modification pattern of active genes revealed through genome-wide chromatin analysis of a higher eukaryote. *Genes Dev* **18,** 1263–1271 (2004).
146. Bannister, A. J. & Kouzarides, T. Regulation of chromatin by histone modifications. *Cell Res.* **21,** 381–395 (2011).
147. Merkenschlager, M. & Odom, D. T. CTCF and cohesin: linking gene regulatory elements with their targets. *Cell* **152,** 1285–1297 (2013).
148. Bernstein, B. E., Mikkelsen, T. S., Xie, X., Kamal, M., Huebert, D. J., Cuff, J., Fry, B., Meissner, A., Wernig, M., Plath, K., Jaenisch, R., Wagschal, A., Feil, R., Schreiber, S. L. & Lander, E. S. A bivalent chromatin structure marks key developmental genes in embryonic stem cells. *Cell* **125,** 315–326 (2006).

149. Venkatesh, S. & Workman, J. L. Histone exchange, chromatin structure and the regulation of transcription. *Nat. Rev. Mol. Cell Biol.* **16,** 178–189 (2015).
150. Allen, B. L. & Taatjes, D. J. The Mediator complex: a central integrator of transcription. *Nat. Rev. Mol. Cell Biol.* **16,** 155–166 (2015).
151. Li, B., Carey, M. & Workman, J. L. The role of chromatin during transcription. *Cell* **128,** 707–719 (2007).
152. Cairns, B. R. The logic of chromatin architecture and remodelling at promoters. *Nature* **461,** 193–198 (2009).
153. Dor, Y. & Cedar, H. Principles of DNA methylation and their implications for biology and medicine. *Lancet* **392,** 777–786 (2018).
154. Smolle, M. & Workman, J. L. Transcription-associated histone modifications and cryptic transcription. *Biochim. Biophys. Acta* **1829,** 84–97 (2013).
155. Jin, Q., Yu, L.-R., Wang, L., Zhang, Z., Kasper, L. H., Lee, J.-E., Wang, C., Brindle, P. K., Dent, S. Y. R. & Ge, K. Distinct roles of GCN5/PCAF-mediated H3K9ac and CBP/p300-mediated H3K18/27ac in nuclear receptor transactivation. *The EMBO Journal* **30,** 249–262 (2011).
156. Kouzarides, T. Chromatin modifications and their function. *Cell* **128,** 693–705 (2007).
157. Geisler, S. J. & Paro, R. Trithorax and Polycomb group-dependent regulation: a tale of opposing activities. *Development* **142,** 2876–2887 (2015).
158. Wu, J. I., Lessard, J. & Crabtree, G. R. Understanding the words of chromatin regulation. *Cell* **136,** 200–206 (2009).
159. Schuettengruber, B., Bourbon, H.-M., Di Croce, L. & Cavalli, G. Genome Regulation by Polycomb and Trithorax: 70 Years and Counting. *Cell* **171,** 34–57 (2017).
160. Nottke, A., Colaiácovo, M. P. & Shi, Y. Developmental roles of the histone lysine demethylases. *Development* **136,** 879–889 (2009).
161. Pope, S. D. & Medzhitov, R. Emerging Principles of Gene Expression Programs and Their Regulation. *Mol Cell* **71,** 389–397 (2018).
162. Heinz, S., Romanoski, C. E., Benner, C. & Glass, C. K. The selection and function of cell type-specific enhancers. *Nat. Rev. Mol. Cell Biol.* **16,** 144–154 (2015).
163. Calo, E. & Wysocka, J. Modification of enhancer chromatin: what, how, and why? *Mol Cell* **49,** 825–837 (2013).
164. Lee, T. I. & Young, R. A. Transcriptional regulation and its misregulation in disease. *Cell* **152,** 1237–1251 (2013).
165. Reddy, M. A., Zhang, E. & Natarajan, R. Epigenetic mechanisms in diabetic complications and metabolic memory. *Diabetologia* **58,** 443–455 (2015).
166. Barbieri, M., Xie, S. Q., Torlai Triglia, E., Chiariello, A. M., Bianco, S., de Santiago, I., Branco, M. R., Rueda, D., Nicodemi, M. & Pombo, A. Active and poised promoter states drive folding of the extended HoxB locus in mouse embryonic stem cells. *Nat. Struct. Mol. Biol.* **24,** 515–524 (2017).
167. Ruthenburg, A. J., Allis, C. D. & Wysocka, J. Methylation of lysine 4 on histone H3: intricacy of writing and reading a single epigenetic mark. *Mol Cell* **25,** 15–30 (2007).
168. King, A. D., Huang, K., Rubbi, L., Liu, S., Wang, C.-Y., Wang, Y., Pellegrini, M. & Fan, G. Reversible Regulation of Promoter and Enhancer Histone Landscape by DNA Methylation in Mouse Embryonic Stem Cells. *Cell Rep.* **17,** 289–302 (2016).

169. Ernst, J., Kheradpour, P., Mikkelsen, T. S., Shoresh, N., Ward, L. D., Epstein, C. B., Zhang, X., Wang, L., Issner, R., Coyne, M., Ku, M., Durham, T., Kellis, M. & Bernstein, B. E. Mapping and analysis of chromatin state dynamics in nine human cell types. *Nature* 1–9 (2011).
170. Rada-Iglesias, A., Bajpai, R., Swigut, T., Brugmann, S. A., Flynn, R. A. & Wysocka, J. A unique chromatin signature uncovers early developmental enhancers in humans. *Nature* **470,** 279–283 (2011).
171. Heintzman, N. D., Hon, G. C., Hawkins, R. D., Kheradpour, P., Stark, A., Harp, L. F., Ye, Z., Lee, L. K., Stuart, R. K., Ching, C. W., Ching, K. A., Antosiewicz-Bourget, J. E., Liu, H., Zhang, X., Green, R. D., Lobanenkov, V. V., Stewart, R., Thomson, J. A., Crawford, G. E., Kellis, M. & Ren, B. Histone modifications at human enhancers reflect global cell-type-specific gene expression. *Nature* **459,** 108–112 (2009).
172. Hyun, K., Jeon, J., Park, K. & Kim, J. Writing, erasing and reading histone lysine methylations. *Exp. Mol. Med.* **49,** e324 (2017).
173. Heintzman, N. D., Stuart, R. K., Hon, G., Fu, Y., Ching, C. W., Hawkins, R. D., Barrera, L. O., Van Calcar, S., Qu, C., Ching, K. A., Wang, W., Weng, Z., Green, R. D., Crawford, G. E. & Ren, B. Distinct and predictive chromatin signatures of transcriptional promoters and enhancers in the human genome. *Nat. Genet.* **39,** 311–318 (2007).
174. Creyghton, M. P., Cheng, A. W., Welstead, G. G., Kooistra, T., Carey, B. W., Steine, E. J., Hanna, J., Lodato, M. A., Frampton, G. M., Sharp, P. A., Boyer, L. A., Young, R. A. & Jaenisch, R. Histone H3K27ac separates active from poised enhancers and predicts developmental state. *Proc. Natl. Acad. Sci. U.S.A.* **107,** 21931–21936 (2010).
175. Hoffman, B. G., Robertson, G., Zavaglia, B., Beach, M., Cullum, R., Lee, S., Soukhatcheva, G., Li, L., Wederell, E. D., Thiessen, N., Bilenky, M., Cezard, T., Tam, A., Kamoh, B., Birol, I., Dai, D., Zhao, Y., Hirst, M., Verchere, C. B., Helgason, C. D., Marra, M. A., Jones, S. J. M. & Hoodless, P. A. Locus co-occupancy, nucleosome positioning, and H3K4me1 regulate the functionality of FOXA2-, HNF4A-, and PDX1-bound loci in islets and liver. *Genome Res.* **20,** 1037–1051 (2010).
176. Campbell, S. A. & Hoffman, B. G. Chromatin Regulators in Pancreas Development and Diabetes. *Trends Endocrinol. Metab.* **27,** 142–152 (2016).
177. Schneider, R., Bannister, A. J., Myers, F. A., Thorne, A. W., Crane-Robinson, C. & Kouzarides, T. Histone H3 lysine 4 methylation patterns in higher eukaryotic genes. *Nat. Cell Biol.* **6,** 73–77 (2004).
178. Saksouk, N., Simboeck, E. & Déjardin, J. Constitutive heterochromatin formation and transcription in mammals. *Epigenetics Chromatin* **8,** 3 (2015).
179. Kingston, R. E. & Tamkun, J. W. Transcriptional regulation by trithorax-group proteins. *Cold Spring Harb Perspect Biol* **6,** a019349 (2014).
180. Wang, A., Yue, F., Li, Y., Xie, R., Harper, T., Patel, N. A., Muth, K., Palmer, J., Qiu, Y., Wang, J., Lam, D. K., Raum, J. C., Stoffers, D. A., Ren, B. & Sander, M. Epigenetic priming of enhancers predicts developmental competence of hESC-derived endodermal lineage intermediates. *Cell Stem Cell* **16,** 386–399 (2015).
181. Zaret, K. S. & Carroll, J. S. Pioneer transcription factors: establishing competence for gene expression. *Genes Dev* **25,** 2227–2241 (2011).

182. Bochyńska, A., Lüscher-Firzlaff, J. & Lüscher, B. Modes of Interaction of KMT2 Histone H3 Lysine 4 Methyltransferase/COMPASS Complexes with Chromatin. *Cells* **7,** (2018).
183. Shilatifard, A. The COMPASS family of histone H3K4 methylases: mechanisms of regulation in development and disease pathogenesis. *Annu. Rev. Biochem.* **81,** 65–95 (2012).
184. Senisterra, G., Wu, H., Allali-Hassani, A., Wasney, G. A., Barsyte-Lovejoy, D., Dombrovski, L., Dong, A., Nguyen, K. T., Smil, D., Bolshan, Y., Hajian, T., He, H., Seitova, A., Chau, I., Li, F., Poda, G., Couture, J.-F., Brown, P. J., Al-awar, R., Schapira, M., Arrowsmith, C. H. & Vedadi, M. Small-molecule inhibition of MLL activity by disruption of its interaction with WDR5. *Biochem. J.* **449,** 151–159 (2013).
185. Dou, Y., Milne, T. A., Ruthenburg, A. J., Lee, S., Lee, J. W., Verdine, G. L., Allis, C. D. & Roeder, R. G. Regulation of MLL1 H3K4 methyltransferase activity by its core components. *Nat Struct Mol Biol* **13,** 713–719 (2006).
186. Schuettengruber, B., Chourrout, D., Vervoort, M., Leblanc, B. & Cavalli, G. Genome regulation by polycomb and trithorax proteins. *Cell* **128,** 735–745 (2007).
187. Takahashi, Y.-H., Westfield, G. H., Oleskie, A. N., Trievel, R. C., Shilatifard, A. & Skiniotis, G. Structural analysis of the core COMPASS family of histone H3K4 methylases from yeast to human. *Proc. Natl. Acad. Sci. U.S.A.* **108,** 20526–20531 (2011).
188. Hu, D., Gao, X., Morgan, M. A., Herz, H.-M., Smith, E. R. & Shilatifard, A. The MLL3/MLL4 branches of the COMPASS family function as major histone H3K4 monomethylases at enhancers. *Mol. Cell. Biol.* **33,** 4745–4754 (2013).
189. Denissov, S., Hofemeister, H., Marks, H., Kranz, A., Ciotta, G., Singh, S., Anastassiadis, K., Stunnenberg, H. G. & Stewart, A. F. Mll2 is required for H3K4 trimethylation on bivalent promoters in embryonic stem cells, whereas Mll1 is redundant. *Development* **141,** 526–537 (2014).
190. Agger, K., Cloos, P. A. C., Christensen, J., Pasini, D., Rose, S., Rappsilber, J., Issaeva, I., Canaani, E., Salcini, A. E. & Helin, K. UTX and JMJD3 are histone H3K27 demethylases involved in HOX gene regulation and development. *Nature* **449,** 731–734 (2007).
191. Sze, C. C., Cao, K., Collings, C. K., Marshall, S. A., Rendleman, E. J., Ozark, P. A., Chen, F. X., Morgan, M. A., Wang, L. & Shilatifard, A. Histone H3K4 methylation-dependent and -independent functions of Set1A/COMPASS in embryonic stem cell self-renewal and differentiation. *Genes Dev* **31,** 1732–1737 (2017).
192. Dorighi, K. M., Swigut, T., Henriques, T., Bhanu, N. V., Scruggs, B. S., Nady, N., Still, C. D., Garcia, B. A., Adelman, K. & Wysocka, J. Mll3 and Mll4 Facilitate Enhancer RNA Synthesis and Transcription from Promoters Independently of H3K4 Monomethylation. *Mol Cell* **66,** 568–576.e4 (2017).
193. Cao, K., Collings, C. K., Marshall, S. A., Morgan, M. A., Rendleman, E. J., Wang, L., Sze, C. C., Sun, T., Bartom, E. T. & Shilatifard, A. SET1A/COMPASS and shadow enhancers in the regulation of homeotic gene expression. *Genes Dev* **31,** 787–801 (2017).
194. Rickels, R., Herz, H.-M., Sze, C. C., Cao, K., Morgan, M. A., Collings, C. K., Gause, M., Takahashi, Y.-H., Wang, L., Rendleman, E. J., Marshall, S. A., Krueger, A., Bartom,

E. T., Piunti, A., Smith, E. R., Abshiru, N. A., Kelleher, N. L., Dorsett, D. & Shilatifard, A. Histone H3K4 monomethylation catalyzed by Trr and mammalian COMPASS-like proteins at enhancers is dispensable for development and viability. *Nat. Genet.* **49,** 1647–1653 (2017).

195. Wang, C., Lee, J.-E., Lai, B., Macfarlan, T. S., Xu, S., Zhuang, L., Liu, C., Peng, W. & Ge, K. Enhancer priming by H3K4 methyltransferase MLL4 controls cell fate transition. *Proc. Natl. Acad. Sci. U.S.A.* **113,** 11871–11876 (2016).
196. Ee, L.-S., McCannell, K. N., Tang, Y., Fernandes, N., Hardy, W. R., Green, M. R., Chu, F. & Fazzio, T. G. An Embryonic Stem Cell-Specific NuRD Complex Functions through Interaction with WDR5. *Stem Cell Reports* **8,** 1488–1496 (2017).
197. Tremblay, V., Zhang, P., Chaturvedi, C.-P., Thornton, J., Brunzelle, J. S., Skiniotis, G., Shilatifard, A., Brand, M. & Couture, J.-F. Molecular basis for DPY-30 association to COMPASS-like and NURF complexes. *Structure* **22,** 1821–1830 (2014).
198. Gates, L. A., Foulds, C. E. & O'Malley, B. W. Histone Marks in the 'Driver's Seat': Functional Roles in Steering the Transcription Cycle. *Trends Biochem Sci* **42,** 977–989 (2017).
199. Hödl, M. & Basler, K. Transcription in the absence of histone H3.2 and H3K4 methylation. *Curr. Biol.* **22,** 2253–2257 (2012).
200. Pérez-Lluch, S., Blanco, E., Tilgner, H., Curado, J., Ruiz-Romero, M., Corominas, M. & Guigó, R. Absence of canonical marks of active chromatin in developmentally regulated genes. *Nat. Genet.* **47,** 1158–1167 (2015).
201. Local, A., Huang, H., Albuquerque, C. P., Singh, N., Lee, A. Y., Wang, W., Wang, C., Hsia, J. E., Shiau, A. K., Ge, K., Corbett, K. D., Wang, D., Zhou, H. & Ren, B. Identification of H3K4me1-associated proteins at mammalian enhancers. *Nat. Genet.* **50,** 73–82 (2018).
202. Simon, J. A. & Kingston, R. E. Occupying chromatin: Polycomb mechanisms for getting to genomic targets, stopping transcriptional traffic, and staying put. *Mol Cell* **49,** 808–824 (2013).
203. Jiang, H., Lu, X., Shimada, M., Dou, Y., Tang, Z. & Roeder, R. G. Regulation of transcription by the MLL2 complex and MLL complex-associated AKAP95. *Nat Struct Mol Biol* **20,** 1156–1163 (2013).
204. Hu, D., Gao, X., Cao, K., Morgan, M. A., Mas, G., Smith, E. R., Volk, A. G., Bartom, E. T., Crispino, J. D., Di Croce, L. & Shilatifard, A. Not All H3K4 Methylations Are Created Equal: Mll2/COMPASS Dependency in Primordial Germ Cell Specification. *Mol Cell* **65,** 460–475.e6 (2017).
205. Stein, A. B., Jones, T. A., Herron, T. J., Patel, S. R., Day, S. M., Noujaim, S. F., Milstein, M. L., Klos, M., Furspan, P. B., Jalife, J. & Dressler, G. R. Loss of H3K4 methylation destabilizes gene expression patterns and physiological functions in adult murine cardiomyocytes. *J. Clin. Invest.* **121,** 2641–2650 (2011).
206. Bertero, A., Madrigal, P., Galli, A., Hubner, N. C., Moreno, I., Burks, D., Brown, S., Pedersen, R. A., Gaffney, D., Mendjan, S., Pauklin, S. & Vallier, L. Activin/nodal signaling and NANOG orchestrate human embryonic stem cell fate decisions by controlling the H3K4me3 chromatin mark. *Genes Dev* **29,** 702–717 (2015).

207. Henriques, T., Scruggs, B. S., Inouye, M. O., Muse, G. W., Williams, L. H., Burkholder, A. B., Lavender, C. A., Fargo, D. C. & Adelman, K. Widespread transcriptional pausing and elongation control at enhancers. *Genes Dev* **32,** 26–41 (2018).
208. Dixon, J. R., Jung, I., Selvaraj, S., Shen, Y., Antosiewicz-Bourget, J. E., Lee, A. Y., Ye, Z., Kim, A., Rajagopal, N., Xie, W., Diao, Y., Liang, J., Zhao, H., Lobanenkov, V. V., Ecker, J. R., Thomson, J. A. & Ren, B. Chromatin architecture reorganization during stem cell differentiation. *Nature* **518,** 331–336 (2015).
209. Gifford, C. A., Ziller, M. J., Gu, H., Trapnell, C., Donaghey, J., Tsankov, A., Shalek, A. K., Kelley, D. R., Shishkin, A. A., Issner, R., Zhang, X., Coyne, M., Fostel, J. L., Holmes, L., Meldrim, J., Guttman, M., Epstein, C., Park, H., Kohlbacher, O., Rinn, J., Gnirke, A., Lander, E. S., Bernstein, B. E. & Meissner, A. Transcriptional and epigenetic dynamics during specification of human embryonic stem cells. *Cell* **153,** 1149–1163 (2013).
210. Xie, W., Schultz, M. D., Lister, R., Hou, Z., Rajagopal, N., Ray, P., Whitaker, J. W., Tian, S., Hawkins, R. D., Leung, D., Yang, H., Wang, T., Lee, A. Y., Swanson, S. A., Zhang, J., Zhu, Y., Kim, A., Nery, J. R., Urich, M. A., Kuan, S., Yen, C.-A., Klugman, S., Yu, P., Suknuntha, K., Propson, N. E., Chen, H., Edsall, L. E., Wagner, U., Li, Y., Ye, Z., Kulkarni, A., Xuan, Z., Chung, W.-Y., Chi, N. C., Antosiewicz-Bourget, J. E., Slukvin, I., Stewart, R., Zhang, M. Q., Wang, W., Thomson, J. A., Ecker, J. R. & Ren, B. Epigenomic analysis of multilineage differentiation of human embryonic stem cells. *Cell* **153,** 1134–1148 (2013).
211. Figura, von, G., Fukuda, A., Roy, N., Liku, M. E., Morris, J. P., IV, Kim, G. E., Russ, H. A., Firpo, M. A., Mulvihill, S. J., Dawson, D. W., Ferrer, J., Mueller, W. F., Busch, A., Hertel, K. J. & Hebrok, M. The chromatin regulator Brg1 suppresses formation of intraductal papillary mucinous neoplasm and pancreatic ductal adenocarcinoma. *Nat. Cell Biol.* **16,** 255–267 (2014).
212. McKenna, B., Guo, M., Reynolds, A., Hara, M. & Stein, R. Dynamic recruitment of functionally distinct Swi/Snf chromatin remodeling complexes modulates Pdx1 activity in islet β cells. *Cell Rep.* **10,** 2032–2042 (2015).
213. Anderson, R. M., Bosch, J. A., Goll, M. G., Hesselson, D., Dong, P. D. S., Shin, D., Chi, N. C., Shin, C. H., Schlegel, A., Halpern, M. & Stainier, D. Y. R. Loss of Dnmt1 catalytic activity reveals multiple roles for DNA methylation during pancreas development and regeneration. *Dev. Biol.* **334,** 213–223 (2009).
214. Georgia, S., Kanji, M. & Bhushan, A. DNMT1 represses p53 to maintain progenitor cell survival during pancreatic organogenesis. *Genes Dev* **27,** 372–377 (2013).
215. Dhawan, S., Tschen, S.-I., Zeng, C., Guo, T., Hebrok, M., Matveyenko, A. & Bhushan, A. DNA methylation directs functional maturation of pancreatic β cells. *J. Clin. Invest.* **125,** 2851–2860 (2015).
216. Haumaitre, C., Lenoir, O. & Scharfmann, R. Directing cell differentiation with small-molecule histone deacetylase inhibitors: the example of promoting pancreatic endocrine cells. *Cell Cycle* **8,** 536–544 (2009).
217. Wong, C. K., Wade-Vallance, A. K., Luciani, D. S., Brindle, P. K., Lynn, F. C. & Gibson, W. T. The p300 and CBP Transcriptional Coactivators Are Required for β-Cell and α-Cell Proliferation. *Diabetes* **67,** 412–422 (2018).

218. Haumaitre, C., Lenoir, O. & Scharfmann, R. Histone deacetylase inhibitors modify pancreatic cell fate determination and amplify endocrine progenitors. *Mol. Cell. Biol.* **28,** 6373–6383 (2008).
219. Lenoir, O., Flosseau, K., Ma, F. X., Blondeau, B., Mai, A., Bassel-Duby, R., Ravassard, P., Olson, E. N., Haumaitre, C. & Scharfmann, R. Specific control of pancreatic endocrine β- and δ-cell mass by class IIa histone deacetylases HDAC4, HDAC5, and HDAC9. *Diabetes* **60,** 2861–2871 (2011).
220. Xu, C.-R., Cole, P. A., Meyers, D. J., Kormish, J., Dent, S. & Zaret, K. S. Chromatin 'prepattern' and histone modifiers in a fate choice for liver and pancreas. *Science* **332,** 963–966 (2011).
221. Pethe, P., Nagvenkar, P. & Bhartiya, D. Polycomb group protein expression during differentiation of human embryonic stem cells into pancreatic lineage in vitro. *BMC Cell Biol.* **15,** 18 (2014).
222. Xu, C.-R., Li, L.-C., Donahue, G., Ying, L., Zhang, Y.-W., Gadue, P. & Zaret, K. S. Dynamics of genomic H3K27me3 domains and role of EZH2 during pancreatic endocrine specification. *The EMBO Journal* **33,** 2157–2170 (2014).
223. Xie, R., Everett, L. J., Lim, H.-W., Patel, N. A., Schug, J., Kroon, E., Kelly, O. G., Wang, A., D'Amour, K. A., Robins, A. J., Won, K.-J., Kaestner, K. H. & Sander, M. Dynamic chromatin remodeling mediated by polycomb proteins orchestrates pancreatic differentiation of human embryonic stem cells. *Cell Stem Cell* **12,** 224–237 (2013).
224. Yu, X.-X., Qiu, W.-L., Yang, L., Li, L.-C., Zhang, Y.-W. & Xu, C.-R. Dynamics of chromatin marks and the role of JMJD3 during pancreatic endocrine cell fate commitment. *Development* **145,** (2018).
225. Cervantes, S., Fontcuberta-PiSunyer, M., Servitja, J. M., Fernandez-Ruiz, R., García, A., Sanchez, L., Lee, Y.-S., Gomis, R. & Gasa, R. Late-stage differentiation of embryonic pancreatic β-cells requires Jarid2. *Sci Rep* **7,** 11643 (2017).
226. Tennant, B. R., Robertson, A. G., Kramer, M., Li, L., Zhang, X., Beach, M., Thiessen, N., Chiu, R., Mungall, K., Whiting, C. J., Sabatini, P. V., Kim, A., Gottardo, R., Marra, M. A., Lynn, F. C., Jones, S. J. M., Hoodless, P. A. & Hoffman, B. G. Identification and analysis of murine pancreatic islet enhancers. *Diabetologia* **56,** 542–552 (2013).
227. van Arensbergen, J., García-Hurtado, J., Maestro, M. A., Correa-Tapia, M., Rutter, G. A., Vidal, M. & Ferrer, J. Ring1b bookmarks genes in pancreatic embryonic progenitors for repression in adult β cells. *Genes Dev* **27,** 52–63 (2013).
228. Schonhoff, S. E., Giel-Moloney, M. & Leiter, A. B. Neurogenin 3-expressing progenitor cells in the gastrointestinal tract differentiate into both endocrine and non-endocrine cell types. *Dev. Biol.* **270,** 443–454 (2004).
229. Sugiyama, T., Benitez, C. M., Ghodasara, A., Liu, L., McLean, G. W., Lee, J., Blauwkamp, T. A., Nusse, R., Wright, C. V. E., Gu, G. & Kim, S. K. Reconstituting pancreas development from purified progenitor cells reveals genes essential for islet differentiation. *Proc. Natl. Acad. Sci. U.S.A.* **110,** 12691–12696 (2013).
230. Trapnell, C., Roberts, A., Goff, L., Pertea, G., Kim, D., Kelley, D. R., Pimentel, H., Salzberg, S. L., Rinn, J. L. & Pachter, L. Differential gene and transcript expression analysis of RNA-seq experiments with TopHat and Cufflinks. *Nat Protoc* **7,** 562–578 (2012).

231. Tennant, B. R., Hurley, P., Dhillon, J., Gill, A., Whiting, C. & Hoffman, B. G. The TrxG Complex Mediates Cytokine Induced De Novo Enhancer Formation in Islets. *PLoS ONE* **10,** e0141470 (2015).
232. Takahashi, T., Nowakowski, R. S. & Caviness, V. S. Cell cycle parameters and patterns of nuclear movement in the neocortical proliferative zone of the fetal mouse. *J. Neurosci.* **13,** 820–833 (1993).
233. Kretzschmar, K. & Clevers, H. Organoids: Modeling Development and the Stem Cell Niche in a Dish. *Dev Cell* **38,** 590–600 (2016).
234. Huch, M. & Koo, B.-K. Modeling mouse and human development using organoid cultures. *Development* **142,** 3113–3125 (2015).
235. Fatehullah, A., Tan, S. H. & Barker, N. Organoids as an in vitro model of human development and disease. *Nat. Cell Biol.* **18,** 246–254 (2016).
236. Mustata, R. C., Vasile, G., Fernandez-Vallone, V., Strollo, S., Lefort, A., Libert, F., Monteyne, D., Pérez-Morga, D., Vassart, G. & Garcia, M.-I. Identification of Lgr5-independent spheroid-generating progenitors of the mouse fetal intestinal epithelium. *Cell Rep.* **5,** 421–432 (2013).
237. Greggio, C., De Franceschi, F., Figueiredo-Larsen, M., Gobaa, S., Ranga, A., Semb, H., Lutolf, M. & Grapin-Botton, A. Artificial three-dimensional niches deconstruct pancreas development in vitro. *Development* **140,** 4452–4462 (2013).
238. Grapin-Botton, A. Three-dimensional pancreas organogenesis models. *Diabetes Obes Metab* **18 Suppl 1,** 33–40 (2016).
239. Lee, J., Sugiyama, T., Liu, Y., Wang, J., Gu, X., Lei, J., Markmann, J. F., Miyazaki, S., Miyazaki, J.-I., Szot, G. L., Bottino, R. & Kim, S. K. Expansion and conversion of human pancreatic ductal cells into insulin-secreting endocrine cells. *eLife* **2,** e00940 (2013).
240. Loomans, C. J. M., Williams Giuliani, N., Balak, J., Ringnalda, F., van Gurp, L., Huch, M., Boj, S. F., Sato, T., Kester, L., de Sousa Lopes, S. M. C., Roost, M. S., Bonner-Weir, S., Engelse, M. A., Rabelink, T. J., Heimberg, H., Vries, R. G. J., van Oudenaarden, A., Carlotti, F., Clevers, H. & de Koning, E. J. P. Expansion of Adult Human Pancreatic Tissue Yields Organoids Harboring Progenitor Cells with Endocrine Differentiation Potential. *Stem Cell Reports* **10,** 712–724 (2018).
241. Kopp, J. L., Dubois, C. L., Hao, E., Thorel, F., Herrera, P. L. & Sander, M. Progenitor cell domains in the developing and adult pancreas. *Cell Cycle* **10,** 1921–1927 (2011).
242. Jin, L., Feng, T., Shih, H. P., Zerda, R., Luo, A., Hsu, J., Mahdavi, A., Sander, M., Tirrell, D. A., Riggs, A. D. & Ku, H. T. Colony-forming cells in the adult mouse pancreas are expandable in Matrigel and form endocrine/acinar colonies in laminin hydrogel. *Proc. Natl. Acad. Sci. U.S.A.* **110,** 3907–3912 (2013).
243. Candiello, J., Grandhi, T. S. P., Goh, S. K., Vaidya, V., Lemmon-Kishi, M., Eliato, K. R., Ros, R., Kumta, P. N., Rege, K. & Banerjee, I. 3D heterogeneous islet organoid generation from human embryonic stem cells using a novel engineered hydrogel platform. *Biomaterials* **177,** 27–39 (2018).
244. Moreira, L., Bakir, B., Chatterji, P., Dantes, Z., Reichert, M. & Rustgi, A. K. Pancreas 3D Organoids: Current and Future Aspects as a Research Platform for Personalized Medicine in Pancreatic Cancer. *Cell Mol Gastroenterol Hepatol* **5,** 289–298 (2018).

245. Hohwieler, M., Illing, A., Hermann, P. C., Mayer, T., Stockmann, M., Perkhofer, L., Eiseler, T., Antony, J. S., Müller, M., Renz, S., Kuo, C.-C., Lin, Q., Sendler, M., Breunig, M., Kleiderman, S. M., Lechel, A., Zenker, M., Leichsenring, M., Rosendahl, J., Zenke, M., Sainz, B., Mayerle, J., Costa, I. G., Seufferlein, T., Kormann, M., Wagner, M., Liebau, S. & Kleger, A. Human pluripotent stem cell-derived acinar/ductal organoids generate human pancreas upon orthotopic transplantation and allow disease modelling. *Gut* **66,** 473–486 (2017).
246. Kim, Y., Kim, H., Ko, U. H., Oh, Y., Lim, A., Sohn, J.-W., Shin, J. H., Kim, H. & Han, Y.-M. Islet-like organoids derived from human pluripotent stem cells efficiently function in the glucose responsiveness in vitro and in vivo. *Sci Rep* **6,** 35145 (2016).
247. Shim, J.-H., Kim, J., Han, J., An, S. Y., Jang, Y. J., Son, J., Woo, D.-H., Kim, S.-K. & Kim, J.-H. Pancreatic Islet-Like Three-Dimensional Aggregates Derived From Human Embryonic Stem Cells Ameliorate Hyperglycemia in Streptozotocin-Induced Diabetic Mice. *Cell Transplant* **24,** 2155–2168 (2015).
248. Ware, M. J., Colbert, K., Keshishian, V., Ho, J., Corr, S. J., Curley, S. A. & Godin, B. Generation of Homogenous Three-Dimensional Pancreatic Cancer Cell Spheroids Using an Improved Hanging Drop Technique. *Tissue Eng Part C Methods* **22,** 312–321 (2016).
249. Bonfanti, P., Nobecourt, E., Oshima, M., Albagli-Curiel, O., Laurysens, V., Stangé, G., Sojoodi, M., Heremans, Y., Heimberg, H. & Scharfmann, R. Ex Vivo Expansion and Differentiation of Human and Mouse Fetal Pancreatic Progenitors Are Modulated by Epidermal Growth Factor. *Stem Cells Dev* **24,** 1766–1778 (2015).
250. Boj, S. F., Hwang, C.-I., Baker, L. A., Chio, I. I. C., Engle, D. D., Corbo, V., Jager, M., Ponz-Sarvise, M., Tiriac, H., Spector, M. S., Gracanin, A., Oni, T., Yu, K. H., van Boxtel, R., Huch, M., Rivera, K. D., Wilson, J. P., Feigin, M. E., Öhlund, D., Handly-Santana, A., Ardito-Abraham, C. M., Ludwig, M., Elyada, E., Alagesan, B., Biffi, G., Yordanov, G. N., Delcuze, B., Creighton, B., Wright, K., Park, Y., Morsink, F. H. M., Molenaar, I. Q., Borel Rinkes, I. H., Cuppen, E., Hao, Y., Jin, Y., Nijman, I. J., Iacobuzio-Donahue, C., Leach, S. D., Pappin, D. J., Hammell, M., Klimstra, D. S., Basturk, O., Hruban, R. H., Offerhaus, G. J., Vries, R. G. J., Clevers, H. & Tuveson, D. A. Organoid models of human and mouse ductal pancreatic cancer. *Cell* **160,** 324–338 (2015).
251. Seino, T., Kawasaki, S., Shimokawa, M., Tamagawa, H., Toshimitsu, K., Fujii, M., Ohta, Y., Matano, M., Nanki, K., Kawasaki, K., Takahashi, S., Sugimoto, S., Iwasaki, E., Takagi, J., Itoi, T., Kitago, M., Kitagawa, Y., Kanai, T. & Sato, T. Human Pancreatic Tumor Organoids Reveal Loss of Stem Cell Niche Factor Dependence during Disease Progression. *Cell Stem Cell* **22,** 454–467.e6 (2018).
252. Seaberg, R. M., Smukler, S. R., Kieffer, T. J., Enikolopov, G., Asghar, Z., Wheeler, M. B., Korbutt, G. & van der Kooy, D. Clonal identification of multipotent precursors from adult mouse pancreas that generate neural and pancreatic lineages. *Nat Biotechnol* **22,** 1115–1124 (2004).
253. Rovira, M., Scott, S.-G., Liss, A. S., Jensen, J., Thayer, S. P. & Leach, S. D. Isolation and characterization of centroacinar/terminal ductal progenitor cells in adult mouse pancreas. *Proc. Natl. Acad. Sci. U.S.A.* **107,** 75–80 (2010).
254. Golson, M. L. & Kaestner, K. H. Epigenetics in formation, function, and failure of the endocrine pancreas. *Mol Metab* **6,** 1066–1076 (2017).

255. Thurner, M., Shenhav, L., Wesolowska-Andersen, A., Bennett, A. J., Barrett, A., Gloyn, A. L., McCarthy, M. I., Beer, N. L. & Efrat, S. Genes Associated with Pancreas Development and Function Maintain Open Chromatin in iPSCs Generated from Human Pancreatic Beta Cells. *Stem Cell Reports* **9,** 1395–1405 (2017).
256. Fontcuberta-PiSunyer, M., Cervantes, S., Miquel, E., Mora-Castilla, S., Laurent, L. C., Raya, A., Gomis, R. & Gasa, R. Modulation of the endocrine transcriptional program by targeting histone modifiers of the H3K27me3 mark. *Biochim Biophys Acta Gene Regul Mech* **1861,** 473–480 (2018).
257. Al-Khawaga, S., Memon, B., Butler, A. E., Taheri, S., Abou-Samra, A. B. & Abdelalim, E. M. Pathways governing development of stem cell-derived pancreatic β cells: lessons from embryogenesis. *Biol Rev* **93,** 364–389 (2018).
258. Couture, J.-F., Collazo, E. & Trievel, R. C. Molecular recognition of histone H3 by the WD40 protein WDR5. *Nat Struct Mol Biol* **13,** 698–703 (2006).
259. Dharmarajan, V., Lee, J.-H., Patel, A., Skalnik, D. G. & Cosgrove, M. S. Structural basis for WDR5 interaction (Win) motif recognition in human SET1 family histone methyltransferases. *J. Biol. Chem.* **287,** 27275–27289 (2012).
260. Patel, A., Dharmarajan, V. & Cosgrove, M. S. Structure of WDR5 bound to mixed lineage leukemia protein-1 peptide. *J. Biol. Chem.* **283,** 32158–32161 (2008).
261. Wysocka, J., Swigut, T., Milne, T. A., Dou, Y., Zhang, X., Burlingame, A. L., Roeder, R. G., Brivanlou, A. H. & Allis, C. D. WDR5 associates with histone H3 methylated at K4 and is essential for H3 K4 methylation and vertebrate development. *Cell* **121,** 859–872 (2005).
262. Schuetz, A., Allali-Hassani, A., Martín, F., Loppnau, P., Vedadi, M., Bochkarev, A., Plotnikov, A. N., Arrowsmith, C. H. & Min, J. Structural basis for molecular recognition and presentation of histone H3 by WDR5. *The EMBO Journal* **25,** 4245–4252 (2006).
263. Ali, A. & Tyagi, S. Diverse roles of WDR5-RbBP5-ASH2L-DPY30 (WRAD) complex in the functions of the SET1 histone methyltransferase family. *J. Biosci.* **42,** 155–159 (2017).
264. Grebien, F., Vedadi, M., Getlik, M., Giambruno, R., Grover, A., Avellino, R., Skucha, A., Vittori, S., Kuznetsova, E., Smil, D., Barsyte-Lovejoy, D., Li, F., Poda, G., Schapira, M., Wu, H., Dong, A., Senisterra, G., Stukalov, A., Huber, K. V. M., Schönegger, A., Marcellus, R., Bilban, M., Bock, C., Brown, P. J., Zuber, J., Bennett, K. L., Al-awar, R., Delwel, R., Nerlov, C., Arrowsmith, C. H. & Superti-Furga, G. Pharmacological targeting of the Wdr5-MLL interaction in C/EBPα N-terminal leukemia. *Nat. Chem. Biol.* **11,** 571–578 (2015).
265. Carugo, A., Genovese, G., Seth, S., Nezi, L., Rose, J. L., Bossi, D., Cicalese, A., Shah, P. K., Viale, A., Pettazzoni, P. F., Akdemir, K. C., Bristow, C. A., Robinson, F. S., Tepper, J., Sanchez, N., Gupta, S., Estecio, M. R., Giuliani, V., Dellino, G. I., Riva, L., Yao, W., Di Francesco, M. E., Green, T., D'Alesio, C., Corti, D., Kang, Y., Jones, P., Wang, H., Fleming, J. B., Maitra, A., Pelicci, P. G., Chin, L., DePinho, R. A., Lanfrancone, L., Heffernan, T. P. & Draetta, G. F. In Vivo Functional Platform Targeting Patient-Derived Xenografts Identifies WDR5-Myc Association as a Critical Determinant of Pancreatic Cancer. *Cell Rep.* **16,** 133–147 (2016).
266. Chen, X., Xie, W., Gu, P., Cai, Q., Wang, B., Xie, Y., Dong, W., He, W., Zhong, G., Lin, T. & Huang, J. Upregulated WDR5 promotes proliferation, self-renewal and

chemoresistance in bladder cancer via mediating H3K4 trimethylation. *Sci Rep* **5,** 8293 (2015).
267. Hopkin, A. S., Gordon, W., Klein, R. H., Espitia, F., Daily, K., Zeller, M., Baldi, P. & Andersen, B. GRHL3/GET1 and trithorax group members collaborate to activate the epidermal progenitor differentiation program. *PLoS Genet* **8,** e1002829 (2012).
268. Sun, W., Guo, F. & Liu, M. Up-regulated WDR5 promotes gastric cancer formation by induced cyclin D1 expression. *J. Cell. Biochem.* **119,** 3304–3316 (2018).
269. Ali, A., Veeranki, S. N., Chinchole, A. & Tyagi, S. MLL/WDR5 Complex Regulates Kif2A Localization to Ensure Chromosome Congression and Proper Spindle Assembly during Mitosis. *Dev Cell* **41,** 605–622.e7 (2017).
270. Wild, T., Larsen, M. S. Y., Narita, T., Schou, J., Nilsson, J. & Choudhary, C. The Spindle Assembly Checkpoint Is Not Essential for Viability of Human Cells with Genetically Lowered APC/C Activity. *Cell Rep.* **14,** 1829–1840 (2016).
271. Ang, Y.-S., Tsai, S.-Y., Lee, D.-F., Monk, J., Su, J., Ratnakumar, K., Ding, J., Ge, Y., Darr, H., Chang, B., Wang, J., Rendl, M., Bernstein, E., Schaniel, C. & Lemischka, I. R. Wdr5 mediates self-renewal and reprogramming via the embryonic stem cell core transcriptional network. *Cell* **145,** 183–197 (2011).
272. Zhu, E. D., Demay, M. B. & Gori, F. Wdr5 is essential for osteoblast differentiation. *J. Biol. Chem.* **283,** 7361–7367 (2008).
273. Gan, Q., Thiébaud, P., Thézé, N., Jin, L., Xu, G., Grant, P. & Owens, G. K. WD repeat-containing protein 5, a ubiquitously expressed histone methyltransferase adaptor protein, regulates smooth muscle cell-selective gene activation through interaction with pituitary homeobox 2. *J. Biol. Chem.* **286,** 21853–21864 (2011).
274. Wang, L., Collings, C. K., Zhao, Z., Cozzolino, K. A., Ma, Q., Liang, K., Marshall, S. A., Sze, C. C., Hashizume, R., Savas, J. N. & Shilatifard, A. A cytoplasmic COMPASS is necessary for cell survival and triple-negative breast cancer pathogenesis by regulating metabolism. *Genes Dev* **31,** 2056–2066 (2017).
275. Wang, Y.-Y., Liu, L.-J., Zhong, B., Liu, T.-T., Li, Y., Yang, Y., Ran, Y., Li, S., Tien, P. & Shu, H.-B. WDR5 is essential for assembly of the VISA-associated signaling complex and virus-triggered IRF3 and NF-kappaB activation. *Proc. Natl. Acad. Sci. U.S.A.* **107,** 815–820 (2010).
276. Liu, H., Cheng, E. H.-Y. & Hsieh, J. J.-D. Bimodal degradation of MLL by SCFSkp2 and APCCdc20 assures cell cycle execution: a critical regulatory circuit lost in leukemogenic MLL fusions. *Genes Dev* **21,** 2385–2398 (2007).
277. Issaeva, I., Zonis, Y., Rozovskaia, T., Orlovsky, K., Croce, C. M., Nakamura, T., Mazo, A., Eisenbach, L. & Canaani, E. Knockdown of ALR (MLL2) reveals ALR target genes and leads to alterations in cell adhesion and growth. *Mol. Cell. Biol.* **27,** 1889–1903 (2007).
278. Milne, T. A., Hughes, C. M., Lloyd, R., Yang, Z., Rozenblatt-Rosen, O., Dou, Y., Schnepp, R. W., Krankel, C., Livolsi, V. A., Gibbs, D., Hua, X., Roeder, R. G., Meyerson, M. & Hess, J. L. Menin and MLL cooperatively regulate expression of cyclin-dependent kinase inhibitors. *Proc Natl Acad Sci USA* **102,** 749–754 (2005).
279. Simboeck, E., Gutierrez, A., Cozzuto, L., Beringer, M., Caizzi, L., Keyes, W. M. & Di Croce, L. DPY30 regulates pathways in cellular senescence through ID protein expression. *The EMBO Journal* **32,** 2217–2230 (2013).

280. Yang, Z., Augustin, J., Chang, C., Hu, J., Shah, K., Chang, C.-W., Townes, T. & Jiang, H. The DPY30 subunit in SET1/MLL complexes regulates the proliferation and differentiation of hematopoietic progenitor cells. *Blood* **124,** 2025–2033 (2014).
281. Thomas, L. R., Wang, Q., Grieb, B. C., Phan, J., Foshage, A. M., Sun, Q., Olejniczak, E. T., Clark, T., Dey, S., Lorey, S., Alicie, B., Howard, G. C., Cawthon, B., Ess, K. C., Eischen, C. M., Zhao, Z., Fesik, S. W. & Tansey, W. P. Interaction with WDR5 promotes target gene recognition and tumorigenesis by MYC. *Mol Cell* **58,** 440–452 (2015).
282. Kim, J.-Y., Banerjee, T., Vinckevicius, A., Luo, Q., Parker, J. B., Baker, M. R., Radhakrishnan, I., Wei, J.-J., Barish, G. D. & Chakravarti, D. A role for WDR5 in integrating threonine 11 phosphorylation to lysine 4 methylation on histone H3 during androgen signaling and in prostate cancer. *Mol Cell* **54,** 613–625 (2014).
283. Salz, T., Li, G., Kaye, F., Zhou, L., Qiu, Y. & Huang, S. hSETD1A regulates Wnt target genes and controls tumor growth of colorectal cancer cells. *Cancer Res.* **74,** 775–786 (2014).
284. Mueller, C. M., Zhang, H. & Zenilman, M. E. Pancreatic reg I binds MKP-1 and regulates cyclin D in pancreatic-derived cells. *J. Surg. Res.* **150,** 137–143 (2008).
285. Parikh, A., Stephan, A.-F. & Tzanakakis, E. S. Regenerating proteins and their expression, regulation and signaling. *Biomol Concepts* **3,** 57–70 (2012).
286. Bluth, M. H. Pancreatic regenerating protein (regI) and regIreceptor mRNA are upregulated in rat pancreas after induction of acute pancreatitis. *World J. Gastroenterol.* **12,** 4511 (2006).
287. Grzesiak, J. J., Ho, J. C., Moossa, A. R. & Bouvet, M. The integrin-extracellular matrix axis in pancreatic cancer. *Pancreas* **35,** 293–301 (2007).
288. Simeone, D. M., Ji, B., Banerjee, M., Arumugam, T., Li, D., Anderson, M. A., Bamberger, A. M., Greenson, J., Brand, R. E., Ramachandran, V. & Logsdon, C. D. CEACAM1, a novel serum biomarker for pancreatic cancer. *Pancreas* **34,** 436–443 (2007).
289. Jiang, H., Shukla, A., Wang, X., Chen, W.-Y., Bernstein, B. E. & Roeder, R. G. Role for Dpy-30 in ES cell-fate specification by regulation of H3K4 methylation within bivalent domains. *Cell* **144,** 513–525 (2011).
290. Patel, A., Vought, V. E., Dharmarajan, V. & Cosgrove, M. S. A novel non-SET domain multi-subunit methyltransferase required for sequential nucleosomal histone H3 methylation by the mixed lineage leukemia protein-1 (MLL1) core complex. *J. Biol. Chem.* **286,** 3359–3369 (2011).
291. Haddad, J. F., Yang, Y., Takahashi, Y.-H., Joshi, M., Chaudhary, N., Woodfin, A. R., Benyoucef, A., Yeung, S., Brunzelle, J. S., Skiniotis, G., Brand, M., Shilatifard, A. & Couture, J.-F. Structural Analysis of the Ash2L/Dpy-30 Complex Reveals a Heterogeneity in H3K4 Methylation. *Structure* **26,** 1594–1603.e4 (2018).
292. Yang, Z., Shah, K., Khodadadi-Jamayran, A. & Jiang, H. Dpy30 is critical for maintaining the identity and function of adult hematopoietic stem cells. *J Exp Med* **213,** 2349–2364 (2016).
293. Wicksteed, B., Brissova, M., Yan, W., Opland, D. M., Plank, J. L., Reinert, R. B., Dickson, L. M., Tamarina, N. A., Philipson, L. H., Shostak, A., Bernal-Mizrachi, E., Elghazi, L., Roe, M. W., Labosky, P. A., Myers, M. G., Gannon, M., Powers, A. C. &

Dempsey, P. J. Conditional gene targeting in mouse pancreatic ß-Cells: analysis of ectopic Cre transgene expression in the brain. *Diabetes* **59,** 3090–3098 (2010).
294. Sabatini, P. V., Speckmann, T., Nian, C., Glavas, M. M., Wong, C. K., Yoon, J. S., Kin, T., Shapiro, A. M. J., Gibson, W. T., Verchere, C. B. & Lynn, F. C. Neuronal PAS Domain Protein 4 Suppression of Oxygen Sensing Optimizes Metabolism during Excitation of Neuroendocrine Cells. *Cell Rep.* **22,** 163–174 (2018).
295. Luo, X., Shin, D. M., Wang, X., Konieczny, S. F. & Muallem, S. Aberrant localization of intracellular organelles, Ca2+ signaling, and exocytosis in Mist1 null mice. *J. Biol. Chem.* **280,** 12668–12675 (2005).
296. Zhu, L., Tran, T., Rukstalis, J. M., Sun, P., Damsz, B. & Konieczny, S. F. Inhibition of Mist1 Homodimer Formation Induces Pancreatic Acinar-to-Ductal Metaplasia. *Mol. Cell. Biol.* **24,** 2673–2681 (2004).
297. Xuan, S., Borok, M. J., Decker, K. J., Battle, M. A., Duncan, S. A., Hale, M. A., MacDonald, R. J. & Sussel, L. Pancreas-specific deletion of mouse Gata4 and Gata6 causes pancreatic agenesis. *J. Clin. Invest.* **122,** 3516–3528 (2012).
298. Figura, von, G., Morris, J. P., Wright, C. V. E. & Hebrok, M. Nr5a2 maintains acinar cell differentiation and constrains oncogenic Kras-mediated pancreatic neoplastic initiation. *Gut* **63,** 656–664 (2014).
299. Lynn, F. C., Skewes-Cox, P., Kosaka, Y., McManus, M. T., Harfe, B. D. & German, M. S. MicroRNA expression is required for pancreatic islet cell genesis in the mouse. *Diabetes* **56,** 2938–2945 (2007).
300. Karki, A., Humphrey, S. E., Steele, R. E., Hess, D. A., Taparowsky, E. J. & Konieczny, S. F. Silencing Mist1 Gene Expression Is Essential for Recovery from Acute Pancreatitis. *PLoS ONE* **10,** e0145724 (2015).
301. Kopp, J. L., Figura, von, G., Mayes, E., Liu, F.-F., Dubois, C. L., Morris, J. P., Pan, F. C., Akiyama, H., Wright, C. V. E., Jensen, K., Hebrok, M. & Sander, M. Identification of Sox9-dependent acinar-to-ductal reprogramming as the principal mechanism for initiation of pancreatic ductal adenocarcinoma. *Cancer Cell* **22,** 737–750 (2012).
302. Fujikura, J., Hosoda, K., Iwakura, H., Tomita, T., Noguchi, M., Masuzaki, H., Tanigaki, K., Yabe, D., Honjo, T. & Nakao, K. Notch/Rbp-j signaling prevents premature endocrine and ductal cell differentiation in the pancreas. *Cell Metab.* **3,** 59–65 (2006).
303. Benayoun, B. A., Pollina, E. A., Ucar, D., Mahmoudi, S., Karra, K., Wong, E. D., Devarajan, K., Daugherty, A. C., Kundaje, A. B., Mancini, E., Hitz, B. C., Gupta, R., Rando, T. A., Baker, J. C., Snyder, M. P., Cherry, J. M. & Brunet, A. H3K4me3 breadth is linked to cell identity and transcriptional consistency. *Cell* **158,** 673–688 (2014).
304. Chen, K., Chen, Z., Wu, D., Zhang, L., Lin, X., Su, J., Rodriguez, B., Xi, Y., Xia, Z., Chen, X., Shi, X., Wang, Q. & Li, W. Broad H3K4me3 is associated with increased transcription elongation and enhancer activity at tumor-suppressor genes. *Nat. Genet.* **47,** 1149–1157 (2015).
305. Muramoto, T., Müller, I., Thomas, G., Melvin, A. & Chubb, J. R. Methylation of H3K4 Is required for inheritance of active transcriptional states. *Curr. Biol.* **20,** 397–406 (2010).
306. Jensen, J., Heller, R. S., Funder-Nielsen, T., Pedersen, E. E., Lindsell, C., Weinmaster, G., Madsen, O. D. & Serup, P. Independent development of pancreatic alpha- and beta-

cells from neurogenin3-expressing precursors: a role for the notch pathway in repression of premature differentiation. *Diabetes* **49,** 163–176 (2000).
307. Miyatsuka, T., Li, Z. & German, M. S. Chronology of islet differentiation revealed by temporal cell labeling. *Diabetes* **58,** 1863–1868 (2009).
308. Blum, B., Hrvatin, S., Schuetz, C., Bonal, C., Rezania, A. & Melton, D. A. Functional beta-cell maturation is marked by an increased glucose threshold and by expression of urocortin 3. *Nat Biotechnol* **30,** 261–264 (2012).
309. Stolovich-Rain, M., Enk, J., Vikesa, J., Nielsen, F. C., Saada, A., Glaser, B. & Dor, Y. Weaning triggers a maturation step of pancreatic β cells. *Dev Cell* **32,** 535–545 (2015).
310. Scoville, D. W., Cyphert, H. A., Liao, L., Xu, J., Reynolds, A., Guo, S. & Stein, R. MLL3 and MLL4 Methyltransferases Bind to the MAFA and MAFB Transcription Factors to Regulate Islet β-Cell Function. *Diabetes* **64,** 3772–3783 (2015).
311. Deering, T. G., Ogihara, T., Trace, A. P., Maier, B. & Mirmira, R. G. Methyltransferase Set7/9 maintains transcription and euchromatin structure at islet-enriched genes. *Diabetes* **58,** 185–193 (2009).
312. Kim-Muller, J. Y., Fan, J., Kim, Y. J. R., Lee, S.-A., Ishida, E., Blaner, W. S. & Accili, D. Aldehyde dehydrogenase 1a3 defines a subset of failing pancreatic β cells in diabetic mice. *Nature Communications* **7,** 12631 (2016).
313. Dahan, T., Ziv, O., Horwitz, E., Zemmour, H., Lavi, J., Swisa, A., Leibowitz, G., Ashcroft, F. M., in't Veld, P., Glaser, B. & Dor, Y. Pancreatic β-Cells Express the Fetal Islet Hormone Gastrin in Rodent and Human Diabetes. *Diabetes* **66,** 426–436 (2017).
314. Fu, Z., Gilbert, E. R. & Liu, D. Regulation of insulin synthesis and secretion and pancreatic Beta-cell dysfunction in diabetes. *Curr Diabetes Rev* **9,** 25–53 (2013).
315. Gu, C., Stein, G. H., Pan, N., Goebbels, S., HOrnberg, H., Nave, K.-A., Herrera, P., White, P., Kaestner, K. H., Sussel, L. & Lee, J. E. Pancreatic beta cells require NeuroD to achieve and maintain functional maturity. *Cell Metab.* **11,** 298–310 (2010).
316. Aguayo-Mazzucato, C., Koh, A., Khattabi, El, I., Li, W. C., Toschi, E., Jermendy, A., Juhl, K., Mao, K., Weir, G. C., Sharma, A. & Bonner-Weir, S. Mafa expression enhances glucose-responsive insulin secretion in neonatal rat beta cells. *Diabetologia* **54,** 583–593 (2011).
317. Doyle, M. J. & Sussel, L. Nkx2.2 regulates beta-cell function in the mature islet. *Diabetes* **56,** 1999–2007 (2007).
318. Mitchell, R. K., Nguyen-Tu, M.-S., Chabosseau, P., Callingham, R. M., Pullen, T. J., Cheung, R., Leclerc, I., Hodson, D. J. & Rutter, G. A. The transcription factor Pax6 is required for pancreatic β cell identity, glucose-regulated ATP synthesis, and Ca2+ dynamics in adult mice. *J. Biol. Chem.* **292,** 8892–8906 (2017).
319. Guo, S., Dai, C., Guo, M., Taylor, B., Harmon, J. S., Sander, M., Robertson, R. P., Powers, A. C. & Stein, R. Inactivation of specific β cell transcription factors in type 2 diabetes. *J. Clin. Invest.* **123,** 3305–3316 (2013).
320. Gosmain, Y., Katz, L. S., Masson, M. H., Cheyssac, C., Poisson, C. & Philippe, J. Pax6 is crucial for β-cell function, insulin biosynthesis, and glucose-induced insulin secretion. *Mol. Endocrinol.* **26,** 696–709 (2012).
321. Artner, I., Hang, Y., Mazur, M., Yamamoto, T., Guo, M., Lindner, J., Magnuson, M. A. & Stein, R. MafA and MafB regulate genes critical to beta-cells in a unique temporal manner. *Diabetes* **59,** 2530–2539 (2010).

322. Poitout, V., Hagman, D., Stein, R., Artner, I., Robertson, R. P. & Harmon, J. S. Regulation of the insulin gene by glucose and fatty acids. *J. Nutr.* **136,** 873–876 (2006).
323. Lee, J.-E., Wang, C., Xu, S., Cho, Y.-W., Wang, L., Feng, X., Baldridge, A., Sartorelli, V., Zhuang, L., Peng, W. & Ge, K. H3K4 mono- and di-methyltransferase MLL4 is required for enhancer activation during cell differentiation. *eLife* **2,** e01503 (2013).
324. Rada-Iglesias, A. Is H3K4me1 at enhancers correlative or causative? *Nat. Genet.* **50,** 4–5 (2018).
325. Mishra, B. P., Zaffuto, K. M., Artinger, E. L., Org, T., Mikkola, H. K. A., Cheng, C., Djabali, M. & Ernst, P. The histone methyltransferase activity of MLL1 is dispensable for hematopoiesis and leukemogenesis. *Cell Rep.* **7,** 1239–1247 (2014).
326. Bertero, A., Pawlowski, M., Ortmann, D., Snijders, K., Yiangou, L., Cardoso de Brito, M., Brown, S., Bernard, W. G., Cooper, J. D., Giacomelli, E., Gambardella, L., Hannan, N. R. F., Iyer, D., Sampaziotis, F., Serrano, F., Zonneveld, M. C. F., Sinha, S., Kotter, M. & Vallier, L. Optimized inducible shRNA and CRISPR/Cas9 platforms for in vitro studies of human development using hPSCs. *Development* **143,** 4405–4418 (2016).
327. Sun, J., Zhao, Y., McGreal, R., Cohen-Tayar, Y., Rockowitz, S., Wilczek, C., Ashery-Padan, R., Shechter, D., Zheng, D. & Cvekl, A. Pax6 associates with H3K4-specific histone methyltransferases Mll1, Mll2, and Set1a and regulates H3K4 methylation at promoters and enhancers. *Epigenetics Chromatin* **9,** 37 (2016).
328. Jozwik, K. M., Chernukhin, I., Serandour, A. A., Nagarajan, S. & Carroll, J. S. FOXA1 Directs H3K4 Monomethylation at Enhancers via Recruitment of the Methyltransferase MLL3. *Cell Rep.* **17,** 2715–2723 (2016).
329. Conwell, D. L., Greenberger, N. J. & Banks, P. A. Approach to the Patient with Pancreatic Disease in *Harrisons Principles of Internal Medicine* 1–12 (2018).
330. Conwell, D. L., Banks, P. A. & Greenberger, N. J. Acute and Chronic Pancreatitis in *Harrisons Principles of Internal Medicine* 1–32 (2018).
331. Kleeff, J., Korc, M., Apte, M., La Vecchia, C., Johnson, C. D., Biankin, A. V., Neale, R. E., Tempero, M., Tuveson, D. A., Hruban, R. H. & Neoptolemos, J. P. Pancreatic cancer. *Nat Rev Dis Primers* **2,** 16022 (2016).

Appendices

Appendix A The top 30 underrepresented genes from pancreas spheroid RNA-sequencing

Gene Symbol	shScramble FPKM	sh*Wdr5* #1 FPKM	Log2 (Fold Change)
Dbpht2	18.4441	0.0151927	-10.24556539
AK041537	65.5443	0.0960049	-9.415146566
St18	3.98905	0.00836165	-8.898041835
Myt1	4.29753	0.0115955	-8.53379887
Fmod	5.08272	0.0140863	-8.495164233
G6pc2	20.4712	0.0635123	-8.332343943
Hepacam2	13.2516	0.0416274	-8.314417394
Kcnk16	22.193	0.0716519	-8.274884025
Tmsb15b2	35.2542	0.116706	-8.238772599
Angptl7	6.94195	0.0259377	-8.064146608
Rimbp2	12.6241	0.0484964	-8.024087167
Pax6	19.3911	0.0746906	-8.020252243
Baiap3	14.1092	0.0574036	-7.941279257
Rfx6	8.58221	0.0395999	-7.759708606
Slc30a8	8.5851	0.0409617	-7.711415537
Sst	2533.94	13.2415	-7.580171994
Pcsk1	16.5823	0.0882212	-7.554303026
Sphkap	7.35954	0.0430816	-7.416399954
Gdpd2	8.33152	0.0501067	-7.377432388
Npas4	3.22028	0.021341	-7.237414545
Scgn	28.336	0.206902	-7.097544716
Chgb	152.829	1.15245	-7.051070358
Gjd2	9.22147	0.070232	-7.03672442
Ptprn2	33.0078	0.268578	-6.94132204
Scg3	36.7358	0.300931	-6.931610151
Pcsk2	58.286	0.478181	-6.92944878
Ggt7	6.53826	0.0565589	-6.853008876
Pnmal1	2.81259	0.0255707	-6.781263797
Abi3bp	4.5752	0.0423222	-6.756276377
Tmem27	25.8193	0.239747	-6.750793315

Appendix B The top 30 overrepresented genes from pancreas spheroid RNA-sequencing

Gene Symbol	shScramble FPKM	sh*Wdr5* #1 FPKM	Log2 (Fold Change)
Gsta1	0.0399639	9.00655	7.816133391
Snora68	0	146.316	7.19294373
Duox2	0.0350705	4.96171	7.144435606
Snord23	0	140.108	7.130395524
Duoxa2	0.0844276	10.8033	6.99954165
Ly6a	1.82145	175.541	6.590576828
Snora5c	0	92.5131	6.531585763
Snora44	0	81.9879	6.357339103
2210407C18Rik	0.147829	9.78707	6.048875799
Clca3	0.125505	7.92182	5.980015175
Tm4sf5	0.0823571	5.18225	5.975541775
Sprr2a1	0.429344	25.7037	5.903698207
Msln	1.63633	93.3505	5.834122118
Mir1188	0	52.763	5.721454691
Mir96	0.0507582	2.45281	5.594650765
Hist1h4h	0.134584	6.18292	5.521709528
Gpa33	0.0834197	3.75018	5.490427909
Cldn18	0.187291	8.32329	5.473800425
Slc25a48	0.071638	3.14663	5.456938677
Anxa10	0.306968	13.298	5.436977203
Areg	2.28311	98.8421	5.436053387
Gjb4	0.0756206	3.26701	5.433047764
Cym	1.46425	61.1224	5.383467393
1810064F22Rik	0.592995	24.7255	5.381835945
Gsta2	0.16729	6.58449	5.298648587
Syt8	0.119028	4.64456	5.286169034
Ctse	0.686887	25.7637	5.229123207
2200002J24Rik	0.0816339	2.93823	5.169635139
Snora62	0	35.794	5.16164587
Cxcl17	0.778325	26.5996	5.094888043

Appendix C Lineage-specific gene expression from pancreas spheroid RNA-sequencing

Endocrine Gene Symbol	shScramble FPKM	sh*Wdr5* #1 FPKM	Log2 (Fold Change)
Abcc8	35.4201	1.01966	-5.118408206
G6pc2	20.4712	0.0635123	-8.332343943
Gcg	191.745	2.29657	-6.38356439
Gck	3.9464	0.169034	-4.545151824
Iapp	672.854	9.67713	-6.119570441
Ins1	325.186	3.16273	-6.683950938
Ins2	1211.98	16.3774	-6.209515742
Kcnj11	7.97487	1.87469	-2.088808951
Neurod1	7.3122	0.123859	-5.883534922
Neurog3	6.74395	0	-2.75359384
Nkx2-2	8.77542	1.2783	-2.779241718
Nkx6-1	13.5888	2.48283	-2.452360672
Pax6	19.3911	0.0746906	-8.020252243
Ppy	38.2121	0.873466	-5.451134188
Slc2a2	12.1733	15.0838	0.290581341
Slc30a8	8.5851	0.0409617	-7.711415537
Sst	2533.94	13.2415	-7.580171994
Acinar Gene Symbol	**shScramble FPKM**	**sh*Wdr5* #1 FPKM**	**Log2 (Fold Change)**
Amy1	5.26583	6.37193	0.275069471228308
Amy2b	0.0873778	0.0208816	-2.06503452301829
Bhlha15	0.317832	0.176971	-0.84475141841791
Cel	1.30301	0.0386003	-5.0770922856359
Clps	16.209	3.68805	-2.135864968
Cpa1	10.134	0.70492	-3.845600386
Cpa2	4.85841	0.26575	-4.192342647
Nr5a2	4.74418	4.95498	0.043073312
Pnliprp1	13.7745	0.983574	-3.807822542
Prss2	3.22116	0.642367	-2.326110638
Rbpjl	0.104318	0.125944	0.271794278012813
Reg1	1.86511	32.258	4.112324369
Reg3b	2.16967	13.4105	2.627815493
Reg3g	0.203021	4.73419	4.543416739

Progenitor Gene Symbol	**shScramble FPKM**	**sh*Wdr5* #1 FPKM**	**Log2 (Fold Change)**
Foxa1	2.37525	8.47745	1.842224586
Foxa2	4.05072	16.858	2.057183118
Foxo1	7.35783	23.6516	1.665511199
Gata4	1.48159	7.46451	2.332901293
Gata6	22.3808	37.1752	0.71547214
Hes1	12.8042	32.7861	1.3564671823639
Hnf1a	3.04431	6.44476	1.746596059
Hnf1b	10.3319	28.1396	1.44480388
Myc	34.8317	62.6284	0.846416135155145
Onecut2	5.2687	20.2251	1.915358642
Pdx1	8.95962	8.29111	-0.119046991
Rbpj	3.31594	3.73077	0.170055519164257
Sox9	4.6719	12.3287	1.380417516
Spp1	715.844	495.841	-0.529767653405673
Duct Gene Symbol	**shScramble FPKM**	**sh*Wdr5* #1 FPKM**	**Log2 (Fold Change)**
Car2	10.544	242.481	4.523377526
Krt7	122.188	505.273	2.047960483
Krt19	166.336	1071.29	2.687176724
Muc1	49.3224	197.888	2.004369222
Muc4	1.06598	4.31094	2.015822113
Muc20	0.34294	4.47451	3.70570161